UNIVERSITAT POLITÈCNICA DE VALÈNCIA

CENTRO DE RECONOCIMIENTO MOLECULAR
Y DESARROLLO TECNOLÓGICO

New approaches for the development of chromo-fluorogenic sensors for chemical species of biological, industrial and environmental interest

PhD. THESIS

Submitted by

Luis Enrique Santos Figueroa

PhD. Supervisors:

Prof. Ramón Martínez Máñez
Dr. Félix Sancenón Galarza

Valencia, September 2014

RAMÓN MARTÍNEZ MÁÑEZ, PhD in Chemistry and Professor at the *Universitat Politècnica de València*, and FÉLIX SANCENÓN GALARZA, PhD in Chemistry and Lecturer at the *Universitat Politècnica de València*.

CERTIFY:

That the work "*New approaches for the development of chromo-fluorogenic sensors for chemical species of biological, industrial and environmental interest*" has been developed by Luis Enrique Santos Figueroa under their supervision in the Centro de Reconocimiento Molecular y Desarrollo Tecnológico (IDM) of the Universitat Politècnica de València, as a Thesis Project in order to obtain the international degree of PhD in Experimental and Industrial Organic Chemistry at the Universitat Politècnica de València.

Valencia, 05th September 2014.

Prof. Ramón Martínez Máñez Dr. Félix Sancenón Galarza

Dedicada a la memoria de la mujer que guió mis primeros pasos en este mundo y cultivo desde muy joven mi pasión por las ciencias.

Rosa Jeannette Figueroa R. I. P.

“En algún sitio algo increíble espera ser descubierto.
Somos polvo de estrellas que piensa acerca de las estrellas”
Carl Sagan

Acknowledgements

Agradecimientos

Para comenzar quiero agradecer a mis directores de tesis Ramón Martínez y Félix Sancenón, no tan solo por su siempre cordial ayuda y sabio consejo, sino también por brindarme la oportunidad de trabajar estos años bajo su tutela y depositar en mi su confianza al recibirme en su grupo de investigación. Muchas gracias por su guía y aun más por su amistad.

Gracias también a un grupo especial de profesores que me brindaron en muchas ocasiones su incondicional ayuda profesional y personal y cuyas conversaciones y consejos han enriquecido mi vida en estos años. Muchas gracias a vosotros Juan Soto, Dolores Marcos, Luis Villaescusa, José Vicente Ros, Salvador Gil y Knut Rurack.

Mil gracias a todos mis compañeros y colegas que durante estos años me han brindado su incondicional apoyo, ayuda y motivación para seguir adelante y que han hecho de mi estancia en tierras europeas una de las mejores etapas de mi vida. No me bastarían las líneas para expresarles cuanto valoro el haberles conocido y poder nombrarles ahora entre mis buenos amigos. Tan seguro estoy de su amistad que se de hecho, que aun sin nombrarles ya os sabeis aludidos. Gracias por los buenos momentos vividos dentro y fuera de la universidad, sois parte de mis mejores recuerdos y lo mejor de esta etapa.

Gracias también a mis hermanos y mis padres por ser siempre una pieza clave de mi soporte en la vida y ofrecerme aun a la distancia la calidez de su compañía. Nada hubiese sido posible sin vuestro apoyo.

Gracias a ti mi amada esposa, por ser desde hace mucho mi compañía en cada paso. Gracias por alegrar mi vida y hacer que todos los esfuerzos tengan un verdadero significado.

Finalmente, gracias a Dios por todas las bendiciones que me han acompañado en esta etapa de mi vida, en particular por reunir en mi camino a las mejores personas de cuatro diferentes continentes.

Resumen

La presente tesis doctoral titulada "*New approaches for the development of chromo-fluorogenic sensors for chemical species of biological, industrial and environmental interest*" está centrada en el desarrollo de nuevos sensores químicos cromo-fluorogénicos basados en los principios básicos de la química supramolecular; particularmente en el reconocimiento molecular y el auto-ensamblaje.

La primera etapa de este estudio consistió en una amplia y minuciosa exploración bibliográfica que dio lugar a la publicación de un artículo de revisión sobre sensores químicos cromogénicos y fluorogénicos para la detección de aniones que fueron publicados durante los años 2010 y 2011 (Santos-Figueroa, L. E., et al. *Chem. Soc. Rev.*, **2013**, 42, 3489-3613). Esta revisión bibliográfica, si bien no ha sido incluida explícitamente en esta tesis doctoral debido a su larga extensión, constituye sin lugar a duda, parte del sustento teórico del trabajo experimental que está expuesto en ella, por lo que es citado continuamente como referencia bibliográfica.

El trabajo de tesis doctoral está estructurado en cuatro capítulos. El primero de ellos constituye una introducción general que resume los fundamentos teóricos de la química supramolecular en que se basan los estudios prácticos realizados. Los siguientes tres capítulos condensan los principales resultados de la etapa experimental de esta tesis. El orden en que son presentados sigue un esquema lógico que favorece su mejor comprensión en conjunto y no una distribución temporal del momento en que fueron realizados.

El capítulo dos está dedicado a la síntesis, caracterización y estudios de coordinación con cationes metálicos de un receptor cromo-fluorogénico construido mediante la aproximación unidad coordinante-unidad indicadora. El receptor sintetizado emplea una chalcona como unidad indicadora que esta

funcionalizada con dos grupos que conforman un sistema electrón dador-electrón aceptor, formando una molécula que presenta una banda de transferencia de carga en la zona visible del espectro. De todos los cationes y aniones ensayados, solo los trivalentes (Fe^{3+}, Al^{3+} y Cr^{3+}) son capaces de inducir cambios significativos en las bandas de absorción de la zona visible y en las de emisión. El receptor preparado permite la detección selectiva de los cationes trivalentes con notables límites de detección que se encuentran en el rango de concentraciones 2-4 nM y con cambios ópticos apreciables a simple vista (*Chem. Eur. J.,* **2014**, submitted).

Por otra parte, el capítulo tres está dedicado a la síntesis, caracterización y estudios de coordinación con aniones de sensores químicos cromo-fluorogénicos construidos mediante las aproximaciones de unidad coordinante-unidad indicadora, ensayos de desplazamiento y dosímetro químico. Mediante la aproximación de unidad coordinante-unidad indicadora se han preparado 7 receptores basados en tiosemicarbazonas funcionalizadas con anillos de furano y diferentes grupos dadores y aceptores de electrones con el fin de modular la selectividad hacia la coordinación con aniones. En presencia de aniones básicos (fluoruro, cianuro, acetato y dihidrógeno fosfato) se observan cambios de color y fluorescencia significativos asociados a procesos de coordinación y desprotonación de los receptores (*Org. Biomol. Chem.,* **2012**, 10, 7418–7428). Empleando también tiosemicarbazonas pero con anillos de tiofeno se sintetizaron 4 nuevas sondas que también presentaron cambios de color y de fluorescencia significativos con los mismos aniones básicos (*Tetrahedron*, **2012**, 68, 7179-7186). La aproximación de ensayos de desplazamiento ha sido empleada para el desarrollo de un sensor fluorimétrico selectivo para el anión hidrógeno sulfuro en ambientes acuosos y medios celulares. Para ello se ha preparado un complejo no fluorescente de ciclam-Cu(II) con antraceno. En este caso, el anión hidrógeno sulfuro es capaz de desplazar al Cu(II) del anillo de ciclam obteniéndose un encendido de la fluoresencia del sistema con un paulatino aumento de intensidad de emisión en función de la cantidad de analito detectada (*Eur. J. Inorg. Chem.,* **2014**, 41–45). Posteriormente, la aproximación del dosímetro químico fue

empleada para la preparación de un sensor cromo-fluorogénico para la detección del anión hidrógeno sulfuro en soluciones acuosas. En este caso, se sintetizó un colorante azoico funcionalizado con un grupo sulfonilazida. En presencia de hidrógeno sulfuro se produce la reducción del grupo sulfonilazida a sulfonilamida que conlleva asociado un cambio de color apreciable a simple vista y un aumento de la intensidad de fluorescencia (*Eur. J. Org. Chem.,* **2014**, 1848–1854).

Finalmente, el capítulo 4 de esta tesis doctoral presenta el desarrollo de un material híbrido sensor para la detección del anión sulfito en medios acuosos. Para ello se ha encapsulado un dosímetro químico, basado en un esqueleto estilbénico, dentro de las cavidades hidrófobas de nanopartículas mesoporosas de sílice. Al añadir el anión sulfito a suspensiones acuosas de las nanopartículas sensoras se observa un aumento significativo de la fluorescencia debido a la reacción entre el anión y el dosímetro dentro de las cavidades del soporte. De forma adicional, un sistema funcional con el uso del material híbrido preparado y un soporte polimérico tipo monolito fueron empleados para realizar ensayos de detección de sulfitos en vinos comerciales (*Angew. Chem. Int. Ed.,* **2013**, 52, 13712–13716).

Por todo lo anterior es posible decir que la presente tesis doctoral constituye un aporte científico original al desarrollo de la química molecular y supramolecular. Su contenido, así como las publicaciones que derivan de los estudios presentados en la tesis, deja abiertas rutas para continuar con el estudio y la preparación de nuevos y más eficientes sensores químicos y sistemas híbridos de detección con aplicaciones biológicas, industriales y ambientales.

Resum

La present tesi doctoral titulada "*New approaches for the development of chromo-fluorogenic sensors for chemical species of biological, industrial and environmental interest*" està centrada en el desenvolupament de nous sensors químics cromo-fluorogènics basats en els principis bàsics de la química supramolecular; particularment en el reconeixement molecular i l'autoacoplament.

La primera etapa d'este estudi va consistir en una àmplia i minuciosa exploració bibliogràfica que va donar lloc a la publicació d'un article de revisió sobre sensors químics cromogènics i fluorogènics per a la detecció d'anions que van ser publicats durant els anys 2010 i 2011 (Santos-Figueroa, L. E., et al. *Chem. Soc. Rev*, **2013**, 42, 3489-3613). Esta revisió bibliogràfica, si bé no ha sigut inclosa explícitament en esta tesi doctoral a causa de la seua llarga extensió, constituïx sense dubte, part del suport teòric del treball experimental que està exposat en ella, per la qual cosa és citat contínuament com a referència bibliogràfica.

El treball de tesi doctoral està estructurat en quatre capítols. El primer d'ells constituïx una introducció general que resumix els fonaments teòrics de la química supramolecular en que es basen els estudis pràctics realitzats. Els següents tres capítols condensen els principals resultats de l'etapa experimental d'esta tesi. L'orde en què són presentats seguix un esquema lògic que afavorix la seua millor comprensió en conjunt i no una distribució temporal del moment en què van ser realitzats.

El capítol dos està dedicat a la síntesi, caracterització i estudis de coordinació amb cations metàllics d'un receptor cromo-fluorogènic construït a través de l'aproximació unitat coordinant- unitat indicadora. El receptor sintetitzat empra una chalcona com a unitat indicadora que esta funcionalitzada amb dos grups que conformen un sistema electró dador-electró acceptor, formant una molècula que

presenta una banda de transferència de càrrega en la zona visible de l'espectre. De tots els cations i anions assajats, només els trivalents (Fe^{3+}, Al^{3+} i Cr^{3+}) són capaços d'induir canvis significatius en les bandes d'absorció de la zona visible i en les d'emissió. El receptor preparat permet la detecció selectiva dels cations trivalents amb notables límits de detecció que es troben en el rang de concentracions 2-4 nM i amb canvis òptics apreciables a simple vista (Chem. Eur. J., 2014, submitted).

D'altra banda, el capítol tres està dedicat a la síntesi, caracterització i estudis de coordinació amb anions de sensors químics cromo-fluorogènics construïts mitjançant les aproximacions d'unitat coordinant-unitat indicadora, assajos de desplaçament i dosímetre químic. A través de l'aproximació d'unitat coordinant-unitat indicadora s'han preparat 7 receptors basats en tiosemicarbazones funcionalizades amb anells de furà i diferents grups dadors i acceptors d'electrons a fi de modular la selectivitat cap a la coordinació amb anions. En presència d'anions bàsics (fluorur, cianur, acetat i dihidrogen fosfat) s'observen canvis de color i fluorescència significatius associats a processos de coordinació i desprotonación dels receptors (*Org. Biomol. Chem.,* **2012**, 10, 7418–7428). Emprant també tiosemicarbazones però amb anells de tiofè es van sintetitzar 4 noves sondes que també van presentar canvis de color i de fluorescència significatius amb els mateixos anions bàsics (*Tetrahedron*, **2012**, 68, 7179-7186). L'aproximació d'assajos de desplaçament ha sigut empleada per al desenvolupament d'un sensor fluorimètric selectiu per a l'anió hidrogen sulfur en ambients aquosos i mitjans cellulars. Per a això s'ha preparat un complex no fluorescent de ciclam-Cu (II) amb antracé. En este cas, l'anió hidrogen sulfur és capaç de desplaçar al Cu (II) de l'anell de ciclam obtenint-se una encesa de la fluoresencia del sistema amb un gradual augment d'intensitat d'emissió en funció de la quantitat d'anàlit detectada (*Eur. J. Inorg. Chem.,* **2014**, 41–45). Posteriorment, l'aproximació del dosímetre químic va ser empleada per a la preparació d'un sensor cromo-fluorogènic per a la detecció de l'anió hidrogen sulfur en solucions aquoses. En este cas, es va sintetitzar un colorant azoic

funcionalitzat amb un grup sulfonilazida. En presència d'hidrogen sulfur es produïx la reducció del grup sulfonilazida a sulfonilamida que comporta associat un canvi de color apreciable a simple vista i un augment de la intensitat de fluorescència (*Eur. J. Org. Chem.,* **2014**, 1848–1854).

Finalment, el capítol 4 d'esta tesi doctoral presenta el desenvolupament d'un material híbrid sensor per a la detecció de l'anió sulfit en mitjans aquosos. Per a això s'ha encapsulat un dosímetre químic, basat en un esquelet estilbènic, dins de les cavitats hidròfobes de nanopartícules mesoporoses de sílice. A l'afegir l'anió sulfit a suspensions aquoses de les nanopartícules sensores s'observa un augment significatiu de la fluorescència degut a la reacció entre l'anió i el dosímetre dins de les cavitats del suport. De forma adicional, un sistema funcional amb l'ús del material híbrid preparat i un suport polimèric tipus monòlit van ser empleats per a realitzar assajos de detecció de sulfits en vins comercials (*Angew. Chem. Int. Ed.,* **2013**, 52, 13712–13716).

Per tot l'anterior és possible dir que la present tesi doctoral constituïx una aportació científica original al desenvolupament de la química molecular i supramolecular. El seu contingut, així com les publicacions que deriven dels estudis presentats en la tesi, deixa obertes rutes per a continuar amb l'estudi i la preparació de nous i més eficients sensors químics i sistemes híbrids de detecció amb aplicacions biològiques, industrials i ambientals.

Abstract

This thesis entitled "*New approaches for the development of chromo-fluorogenic sensors for chemical species of biological, industrial and environmental interest*" is focused on the development of new chromo-fluorogenic chemosensors based on the basic principles of supramolecular chemistry; particularly in molecular recognition and self-assembly.

The first stage of this work consisted on an extensive and thorough literature exploration that led to the publication of a review article about chromogenic and fluorogenic chemosensors for anions recognition that were published during the years 2010 and 2011 (Santos-Figueroa, LE, et al. *Chem Soc Rev*., **2013**, 42, 3489-3613). This literature review, although not has been explicitly included in this PhD thesis, due to its long stretch, is without a doubt a part of the theoretical basis of the experimental work exposed here, thus it is continually cited as reference.

This PhD thesis is structured in four chapters. The first is a general introduction that summarizes the theoretical foundations of supramolecular chemistry in which the practical studies are based. In the next three chapters, the main results of the experimental phase of this thesis are condensed. The order in which they are shown follows a logical scheme that promotes a better understanding and it does not represent timing of when they were made.

Chapter 2 is devoted to the synthesis, characterization and coordination studies with metal cations of a chromo-fluorogenic receptor constructed by binding site-signaling subunit approach. The synthetic receptor employs a chalcone skeleton as signaling subunit and it is functionalized with two groups that make up an electron donor-acceptor system, forming a molecule, which have a charge transfer band in the visible spectrum region. Of all cations and anions tested, only the trivalent (Fe^{3+}, Al^{3+} and Cr^{3+}) are able to induce significant changes in the absorption bands of the visible zone and in the emission. The receptor

allows screening of trivalent cations with remarkable limits of detection in the 2-4 nM range of concentrations and optical changes noticeable to the naked eye (*Chem Eur J*., **2014**, submitted).

Moreover, chapter three is devoted to the synthesis, characterization and anion coordination studies of chromo-fluorogenic chemosensors constructed by binding site-signaling subunit approach, displacement assays and chemodosimeter. By binding site-signaling subunit approach, seven thiosemicarbazones-based receptors have been prepared with furan ring functionalized with two electron donor and acceptor groups in order to modulate the selectivity in coordination towards anions. In the presence of basic anions (fluoride, cyanide, acetate and dihydrogen phosphate) significant color and emission changes has been associated to coordination and deprotonation processes into the receptors (*Org. Biomol. Chem*, **2012**, 10, 7418-7428). Other four thiosemicarbazones-based probes synthesized using thiophene rings, also showed significant fluorescence and color changes in the presence of the same basic anions (*Tetrahedron*, **2012**, 68, 7179-7186). The displacement assays approach have been used to develop a selective fluorimetric sensor for hydrogen sulfide anion in aqueous environments and cell media. With this goal, we have prepared a non-fluorescent cyclam-Cu(II) complex with anthracene moiety. In this case, hydrogen sulfide anion is capable of displacing the Cu(II) from cyclam ring, this causes a swich on in the fluoresence of the system with a gradual increase in emission intensity as a function of the amount of analyte detected (*Eur. J. Inorg. Chem*, **2014**, 41-45). Subsequently, the approach of the chemodosimeter was used to prepare a chromo-fluorogenic probe for detection of hydrogen sulfide in aqueous solutions. In this case, an azo dye functionalized with a sulfonyl azide group was synthesized. In the presence of hydrogen sulfide a reduction from sulfonyl azide to sulfonyl amide taking place with a noticeable color change with the naked eye and an enhancement fluorescence intensity (*Eur. J. Org. Chem*, **2014**, 1848-1854).

Finally, Chapter 4 of this thesis shown the development of a sensor hybrid material for sulfite anion recogniton in aqueous media. For it, a stilbene skeleton-base chemodosimeter has been encapsulated within the hydrophobic pockets of mesoporous silica nanoparticles. Upon addtion of the sulfite anion to aqueous nanoparticles suspensions, a significant increase in fluorescence due to the reaction between the anion and the chemodosimeter within the cavities of the support is observed. Additionally, a functional system with the use of the hybrid material prepared and a monolith as polymeric support were employed for testing detection of sulfite in commercial wine (*Angew. Chem Int Ed*, **2013**, 52, 13712-13716).

For all the above we can say that this PhD thesis constitutes an original scientific contribution to the development of molecular and supramolecular chemistry. Its content and publications derived from the studies presented in the thesis leaves open routes to continue the study and development of new and more efficient chemical sensors and hybrid detection systems with biological, industrial and environmental applications.

Publications

Results of this PhD Thesis and other contributions have resulted in the following scientific publications:

- **Luis E. Santos-Figueroa**, María E. Moragues, Estela Climent, Alessandro Agostini, Ramón Martínez-Máñez, Félix Sancenón, "*Chromogenic and fluorogenic chemosensors and reagents for anions. A comprehensive review of the years 2010-2011.*" *Chemical Society Reviews*, **2013**, *42,* 3489-3613.

- **Luis Enrique Santos-Figueroa**, Cristina Giménez, Alessandro Agostini, Elena Aznar, María D. Marcos, Félix Sancenón, Ramón Martínez-Máñez, Pedro Amorós, "*Selective and Sensitive Chromofluorogenic Detection of the Sulfite Anion in Water Using Hydrophobic Hybrid Organic-Inorganic Silica Nanoparticles*", *Angewandte Chemie International Edition*, **2013**, *52,* 13712 – 13716.

- **Luis E. Santos-Figueroa**, María E. Moragues, M. Manuela M. Raposo, Rosa M. F. Batista, Susana P. G. Costa, R. Cristina M. Ferreira, Félix Sancenón, Ramón Martínez-Máñez, José Vicente Ros-Lis, Juan Soto, "*Synthesis and evaluation of thiosemicarbazones functionalized with furyl moieties as new chemosensors for anion recognition*", *Organic & Biomolecular Chemistry*, **2012**, *10,* 7418-7428.

- **Luis E. Santos-Figueroa**, María E. Moragues, M. Manuela M. Raposo, Rosa M. F. Batista, R. Cristina M. Ferreira, Susana P. G. Costa, Félix Sancenón, Ramón Martínez-Máñez, Juan Soto, José Vicente Ros-Lis, *"Synthesis and evaluation of fluorimetric and colorimetric chemosensors for anions based on (oligo)thienyl-thiosemicarbazones", Tetrahedron,* ***2012****, 68,* 7179-7186.

- **Luis E. Santos-Figueroa**, Cristina de la Torre, Sameh El Sayed, Félix Sancenón, Ramón Martínez-Máñez, Ana M. Costero, Salvador Gil, Margarita Parra, "*Highly Selective Fluorescence Detection of Hydrogen Sulfide by Using an Anthracene-Functionalized Cyclam–Cu(II) Complex*", European Journal of Inorganic Chemistry, 2014, 41–45

- **Luis Enrique Santos-Figueroa**, Cristina de la Torre, Sameh El Sayed, Félix Sancenón, Ramón Martínez-Máñez, Ana M. Costero, Salvador Gil, Margarita Parra, "*A Chemosensor Bearing Sulfonyl Azide Moieties for Selective Chromo-Fluorogenic Hydrogen Sulfide Recognition in Aqueous Media and in Living Cells*", *European Journal of Organic Chemistry, **2014**,* 1848–1854.

- **Luis Enrique Santos-Figueroa**, Antonio Llopis-Lorente, Santiago Royo, Félix Sancenón, Ramón Martínez-Máñez, "*A chalcone-based probe for the highly selective and sensitive chromo-fluorogenic sensing of trivalent metal cations*", ***2014**,* submitted.

- María E. Moragues, **Luis E. Santos-Figueroa**, Tatiana Ábalos, Félix Sancenón, Ramón Martínez-Máñez, "Synthesis of a new tripodal chemosensor based on 2,4,6-triethyl-1,3,5-trimethylbenzene scaffolding bearing thiourea and fluorescein for the chromo-fluorogenic detection of anions", *Tetrahedron Letters, **2012**, 53,* 5110–5113.

- Sameh Elsayed, Alessandro Agostini, **Luis E. Santos-Figueroa**, Ramón Martínez-Mañez, Félix Sancenón, "*An Instantaneous and Highly Selective Chromofluorogenic Chemodosimeter for Fluoride Anion Detection in Pure Water*", *Chemistry Open, **2013**, 2,* 58– 62.

- Sameh El Sayed, Cristina de la Torre, **Luis E. Santos-Figueroa**, Enrique Pérez-Payá, Ramón Martínez-Máñez, Félix Sancenón, Ana M. Costero, Margarita Parra, Salvador Gil, "*A new fluorescent "turn-on" chemodosimeter for the detection of hydrogen sulfide in water and living cells*", *RSC Advances, **2013**, 3,* 25690–25693.

- Sameh El Sayed, **Luis E. Santos-Figueroa**, Cristina de la Torre, Ramón Martínez-Máñez, Félix Sancenón, Ana M. Costero, Margarita Parra, Salvador Gil, "*2,4-dinitrophenyl ether-containing chemodosimeters for the selective and sensitive "in vitro" and "in vivo" detection of hydrogen sulfide*", **2014**, submitted.

- Sameh El Sayed, Cristina de la Torre, **Luis E. Santos-Figueroa**, Cristina Marín-Hernández, Ramón Martínez-Máñez, Félix Sancenón, Ana M. Costero, Salvador Gil, Margarita Parra, "*Azide and sulfonylazide functionalized fluorophores for the selective and sensitive detection of hydrogen sulfide*", *Sensors and Actuators B: Chemical,* **2014**, accepted.

- Cristina Marín-Hernández, **Luis E. Santos-Figueroa**, María E. Moragues, M. Manuela M. Raposo, Rosa M. F. Batista, Susana P. G. Costa, Ramón Martínez-Máñez and Félix Sancenón, "*Imidazo-anthraquinone derivatives for the chromo-fluorogenic sensing of basic anions and trivalent metal cations*", *Journal of Organic Chemistry,* **2014**, accepted.

- Cristina Marín-Hernández, **Luis E. Santos-Figueroa**, María E. Moragues, M. Manuela M. Raposo, Rosa M. F. Batista, Susana P. G. Costa, Ramón Martínez-Máñez and Félix Sancenón, *"Synthesis and evaluation of quinolines derivatives as chromo-fluorogenic chemosensor*", **2014**, submitted.

Abbreviations and Acronyms

2D	Bi-dimensional
3D	Three-dimensional
ACN	Acetonitrile
ACS	American Chemical Society
APTS	Aminopropyltriethoxysilane
BET	Brunauer–Emmett–Teller theory
BJH	Barrett-Joyner-Hale method
BODIPY	Boron-dipyrromethene
Bu_4N	Tetra-n-butylammonium
β2AR	β2 adrenergic receptor
CCD	Charge-Coupled Device
CD3CN	Deuterated Acetonitrile
CDCl3	Deuterated Chloroform
CHEF	Chelation Enhanced Fluorescence
CHEQ	Chelation Enhancement Quenching
CIBER-BBN	Centro de Investigación Biomédica en Red en Bioingeniería, Biomateriales y Nanomedicina
COSY	Correlation spectroscopy
CT	Charge tranfer
CTAB	*n*-cetyltrimethylammonium bromide
CyS	Cysteine
DBU	1,8-diazabicyclo[5.4.0]undec-7-ene
DHB	2,5-dihydroxybenzoic acid
DM	Dichroic Mirror
DMEM	Dulbecco's Modified Eagle's Medium
DMF	Dimethyl Formamide
DMSO	Dimethylsulfoxide
DNA	Deoxyribonucleic Acid
DSMZ	German Resource Centre for Biological Materials (Deutsche Sammlung von Mikroorganismen und Zellkulturen)
EM	Electron Microscopy
Em and em	Emission
ESIPIT	Excited-State Intramolecular Proton Transfer
EtOH	Ethanol

FBS	Fetal Bovine Serum
FF-ISC	Formally Forbidden Intersystem Crossing
Fl	Fluorescence
FRET	Fluorescence Resonance Energy Transfer
GPCR	G Protein-Coupled Receptors
GSH	Glutathione
Hcy	Homocysteine
HeLa	Henrietta Lacks (human cell line)
HEPES	[4-(2-hydroxyethyl)-1-piperazineethanesulfonic acid
HMDS	Hexamethyldisilazane
HOMO	Highest Occupied Molecular Orbital
HRMS	High Resolution Mass Spectra
HSQC	Heteronuclear Single Quantum Coherence
ICT	Internal Charge Transfer
IDM	Instituto de Reconocimiento Molecular y Desarrollo Tecnológico
IR	Infrared
IUPAC	International Union of Pure and Applied Chemistry
LOD	Limit of Detection
LUMO	Lowest Unoccupied Molecular Orbital
MCM	Mobil Composition Of Matter
MCR	Molecular Chemical Receptor
MeCN	Methyl Cyanide (Acetonitrile)
MeOH	Methanol
MLCT	Metal-to-Ligand Charge Transfer
Mp	Melting Point
MscL	Mechanosensitive Channel of Large Conductance
MS-EI	Mass Spectrometry by Electron Impact Ionization
NMR	Nuclear Magnetic Resonance
PBS	Phosphate Buffered Saline
PCT	Photoinduced Change Transfer
PET	Photoinduced Electron Transfer
Ph	Phenyl Groups
PhD	Doctor of Philosophy of Philosophy Doctorate
PIPES	Piperazine-N,N'-bis(2-ethanesulfonic acid)
PM3	Parameterized Model number 3
PT	Proton Transfer
PTI	Photon Technology Internation

PTMS	(Propyl)trimethoxysilane
PUF	Polyurethane Foams
PXRD	Powder X-ray diffraction
RA	Regression Approach
RMS	Root Mean Square
RNA	Ribonucleic Acid
SEM	Scanning Electron Microscope
TEM	Transmission Electron Microscope
TEOS	Tetraethylorthosilicate
TGA	Thermo-Gravimetric Analysis
TICT	Twisted Internal Charge Transfer
TMS	Trimethylsilyl
TRIS	Tris(hydroxymethyl)aminomethane)
UV/VIS and UV-Vis	Ultraviolet–visible
UPV	Universidad Politécnica de Valencia
Ex and ex	Excitation

Table of contens

Chapter 1: General introduction

1. GENERAL INTRODUCTION

1.1. Supramolecuar Chemistry

Nowadays, the development of new chromo-fluorogenic sensors systems is framed in the field of supramolecular chemistry. In this direction, all the research described in this PhD thesis is based on the fundaments of this dynamic field, therefore, the general introduction is aimed at present briefly their basics and some of their expansion lines in recent years.

1.1.1. Historical foundations on supramolecular chemistry.

Historically, the first bases of supramolecular chemistry can be traced by the late nineteenth century in the hands of some large researchers, beginning with the discovery of intermolecular forces in 1873 by Dr Johannes van der Waals Diderik (Nobel Prize in Physics of 1910)[1] and the synthesis and study of cyclodextrins by Dr. Villiers in 1891.[2] These were followed by the studies of the enzyme-substrate interactions the lock and key approach model reported in 1894 by Dr. Hermann Emil Fischer (Nobel Prize in Chemistry in 1902)[3] and the application of the theory of coordination and study of metal complexes presented in 1893 by Dr. Alfred Werner (Nobel Prize in Chemistry 1913).[4]

[1] Van der Waals, J. D. *Nobel Lecture: Physics 1901-1921*, **1967**, 255-265; Van der Waals, J. D. *"On the continuity of the gaseous and liquid state"*, PhD Dissertation. Leiden University, **1873**.

[2] Villiers, A. C. R. *Hebd. Seances. Acad. Sci*., **1891**, 112, 536-538.

[3] Fischer, H. E. *Nobel Lecture: Chemistry 1901-1921*, **1966**, 21-35; Fischer, E. *Ber. Dtsch. Chem. Ges*., **1895**, 28, 1429-1438.

[4] Werner, A. *Nobel Lecture: Chemistry 1901-1921*, **1966**, 256-269; Bowman-James, K. *Acc. Chem. Res.*, **2005**, 38, 671–678.

From these works, a new chemistry field, parallel to the current classical molecular chemistry, was developed with a main emphasis on the study of intermolecular interactions. Thus, in the early twentieth century many studies were performed within this new approach, emphasizing increasingly in the importance of interactions between molecules in many chemical and biological processes, providing a new structure in the chemical sciences.

Unquestionably, some of the most relevant works of twenty century, which were used to define the specific field of the new supramolecular chemistry discipline, were the pioneered studies on immunology about description of selective cell surface receptors presented in 1906 by the Dr. Paul Ehrlich (Nobel Prize in Physiology or Medicine of 1908).[5] Moreover, the introduction of supermolecule concept (Übermoleküle) to describe the hydrogen-bonded acetic acid dimers by Lothar Karl Wolf in 1937,[6] and the description of the hydrogen-bond nature published in 1939[7] by Dr. Linus Pauling (Award Novel Chemistry in 1954[8] and Nobel Peace after 1962). Finally, the discovery and study of the specific interactions of crown ethers and cryptands performed in 1967-1973 by considered parents of supramolecular chemistry, the Doctors Jean-Marie Lehn,[9] Donald J. Cram[10] and Charles J. Pedersen[11] (Nobel Prize *ex aequo* in Chemistry of 1987) definitely established the specific field of supramolecular chemistry and began their development as a new interdiscipline field.

[5] Ehrlich, P. *Nobel Lecture: Physiology or Medicine 1901-1921*, **1967**, 304-320.

[6] Wolf, K. L.; Frahm, H.; Harms, H. *Z Phys. Chem., Abt. B*, **1937**, 36, 237–287.

[7] Pauling, L. The Nature of the Chemical Bond, Cornell Universty, Ithaca, NY, 1st ed., **1939**.

[8] Pauling, L. Nobel Lecture: Chemistry 1942-1962, **1964**, 429-437.

[9] Lehn, J. M. *Nobel Lecture: Chemistry 1981-1990*, **1992**, 444-491;

[10] Cram, D. J. *Nobel Lecture: Chemistry 1981-1990*, **1992**, 419-437.

[11] Pedersen, C.J. *Nobel Lecture: Chemistry 1981-1990*, **1992**, 495-511.

1.1.2. Keywords and definitions of supramolecular chemistry.

While the molecular chemistry allows us, the understanding of the structure, reactivity and properties of molecules formed by the union of atoms by covalent bonds, the supramolecular chemistry or supermolecular chemistry provides us the tools to understand how the molecules organize themselves by intermolecular forces to build up more complex units, which are referred to as supra or supermolecules. Thus, the main purpose of the supramolecular chemistry is to gain control over the intermolecular bond.

Inspired by those concepts today supramolecular chemistry has been defined with many expressions, such as the "chemistry beyond the molecule", "chemistry of molecular assemblies and of the intermolecular bonds", "chemistry of non-covalent bond" or "non-molecular chemistry".[12]

In the official IUPAC terminology, the supramolecular chemistry is defined as "a field of chemistry related to species of greater complexity than molecules that are held together and organized by means of intermolecular interactions. The objects of supramolecular chemistry are supermolecules and other polymolecular entities that result from the spontaneous association of a large number of components into a specific phase (membranes, vesicles, micelles, solid state structures etc.)"[13]

A simple way to understand the nature of supramolecular chemistry have been presented by Dr. Jean Marie Lehn, by the following analogy: "…if we considerate the molecules are like individuals, so molecular chemistry deals with individuals and supermolecular chemistry deals with the society. Supermolecular

[12] Lehn, J. M. *Angew. Chem*., **1988**, 100, 91–116.

[13] Minkin, V. I. *Pure Appl. Chem*., **1999**, 71, 1919-1981.

chemistry is a chemical sociology, so to speak"[14] (Figure 1). Following this analogy, the molecular chemistry has allowed the study and construction of individual entities (molecules) by linking (covalently) their parts (atoms) according to their specific functions, thus giving to end-entity the particular characteristics that result from the sum and interaction between their functional groups.

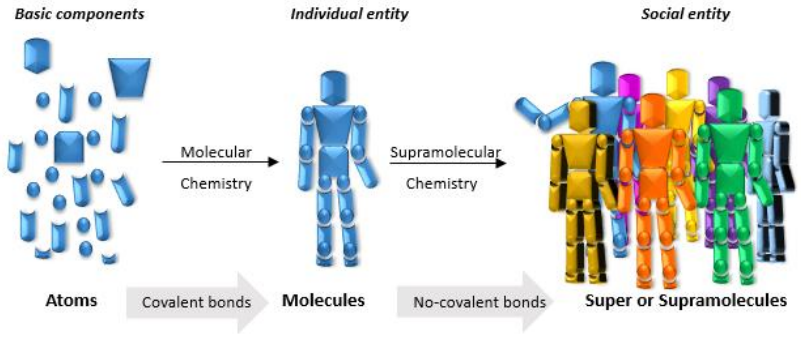

Figure 1. Schematic representation of Lehn´s analogy about nature of supramolecular chemistry.

Moreover, supramolecular chemistry exploits the interactions among individual entities, which never are merged into a single but can interact with each other forming clusters with an organized structure and specific characteristics, such as a society. Further, while covalent bonds allow atoms to remain tightly bound and communicated with each other in a molecule, such as the body's organs in an individual, the molecules interact together by individual weak bonds which when combined among themselves allow the formation of structural "societies" calls supra or supermolecules.

DNA is a good example of a well-structured and stable biological supermolecule. DNA consists of two polynucleotide strands with arrays of base-pairs complementary nitrogen that are joined together by non-covalent hydrogen bonds. In this case, the electrostatic interactions are caused by the attraction

[14] Lehn, J. M. "Supramolecular chemistry can help to understand better how to make efficient drugs". Universitat Autònoma de Barcelona, Spain. October **2012**. Lecture.

between the dipoles of proton-donor groups (NH) and proton-acceptor groups (C=O and C-N), the hydrogen bonds formed granted bond strength and high degree of directionality in this complex structure **1** (Figure 2). Besides, other non-covalent bond is the responsible to reduce the Gibbs free energy, minimizing solvation effect and produce an align perpendicular to DNA axis of the polynucleotides, namely π-stacking interactions among aromatic rings of nucleobases such as into structure **2**.

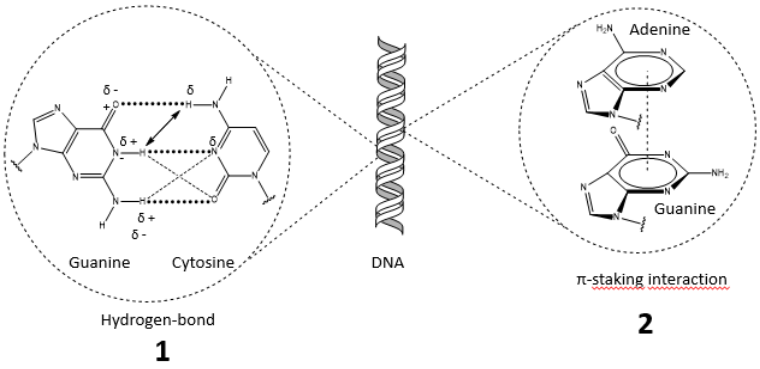

Figure 2. Noncovalents interactions between nucleobases-pair inside of DNA structure. Left: Primary and secondary hydrogen bond interactions **1**. Right: sandwich π-staking interaction between aromatic rings **2**.

As in the DNA, several supermolecules possess highly organized structures because of the sum of several weak intermolecular forces and high complementarity between their components. In fact, the relative ease to break these interactions is just what allows that certain processes such as replication and the recombination of DNA occur.

Nowadays, the synthesis of supermolecules with complex structure and similar properties as well as the biosupermolecules are also possible. In fact, in some cases the modulation of noncovalent interactions in these synthetic supermolecules has enabled the preparation of complex molecular machines. A good example of the cited above is the pH-switchable glycorotaxanes **3** preparated by the group of F. Coutrot and E. Busseron, that behaves as a molecular muscle and which has the ability to contract and stretch induced by

changes in the affinities of the macrocycles for two molecular stations depending of pH modulations (Figure 3).[15]

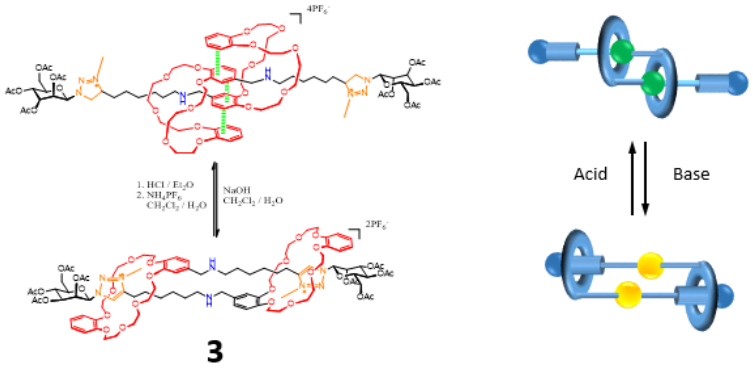

Figure 3. Schematic representation of stretching/contraction of "molecular muscle" based in pH-switchable mannosyl[c2]daisy chains rotaxanes **3**.

In order to structure and sort the new discipline, in recent decades the studies of supermolecules and in general, the development of supramolecular chemistry has been classified into three main areas:

- ***Molecular recognition,*** chemistry process associated with a molecule recognizing a partner compound, also defined as Host-Guest chemistry.

- ***Molecular self-assembly,*** chemistry process of spontaneous formation of supermolecules without guidance from an outside source.

- **Preparation of functional systems**, interdisciplinar applications of supramolecular chemistry to prepare functional systems such as chemical templated capsules, control release systems, nano superstructures or mechanically interlocked switchable scaffolds (molecular machines).

[15] Coutrot, F.; Busseron, E. and Montero, J. L. *Org. Lett.*, **2008**, 10, 753–756; Coutrot, F. and Busseron, E. *Chem.-Eur. J.*, **2008**, 14, 4784–4787; Coutrot, F.; Romuald, C. and Busseron, E. *Org. Lett.*, **2008**, 10, 3741–3744; Coutrot, F. and Busseron, *Chem. -Eur. J.*, **2009**, 15, 5186–5190.

1.1.3. Molecular recognition chemistry.

Through supramolecular studies, nowadays we know that all biological functions are associated with a selective recognition between two or more molecules through specific interactions. This process is known as "molecular recognition". More specifically, molecular recognition is considerated the way that molecules can recognize each other to form complex structures through a privileged relationship resting on the mutual interest of interacting partners possessing special qualities. Usually, the interaction between these partners (host-guest) is of the kind of noncovalent interactions as hydrogen bonding, metal coordination, hydrophobic forces, Van der Waals forces and $\pi-\pi$ interactions.[16]

The first and simplest model of molecular recognition is the lock-key principle suggested by Dr. Hermann Emil Fischer in 1894.[17] In this model, an enzyme (host) can discriminate among different substrates (guests) through the specific geometric complementarity between host and guest. Thus, only one guest fit exactly into one host like only a key enter in a specific lock. Knowledge of this simple principle allowed explaining the enzymatic catalysis (Figure 4), the compression of many complex biological processes and setting up the foundation for the preparation and optimization of new synthetic hosts (receptors).[18]

[16] Schmidtchen, F. P. *Chem. Soc. Rev.,* **2010**, 39, 3916-3935; Smith, D. K. *J. Chem. Edu.,* **2005**, 82, 393-400.

[17] Fischer, E. *Ber. Dtsch. Chem. Ges*., **1895**, 28, 1429-1438.

[18] Lichtenthaler, F. W. *Angew. Chem*., **1992**, 104, 1577–1593; Koshland, D. E. *Angew. Chem*., **1995**, 33, 2375–2378.

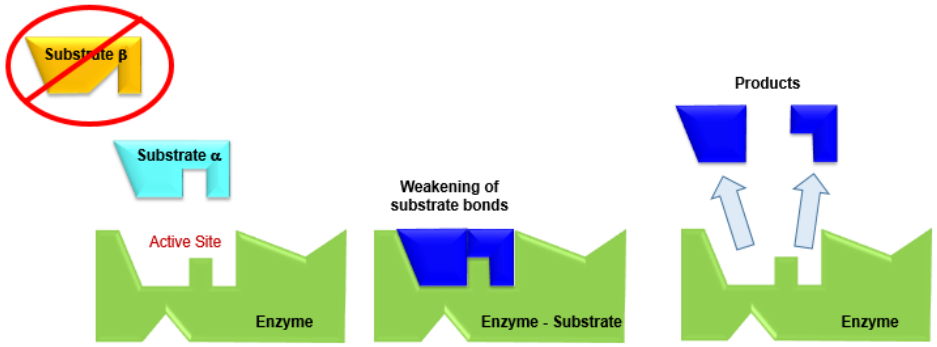

Figure 4. Schematic representation of enzymatic catalysis process by simple geometric recognition of a sustrate α, based on lock-key principle.

Although currently we know that molecular recognition is a more complex phenomenon with action of dynamic processes as self-assembly, molecular folding, steric effect, and others, that lead to adaptive effects like cooperativity or allosterism,[19] the host-guest chemistry principle remains very similar: a molecular host selectively recognizes a specific molecular guest.

1.1.3.1. Molecular chemical receptor.

A molecular chemical receptor (MCR) is a particular molecule designed and optimized for molecular recognition of a given substrate, so its preparation has to take into account the physical and chemical characteristics of the latter in order to ensure the greatest possible complementarity in the Host-Guest pair.

During the design of a MCR is necessary an extensive evaluation of the size, shape, geometry, charge, hydrophilic/lipophilic character and other physico-chemical characteristics of guest-analyte to provide the best and largest amount of intermolecular forces between the host and the guest that are possible. In addition, an assessment of the environment in which molecular recognition takes

[19] Baron, R. and McCammon, J. A. *Ann. Rev. Phys. Chem.,* **2013**, 64, 151 -175; Hummer, G. Nature *Chemistry*, **2010**, 2, 906–907.

places is very important when designing the MCR due to the influence of intermolecular processes such as solvation and electrostatic interactions between MCR, medium and analyte.[20]

Moreover, the effectiveness of a MCR is associated to the degree of complementarity between host and guest, which promotes the action of one or more intermolecular forces during the recognition process. Furthermore, the MCR efficiency is determined by its ability to selectively recognize a specific guest, including on the presence of other substrates with similar features. Therefore, it is intended that the MCR have more than one form of interaction type with the analyte (Figure 5), such as biological receptors whose complexity and complementarity with certain substrates ensures the activation of biological processes in a consistent and very specific manner.[21]

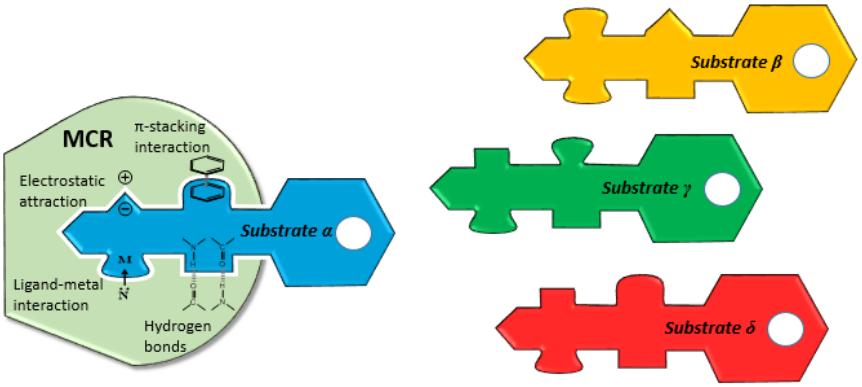

Figure 5. Schematic representation of host-guest complementarity to a specific MCR and a specific substrate α by multiple noncovalent interactions.

As mentioned above, the first studies with biological MCR were conducted by Dr. Villiers in 1891 with cyclodextrins,[22] although his skill as MCR was not studied

[20] Oshovsky, G. V.; Reinhoudt, D. N. and Verboom, W. *Angew. Chem. Int. Ed*. **2007**, 46, 2366 – 2393; Kubik, S. *Chem. Soc. Rev.,* **2010**, 39, 3648-3663.

[21] Joyce, L. A.; Shabbir, S. H. and Anslyn, E. V. *Chem. Soc. Rev*., **2010**, 39, 3621–3632.

[22] Villiers A. *Compt. Rend. Fr. Acad. Sci.* **1891**, 112, 435-438.

until 1935, by Dr. Pringsheim[23] demonstrated their ability to form complexes with certain specific substrates. Since these pioneering studies, the understanding of biological MCR has significantly increased. In fact, the most drugs used today are based on studies of specific biological receptors, such as those coupled to G proteins that have been investigated extensively by Dr. Robert Lefkowitz and Dr. Brian Kobilka and for which they were awarded the Nobel Prize in chemistry in 2012.[24] Besides, Dr. Brian Kobilka and co-workers were also the responsibles of other significant progress in this area in 2011, when reported the first picture of high-resolution structure of a GPCR-G protein complex (**4**) formed by the transmembrane signaling (molecular recognition) between the β_2 adrenergic receptor (β_2AR) and the G protein (Figure 6).[25] This agonist-GPCR-G protein complex is responsible for a majority of cellular responses to hormones and neurotransmitters in humans.

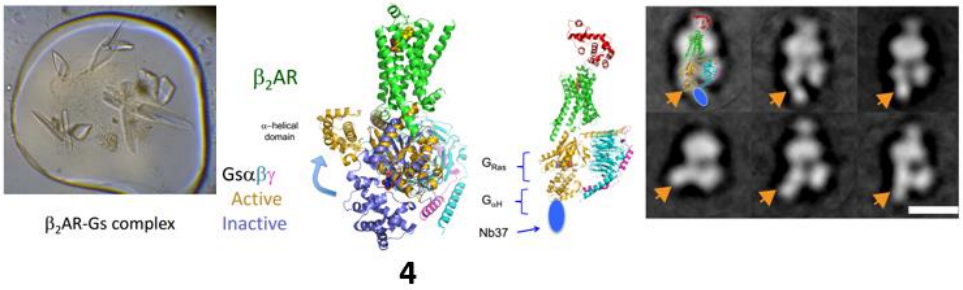

Figure 6. Picture and schematic representation of molecular recognition of G protein by β_2AR receptor. Left: Picture on HD of β_2AR-Gs complex. Center: schematic representation of active and inactive complex **4**. Right: mobility of alpha helical domain confirmed by EM.[26]

[23] Pringsheim, H. Chemistry of the Saccharides; McGraw-Hill: New York, **1932**; p 280.

[24] Kobilka, B. C. *Nobel Lecture: Chemistry Nobel Prizes*, **2012**, 195-213.

[25] Rasmussen, S. G. F.; DeVree, B. T.; Zou, Y.; Kruse, A. C.; Chung, K. Y.; Kobilka, T. S.; Thian, F. S.; Chae, P. S.; Pardon, E.; Calinski, D.; Mathiesen, J. M.; Shah, S. T. A.; Lyons, J. A.; Caffrey, M.; Gellman, S. H.; Steyaert, J.; Skiniotis, G.; Weis, W. I.; Sunahara, R. K. and Kobilka, B. K. *Nature,* **2011**, 477, 549-555.

[26] Kobilka, B. C. *Nobel Lecture Slides: "The structural basis of G protein coupled receptor signaling",* **2012**.

On the other hand, the first synthetic MCRs were reported in 1960 by the parents of the supramolecular chemistry the Drs Jean-Marie Lehn,[27] Donald J. Cram[28] and Charles J. Pedersen[29] who prepared crown ethers (**5** and **6**) and cryptands (**7** and **8**) capable of a specific molecular recognition of certain metal cations by coordination processes (Figure 7).

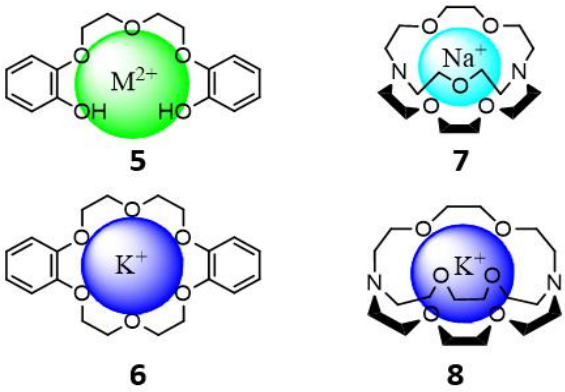

Figure 7. Metal complex based on MCR of crown ethers and cryptands. Left: Pederson´s complexes of divalent cations (**5**) and K^+ (**6**) with crown ethers. Right: Structures of metal complex of Na^+ (**7**) and K^+ (**8**) with two of the first sintetic cryptands.

Then, on the end of the same decade, the first anion receptors were also reported by Drs. Shriver and Biallas[30] and by Drs Park and Simmons.[31] These receptors were based in donor-acceptor formation of bidentate complexes between macrobicyclic amines **9** or triphenylmethyl ethers **10** with several anions, such as Cl^- (Figure 8).

[27] Lehn, J. M. *Acc. Chem. Res.*, **1978**, 11, 49–57; Lehn, J. M. *Pure Appl. Chem.,* **1978**, 50, 9, 871-892.

[28] Cram, D. J. *J. Am. Chem. Soc.* **1978**, 100, 8190-8202; Cram, D. J.; Cram, J. M. *Science*, **1974**, 183, 803-809.

[29] Pedersen, C.J. *J. Am. Chem. Soc.* **1957**, 79, 2295-2299; Pedersen, C. J. *J. Am. Chem. Soc.* **1967**, 89, 7017-7036.

[30] Shriver, D. F. and Biallas, M. J. *J. Am. Chem. Soc.*, **1967**, 89, 1078-1081.

[31] Park, C. H. and Simmons, H. E. *J. Am. Chem. Soc.*, **1968**, 90, 2429-2431.

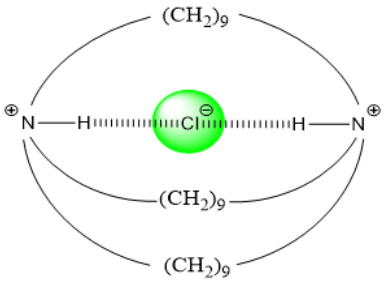

9

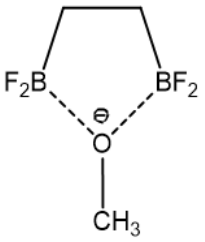

10

Figure 8. Representation of first anion receptors. Left: chelated complex (**9**) formed between macrobicyclic amines and Cl^- anion, reported by Park and Simmons. Right: chelated complex (**10**) formed between bidentade 1,2-bis(difluoroboryl)ethane and methoxide anion, reported by Shriver and Biallas.

In the following decades, the study and preparatio of new and more efficient MCR has been widely developed for many applications.[32] In particular, a strong line on development of MCR that is becoming increasingly important is the preparation of receptors designed for the sensing of chemical species of industrial, biological or enviromental interest, which are know as chemical sensor or chemosensors and which are the main focus in this PhD thesis.

1.1.4. Molecular chemical sensors (chemosensor).

Acording with IUPAC definition a chemical sensor or chemosensor "…transforms chemical information, ranging from the concentration of a specific sample component to total composition analysis, into an analytically useful signal".[33] In this particular, a molecular chemical sensor or chemosensor is really a molecular probe, which produces a detectable signal when interacting with a specific analyte.

[32] Reinhoudt, D. N.; Stoddart, J. F. and Ungaro, R. *Chem. Eur. J.*, **1998**, 4, 1349-1351; Lusby, P. J. *Annu. Rep. Prog. Chem., Sect. A: Inorg. Chem.*, **2013**, **109**, 254-276.

[33] Hulanicki, A.; Geab, S. and Ingman, F. *Pure. App. Chern.,* **1991**, 63, 1247-1250.

A molecular chemosensor is usually composed of two basic functional groups: a receptor subunit and a signaling subunit or trasducer (Figure 9) and which have a specific mechanism for communication between both. The receptor subunit is the part able to display a molecular recognition process in which the chemical information is transformed into a form of energy that is transduced by the signaling subunit into a macroscopic measurable signal as an alarm signal or output response.[34]

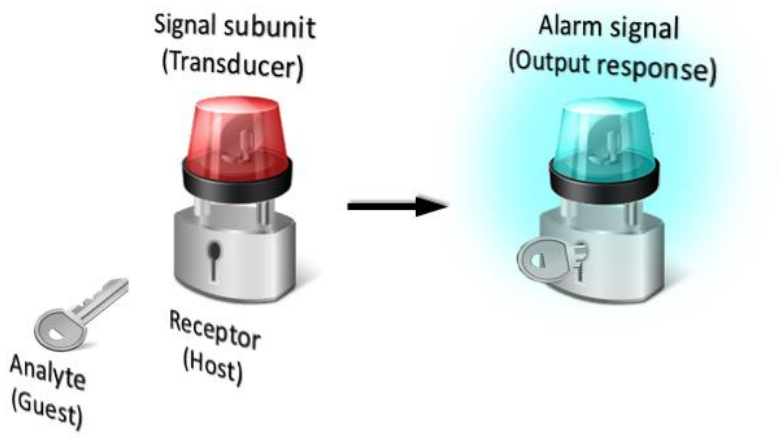

Figure 9. Schematic representation of the operation mechanism of a chemosensor.

As previously mentioned, the receptor subunit is the main responsible of selectivity of chemosensor in agreement of their complementary with the analyte-guest (see Figure 5), whereas, the chemosensor sensitivity is the result of both the receptor ability to effect the molecular recognition at low concentrations of guest and of the signaling subunit ability to report the event. Both selectivity and sensitivity are strongly influenced by environmental conditions and physico-chemical characteristics of the enviroment in which the molecular recognition takes place.

[34] Czarnik, A. W. *Acc. Chem. Res*., **1994**, 27, 302–308.

According to the operating principle of the signal subunit, the chemical sensor could be classified as:

- Optical sensors, if the molecular recognition is transduced in optical phenomena as changes in absorbance, transmittance, fluorescence, luminescence, light scattering or optothermal effect.

- Electrochemical sensors, when the final signal result in a modulation of electrical current condition by redox process.

- Mass sensitive sensors, when the recognition process is reported as the mass change at a specially modified surface that resulting into a change of a property of the support material.

- Magnetic sensors, when the analitical signal is a change of paramagnetic properties.

- Thermometric sensors, when the signal is based in the measurement of the heat effects of a specific chemical reaction or adsorption molecules, which involve the analyte.

- Radiation sensors, if non-optical radiation as α-, β-, γ- or X-rays is the basis for the signaling.

Of all the types of chemical sensors, the optical and electrochemical chemosensors are the most appealing to design applied molecular systems. These kinds of chemosensors are extensively used for the detection of anions, cations or neutral molecules in biological and environmental samples by their versatility and ease of measuring its response.

1.1.5. Molecular self-assembly.

Additionaly to molecular recognition, the supramolecular chemistry also has been developed as an important tool in the construction of new molecular topologies through self-assembly processes.

Following the recommended IUPAC terminology molecular self-assembly could be defined as "the spontaneous and reversible organization of molecular entities by noncovalent interactions…Self-assembly is a process in which a system of pre-existing components, under specific conditions, adopts a more organized structure through interactions between the components themselves".[35] In practical, if this self-organization is carried out by atoms in intramolecular rearrangement, the common term used is "folding", while, if the spontaneous reorganization is produced intermolecularly the self-assembly term is really used.

Although the two terms "self-assembly" and "folding" are analogous, since noncovalent intermolecular interactions are weaker than covalent bonds, thus to overcoming the entropic cost of reorganization, large areas of complementarity are necessary to allow the self-assembling process to occur.[36]

The classic self-assembly was studied and employed to model micellar and colloidal molecular systems, but recently other complex constructions have been achieved by modern supramolecular self-assembly techniques such as novel macrocycles, organic frameworks, rotaxanes systems, molecular capsules, supramolecular aggregates templates and polymeric and siliceous nanostructures.[37]

---

[35] Jones, R. G.; Ober, C. K.; Hodge, P.; Kratochvíl, P.; Moad, G. and Vert, M. *Pure Appl. Chem*., **2013**, 85, 463–492.

[36] De Mendoza, J. *Chem. Eur. J.* **1998**, 4, 1373-1377.

[37] Leininger, S.; Olenyuk, B.; Stang, P. J. *Chem. Rev.* **2000**, 100, 853-908.

A good example of the use of modern self-assembly techniques in the construction of ordered structures is seen in the preparation of mesoporous siliceous nanomaterials through the use of supramolecular aggregate templates (Figure 10).

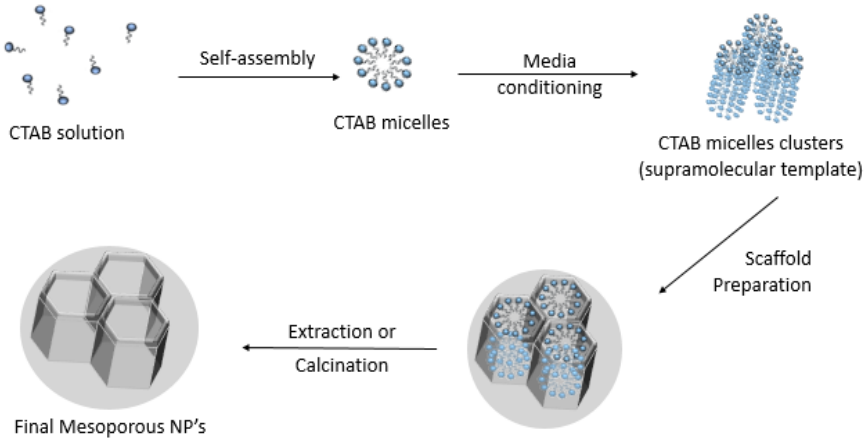

Figure 10. Schematic representation of mesoporous silica nanoparticle synthesis by self-assembly template.

In this case, first, micellar systems are formed by self-assembly via simple non-covalent hydrophobic interactions between molecules of surfactants over critical micelle concentration. Then, using specific conditions of concentration, temperature and presure, nano-aggregates are organized and packaging with definite structure (lamellar, cubic or hexagonal) over which a silica precursor is solidified by sol-gel reaction. Finally, the template is removed and the especific mesoporous silica nano-particles are obtained.

Another example of self-assembly used to build supermolecules on 2D and 3D was reported by Stang, Zheng and co-workers, who recently described the preparation of multicomponent supramolecular structures by selective self-

assembly.[38] Upon combination of a 90° Pt(II) acceptor **11** and a carboxylate ligand **12** with appropriate pyridyl donors **13** or **14**, in a proper ratio, coordination-driven self-assembly allows for the selective formation of multicomponent supramolecular rectangle **15** on 2D and prisms **16** on 3D (Figure 11).

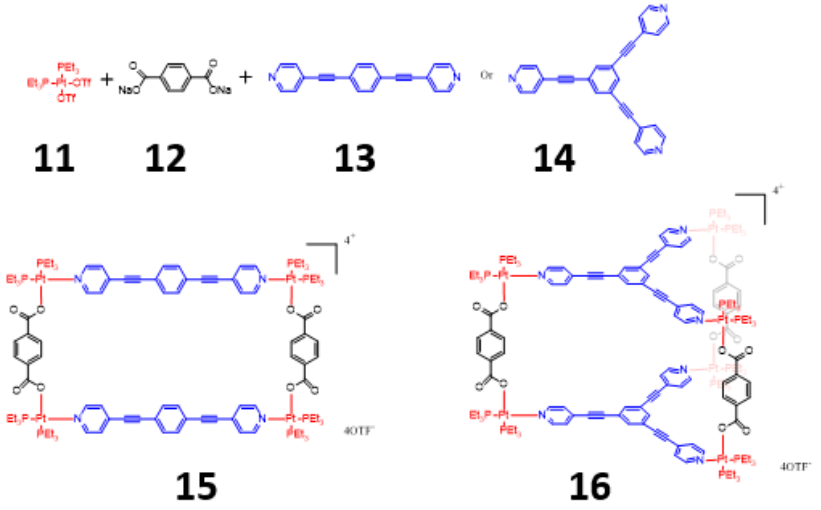

Figure 11. Selective self-assembly of multicomponents 2D rectangle **15** (left) and 3D trigonal prism **16** (right) by combination of cis-$Pt(PEt_3)_2(OTf)_2$ (**11**), dicarboxylate ligand (**12**), and dipyridyl donors (**13** and **14**).

The emerging science of materials engineering, especially on nanotechnology, have promoted the development of new supramolecular applications beyond of simple self-assembly or molecular recognition. Complex supramolecular applications involving both molecular recognition and self-assembling, are grouped in a different category known as "preparation of functional systems" which is discussed below.

[38] Zheng, Y.-R.; Zhao, Z.; Wang, M.; Ghosh, K.; Pollock, J. B.; Cook, T. R.; Stang, P. J., *J. Am. Chem. Soc.* **2010**, 132, 16873-16882.

1.1.6. Preparation of functional systems.

The combined use of molecular recognition and self-assembly processes has enabled the preparation of highly sophisticated functional biologically inspired supramolecular systems with novel aplications in industry, medicine, farmacology, materials engineering and biology.

This category of supramolecular chemistry implementation has recently received a great interest of the international scientific community and some applications are currently used into interdisciplinary areas. In fact, such as the Dr. Jean Marie Lehn notes "a major feature is the range of perpectives offered by the cross reutilization of supramolecular chemistry research, owing to its location at the intersection of chemistry, biology and physics. Such wide horizons are a challenge and a stimulus to the creative imagination of the chemist".[39]

One of the applications of these functional systems that has attracted the interest is the preparation of controlled release systems. Some examples of preparation of this kind of nanodevices, using mesoporous hybrid materials container and complex molecular gates, have been reported.[40] In this respect, the ability to control delivery of drugs on cells or the capture and release of specific molecules has important applications on nanomedicine. As a particular example, a work report by Climent, et al. offers a competitive method to *Mycoplasma* sensing. In this design, a fragment of the 16S ribosomal RNA subunit is incorporated as molecular gate adsorbed into the external surface of mesoporous silica nanoparticles that containing an encapsulated dye (**S1-O1**). In the presence of the genomic DNA of *Mycoplasma* fermentans, an uncapping of the solid occurs

[39] Lehn, J. M. *Science*, **1993**, 260, 1762-1763

[40] Coll, C.; Bernardos, A.; Martínez-Máñez, R.; Sancenón, F., *Acc. Chem. Res.,* **2012**, 46, 339-349.

inducing the release of the entrapped dye as optical output of the molecular recognition (Figure 12).[41]

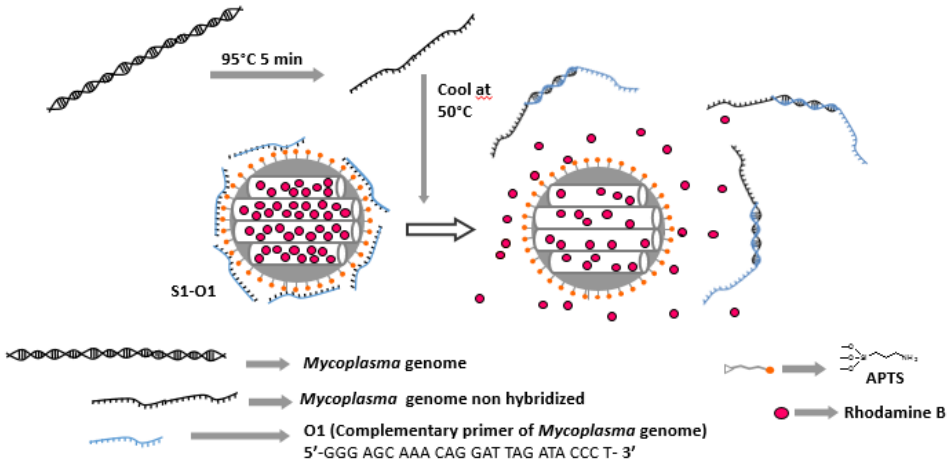

Figure 12. Schematic representation of the molecular gated material **S1-O1** functionalized with **APTS** and capped with a single-stranded oligonucleotide (**O1**).

Another example of functional nanosystem was reported by Koçer, et al. in the design of a molecular valve embedded in a membrane that can be opened by illumination with long-wavelength ultraviolet (366 nm) light and then resealed by visible irradiation. In this case, the valve consists of a channel protein, the mechanosensitive channel of large conductance (MscL) from *Escherichia coli*, modified by attachment of synthetic spiropyran photoswitches (**17** and **18**) that undergo light-induced charge separation to reversibly open and close a 3-nanometer pore (Figure 13).[42]

[41] Climent, E., Mondragón, L., Martínez-Máñez, R., Sancenón, F., Marcos, M. D., Murguía, J. R., Amorós, P., Rurack, K. and Pérez-Payá, E. *Angew. Chem. Int. Ed.,* **2013**, 52, 8938–8942.

[42] Koçer, A.; Walko, M.; Meijberg, W. and Feringa B. L. A., *Science*, **2005**, 309, 755–758.

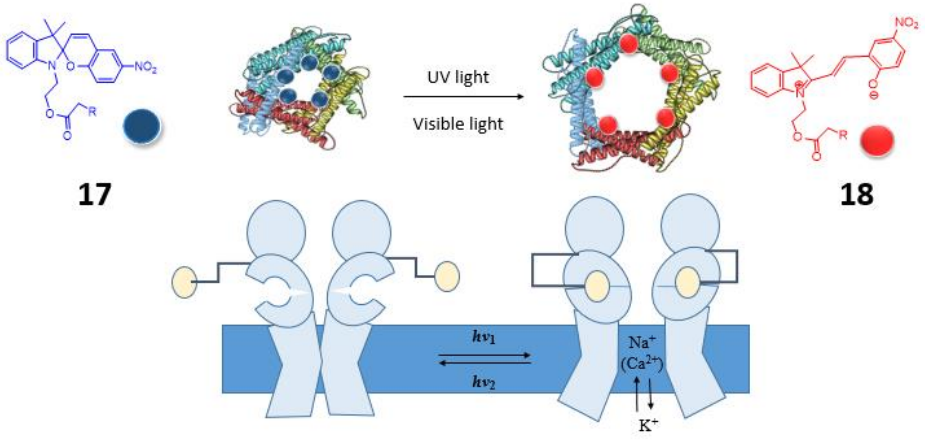

Figure 13. Schematic representation of light-actuated nanovalve based on a mechano-sensitive channel protein modified with spiropyran **17** and **18** photoswitches.

Further, other electrochemical and biological systems have also been implemented into supramolecular nanodevices with good perspectives to be used in real applications.[43]

1.2. Optical Chemosensors.

As mentioned above, an optical chemosensor is a special kind of chemosensor, which reports a molecular recognition process through an optical signal such as changes of colour or fluorescence. The development of optical chemosensors has gained prime importance in recent years due the simple and low-cost instrumentation required, the usually low limit of detection obtained and the high quantity of fluorophores and dyes comercially available. Especially, chromogenic recognition has drawn attention because it offers the possibility of straightforward semiquantitative "naked-eye" detection.[44]

[43] Dalgarno, S. J. *Annu. Rep. Prog. Chem., Sect. B*, **2010**, 106, 197–215.

[44] Santos-Figueroa, L. E.; Moragues, M. E.; Climent, E.; Agostini, A.; Martínez-Máñez, R.; Sancenón, F. Chem. Soc. Rev., **2013**, 42, 3489-3613; Formica, M.; Fusi, V.; Valeur, B.; Leray, I. Coord. Chem. Rev., **2000**, 205, 3-40.

1.2.1. Different design principles for optical chemosensors.

Nowadays, most of the reported examples of optical chemosensors still use one of the following three main approaches: (i) the ‘‘binding site-signaling subunit’’ protocol, (ii) the ‘‘displacement’’ approach and (iii) the ‘‘chemodosimeter’’ paradigm.

The choice of one protocol or another depends largely on the most important aspects of chemosensor design such as analyte affinity, binding selectivity, the medium in which the sensing is performed, the optical signaling mechanism and the synthetic effort that it desired to made in the chemosensor preparation.

1.2.1.1. “Binding site-signaling subunit” aproach.

The binding site-signaling subunit approach is perhaps the most popular method for the development of optical chemosensors. On this approach, the binding site and the optical signaling subunit are covalently bonded in such a way that the interaction of the analite with the binding site induces modulations in the signaling unit. If the two units are electronically connected, then the modulations in signaling unit can result in colour and emission changes, otherwise, only changes in fluorescence could be observed.

In general, the binding site subunit is designed to have effective noncovalent interactions with a specific analite, while, the signaling subunit is usually a chromophore or fluorophore.

One of the most remarkable drawbacks to this approach, especially for anion recognition, is that, the interaction of the analyte with the binding sites usually relies on relatively weak interactions, thus the optical modulation is strongly affected by the environment and the probes usually requires a large synthetic effort to overcome this problem.

As an example, Figure 14 shows the metal complex **19** reported by Goswami and co-workers, which contained two quinoline fluorophores as signaling subunits and a coordination cavity able to form hydrogen bonds and electrostatic interactions with anions.[45] The selectivity to $H_2PO_4^-$ over other several anions, in acetonitrile solution, was due to the cavity of **19** that perfectly fits the size and shape of this specific $H_2PO_4^-$ anion. In this case, the molecular recognition was reported by an increase of the emission intensity at 398 nm upon excitation at 285 nm.

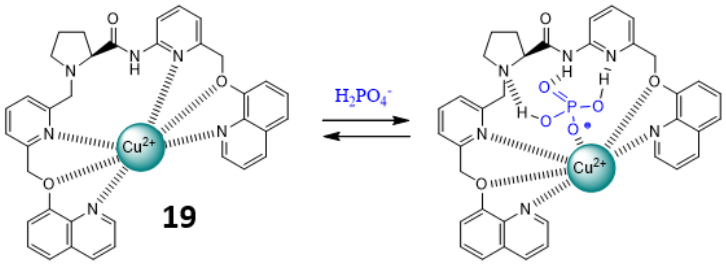

Figure 14. Schematic representation of the binding mode between receptor **19** and $H_2PO_4^-$.

Another example is for Hg^{2+} sensing via the use of the rhodamine-based chemosensor **20** reported by Ali group (Figure 15).[46] The formation of 1:1 coordination metal complexes is signalled by both colorimetric and fluorogenic changes in organic-water mixtures. In addition, the reversible binding of **20** with Hg^{2+} by addition of KI offered the potential design of INHIBIT logic devices.

[45] S. Goswami, D. Sen and N. K. Das, *Tetrahedron Lett.,* **2010**, 51, 6707–6710.

[46] Mistri, T., Alam, R., Dolai, M., Kumar Mandal, S., Guha, P., Rahman Khuda-Bukhsh, A. and Ali, M., *Eur. J. Inorg. Chem.*, **2013**, 5854–5861.

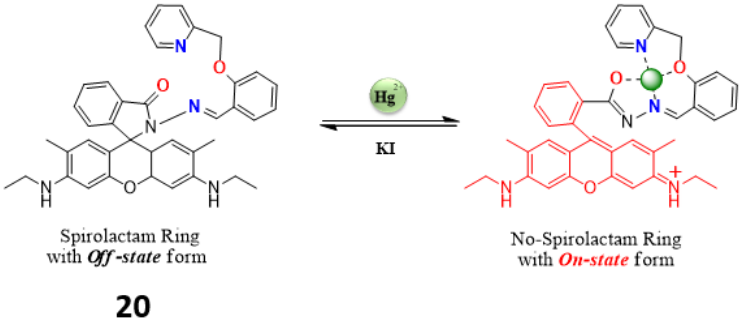

20

Figure 15. Schematic reprecentation of binding mode of **20** chemosensor towards Hg^{2+}.

Less common, but equally important, is the design of probes for neutral species using the binding-site-signaling-subunit approach. As an example, D'Souza, et al. reported a group of metalloporphyrin-based fluorescent chemosensors (**21**-**23**) for the selective detection of dinitrogen alkaloids such as nicotine and cotinine in solution of organic solvents such as toluene, *o*-dichlorobenzene or acetonitrile.[47] These probes showed selectivity with respect to the presence of other axially coordinating nitrogenous bases. The recognition strategy in this case, was based on the use of 'two-point' binding for dinitrogen alkaloids (Figure 16).

[47] Deviprasad, G. R.; D'Souza, F., *Chem. Commun.*, **2000,** 19, 1915-1916.

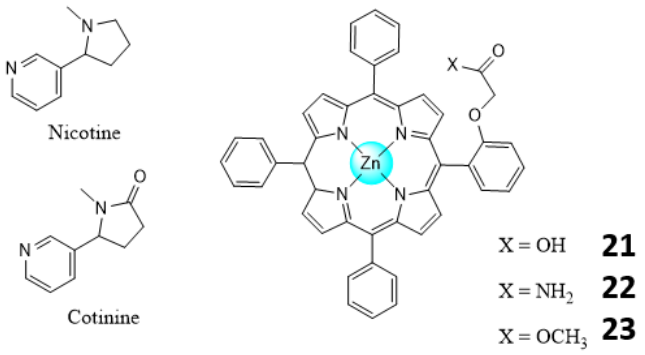

Figure 16. Schematic representation of metalloporphyrin chemosensors **21**-**23** for nicotine and cotinine dinitrogen alkaloids sensing.

1.2.1.2. "Displacement" approach.

Displacement assays have also been widely used to develop chromo-fluorogenic chemosensors since the pioneering work of authors such as Anslyn[48] and Fabbrizzi,[49] who were inspired in displacement reactions in immunoassay protocols.

Like in the previous approach, in the displacement assays also a binding site (receptor) and a signalling subunit (indicator group) is used but in this case, they are not covalently anchored but form a coordination ensemble. A clear advantage of this paradigm is that it allows testing a large number of binding site/signalling subunit combinations in order to obtain tuned sensing probes.

[48] Metzger, A. and Anslyn, E. V. *Angew. Chem., Int. Ed.,* **1998**, 37, 649–652; Niikura, K.; Metzger, A. and Anslyn, E. V. *J. Am. Chem. Soc.,* **1998**, 120, 8533–8534; Ait-Haddou, H.; Wiskur, S. L.; Lynch, V. M. and Anslyn, E. V. *J. Am. Chem. Soc*., **2001**, 123, 11296–11297; Wiskur, S. L. and Anslyn, E. V. *J. Am. Chem. Soc*., **2001**, 123, 10109–10110; Zong, Z. and Anslyn, E. V. *J. Am. Chem. Soc*., **2002**, 124, 9014–9015; Lavigne, J. J. and Anslyn, E. V. *Angew. Chem., Int. Ed*., **1999**, 38, 3666–3669; Wiskur, S. L.; Floriano, P. N.; Anslyn, E. V. and McDevitt, J. T. *Angew. Chem., Int. Ed*., **2003**, 42, 2070–2072.

[49] Fabbrizzi, L.; Marcotte, N.; Stomeo, F. and Taglietti, A. *Angew. Chem., Int. Ed*., **2002**, 41, 3811–3814; Hortala, M. A.; Fabbrizzi, L.; Marcotte, N.; Stomeo, F. and Taglietti, A. *J. Am. Chem. Soc*., **2003**, 125, 20–21; Fabbrizzi, L.; Leone, A. and Taglietti, *A. Angew. Chem., Int. Ed*., **2001**, 40, 3066–3069.

Traditionally in this paradigm, the receptor forms an inclusion complex with a select indicator molecule, such as a dye or a fluorophore, and upon addition of the target analyte, for which the receptor has a high affinity, a displacement reaction occurs; i.e. the receptor binds to the analyte and releases the indicator group to the medium. The difference in optical properties between the free indicator and the complexed indicator leads to the detection of the corresponding analyte.

An advantage of this approach is that most of the designed ensembles usually display sensing features in water or organic–aqueous mixed solutions allowing the design of realistic sensing protocols.

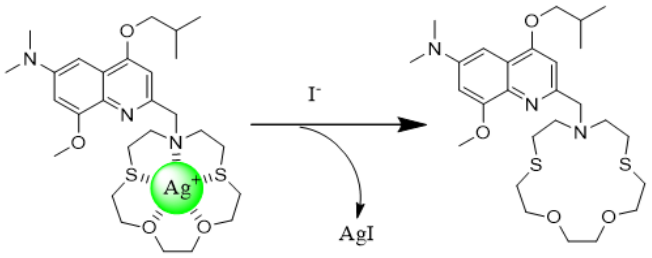

24

Figure 17. Schematic representation of a displacement assay using **24** metal complex for I^- sensing.

As an example, Jiang et al. developed a displacement assay for the fluorimetric sensing of I^- anion in water (Figure 17).[50] In this case, upon addition of I^- anion to probe **24**, a selective release of the Ag^+ cation from the metal complex was observed, due to the formation of highly insoluble AgI. The significative change on maximum emission, from 481 to 565 nm upon excitation at 405 nm, was used as optical output.

[50] Wang, H.; Xue L.; and Jiang, H. *Org. Lett*., **2011**, 13, 3844–3847.

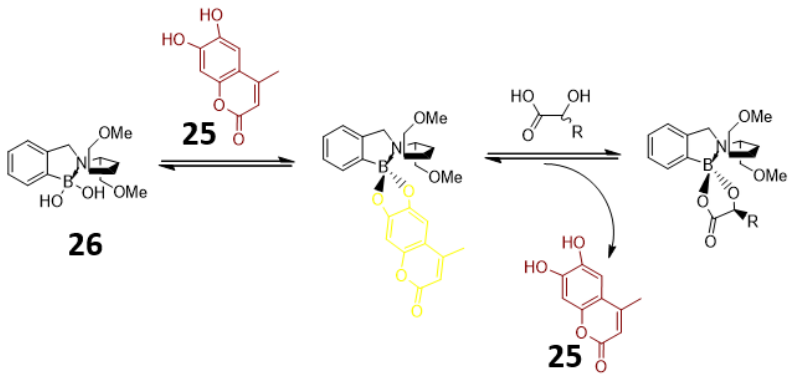

Figure 18. Enantioselective displacement assays for the fluorescent indicator 4-methylesculetin **25**.

In another example, Anslyn and co-workers took advantage of enantioselective association events between boronic acid receptor **26** and bifunctional substrates such as (R)-hydroxycarboxylates and vicinal diols **25** to develop enantioselective colorimetric and fluorescent indicators by displacement assays (Figure 18).[51] Large fluorescence intensity enhancement and a colour change from brown to yellow were observed in solutions of indicator **25** upon reversible binding with the receptor **26**. Upon addition of hydroxycarboxylates a displacement of indicator **25** occurred and a return to the original color and fluorescence of the free indicator was observed.

1.2.1.3. "Chemodosimeter" paradigm.

The chemodosimeter paradigm is an approach that takes advantage of classical reactions, usually irreversible, that result in an optical modulation, such as change in fluorescence or in colour.

[51] Zhu, L.; Zhong, Z. L. and Anslyn, E. V. *J. Am. Chem. Soc.,* **2005**, 127, 4260 –4269; Zhu, L. and Anslyn, E. V. *J. Am. Chem. Soc.*, **2004**, 126, 3676 –3677.

Even though, this approach was marginal some years ago, today it is a well-established procedure for the design of optical chemosensor and probably is the approach that has been growing more in number of examples in the last years, especially for the chromo-fluorogenic recognition of anions and neutral molecules.

One major advantage of this approach is that the structural chemical modification of the chemosensor, when reacts with a target analyte, is accumulative, is typically associated with remarkable spectroscopic modulations and the probes are usually highly selective.

The design of new chemodosimeters involves the finding of quich selective reactions preferably in water or in mixed organic–aqueous solutions. In most cases, the probes take advantage of the nucleophilic attack of target species to electron deficient functional groups that results in a re-organization of the electron density in the whole molecule and optical modulation.

As an example, a ratiometric fluorescent CN^- probe was developed by W. Guo et al., based on the hybrid coumarin–hemicyanine dye **27**.[52] In this case, the CN^- nucleophilic attack to the indolium group resulted in an interruption of the π-conjugation, which blocked the ICT process and quenched the emission at 630 nm whereas an increase in the emission of the coumarin moiety at 514 nm was also observed. Aditionally, a remarkable colour change from purple to pale yellow was found due to a decrease of the absorption at 434 nm together the appearance of a new band at 415 nm (Figure 19).

[52] Lv, X.; Liu, J.; Liu, Y.; Zhao, Y.; Sun, Y.-Q.; Wang, P. and Guo, W. *Chem. Commun.,* **2011,** *47* (48), 12843-12845.

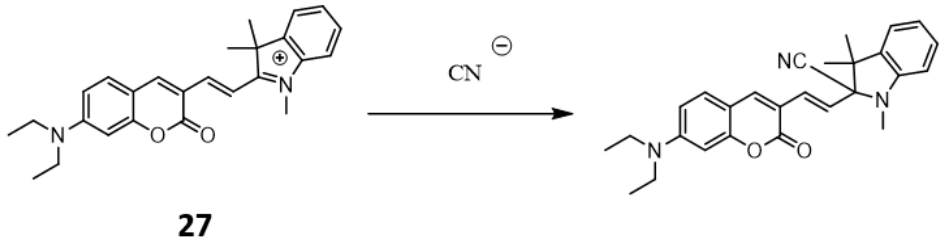

27

Figure 19. Chemical reaction of probe **27** with CN^-.

Another example of chemodosimeter was presented by J. Tae, et al.[53] In this work, a thiosemicarbazide moiety of a rhodamine-based probe (**28**) underwent an irreversible Hg^{2+} promoted cyclization to form a 1,3,4-oxadiazole in water-methanol (4:1 v/v), causing the opening of the spirocyclic form of rhodamine (Figure 20). An instantaneous development of a pink color and an increase of a strong yellow fluorescence centered at 556 nm was associated with the chemical reaction and used as optical output.

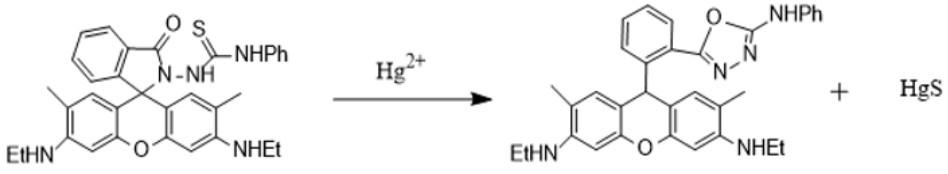

28

Figure 20. Chemical reaction of probe **28** with Hg^{2+}.

[53] Yang, Y.-K.; Yook, K.-J.; Tae, J., *J. Am. Chem. Soc.,* **2005**, 127, 16760-16761.

1.2.2. Optical signaling mechanisms.

One of the most important aspects in optical chemosensors design is the choice of the optical signaling mechanism, i. e. the mechanism whereby the molecular recognition is transduced in a measurable optical signal. In this respect, the first step is the choice of an optical reporter (a chromophore or a fluorophore) according with its properties such as light-absorbing behavior, stability, reactivity, etc. Moreover the binding site and the optical reporter should be structurally integrated as much as possible in order to maximize their communication and the optical effects observed upon guest binding. Furthermore, it should be taken into account that sometimes the integration of an optical reporter into a molecular receptor can modify the optical properties of the chromophore or fluorophore used. For instancet the latter effect is directly utilized in the design of probes based in the displacement approach.

Additionally, there is an important distinction between the guest binding effects on chromophores and fluorophores. While the chromophores display useful absorbance effects generally as result from changes in the molecular structure, including proton transfer, charge transfer, and isomerization, the effects exhibited by the fluorophores are much more sensitive to subtle changes in the geometry and electronic structure of the ground state, as well as the electronic excited state. Moreover only the fluorophores are responsive to physical processes affecting depopulation of the emissive excited state, such as conformational restriction occurring upon analyte complexation (Table 1).

Table 1: Main optical signaling mechanisms reported to molecular sensing by chromogenic and fluorogenic chemosensors

Optical signaling mechanisms	Optical chemosensors	
	Chromogenic	**Fluorogenic**
Irreversible reaction-based	X	X
Tautomerism	X	X
Skeletal isomerism	X	X
Proton transfer (PT)	X	X
Charge tranfer (CT)	X	X
Photoinduced charge transfer (PCT)	X	X
Fluorescence resonance energy transfer (FRET)		X
Photoinduced electron transfer (PET)		X
Excimer or exciplex formation		X
Quenching by guest		X

Studies on optical signaling mechanisms are nowadays a fertile field to study, and even today, the mechanism of many known probes is not yet well understood. As it can be seen on Table 1, among different optical signaling mechanisms operative in chemosensors, only some structural mechanisms are available in chromogenic chemsensors, which somehow limits their design when compared with the large number of photophysical processes than can be used to design fluorogenic probes.[54] These optical signaling mechanisms are discussed below.

1.2.2.1. Irreversible reaction-based.

As already mentioned, the reaction-based mechanism is the fundation of the chemodosimeter paradigm. In this case, optical signaling is promoted by an irreversible chemical reaction and the formation of new compounds is the cause

[54] Bell, T. W.; Hext, N. M. *Chem. Soc. Rev.,* **2004**, 33, 589-598

of variation of optical properties (colour of fluorescent changes). Many chemical irreversible reactions have been used to prepare a number of chromogenic, fluorogenic or chromo-fluorogenic chemosensors. As an example, Lu et al. reported a chemodosimeter for F^- anion based in an irreversible elimination reaction of the trimethylsilyl (TMS) substituents in the pyrene derivative probe **29**.[55] The strong interaction between the F^- anion and the silicon atoms with subsequent elimination of the four TMS moieties caused a noticeable colour change from light green to colourless and an emission change from blue to purple on solutions of **29** in THF (Figure 21).

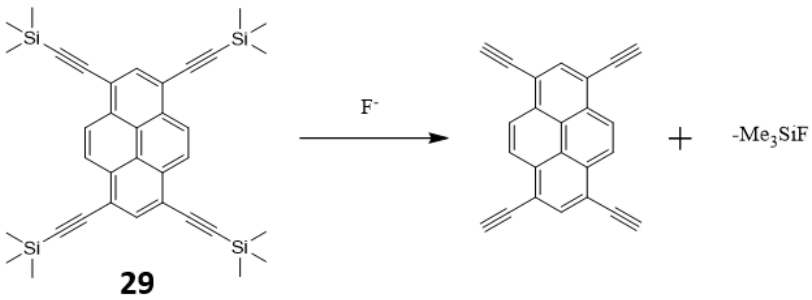

Figure 21. Chemical reaction of the pyrene derivative **29** with the F^- anion.

1.2.2.2. Tautomerism.

In this mechanism, the migration of a hydrogen atom or proton and a switch of a single bond and adjacent double bond causes the modulation of the optical signal. This very fast interconversion between constitutional isomers or tautomerization has been used in molecular recognition of some compounds and in some biorecognition processes suc as RNA-DNA pair recognition.[56] As example of optical chemosensor based in this mechanism, Elango and co-workers reported

[55] Lu, H.; Wang, Q.; Li, Z.; Lai, G.; Jiang, J. and Shen, Z. *Org. Biomol. Chem*., **2011**, 9, 4558–4562.

[56] Douhal, A.; Kim, S. K. and Zewail, A. H. *Nature* **1995**, 378, 260 - 263

the use of an azo-hydrazone tautomerism to colorimetrically sense fluoride.[57] Addition of F^- anion induced a change in probes **30** and **31** from C=N (hydrazone form) to N=N (azo form) which resulted in a visible color change from yellow to red and a significant quenching of emission intensity (Figure 22).

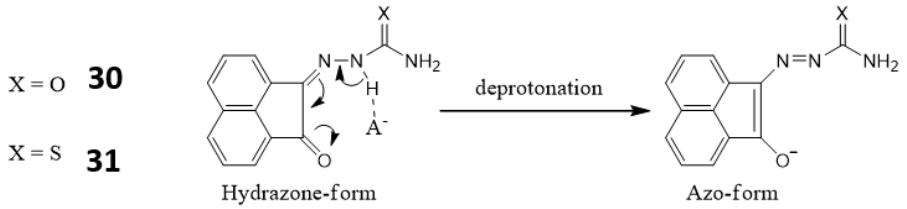

Figure 22. Fluoride sensing by tautomerization process of **30** and **31** chemosensors.

1.2.2.3. Skeletal isomerism.

The reorganization between regioisomers has also been used to optically sense certain analytes. For example, the transformation between distortional supramolecular isomers (**32** and **33**) of polyrotaxanes was used to sense nitro derivatives by S. S. Lee and J. J. Vittal and co-workers.[58] Both supramolecular isomers, the polyrotaxanes **32** and **33**, exhibited a blue emission in the region 458–473 nm when excited at 360 nm. However, in the presence of 2,4-dinitrophenylhydrazine, the isomers exhibit different photochemical reactivity and different sensing efficiencies to emission quenching. Upon addition of 2,4-dinitrophenylhydrazine, **32** showed a larger quenching of fluorescence (up to about one twenty-third of its initial intensity) as compared to **33** (which only displayed up to one sixth of fluorescence quenching). The difference in response

[57] Satheshkumar, A.; El-Mossalamy, E.H.; Manivannan, R.; Parthiban, C.; Al-Harbi, L. M.; Kosa, S.; Elango, K. P. *Spectrochim. Acta A* **2014**, 128, 798–805.

[58] Park, I. H.; Medishetty, R.; Kim, J. Y.; Lee, S. S. and Vittal, J. J. *Angew. Chem. Int. Ed.,* **2014**, 53, 5591 –5595.

between both supramolecular isomers was ascribed to the different alignments of the rotaxanes units (Figure 23).

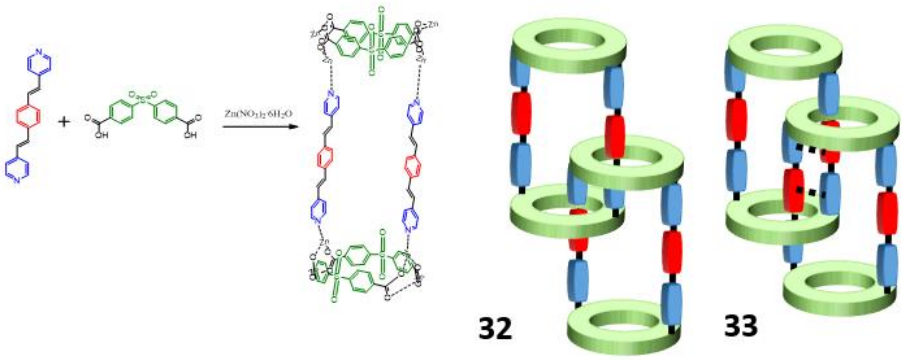

Figure 23. Structural representation of supramolecular isomers of polyrotaxanes **32** and **33**. Left: scheme of general preparation of polyrotaxanes. Right: representation of the alignments of the rotaxanes units in **32** and **33**.

1.2.2.4. Proton transfer (PT).

Proton transfer is another mechanism widely utilized in the design of chromo-fluorogenic probes. Different proton transfer processes, from the simple use of an acid-base protonation to a Grotthuss mechanism can be used to modulate the optical signal in some chromofluorgenic chemosensors. As an example, Kim and Helal reported the thiazole-based chemosensors **34** and **35** for the selective fluorogenic sensing of AcO^- over several another anions, based on an inhibition of an excited-state intramolecular proton transfer (ESIPT) process.[59]

In this case, excitation at 339 nm of acetonitrile solutions of **34** induced an ESIPT process and a dual emission with two bands at 389 (normal emission) and 556 nm (tautomer emission) was observed. Addition of AcO^- induced the

[59] Helal, A. and Kim, H. S., *Tetrahedron*, **2010**, 66, 7097–7103.

formation of 1:1 hydrogen-bonding complexes that resulted in a significant quenching of the tautomer fluorescence and a growth of a new emission at 479 nm. A similar behavior was shown by receptor **35** (Figure 24).

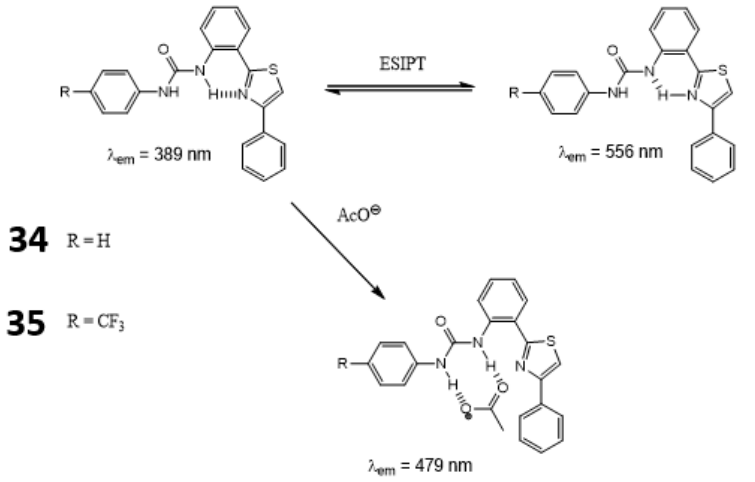

Figure 24. Chemical structures and coordination mode of thiazole-based receptors **34** and **35** with AcO^- anion upon deactivation of ESIPT process.

1.2.2.5. Charge tranfer (CT).

In a CT transition a fraction of electronic charge is transferred between a system of conjugated bonds from an electron donor group to a electron acceptor unit. The energy difference between the HOMO and the LUMO of these two groups is the cause of the appearance an absorption band. This HOMO-LUMO difference, and therefore the colour of the probe, can be modulated by the presence of electron-donor or electron-acceptor groups in the molecule. Moreover, from a sensing point of view, the strength of the electron donor or the electron acceptor groups can be easily altered by coordination with target guests. As an example if the target analyte (**T**) is a cation, its interaction with acceptor group (**A**) is expected to induce an increase in the electronic conjugation of the system that results in a red-shift (bathochromic effect) whereas if the interaction

occurs with a donor group (**D**) a blue-shift (hypsochromic effect) occurs (Figure 25).

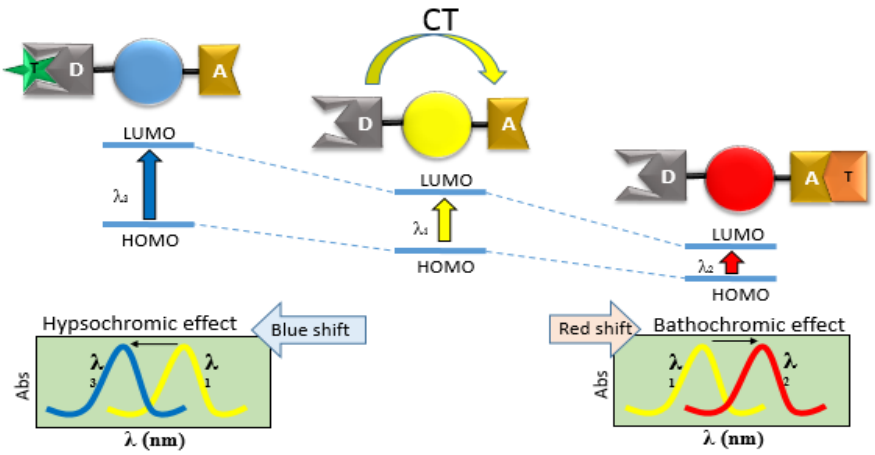

Figure 25. Spectral shifts caused by charge transfer (CT) interaction of a target analyte (**T**) with an electron-donating moiety (**D**) or an electron-withdrawing group (**A**) of the chemosensor.

Depending on the relative position and nature of the donor-aceptor pair, charge transfer probes can be classified depending on the nature of the CT and probes based in the use of metal-to-ligand charge transfer (MLCT),[60] twisted internal charge transfer (TICT),[61] internal charge transfer (ICT), or charge transfer through the bonds[62] have been reported.

1.2.2.6. Photoinduced charge transfer (PCT).

PCT is a particular partial charge transfer mechanism of a fully conjugated system in which transfer of an electron between an electron donor group (**D**) and an electron withdrawing group (**A**), both integrated into a single molecule, is induced by light excitation. In this context the formation of a complex with target

[60] Vlček Jr, A. *Coord. Chem. Rev.* **1998,** *177* (1), 219-256.

[61] Grabowski, Z. R.; Rotkiewicz, K.; Rettig, W., *Chem. Rev.* **2003,** *103* (10), 3899-4032.

[62] de Silva, A. P.; Gunaratne, H. Q. N.; Gunnlaugsson, T.; Huxley, A. J. M.; McCoy, C. P.; Rademacher J. T. and Rice, T. E. *Chem. Rev*. **1997**, 97, 1515-1566.

species (**T**) gives rise to an alteration of electron energy levels causing variation in emission and absorption wavelengths, which is used for optical signaling in some probes (Figure 26).

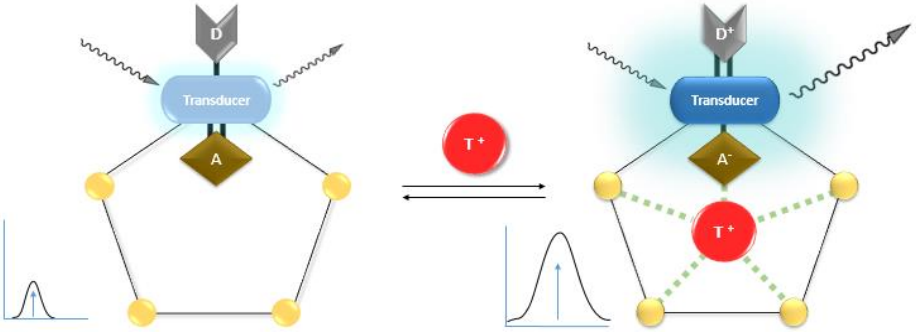

Figure 26. Schematic representation of the increased optical output on photoinduced charge transfer process (PCT) induced by formation of complex with a target specie (**T**).

1.2.2.7. Photoinduced electron transfer (PET).

In a PET mechanism, the excitation of a fluorophore by light induces an electron transfer from HOMO to LUMO that results in an excited state of the fluorophore. This new state, of higher energy content, can be a strong reducing or oxidizing system. In this context when another species able to donate or to accept an electron interacts with the excited fluorophore a deactivation by redox reaction occurs and the emisión is quenched. Coordination of target analytes with the binding site can change this procces resulting in a change in the emission that is used as optical output (Figure 27).

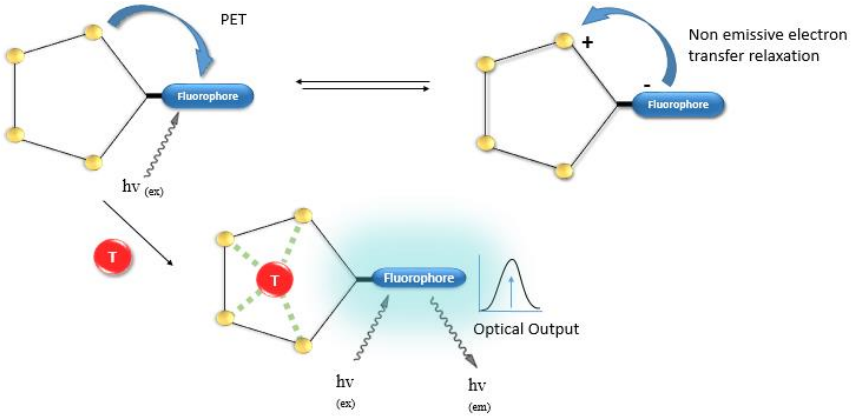

Figure 27. Schematic representation of photoinduced electron transfer process (PET).

1.2.2.8. Fluorescence resonance energy transfer (FRET).

In FRET chemosensor design, normally two fluorophores are joined by a flexible binding-site spacer. The presence of an external target analyte forces the two fluorophores to move close (turn-on FRET) or far (turn-off FRET) each other. When the FRET is turn-on the excitation of a fluorophore is transferred to the second fluorophore and the emission of the latter is shown, else (turn-off FRET) the emission from the electronic excited state of the former is detected (Figure 28).

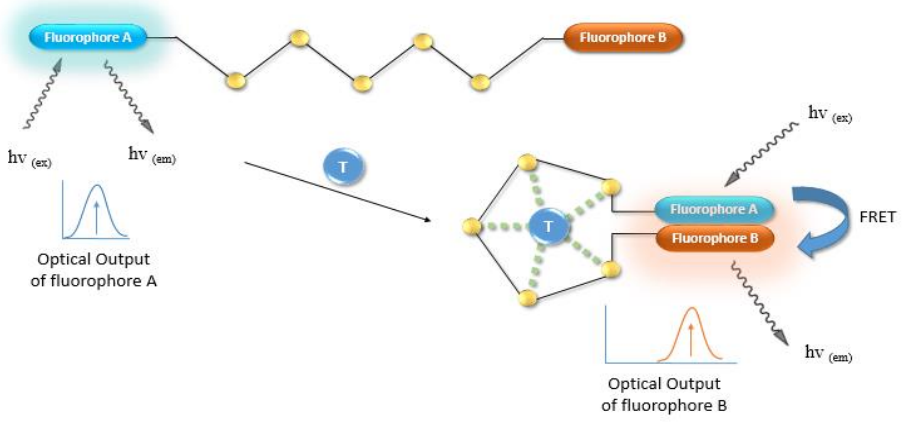

Figure 28. Schematic representation of fluorescence resonance energy transfer (FRET).

1.2.2.9. Excimer or exciplex formation (EF).

As in FRET, the EF process is a distance-dependent interaction between the excited state and the ground-state of two fluorophores. In chemosensor designing by EF, the distance between both fluorophores is modulated by complexation with a second chemical species which can favor or hinder excimer/exciplex formation (Figure 29).

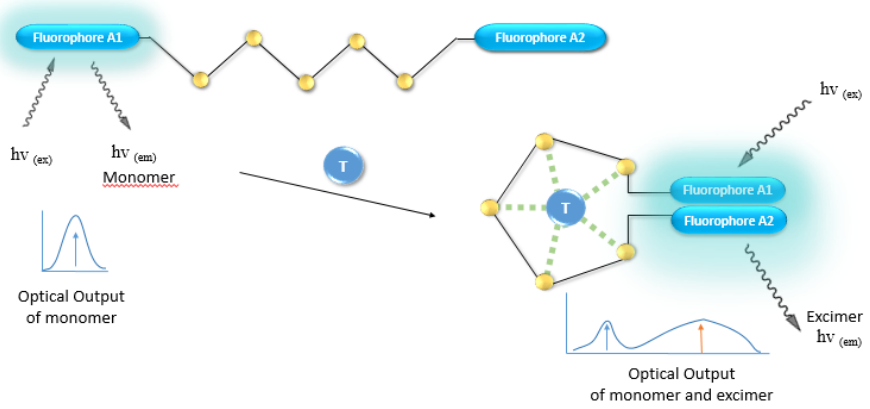

Figure 29. Schematic representation or excimer or exciplex formation.

In addition, the ratio between the emission intensity of the monomer and the excimer can be used to quantitative measures. In this case, "radiometric sensors" could be developed.

1.2.2.10. Quenching by guest.

Several fluorogenic chemosensor take advantage of the formally forbidden intersystem crossing (FF-ISC), namely, the forbidden radiationless transition between two electronic states with different spin multiplicity, to design an optical signaling mechanism. In this case, the presence of a particular atom or molecule (usually a paramagnetic metal) in the proximity of the fluorophore brings the switched-on of FF-ISC and caused a fluorescence quenching.

The most popular case of these systems occur when a probe forms a supramolecular complex with a strongly paramagnetic metals (such as Cu^{2+}, Fe^{3+}, Cr^{3+} or Co^{2+}). In this case the metal complex undergo FF-ISC by excitation and normal radiative transition of the fluorophore from exited state S1 to ground state S0 is replaced by transition from S1 to T1 state (with more energy that S0) which is deactivated by bimolecular non-radiative processes and a remarkable fluorescence quenching is displayed (Figure 30).

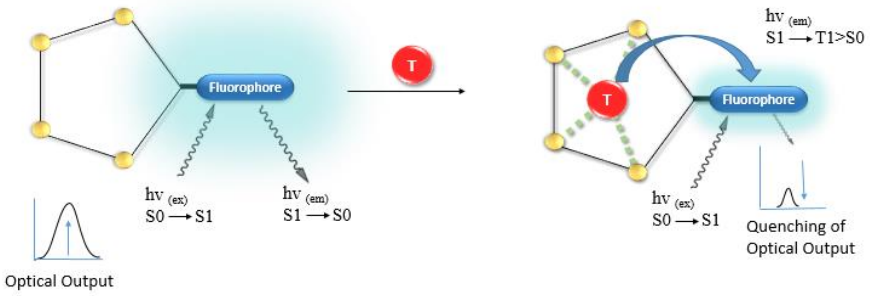

Figure 30. Schematic representation of paramagnetic fluorescence quenching.

The use of logic gates via the use of more than one of the above mechanisms[63] and the design of other more complex mechanisms for instance through the use of intermediate excited state reactions[64] have also been recently reported as optical signaling mechanisms.

It should be noted that, all chromogenic and fluorogenic optical signaling mechanisms can be used to turn-on and turn-off measurable signals depending on the approach used and whether the analyte is who directly causes the activation or deactivation of the optical signaling mechanism. Further, in some cases, when

[63] De Silva, A. P.; Fox, D. B.; Moody, T. S. and Weir, S. M. *Pure Appl. Chem.,* **2001**, 73, 503–511.
[64] Valeur, B. and Leray, I. *Coord. Chem. Rev.,* **2000**, 205, 3–40.

more than one signal is measurable, the modulation of several signals or radiometric measurements is also used as quantitative optical output.

In addition, chromo-fluorogenic chemosensors also offer the ability to report both colour and emission changes as optical signalling by one or several different mechanism. These features are highly desirable in the preparation of chemosensors and also for their application in real measurements.

Chapter 2:
Optical Chemosensors for Cations

2. OPTICAL CHEMOSENSORS FOR CATIONS

2.1. About this chapter

This chapter is focused on the study of optical chemical sensors for cations recognition. Their main purpose is to shown the experimental results obtained with the development of a new chromo-fluorogenic chemosensor for selective detection of trivalent cations.

Previously to the presentation of experimental results, an introduction to the theorical and experimental considerations into design of optical chemical sensors for cations is presented to the reader. The purpose is provide a concise overview of the context on which the research project has been developed and establish the foundations that have inspired the design of this new chemical detection system.

2.2. Preliminary discussion

As previously mentioned in Chapter 1, one of the first areas in which the concepts of supramolecular chemistry was applied consisted in the study and preparation of receptors for cation recognition (see section 1.1 into this PhD thesis). In fact, the cation sensing is nowadays a well-established field into supramolecular chemistry.

Based in the first crown ethers and cryptands cation receptors preparated in sixties decade of the past century, many efforts has been dedicated to the synthesis of new cation receptors, specially for metal cations of group I and II and for non metalic cations such as amonium.[1] Recently the enantiospecific binding of

[1] Veale, E. B.; Gunnlaugsson, T., *Annu. Rep. Prog. Chem., Sect. B: Org. Chem*., **2010**,106, 376-406.

chiral species such as protonated amino acids also has been studied and some molecular probes to selective sensing of these biospecies has been reported.[2] In addition, a special emphasis on the sensing of transition metal ions has become of greater interest in last decade due to better understanding of their biological roles, their use in modern industry as well as their recently environmental regulation in several countries.

2.3. Theorical considerations

The classic cation receptors have been prepared based primarily on the forming of metal coordination complexes.[3] In this respect, the most popular receptors are the crown ethers, podands, lariat ethers, cryptands and spherands. All clasic receptors present cavities with hard atoms such as oxygen, nitrogen or sulfur which act as binding site to cations.

The shape and size of the cavities formed by binding atoms in these receptors are designed to encapsulate specific complementary cations. Thus, the selectivity of these clasic receptors for cations is mainly subject to the size complementarity between the cavity and the target cation. Besides, other general consideration such as electrostatic charge, solvent polarity, solvation energies, preorganization of the receptor, chelate ring size, nature of the counter-anion and binding kinetic should be considered into receptor design.

Currently, cation chemosensors based on the three approaches presented in chapter one have been reported, using one or more of the optical signaling mechanisms that have been previously discussed (see section 2).

[2] Qian, X.; Xiao, Y.; Xu, Y.; Guo, X.; Qian, J.; Zhu, W., *Chem. Commun.* **2010,** *46*, 6418-6436.
[3] Liu, Z.; He, W.; Guo, Z., *Chem. Soc. Rev.* **2013**, 42, 1568-1600.

The majority of the chemosensors reported have been designed to contain a molecular structure with one or more signal subunits linked by a spacer to a specific cation receptor. According to what has been mentioned in chapter 1 (section 1.2.2), the use of a spacer between binding site and the signaling subunit in chemosensors can be unfavorable for chromogenic changes, but may simultaneously promote fluorogenic changes, due to an improvement in the electronic conjugation of the probe.

Open chain or macrocyclic receptor topologies of chemosensor for cations sensing are normally based on arrays of electron-donor functions of known coordination groups such as polyamines, polyethers, polysulfides, carboxylic acids or hydroxamic acids.[4]

Due to special interest in the development of chemosensor for biological and environmental relevant cations, such as monovalent Na^+, K^+, Li^+ divalent Zn^{2+}, Ca^{2+} and Mg^{2+} and trivalent metal cations Fe^{3+}, Cr^{3+} and Al^{3+}, as well as heavy metal and other non metal cations, a high amount of fluorogenic and chromogenic chemosensors has been prepared.[5]

In general, the cation interaction with a fluorogenic chemosensor could cause an enhancement of the fluorescence emission, also called chelation enhanced fluorescence effect (CHEF) or a quenching of the fluorescence know as chelation enhancement quenching effect (CHEQ). Both CHEF and CHEQ effects can be coupled with a red or blue shift of the emission band, similarly to chromogenic changes discussed in the section 1.2.2.5. This interaction and emission changes are especially useful in cation recognition on cellular media.

[4] Giorgi, L. and Micheloni, M. *Coord. Chem. Rev*., **2012**, 256, 170-192.

[5] Albelda, M. T.; Frias, J. C.; Garcia-Espana, E.; Schneider, H.-J., *Chem. Soc. Rev.* **2012**, 41, 3859-3877.

2.4. Cation chemosensor by binding site-signaling subunit approach

2.4.1. Experimental objectives

Taking into account the growing current interest in the development of chemosensors to biorelevant cations, the small quantity of described probes for simultaneous detection of trivalent cations and our interest in the development of new chromo-fluorogenic systems; we decided to prepare a new optical chemosensor cable of a selective trivalent cations recognition.

In particular our main aims in this project were:

- Design and synthesize a new chemosensor for selective and sensitive trivalent cation recognition, based on the binding site-signaling subunit approach.

- Characterize the new probe by standard methods (NMR, HRMS, IR, UV/Vis and emission spectroscopy).

- Evaluate the sensibility and selectivity of the synthesized probe toward trivalent cations recognition.

2.4.2. Chemosensor design

During the design phase, emphasis was given to the search for a selective response to trivalent cations over common interferents. A "binding site-signaling subunit" approach was selected for the chemosensor design by their versatility and major control of selectivity. In addition, two potential binding units were included in the chemosensor design, one for anion coordination and other to interact with cations, to discriminate among the anions and cations responses.

Moreover, a dual optical response with both chromogenic and fluorogenic output signals was also searched. Thus, a strong electronic conjugation in the molecular structure and donor/acceptor moieties were used to favor internal charge transfer character. Finally, biocompatibility was promoted with the use of a chalcone derivative body. The chalcones are one of the major classes of natural products with a stable electronic conjugation containing two aromatic rings with an unsaturated chain. Furthermore, several chalcone derivatives have been recently evaluated into biomedical and farmacological studies with very good cell compatibiliy.[1]

2.4.3. A chalcone-based probe for the highly selective and sensitive chromo-fluorogenic sensing of trivalent metal cations

Below, the study and preparation of a new chalcone-containing probe for the chromo-fluorogenic sensing of Al^{3+}, Fe^{3+} and Cr^{3+} over mono and divalent cations and several anions, with a remarkable limit of detection about nM range is presented (Figure 31).

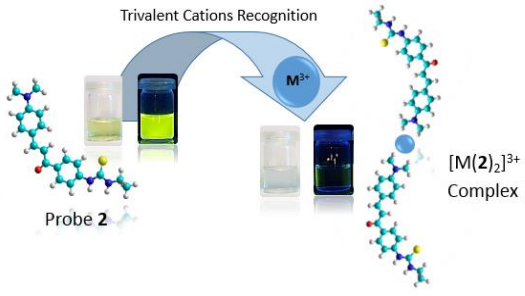

Figure 31. Schematic representation of a new chemosensor for trivalent cations recognition (front cover of publised communication)

[1] El Sayed Aly, M. R.; Abd El Razek Fodah, H. H.; Saleh, S. Y., *Eu. J. Med. Chem.* **2014**, 76, 517-530; Neves, M. P.; Cravo, S.; Lima, R. T.; Vasconcelos, M. H.; Nascimento, M. S. J.; Silva, A. M. S.; Pinto, M.; Cidade, H.; Corrêa, A. G., *Bioorg. Med. Chem.* **2012**, 20, 25-33.

A chalcone-based probe for the highly selective and sensitive chromo-fluorogenic sensing of trivalent metal cations

Luis E. Santos-Figueroa,[abc] Antonio Llopis-Lorente,[abc] Santiago Royo,[abc] Félix Sancenón,[abc] Ramón Martínez-Máñez,[abc] Ana M. Costero,[ad]* Salvador Gil[ad] and Margarita Parra[ad]*

[a] *Centro de Reconocimiento Molecular y Desarrollo Tecnológico (IDM), Unidad Mixta Universidad Politécnica de Valencia-Universidad de Valencia, Spain.*

[b] *Departamento de Química, Universidad Politécnica de Valencia, Camino de Vera s/n, 46022, Valencia, Spain.*

[c] *CIBER de Bioingeniería, Biomateriales y Nanomedicina (CIBER-BBN).*

[d] *Departamento de Química Orgánica, Facultad de Ciencias Químicas, Universidad de Valencia, Dr. Moliner 50, Burjassot 46100, Valencia, Spain.*

Chemistry - A European Journal, **2014**, submitted

2.4.3.1. Abstract

A new chalcone-containing probe for the chromo-fluorogenic sensing of Al^{3+}, Fe^{3+} and Cr^{3+} over mono and divalent cations and anions is reported.

2.4.3.2. Introduction

Recently, an increasing interest in the recognition and sensing of transition metal cations has boosted due to the better understanding of their biological and environmental role in several fundamental natural and physiologic process as well as their widespread use in industrial applications and in organic synthesis protocols.[1] Among metal cations, Al^{3+}, Fe^{3+} and Cr^{3+} played crucial roles in biological processes and their detection is a timely topic.

For instance, iron is the most abundant transition metal in cellular systems. More specifically, Fe^{3+} cation is an essential element in the growth and development of living systems as well as in many biochemical processes at the cellular level[2] and its deficiency is associated with several diseases such as anemia, hemochromatosis, diabetes, Parkinson's and dysfunction of all principal human organs such as heart, pancreas, and liver.[3]

On the other hand, aluminum is the third element in earth and the most abundant metallic element. Aluminum is highly used in several commercial applications such as water treatment, food additives, medicines and metallic dispositives. Besides, some studies indicate that abnormal levels of aluminum ions in certain human tissues and cells[4] could induce Alzheimer's[5] and Parkinson's diseases.[6]

Finally, Cr^{3+} cation is one of the most important nutrient in human and animal diet and plays a fundamental role in the metabolism of carbohydrates, proteins, lipids and nucleic acids.[7] The deficiency of Cr^{3+} is associated to the development of

diabetes and some cardiovascular diseases.[8] As for Al^{3+}, an overdose of Cr^{3+} cation could induce serious toxic effects,[9] moreover their use in metal industry has resulted in increased levels of chromium in the environment and today has come to be regarded as a pollution element.[10]

Consequently, trivalent cation detection is now a focus of interest and a timely topic of research. In this context, the development of optical probes able to selectively recognize trivalent cations are highly appealing due to the possibility of using for their detection widely available low-cost instrumentation and also because optical probes offer the possibility to develop simple tests for sensing these target species to the "naked eye".[11] In fact, some selective fluorogenic and chromogenic probes for the detection of Fe^{3+},[12] Al^{3+},[13] and Cr^{3+} [14] cations have been reported recently. However, just a few probes able to recognize simultaneously two[15] or three[16] trivalent cations have been described in the literature. This lack of multiresponsive probes is due, in most of the cases, to the severe interferences caused by mono and divalent metal cations.

Taking into account the above mentioned facts and our interest in the development of new chromo-fluorogenic chemosensors[11a,11b,17] we report herein a new probe able to selectively detect the trivalent metal cations Fe^{3+}, Al^{3+} and Cr^{3+} via remarkable changes in the UV-visible and fluorescence spectra of the probe. Moreover low detection limits, in the nM range when fluorescence was used, were determined.

2.4.3.3. Results and discussion

Probe **2** was readily synthetized by a two steps procedure (see Scheme 1). The first step consisted in the synthesis of thiourea derivative **1** by the reaction of commercially available 4-aminoacetophenone and ethylisothiocyanate. Probe **2** was obtained by an aldol condensation between compound **1** and 4-dimethylaminobenzaldehyde (see Supporting Information for further details).

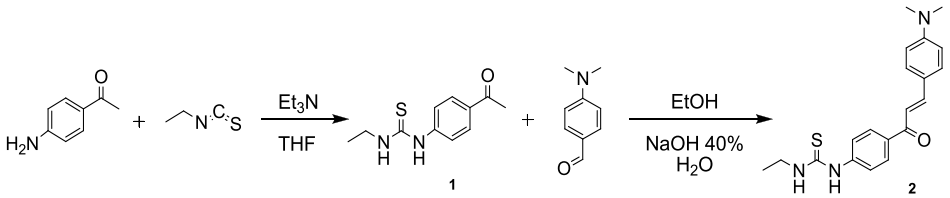

Scheme 1. Synthesis of probe **2**.

Acetonitrile solutions of probe **2** showed (see Figure 1) an absorption band in the visible zone centered at 414 nm (ε = 2.64 x 10^4 M^{-1} cm^{-1}) and two less intense bands in the UV domain at 317 (ε = 1.54 x 10^4 M^{-1} cm^{-1}) and 257 nm (ε = 1.50 x 10^4 M^{-1} cm^{-1}). As a consequence, solutions of **2** showed an intense yellow color. Furthermore, when acetonitrile solutions of **2** were excited at 412 nm a very strong emission band at 538 nm (stokes shift = 5567.23 cm^{-1}) was displayed with a remarkable quantum yield of Φ = 0.63 ± 0.02 (calculated using fluorescein in 0.1M NaOH as standard).[18]

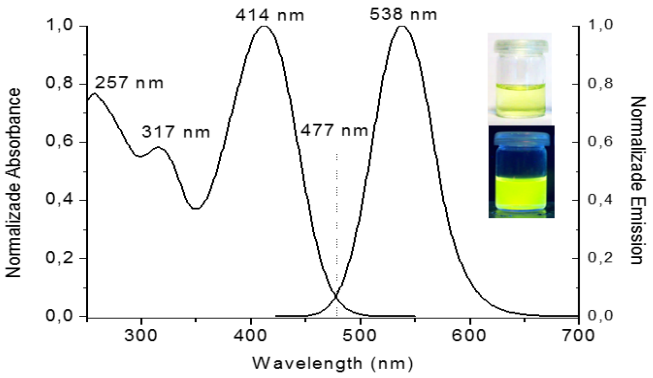

Figure 1. UV-visible and emission (λ_{ex} = 412 nm) spectra of probe **2** in acetonitrile (1.0 x 10^{-5} mol dm^{-3}). Insert: color and fluorescence (under UV lamp, λ_{ex} = 365nm) of acetonitrile solutions of **2** observed to naked eye.

The charge-transfer character of the visible band was assessed by quantum chemical calculations at semi empirical level using the PM3 model (with an RMS gradient of 0.001) using HyperChem software. As seen in Figure 2 the HOMO

orbital was mainly centered in the *N*,*N*-dimethylaniline donor fragment, whereas the LUMO orbital was located in the acceptor phenylthourea moiety.

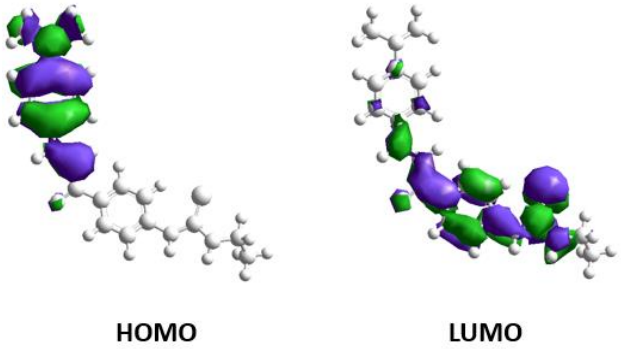

Figure 2. HOMO and LUMO orbitals for probe **2**.

Probe **2** contains, in its structure, two potential binding units, namely the thiourea moiety (for anion coordination) and an aniline donor nitrogen atom (able to interact with cations). Therefore the chromogenic and fluorogenic behavior of acetonitrile solutions of probe **2** were tested in the presence of 10 eq. of selected anions (F^-, Cl^-, Br^-, I^-, OH^-, AcO^-, BzO^-, CN^-, OCN^-, $H_2PO_4^-$ HSO_4^-, and ClO_4^-) and cations (K^+, Li^+, Mg^{2+}, Co^{2+}, Fe^{3+}, Fe^{2+}, Al^{3+}, Hg^{2+}, Cr^{3+}, Pb^{2+}, Cd^{2+}, Ba^{2+}, Ni^{2+}, Zn^{2+}, Ca^{2+}, and Cu^{2+}). The obtained results in the presence of cations are depicted in Figure 3. Of all the anions and cations tested only Al^{3+}, Fe^{3+} and Cr^{3+} induced remarkable and inmmediate color changes. At this respect, the color of acetonitrile solutions of probe **2** changes from yellow to colorless and the strong yellow fluorescence is quenched and substituted with a weakly blue emission. Moreover, and despite the presence of a thiourea moiety in the probe, **2** was unable to display sensing features in the presence of the tested anions (see Supporting Information).

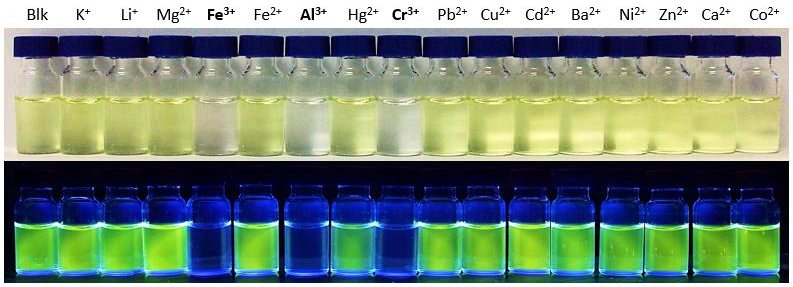

Figure 3. Photograph of color and fluorescence (λ_{ex} = 365 nm) modulation of **2** upon the addition of 10 eq. of selected cations.

Having assessed the highly selective response of **2** toward trivalent metal cations, the sensitivity of the probe was studied by monitoring of UV-visible and emission changes at 25 ^{o}C in acetonitrile solutions upon the addition of increasing quantities of Fe^{3+}, Al^{3+} and Cr^{3+}. The UV-visible and emission profiles obtained in the presence of the three trivalent cations were quite similar and, as an example, the complete set of spectra obtained for probe **2** and Al^{3+} cation are shown in Figure 4. As seen, addition of increasing amounts of Al^{3+} cation induced a progressive decrease of the visible band at 414 nm together with a simultaneous growth of new blue-shifted absorption at 292 nm (ε = 1.39 x 10^4 M^{-1} cm^{-1}) with a clear isosbestic point at 361 nm. The disappearance of the absorption band at 414 nm was the responsible of the yellow-to-colorless color modulation observed (see Figure 3).

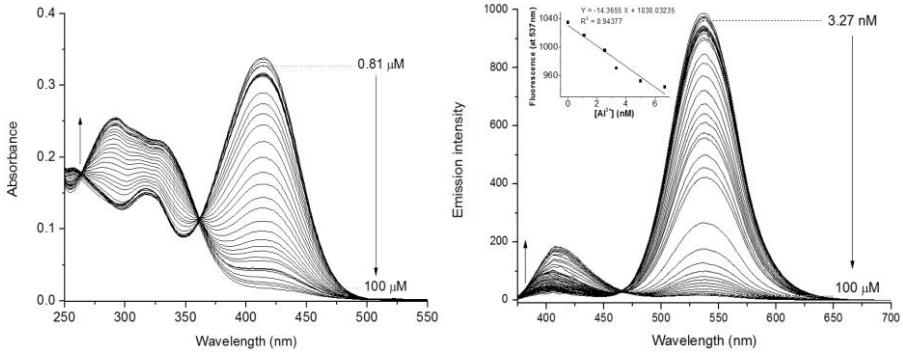

Figure 4. UV-visible (left) and emission (right) profile of the titrations of acetonitrile solution (1.0 x 10-5 mol dm-3) of probe **2** upon addition of increasing quantities of Al^{3+} cation. Insert: fluorescence changes of 537nm emission band into nM range.

On the other hand, upon excitation at the isosbestic point observed in the course of UV-visible titration between **2** and Al^{3+} (λ_{ex} = 361 nm), an intense emission band at 538 m was observed. Addition of increasing amounts of Al^{3+} cation induced a progressive quenching of the fluorescence at 538 nm together with the simultaneous growth of a new blue shifted emission at 406 nm (see Figure 4). The overall result is a remarkable reduction of the quantum yield of probe **2** to 0.070 ± 0.005 in the presence of Al^{3+} cation.

From the UV-visible and fluorescence titrations the limits of detection for probe **2** and Al^{3+}, Fe^{3+} and Cr^{3+} cations were evaluated (see table 1) using the IUPAC Regression Approach (see Supporting Information for details).[19] When changes in the absorption bands were studied the limits of detection were in the μM range whereas when fluorescence was used limits of detection were found to be in the nM range.

Moreover, in order to determine the binding stoichiometry between probe **2** and the trivalent metal cations Job's plots were calculated.[20] As an example Figure 5 shows the Job's plot obtained for Al^{3+} that clearly shows the formation of 2:1 probe-cation complexes. The same stoichiometries were determined for probe **2** with Fe^{3+} and Cr^{3+} cations (data not shown).

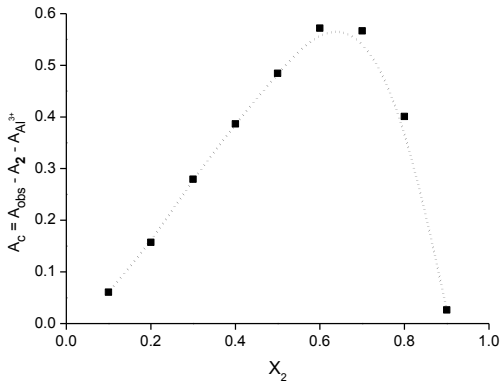

Figure 5. Job's plot for the complexation between probe **2** and Al^{3+} cation determined by UV-visible measurements at 414 nm in acetonitrile solution with [**2**] + [Al^{3+}] = 1x10^{-4} mol dm^{-3}.

Based in the Job's plots information the corresponding stability constants for the formation of $[M(\mathbf{2})_2]^{3+}$ complexes were determined using the HypSpec software (V 1.1.18) and adjusting the data to the equilibrium equation 1:

$$M^{3+} + 2L \rightleftharpoons [M(L)_2]^{3+} \quad (1)$$

The estimated values of log *K* obtained by UV-visible and emission titration profile data are shown in Table 1.

Table 1. Limits of detection and logarithms of binding constants for the interaction of probe **2** with trivalent cations.

Cation	Limit of detection [M^{3+}]		log K[a]	
	UV/Vis (μM)	Emission (nM)	UV/Vis	Emission
Al^{3+}	0.81	3.27	13.10 ± 0.043	12.35 ± 0.039
Fe^{3+}	0.43	2.87	12.79 ± 0.047	12.70 ± 0.034
Cr^{3+}	0.34	2.44	14.02 ± 0.007	15.21 ± 0.071

[a] Log *K* values for the formation of 2:1 probe-metal complexes (eq. 1).

The remarkable hypsochromic shift observed in the visible band in the presence of the metals cations Al^{3+}, Fe^{3+} and Cr^{3+} appears to be indicative of a preferential coordination with the donor part of probe **2**, i.e. the *N*,*N*-dimethylaniline moiety. Moreover the selective response observed is most likely related with the small size and high charge of the trivalent cations. Both characteristics endowed these cations with a strong polarization power that induced changes in the electronic distribution of **2** resulting in remarkable modulations of the UV-visible and fluorescence spectra.

In order to confirm the binding mode of probe **2** with trivalent cations ^{1}H NMR titration studies were carried out with Al^{3+}. The most representative signal of probe **2** in the aliphatic zone was a singlet centered at 3.02 ppm that was ascribed

to the methyl groups linked with the nitrogen atom of the aniline ring (Hj protons in Figure 6). Dealing with the aromatic zone, the most remarkable signals appeared as doublets at 6.76 and 7.63 ppm (Hh and Hd protons of the *N,N*-dimethylaniline 1,4-disubstituted ring) and at 7.54 and 8.04 ppm (He and Ha protons of the 1,4-disubstitute aromatic ring bearing carbonyl and thiourea moieties). Also, two doublets centered at 7.48 and at 7.72 ppm with a coupling constant of 15.4 Hz ascribed to the trans double bond was observed.

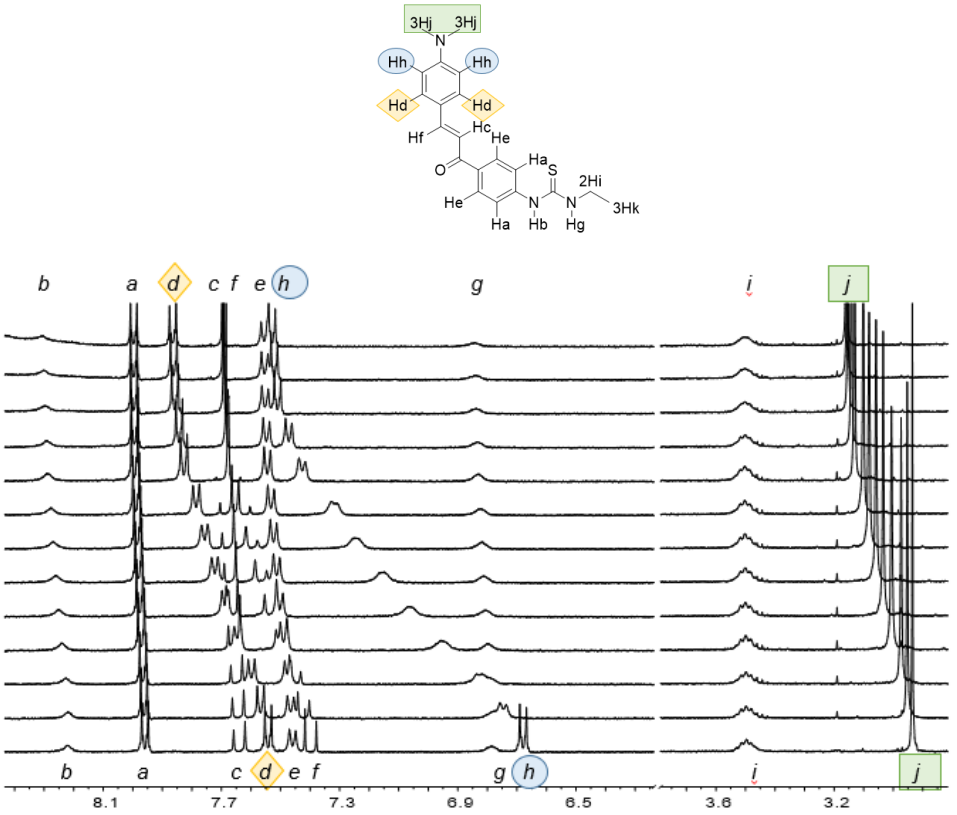

Figure 6. ^{1}H NMR shifts of the protons of probe **2** in the presence of increasing quantities of Al^{3+} in CD_3CN.

As seen in the family of ^{1}H NMR spectra shown in Figure 6, addition of increasing quantities of Al^{3+} to a CD_3CN solution of probe **2** induced remarkable

downfield shifts for Hh, Hd and Hj protons. These protons are located in the *N*,*N*-dimethylaniline ring and pointed toward a coordination of Al^{3+} with the nitrogen donor nitrogen atom located in this fragment of probe **2**. A similar coordination mode is expected for Fe^{3+} and Cr^{3+}.

2.4.3.4. Conclusions

In summary, we report herein a simple chromo-fluorogenic probe with a chalcone-like structure able to selectively detect Al^{3+}, Fe^{3+} and Cr^{3+} over mono and divalent cations and anions. In the presence of trivalent metal cations the probe was able to display a remarkable color change from yellow to colorless clearly visible to the naked eye. Also the initial strong yellow emission was gradually quenched and substituted by a weakly blue shifted band. Moreover the new probe showed remarkable limits of detection in the μM range when UV-visible was used and in the nM order by using fluorescence. The probe displayed a significant selectivity, remarkable low limits of detection and a simple to detect to-naked-eye chromo-fluorogenic response making it suitable for the effective, sensitive, fast and low-cost detection of trivalent cations in organic solvents.

2.4.3.5. Acknowledgements

The authors thank the Spanish Government (project MAT2012-38429-C04-01), and CIBER de Bioingeniería, Biomateriales y Nanomedicina (CIBER-BBN) for their support. The authors are also grateful to Carolina Foundation for doctoral grant to L. E. Santos-Figueroa.

2.4.3.6. References and Notes

Keywords: chromo-fluorogenic sensing • trivalent cations • cation recognition • Al^{3+}, Fe^{3+} and Cr^{3+} recognition • chalcone-based probe

1 J. Burgess, *Chem. Soc. Rev.* **1996**, *25*, 85-92.

2 W. E. Winter, L. A. Bazydlo, N. S. Harris, *Lab. Med.* **2014**, *45*, 92-102.

3 S. von Haehling, S. D. Anker, *Dtsch. Med. Wochenschr.* **2014**, *139*, 841-844.

4 a) V. Rondeau, *Rev. Environ. Health* **2002**, *17*, 107-121; b) K. Cooke, M. H. Gould, *J. R. Soc. Health* **1991**, *111*, 163-168.

5 a) D. Perl, A. Brody, *Science* **1980**, *208*, 297-299; b) G. Belojevic, B. Jakovljevic, *Srp. Arh. Celok. Lek.* **1998**, *126*, 283-289.

6 D. Perl, D. Gajdusek, R. Garruto, R. Yanagihara, C. Gibbs, *Science* **1982**, *217*, 1053-1055.

7 W. Mertz, *J. Nutr.* **1993**, *123*, 626-633.

8 S. Wallach, *J. Am. Coll. Nutr.* **1985**, *4*, 107-120.

9 D. A. Eastmond, J. T. MacGregor, R. S. Slesinski, *Crit. Rev. Toxicol.* **2008**, *38*, 173-190.

10 J. Szczygiel, K. Dyrek, K. Kruczala, E. Bidzinska, Z. Brozek-Mucha, E. Wenda, J. Wieczorek, J. Szymonska, *J. Phys. Chem. B* **2014**, *118*, 7100-7107.

11 a) L. E. Santos-Figueroa, M. E. Moragues, E. Climent, A. Agostini, R. Martinez-Manez, F. Sancenon, *Chem. Soc. Rev.* **2013**, *42*, 3489-3613; b) L. E. Santos-Figueroa, C. de laTorre, S. El Sayed, F. Sancenón, R. Martínez-Máñez, A. M. Costero, S. Gil, M. Parra, *Eur. J. Org. Chem.* **2014**, *2014*, 1848-1854; c) M. Formica, V. Fusi, L. Giorgi, M. Micheloni, *Coord. Chem. Rev.* **2012**, *256*, 170-192; d) Y. Yang, Q. Zhao, W. Feng, F. Li, *Chem. Rev.* **2012**, *113*, 192-270.

12 See for example: a) M. Venkateswarulu, T. Mukherjee, S. Mukherjee, R. R. Koner, *Dalton Trans.* **2014**, *43*, 5269-5273; b) J. Piao, J. Lv, X. Zhou, T. Zhao, X. Wu, *Spectrochim. Acta A* **2014**, *128*, 475-480; c) T.-B. Wei, P. Zhang, B.-B. Shi, P. Chen, Q. Lin, J. Liu, Y.-M. Zhang, *Dyes Pigments* **2013**, *97*, 297-302; d) J. Bordini, I. Calandreli, G. O. Silva, K. Q. Ferreira, D. P. S. Leitão-Mazzi, E. M. Espreafico, E. Tfouni, *Inorg. Chem. Commun.* **2013**, *35*, 255-259; e) M. H. Lee, T. V. Giap, S. H. Kim, Y. H. Lee, C. Kang, J. S. Kim, *Chem. Commun.* **2010**, *46*, 1407-1409.

13 See for examole: a) S. A. Lee, G. R. You, Y. W. Choi, H. Y. Jo, A. R. Kim, I. Noh, S.-J. Kim, Y. Kim, C. Kim, *Dalton Trans.* **2014**, *43*, 6650-6659; b) L. Wang, W. Qin, X. Tang, W. Dou, W. Liu, Q. Teng, X. Yao, *Org. Biomol. Chem.* **2010**, *8*, 3751-3757; c) D. Maity, T. Govindaraju, *Chem. Commun.* **2010**, *46*, 4499-4501; d) T.-H. Ma, M. Dong, Y.-M. Dong, Y.-W. Wang, Y. Peng, *Chem. Eur. J.* **2010**, *16*, 10313-10318.

14 See for example: a) J. P. Metters, R. O. Kadara, C. E. Banks, *Analyst* **2012**, *137*, 896-902; b) Y. Wan, Q. Guo, X. Wang, A. Xia, *Anal. Chim. Acta* **2010**, *665*, 215-220; c) M. G. Basallote, P. V. Bernhardt, T. Calvet, C. E. Castillo, M. Font-Bardia, M. Martinez, C. Rodriguez, *Dalton Trans.* **2009**, 9567-9577.

15 a) M. Wang, J. Wang, W. Xue, A. Wu, *Dyes Pigments* **2013**, *97*, 475-480; b) L. Wang, H. Li, D. Cao, *Sensors Act. B Chem.* **2013**, *181*, 749-755; c) V. Bravo, S. Gil, A. M. Costero, M. N. Kneeteman, U. Llaosa, P. M. E. Mancini, L. E. Ochando, M. Parra, *Tetrahedron* **2012**, *68*, 4882-4887.

16 a) Y. Xu, D. Zhang, B. Li, Y. Zhang, S. Sun, Y. Pang, *RSC Advances* **2014**, *4*, 11634-11639; b) M. Venkateswarulu, S. Sinha, J. Mathew, R. R. Koner, *Tetrahedron Lett.* **2013**, *54*, 4683-4688; c) X. Chen, X. Y. Shen, E. Guan, Y. Liu, A. Qin, J. Z. Sun, B. Z. Tang, *Chem. Commun.* **2013**, *49*, 1503-1505; d) A. Barba-Bon, A. M. Costero, S. Gil, M. Parra, J. Soto, R. Martinez-Manez, F. Sancenon, *Chem. Commun.* **2012**, *48*, 3000-3002.

17 a) L. E. Santos-Figueroa, C. de la Torre, S. El Sayed, F. Sancenón, R. Martínez-Máñez, A. M. Costero, S. Gil, M. Parra, *Eur. J. Inorg. Chem.* **2014**, *2014*, 41-45; b) L. E. Santos-Figueroa, C. Giménez, A. Agostini, E. Aznar, M. D. Marcos, F. Sancenón, R. Martínez-Máñez, P. Amorós, *Angew. Chem. Int. Ed.* **2013**, *52*, 13712-13716 c) S. Elsayed, A. Agostini, L. E. Santos-Figueroa, R. Martínez-Máñez, F. Sancenón, *ChemistryOpen* **2013**, *2*, 58-62; d) S. El Sayed, C. de la Torre, L. E. Santos-Figueroa, E. Perez-Paya, R. Martinez-Manez, F. Sancenon, A. M. Costero, M. Parra,

S. Gil, *RSC Advances* **2013**, *3*, 25690-25693; e) E. Climent, M. D. Marcos, R. Martínez-Máñez, F. Sancenón, J. Soto, K. Rurack, P. Amorós, *Angew. Chem. Int. Ed.* **2009**, *48*, 8519-8522.

18 a) U. Resch-Genger, K. Rurack, *Pure Appl. Chem.* **2013**, *85*, 2005-2026; b) M. Brouwer Albert, *Pure Appl. Chem.* **2011**, *83*, 2213-2228.

19 J. Mocak, A. M. Bond, S. Mitchell, G. Scollary, *Pure Appl. Chem.* **1997**, *69*, 297-328.

20 a) J. S. Renny, L. L. Tomasevich, E. H. Tallmadge, D. B. Collum, *Angew. Chem. Int. Ed.* **2013**, *52*, 11998-12013; b) K. Hirose, *J. Incl. Phenom. Macro. Chem.* **2001**, *39*, 193-209.

2.4.3.7. Supporting Information

A chalcone-based probe for the highly selective and sensitive chromo-fluorogenic sensing of trivalent metal cations

Luís E. Santos-Figueroa, Antonio Llopis-Lorente, Santiago Royo, Félix Sancenón, Ramón Martínez-Máñez, Ana M. Costero,* Salvador Gil and Margarita Parra*

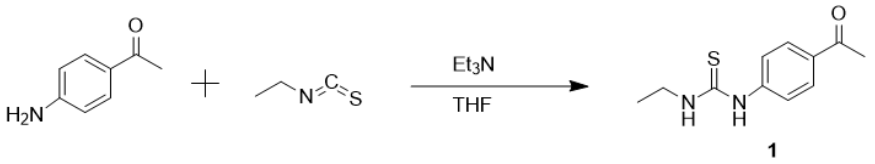

Scheme S-1 Synthesis of compound **1**.

4-aminoacetophenone (1.045 g, 7.73 mmol) was dissolved THF (10 mL) and then ethylisothiocyanate (698 µL, 7.73 mmol) and triethylamine (1.077 mL, 7.33 mmol) were added to the initial solution. The resultant mixture was refluxed for 18h. Afterward, the solvent was removed under reduced pressure and the final solid was diluted with dichloromethane (30 mL), washed with HCl 10% (3 x 20 mL), dried over anhydrous $MgSO_4$ and finally concentrated to yield **1** as a pale yellow solid (1.37 g, 6.16 mmol, 80%). ^{1}H NMR (300 MHz, $CDCl_3$) δ 8.03 (d, *J* = 8.6 Hz, 2H), 7.95 (s, 1H), 7.30 (d, *J* = 8.5 Hz, 2H), 6.26 (s, 1H), 3.75 – 3.61 (m, 2H), 2.60 (s, 3H), 1.24 (t, *J* = 7.3 Hz, 3H). ^{13}C NMR (75 MHz, $CDCl_3$) δ 197.20, 180.43, 141.48, 134.79, 130.78, 123.38, 40.88, 26.97, 14.53. Calc. for $C_{11}H_{14}N_2OS$: 222.0827; Found: 222,0822.

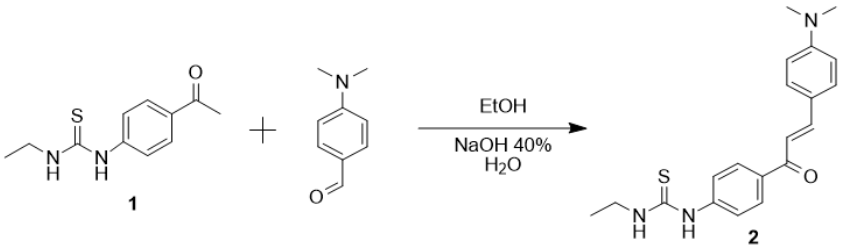

Scheme S-2 Synthesis of probe **2**.

4-(dimethylamino)benzaldehyde (456 mg, 3.06 mmol) and compound **1** (679 mg, 3.06 mmol) were dissolved in ethanol (10 mL). Then, NaOH 40% solution in water-EtOH 4:1 v/v (2 mL) was added and the mixture was stirring at room temperature for 12 h. Afterward, the crude was poured over 100 mL of water. The precipitate was filtered off and dried at 60 ^{o}C. The solid was recrystallized from MeOH to yield probe **2** as red crystals (487 mg, 1.38 mmol, 45%). ^{1}H NMR (400 MHz, $CDCl_3$) δ 8.07 (d, *J* = 8.8 Hz, 2H), 7.81 (d, *J* = 15.4 Hz, 1H), 7.68 (s, 1H), 7.55 (d, *J* = 8.8 Hz, 3H), 7.34 – 7.27 (m, 3H), 6.70 (d, *J* = 8.9 Hz, 2H), 6.18 (s, 1H), 3.76 – 3.66 (m, 2H), 3.05 (s, *J* = 6.2 Hz, 6H), 1.24 (dd, *J* = 9.5, 5.0 Hz, 4H). ^{13}C NMR (101 MHz, $CDCl_3$) δ 189.10 (s), 180.42 (s), 152.38 (s), 146.65 (s), 130.75 (s), 130.58 (s), 123.67 (s), 116.19 (s), 111.97 (s), 40.28 (s), 29.85 (s), 14.32 (s). Calc. for $C_{20}H_{23}N_3OS$: 353.1562; Found: 353.1575.

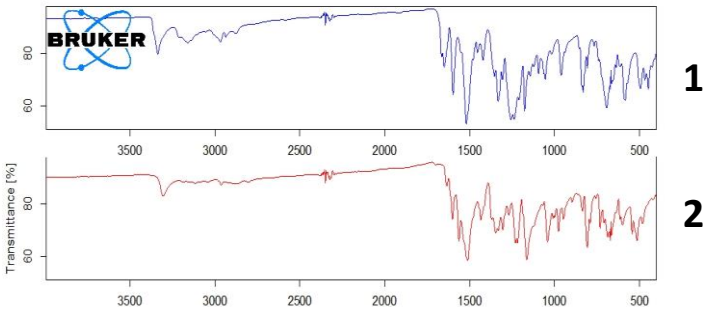

Figure S-1 IR spectra of **1** and **2**.

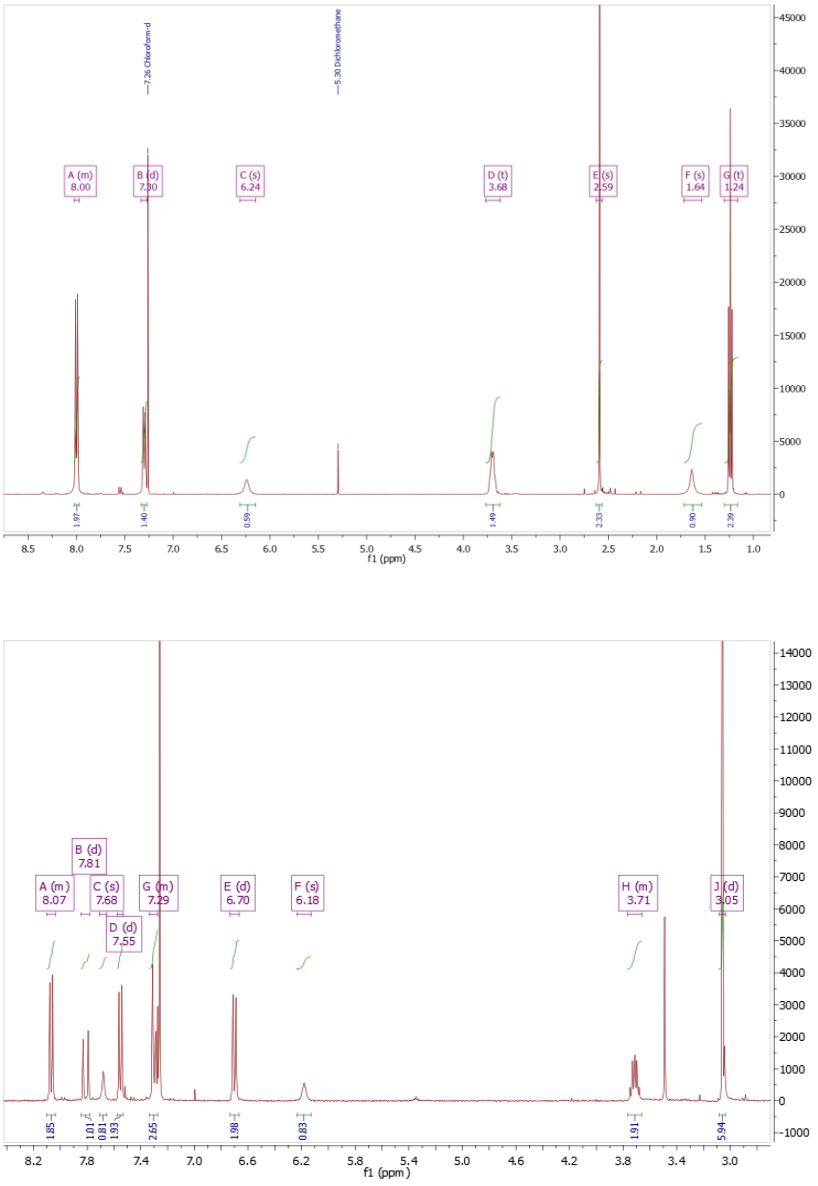

Figure S-2 ^{1}H RMN spectra of probes **1** (up) and **2** (down) in $CDCl_3$.

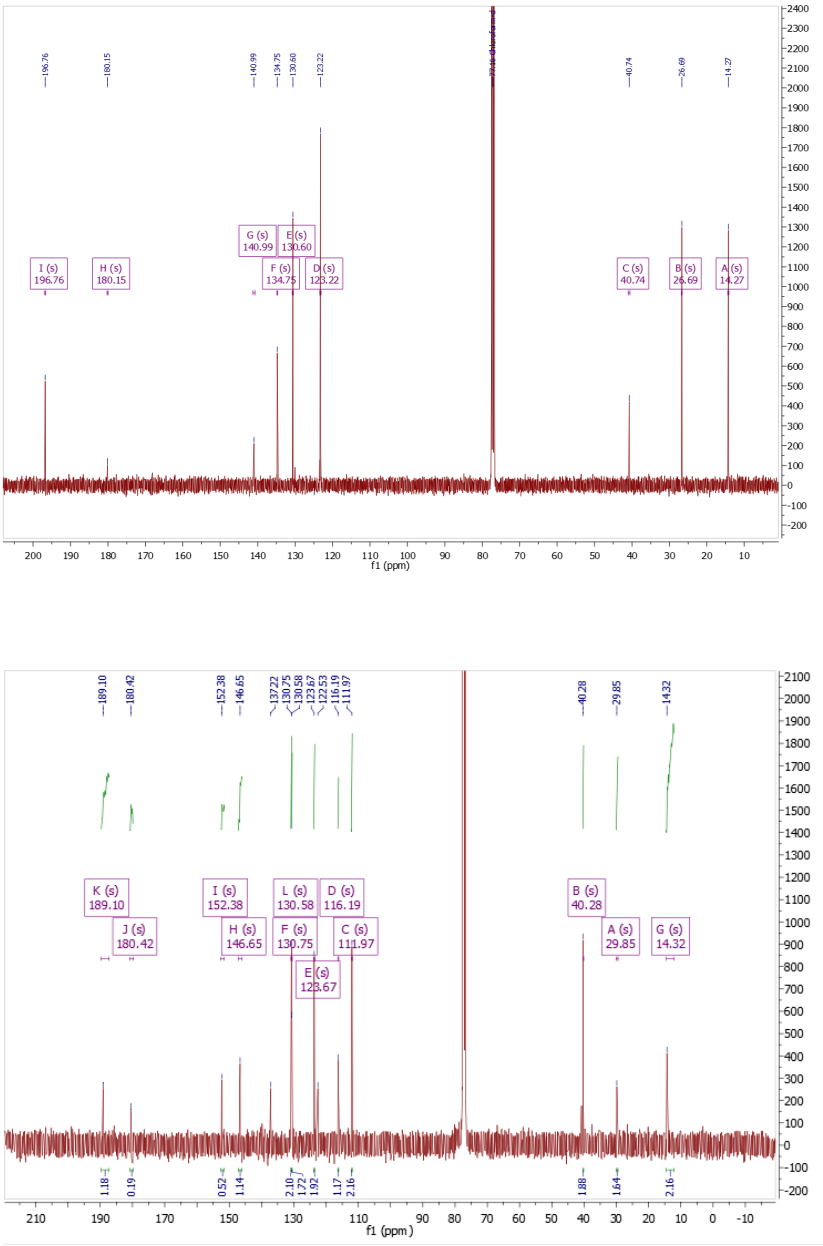

Figure S-3 ^{13}C RMN spectra of probes **1** (up) and **2** (down) in $CDCl_3$.

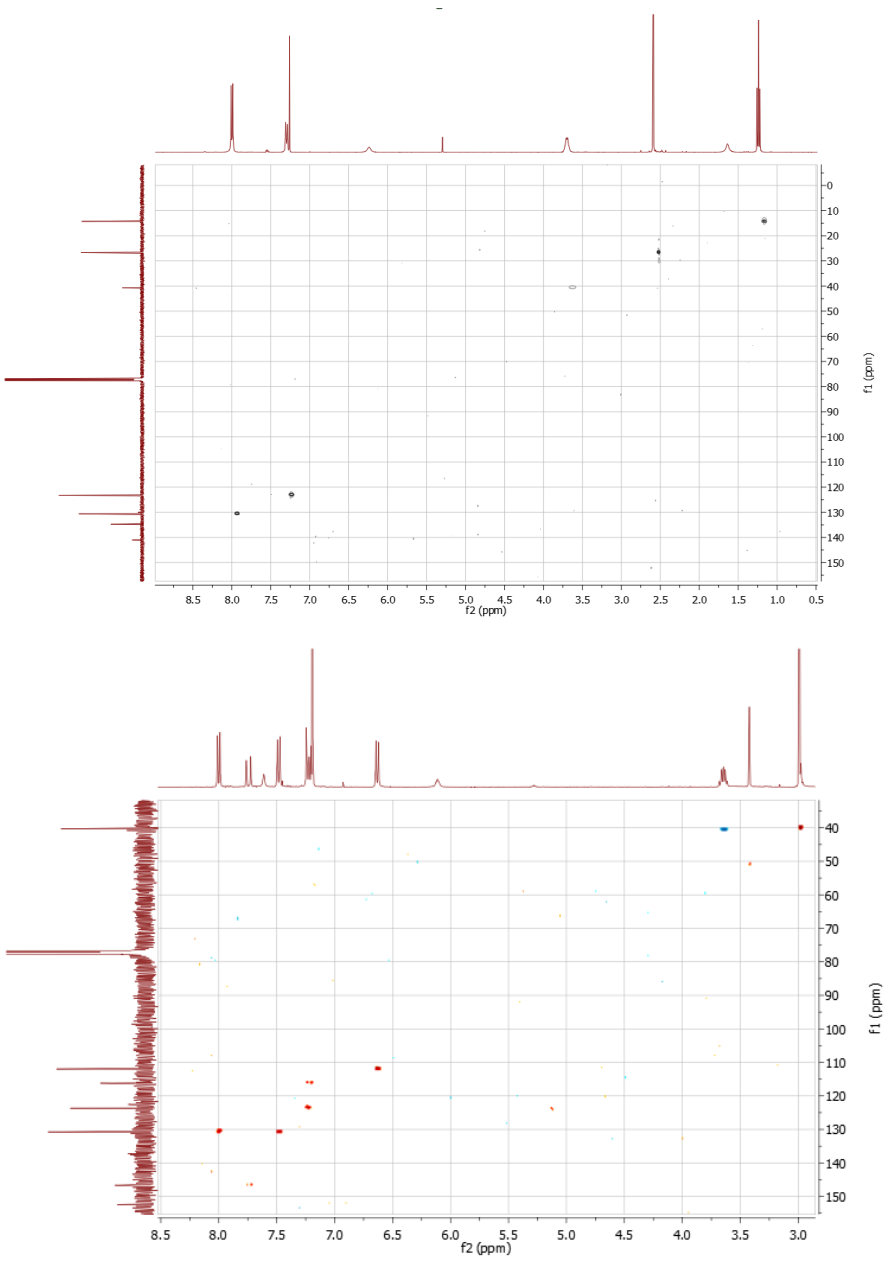

Figure S-4 ^{13}C-^{1}H HSQC NMR 2D spectra of probes **1** (up) and **2** (down) in $CDCl_3$.

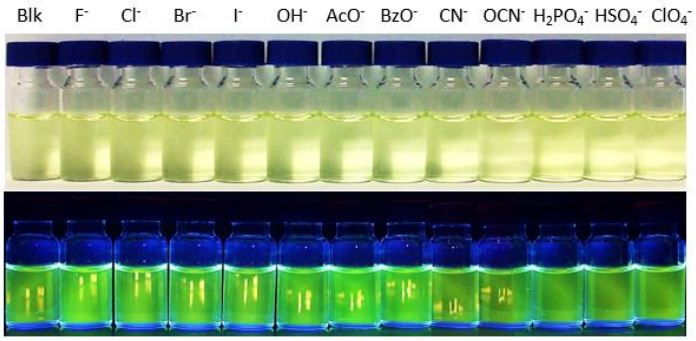

Figure S-5 Photograph of color and fluorescence (λ_{ex} = 365 nm) modulation of **2** upon the addition of 10 eq. of selected anions.

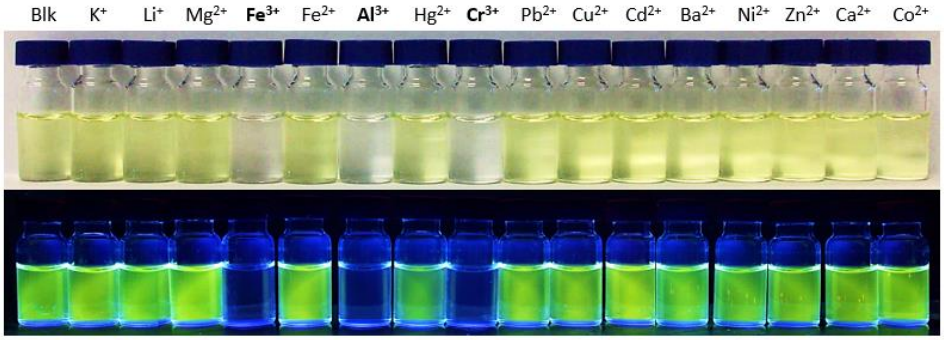

Figure S-6 Photograph of color and fluorescence (λ_{ex} = 365 nm) modulation of **2** upon the addition of 10 eq. of selected cations and HCl.

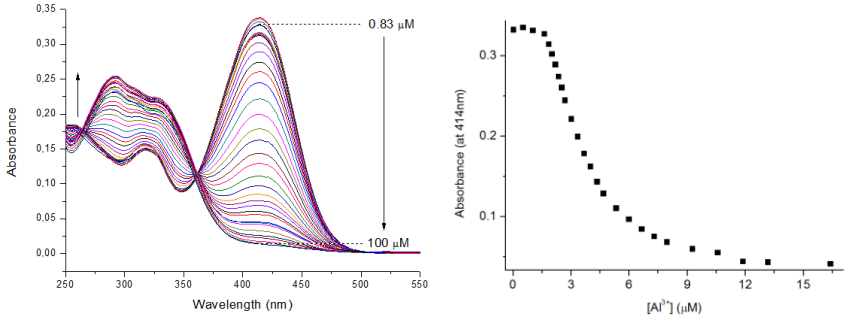

Figure S-7 UV/Vis profile of the titrations of acetonitrile solution (1.0 x 10^{-5} mol dm^{-3}) of probe **2** upon addition of increasing quantities of Al^{3+} cation (LOD = 0.83μM). Left: Absorbance spectra changes. Right: change in the intensity of the 414 nm band.

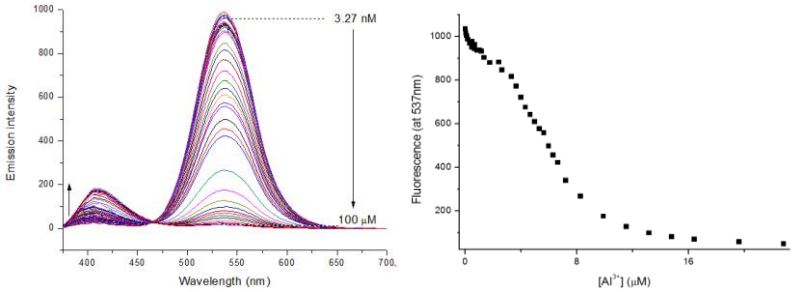

Figure S-8 Emission profile of the titrations of acetonitrile solution (1.0 x 10^{-5} mol dm^{-3}) of probe **2** upon addition of increasing quantities of Al^{3+} cation (LOD = 3.27nM). Left: emission Spectra changes. Right: change in the intensity of the 537 nm band.

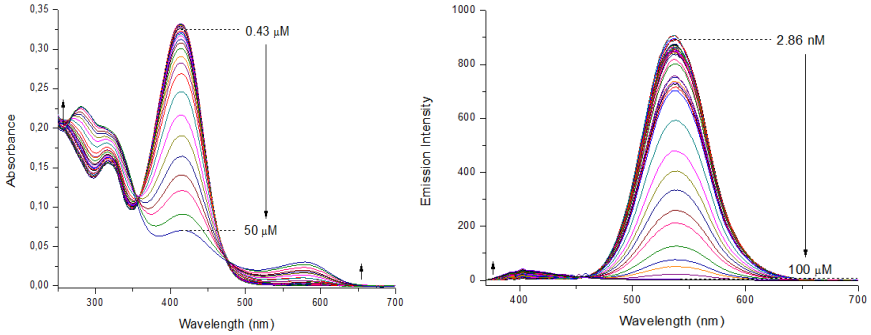

Figure S-9 UV-visible and emission profile of the titrations of acetonitrile solution (1.0 x 10^{-5} mol dm^{-3}) of probe **2** upon addition of increasing quantities of Fe^{3+} cation.

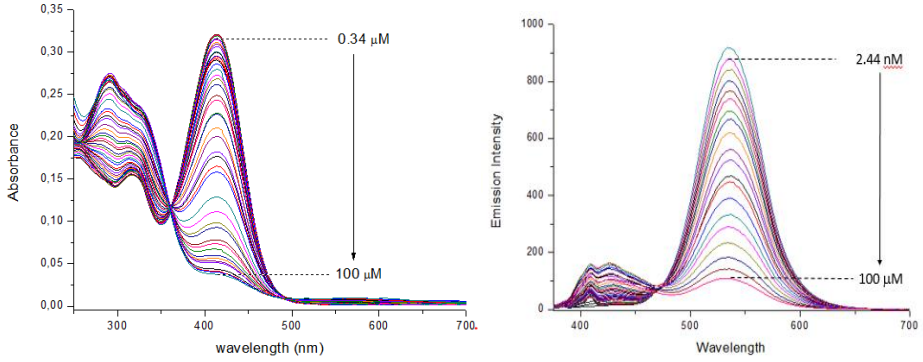

Figure S-10 UV-visible and emission profile of the titrations of acetonitrile solution (1.0 x 10^{-5} mol dm^{-3}) of probe **2** upon addition of increasing quantities of Cr^{3+} cation.

Quantum yield determination

The quantum yields were calculated using the equation S-1 eq.

$$\phi = \phi_R \times \frac{I}{I_R} \times \frac{A_R}{A} \times \frac{\eta^2}{\eta_R^2} \qquad \text{(S-1)}$$

Where Φ is the quantum yield, I is the integrated fluorescence intensity, η is the refractive solvent index, and A is the absorbance intensity. The subscript R refers to the reference fluorophore of known quantum yield. Fluorescein solution in NaOH 0.1 M was used as photoluminescence standards with quantum yield reported as 0.95 ± 0.03 by IUPAC.[1] The blank, polarization, reabsorption, base line, dilution and refractive index effect were considerate and the necessary correction were carried out on base a standard IUPAC procedure.[2]

Limits of detection determination

The limits of detection were estimated using the method denoted as RA (Regression Approach) of ACS and IUPAC standard procedure.[3] Limits of detection were evaluated from the equations S-2, S-3 and S-4.

$$LOD = 3.3S_y/q_1 \qquad \text{(S-2)}$$

$$S_y = \sqrt{\frac{1}{N-m}\sum_{i=1}^{N}(Y_i - q_0)^2} \qquad \text{(S-3)}$$

$$Y = q_0 + q_1 C \qquad \text{(S-4)}$$

[1] M. Brouwer Albert, *Pure Appl. Chem.*, 2011, **83**, 2213-2228

[2] U. Resch-Genger and K. Rurack, *Pure Appl. Chem.*, 2013, **85**, 2005-2026.

[3] J. Mocak, A. M. Bond, S. Mitchell and G. Scollary, in *Pure Appl. Chem.*, 1997, **69**, 297-328

Where:

Sy = regression statistic deviation

Y = optical response (absorbance or emission)

N = number of repeat blank measures

C = molar concentration to metal cation trivalent added during standard titrations

q_0 = intercept of regression line to calibration curve

q_1 = slope of regression line to calibration curve

Regression statistic (S_y) was used on replace of the blank signal standard deviation (σ) in order of express the variation of the signal values around the regression values. Moreover, the intercept of regression line (q_o) was used as the point of reference instead of the mean blank signal to compensate the classic error in the limit of detection estimation when the calibration curve is not crossing for cero, cero point.

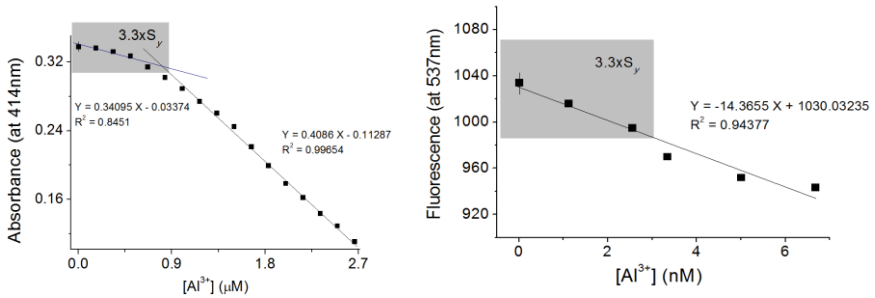

Figure S-11 Representation of 3.3S_y areas of the statistic regressions to UV-vis (left) and emission (rigth) intensity band changes upon addition of increasing quantities of Al^{3+} cation

Bindig constants estimation and technical titration experiments considerations

The binding constants of probe **2** towards trivalent cations (M^{3+}) were evaluated by UV–visible and fluorescence titrations in acetonitrile at room temperature. The log K values were calculated by the spectrophotometric titration curves with base line and blank corrections, using HypSpec software (V 1.1.18). Typically, acetonitrile solution of probe **2** (1.0×10^{-5} mol dm^{-3}) were titrated by addition of 0.1 equivalents aliquots of the M^{3+} solution (1.0×10^{-3} mol dm^{-3}) at room temperature, and the UV-visible or emission spectrum were recorded. The maximum volume of M^{3+} add always was ≤ 10% of probe volume to minimize the dilution effect, and blank solvent correction were permanently carried out in all titration experiment. The pure M^{3+} and probe **2** spectrum were loaded as standards relating to HypSpec refinement calculations.

HOMO and LUMO determination

The HOMO and LUMO determination was performed by quantum chemical calculations at the semi-empirical level, employing a PM3 model (with RMS gradient of 0.01) through of Polak-Ribiere algorithm (Conjugate gradient) on HyperChem software (V 8.0.6). In addition a global molecular hardness value was estimated as $\boldsymbol{\eta = \frac{E_{HOMO} - E_{LUMO}}{2} = 3.675\ eV}$ for probe **2** in vacuum conditions.

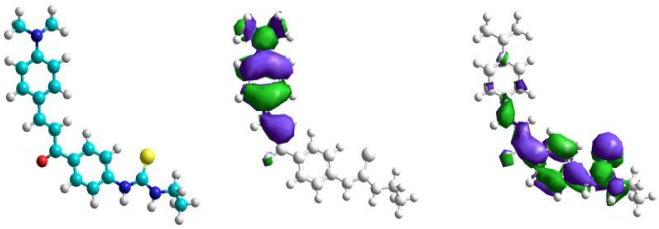

Figure S-12 HOMO and LUMO orbitals distribution and energy values of probe 2.

Chapter 3: Optical Chemosensors for Anions

3. OPTICAL CHEMOSENSORS FOR ANIONS

3.1. About this chapter

The chapter 3 of this PhD thesis is devoted to the study of optical chemosensors for anions recognition. The synthesis and evaluation of sensing behaviour of 13 new cromofluorogenic chemosensor are shown along this chapter. All of experimental results presented are in the form as they have been published, and they are presented with the authorization of the publisher and with the permission of the co-authors.

As in the previously chapter, first a brief introduction to the theorical and experimental considerations into the design of optical chemical sensors for anions is presented to the reader. Next, the experimental results in a systematic form are shown, sorting the paper according to the approach used in the preparation of each chemosensor.

3.2. Preliminary discussion

While the first receptors for anion were born almost parallelly to the first receptors for cations in the sixties decade of the past century, the specific field of the anion chemosensors was developed slowly during the next 20 years, due to the greater complexity required for a suitable coordination. In general anions present larger sizes, lower charge-radius ratio and less effective electrostatic interactions that the cations. In addition, several anions have a pH dependent charge, complex geometries, different hydrophobicity and high solvation energies.[1] Therefore, the preparation of selective receptors and chemosensors for

[1] Beer, P. D.; Gale, P. A., *Angew. Chem. Int. Ed.* **2001**, 40, 486-516.

anions is more complex and required more synthetic efforts than for their cation counterparts.

However, the great relevance of anions in several biological processes and their implication in industrial and agricultural pollution has caused than in the last years a large effort has been devoted to the development of anion chemosensors. Nowadays, the supramolecular chemistry of anions has become one fertile sub-area of research in the supramolecular chemistry field.[2]

3.3. Theoretical considerations

The ability of anions to give electrostatic ion-pair and hydrogen bond interaction with electron-acceptor groups is considered on the synthesis of appropriate binding sites for chemosensors.

The strong electrostatic interactions between an anion and the chemosensors is used to compete with the high solvation in aqueous environments. Nevertheless, the anion receptors based only on simple electrostatic arguments have a poor selectivity. Thus, the use of hydrogen bond is usually included on design of anion chemosensors in order to take advantage of their directionality for differentiating between anions of different size, geometry and hydrogen bonding ability.[3]

In particular, many of recently reported chemosensors for anions have been designed to contain binding subunits with nitroaromatic derivatives, N-heterocycles or aromatic alcohols to use the hydrogen bond properties on the processes of anion recognition.[4] In addition, the studies of behavior of anion receptors with appropriate proton donor groups for binding have allowed the

[2] Bowman-James, K.; Bianchi, A.; García-Espana, E., *Anion Coordination Chemistry.* Wiley: **2012**.

[3] Juwarker, H.; Jeong, K.-S., *Chem. Soc. Rev.* **2010,** *39*, 3664-3674.

[4] Sessler, J. L.; Gale, P. A.; Cho, W. S., *Anion Receptor Chemistry.* Royal Society of Chemistry: **2006**.

preparation of foldamers based in synthetic linear oligomers or polymers, which fold to create binding cavities, similarly as makes nature in proteins and enzymes.[5]

The interaction of cationic complexes with anions also has been widely used in the design of chemosensors for anions which combine both the electrostatic attraction of the metal centre and the directional binding effects of proton-donor moieties. In this respect, metal-based anions chemosensors that used simple electrostatic interactions and more sophisticated probes, which used the first- and second-sphere coordination, has been reported.[6] Many guanidinium-based chemosensor for anions also has been reported. [7]

On the other hand, as we discussed in chapter 1 (section 1.2.1.3), the knowledge of several selective chemical reactions for specific anions has also enabled the preparation of many efficient chemodosimeters for anion sensing.[8]

In general, the supramolecular concepts of preorganization and complementarity are the main base of the design of chemosensors for anions independently of the pattern of construction used. In fact, currently both concepts are implemented on the three approaches presented in chapter 1 (section 1.2.1) and the selection of one or more of the optical signaling mechanisms (see section 1.2.2), in order to ensure high affinity and selectivity.

[5] Hill, D. J.; Mio, M. J.; Prince, R. B.; Hughes, T. S.; Moore, J. S., *Chem. Rev*. **2001**, 101, 3893-4012.

[6] Mercer, D. J.; Loeb, S. J., *Chem. Soc. Rev.* **2010,** *39*, 3612-3620

[7] Houk, R. T.; Tobey, S.; Anslyn, E., Abiotic Guanidinium Receptors for Anion Molecular Recognition and Sensing. In Anion Sensing, Stibor, I., Ed. Springer Berlin Heidelberg: **2005**; Vol. 255, pp 199-229.

[8] Santos-Figueroa, L. E.; Moragues, M. E.; Climent, E.; Agostini, A.; Martinez-Manez, R.; Sancenon, F., *Chem. Soc. Rev.* **2013,** *42*, 3489-3613.

3.4. Anion chemosensor by binding site-signaling subunit approach

3.4.1. Experimental objectives

Bearing in mind the concepts mentioned above, the relevant role of anions in several biological process and the growing interest in the development of efficient chemosensors for anions; we proposed synthesize and evaluate new thiosemicarbazones-based chemosensors for anion sensing.

In particular our main aims in this project were:

- Design and synthesize a family of new thiosemicarbazones-based chemosensors for anions recognition through "binding site-signaling subunit" approach.

- Characterize the new probes by standard methods (NMR, HRMS, IR, UV/Vis and emission spectroscopy).

- Evaluate the influence of structural changes of thiosemicarbazones-based chemosensors into the modulation of their optical outputs and selectivity to anions of different size, charge and shape.

3.4.2. Chemosensor design

On this project, the main focus on design phase was to prepare a family of chemosensors with structural variations, but with the same specific binding site for anions. In this case a "binding site-signaling subunit" approach was selected for the chemosensors design due to the major influence of molecular structure into binding properties.

A thioureido moiety was included in the chemosensor design as binding site for its known ability to anion coordination and knowing reactivity with other organic groups. A relative good electronic conjugation in the molecular structure was attempted (by push-pull system) with inclusion of a phenyl and thioureido moieties attached together, as electron donor/acceptor groups, in order to favor internal charge transfer character and the final optical output.

Finally, structural variations among chemosensors were design for attempting modulate their anion sensing capability. This was achieved through incorporation of different heterocyclic systems linked to the skeleton of thiosemicarbazone. Furyl and thiophenyl moieties were tested.

3.4.3. Synthesis and evaluation of thiosemicarbazones functionalized with furyl moieties as new chemosensors for anion recognition.

Below, the complete studies of synthesis and evaluation of the ability for chromo-fluorogenic sensing of anions of a family of thiosemicarbazones-based chemosensor functionalized with furyl moieties is presented (Figure 32).

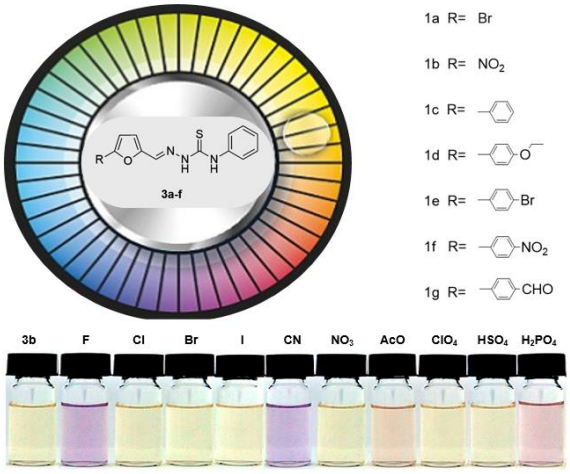

Figure 32. Grafic representation of thiosemicarbazones-based receptors family for anions recognition.

Synthesis and Evaluation of Thiosemicarbazones Functionalized with Furyl Moieties as New Chemosensors for Anion Recognition.

Luis E. Santos-Figueroa, [a, b, c] María E. Moragues, [a, b, c] M. Manuela M. Raposo, [d] Rosa M. F. Batista, [d] Susana P. G. Costa, [d] R. Cristina M. Ferreira, [d] Félix Sancenón, Ramón Martínez-Máñez, [a, b, c]* José Vicente Ros-Lis [a, b, c] and Juan Soto [a, b]*

[a] *Instituto de Reconocimiento Molecular y Desarrollo Tecnológico (IDM), Centro Mixto Universidad Politécnica de Valencia-Universidad de Valencia (Spain)*

[b] *Departamento de Química, Universidad Politécnica de Valencia, Camino de Vera s/n, 46022 Valencia (Spain)*

[c] *CIBER de Bioingeniería, Biomateriales y Nanomedicina (CIBER- BBN)*

[d] *Centro de Química, Universidade do Minho, Campus de Gualtar, 4710-057 Braga, Portugal.*

Received: March 12, 2012
Published online: July 24, 2012

Organic & Biomolecular Chemistry, **2012**, 10, 7418–7428

3.4.3.1. Abstract

A family of heterocyclic thiosemicarbazone dyes (**3a–f** and **4**) containing furyl groups was synthesized in good yields, characterized and their response in acetonitrile in the presence of selected anions was studied. Acetonitrile solutions of **3a–f** and **4** showed absorption bands in the 335–396 nm range which are modulated by the electron donor or acceptor strength of the heterocyclic systems appended to the thiosemicarbazone moiety. Fluoride, chloride, bromide, iodide, dihydrogen phosphate, hydrogen sulphate, nitrate, acetate and cyanide anions were used in recognition studies. From these anions, only sensing features were seen for fluoride, cyanide, acetate and dihydrogen phosphate. Two clearly different chromo-fluorogenic behaviours were observed: (i) a small shift of the absorption band due to the coordination of the anions with the thiourea protons and (ii) the appearance of a new red shifted band due to deprotonation. For the latter effect, a change in the colour of solution from pale yellow to purple was observed. Fluorescence studies were also in agreement with the different effects observed in the UV/Vis titrations. In this case, hydrogen bonding interactions were visible through the enhancement of the emission band, whereas deprotonation induced the appearance of a new red-shifted emission. Logarithms of stability constants for the two processes (complex formation + deprotonation) for receptors **3a–f** in the presence of fluoride and acetate anions were determined from spectrophotometric titrations using the HypSpec V1.1.18 program. Semi-empirical calculations to evaluate the hydrogen-donating ability of the receptors and a prospective electrochemical characterization of compound **3b** in the presence of fluoride were also performed.

3.4.3.2. Introduction

The development of new molecular systems for the detection of anions, cations or neutral molecules has gained prime importance in recent years due to the significance of detecting target species in biological and environmental

samples. In this area, designed receptors are able to transform, upon coordination, host‑guest interactions into a measurable signal which allows analyte recognition and sensing through optical or electrochemical responses.[1] In particular, optical outputs are attractive given the possibility of using low-cost, widely available instrumentation. Apart from the development of fluorescent probes, chromogenic recognition has drawn attention because it offers the possibility of straightforward semiquantitative "naked eye" detection.[2] Moreover, the colorimetric probes showing a simple displacement of the absorption band allow one to develop ratiometric methods, thus avoiding the use of an internal reference. Optical detection for metal cations was developed more than two decades ago,[3] yet anionic chromogenic receptors have only recently been investigated.[4] The latter focus on anions are mainly due to the more challenging chemistry of host-anion interactions, the lower stability constants observed with anionic species when compared with metal cations, the complex and varied shapes found for anions, their possible dependence on pH and the strong competition of water usually found for receptor‑anion complexes based on hydrogen-bonding interactions.[5] Despite these setbacks, the supramolecular chemistry of anions has advanced a great deal in the last few years mainly due to the progress made in the knowledge of how the formation of host-anion complexes operates. Based on these advances, a number of receptors for anion binding have been developed, most of which are based on hydrogen bonding and electrostatic interactions.[6] In contrast to purely electrostatic interactions, which are only distance-dependent, hydrogen bonds offer the advantage of being directional which allows one to discriminate between anions of different geometries or hydrogen-bonding requirements.[7] Among the neutral anion binding groups, thioureas and thiourea-containing fragments have been widely used for the formation of complexes with anions because the hydrogen-bonding ability of these functional groups commonly results in the formation of quite stable complexes, and also because they can be easily synthesized from commercially available reagents by a single-step procedure.[8] In fact, thiourea derivatives have been the subject of intense research given their performance in the development

of anion receptors and, for instance, thioureas (and also ureas) have been demonstrated as good coordinating groups for Y-shaped anions such as carboxylates.[9] Moreover, the hydrogen bonding ability of the thiourea moiety depends on the acidity of the thioureido NH protons and the number of binding sites. A means of tuning this acidity is to introduce electron-donating or electron-withdrawing substituents.[10] Additionally, experimental and theoretical studies have demonstrated that replacing the benzene ring of a chromophore bridge with easily delocalizable five member heteroaromatic rings, such as thiophene, pyrrole and thiazole, results in enhanced intramolecular electronic delocalization.[11]

On the other hand, among the molecules containing thiourea fragments, the use of thiosemicarbazones has recently gained interest as potential receptors. Schiff base compounds containing thiosemicarbazone groups have also grown in the biology and chemistry areas due to ample biological activity,[12] such as antitumoural, fungicidal, bactericidal, or antiviral, and nonlinear optical properties.[13] Moreover, thiosemicarbazones have also gained attention recently as anion receptors due to their easy synthesis. Also, thiosemicarbazones will be easily included in aromatic frameworks functionalized with acceptor and donor moieties in order to fine tune the acidity of the NH protons. In fact, we and others have recently demonstrated that π-conjugated heterocyclic derivatives, containing thiosemicarbazone moieties, are suitable systems for the colorimetric and fluorimetric sensing of anions.[14] Following this previous work on the synthesis and evaluation of thiosemicarbazones as binding groups, and by also considering our interest in the development of new probes for anion recognition, we report herein the synthesis and the characterization of new *N*-phenylthiosemicarbazones. As a special feature, these newly reported derivatives additionally contain heteroaromatic π-conjugated systems (instead of the more commonly used benzene rings) because anion chemosensors containing phenylthioureas functionalized with heterocyclic moieties are still unusual. The new reported receptors contain furan (instead of thiophene as we have reported recently)[14] as aromatic rings. The underlying idea of the present paper was to

evaluate the effect in the binding efficiency of the thiosemicarbazone moiety upon functionalization with furan groups.

3.4.3.3. Results and discussion

Synthesis and characterization

Different formyl precursors **1a–g** containing several substituents, such as bromo, nitro and alkoxy, linked to different π conjugating bridges were used to evaluate the influence of the structure modification (i.e., donating and accepting strength of these groups, and the nature and length of the π-conjugated bridge) on the optical properties of prepared *N*-phenylthiosemicarbazones **3a–f** and **4.** The new compounds containing furan and arylfuran π-conjugated bridges were synthesized in good yields (76–96%) through the Schiff-base condensation of heterocyclic aldehydes 1a–g with 4-phenyl-3-thiosemicarbazide in methanol at room temperature (see Scheme 1).

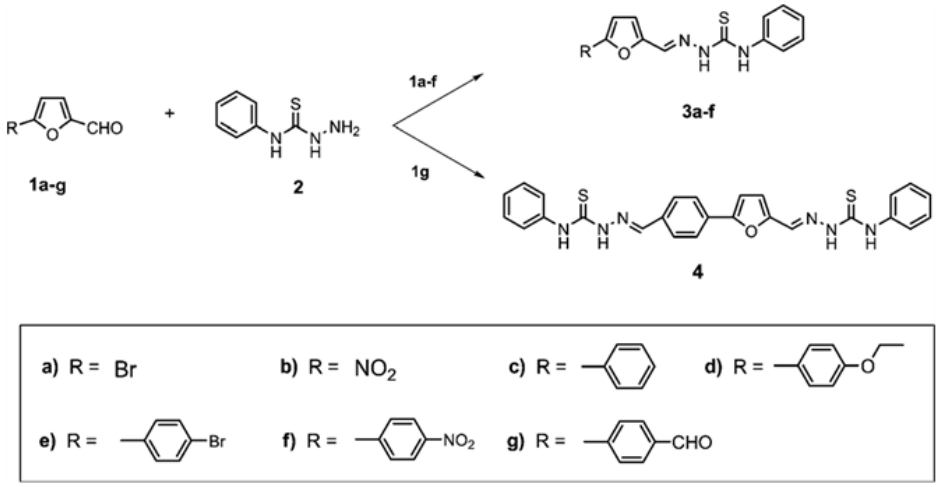

Scheme 1 Synthesis of furyl-thiosemicarbazone receptors **3a–f** and **4.**

Aldehydes **1a–c** and **1e–f** are inexpensive and commercially available, and 5-(4′-ethoxyphenyl)furan-2-carbaldehyde **1d**[15] and the precursor 5-(4′-formylphenyl)furan-2-carbaldehyde **1g** were easily prepared in good yields (75–91%) through Suzuki cross-coupling reactions of 5-bromofuran-2-carbaldehyde with 4-ethoxyphenylboronic acid or 4-formylphenylboronic acid, respectively, using the synthetic procedure previously reported by us.[11a] All the compounds were completely characterized by ^{1}H and ^{13}C NMR, IR, MS, EA or HRMS, and the data obtained were in full agreement with the proposed formulation (see Experimental section). The ^{1}H NMR spectra of this family of thiosemicarbazones show the most characteristic signals for N–H and CH=N protons. ^{1}H NMR studies using deuterated *N,N*-dimethylsulphoxide (DMSO) displayed resonances due to the CH=N protons in the 7.99–8.16 ppm interval, whereas thiourea N–H protons were found in the 9.88–10.18 and 11.84–12.23 ppm range for the N–H groups adjacent to the monosubstituted phenyl ring and for the N–H adjacent to the CH=N moiety, respectively. When the whole family of compounds was considered, the highest variations in δ were found for the N–H protons located in the vicinity of the CH=N moiety adjacent to the furan ring functionalized with electron withdrawing or electron donor groups (Δδ = 0.39 ppm). Additionally, the CH=N protons were the least affected by the substituents located in their vicinity (Δδ = 0.17 ppm), whereas the N–H protons adjacent to the monosubstituted phenyl ring showed an interval of Δδ = 0.30 ppm.

Spectroscopic behaviour of 3a–f and 4

Acetonitrile solutions (C = 1.2 × 10^{-5} mol dm^{-3} at 25 °C) of thiosemicarbazone-functionalised receptors **3a–f** and **4** showed an intense absorption band (log ε ≈ 4.4) in the 335–396 nm region (see Table 1 for spectroscopic data). Compound **3a**, containing the thiosemicarbazone moiety surrounded by a phenyl and a furyl ring functionalized with a bromo group, presented an absorption band at 335 nm, whereas changing the bromo substituent for a better electron acceptor moiety, such as a nitro group (receptor **3b**), induced a pronounced red shift from 335 to

383 nm. The coupling of an additional aromatic ring with the framework of **3a** or **3b** (receptors **3e** and **3f**, respectively) induced a significant bathochromic shift of the band (from 335 to 364 nm and from 383 to 396 nm, respectively), this being a direct consequence of the extension of the conjugation.

Table 1. Spectroscopic Data for Compounds **3a-f** and **4**.

Receptor	λ_{ab} LH (nm)	λ_{ab} L^{-} [a] (nm)	Log ε (LH)	λ_{em} LH (nm)	λ_{em} L^{-} [a] (nm)	Φ	$\Delta\lambda_{ab\text{-}em}$ LH (nm)	$\Delta\nu_{ab\text{-}em}$ LH (cm^{-1})
3a	335	391	4.55	421	431	0.0016	86	6097.78
3b	383	540	4.27	422	409	0.0006	39	2412.98
3c	362	416	4.59	426	491	0.0226	64	4150.13
3d	366	410	4.01	432	462	0.0644	66	4174.26
3e	364	423	4.61	429	476	0.0183	65	4162.50
3f	396	489	4.31	586	546	0.0259	190	8187.68
4	359	443	4.53	486	467	0.0363	127	7279.02

[a] Measured upon addition of 100 equiv. of the fluoride anion.

UV-Vis studies involving anions

The UV-Vis behaviour of receptors **3a–f** and **4** in acetonitrile solutions (C = 1.2 × 10^{-5} mol dm^{-3}) was studied at 25 °C in the presence of selected anions of different sizes and shapes such as fluoride, chloride, bromide, iodide, cyanide, nitrate, acetate, perchlorate, hydrogen sulphate and dihydrogen phosphate. For all the receptors, addition of increasing quantities (up to 10 equiv.) of chloride, bromide, iodide, nitrate, perchlorate and hydrogen sulphate induced negligible changes in the UV-Vis bands, which clearly indicates that no coordination occurs. Much more relevant results were observed in the presence of those anions showing a basic character in acetonitrile, such as fluoride, cyanide, acetate, and dihydrogen phosphate (see Figure 1). The changes in colour observed upon addition of basic anions were almost immediate (see ESI† for the kinetic profile of changes in the 390 nm band of **3b** in the presence of the fluoride anion).

Figure 1. Colour changes of the **3b** solution (1.2×10^{-4} mol dm^{-3}) seen in the presence of 10 equiv. of F^-, Cl^-, Br^-, I^-, CN^-, NO_3^-, AcO^-, ClO_4^-, HSO_4^- and $H_2PO_4^-$.

In most cases, UV-Vis titration experiments with receptors **3a–f** and **4** and fluoride showed similar behaviour; i.e., intensity decreased and there was a slight hypsochromic shift of the absorption band, together with simultaneous growth of a new red-shifted band. However, it was clearly apparent from the titration profiles that both the position of the new band and the reltive intensity of the absorption band of the receptor in relation to the red-shifted band upon addition of fluoride were dependent on the receptor used. Acetonitrile solutions of **3b** were yellow due to the presence of a band at 383 nm. Upon addition of increasing quantities of the fluoride anion, this band progressively decreased, while a new absorption at 540 nm ($\Delta\lambda$ = 157 nm) increased in intensity with a clear isosbestic point at 429 nm (see Figure 2). The formation of this new visible band induced a change in colour from pale yellow to purple (see Figure 1).

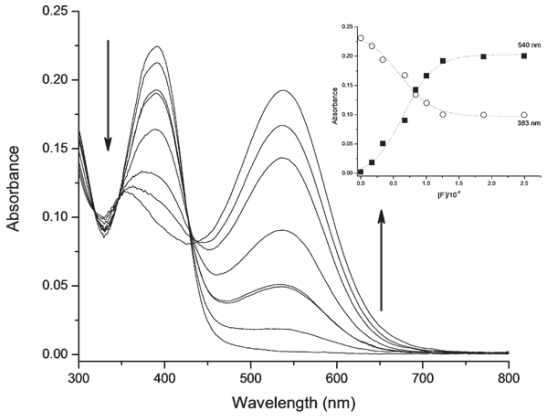

Figure 2. UV-Vis titration of receptor **3b** (1.2×10^{-5} mol dm^{-3}) with F^- anion (0–10 equiv.) in acetonitrile. Inset: Absorbance of a solution of **3b** at 383 and 540 nm versus concentration of F^- anion (mol dm^{-3}).

Fluoride and cyanide anions were able to induce UV-Vis changes for all the receptors tested, whereas acetate and hydrogen phosphate displayed a poorer response with all the receptors (see Figure 3).

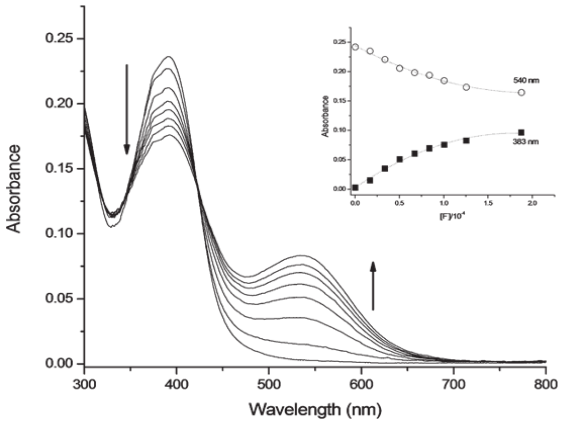

Figure 3. UV-Vis titration of receptors **3b** (1.2×10^{-5} mol dm^{-3}) with AcO^- anion (0–10 equiv.) in acetonitrile. Inset: Absorbance of acetonitrile solutions of receptor **3b** at 383 and 540 nm *versus* concentration of AcO^- anion (mol dm^{-3}).

The selectivity of receptors **3a–b** and **4** for the most basic anions (F^-, CN^-, AcO^- and $H_2SO_4^-$) was demonstrated by further UV-Vis experiments. Figure 4 shows that addition of 10 equiv. of fluoride anion to acetonitrile solutions of receptor **3b** induced the appearance of an absorbance band at 540 nm. The same red-shifted band with identical absorbance was obtained upon addition of a mixture of anions (10 equiv. of fluoride, chloride, bromide, iodide, perchlorate, hydrogen sulfate and nitrate). Similar chromogenic behaviors were observed for CN^- and AcO^- in mixtures with other anions (i.e. chloride, bromide, iodide, perchlorate, hydrogen sulfate and nitrate).

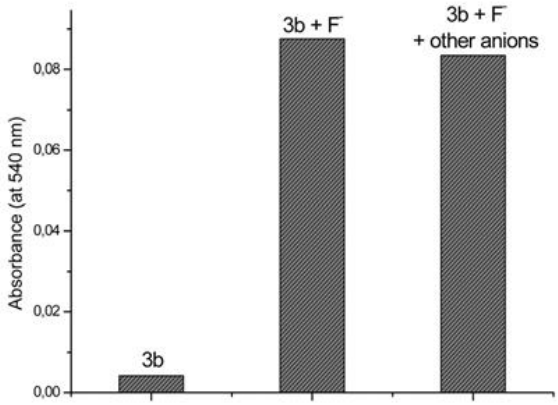

Figure 4. Absorbance at 540 nm of receptor **3b** (1.0×10^{-5} mol dm^{-3}) alone and upon addition of 10 equiv. of F^- and 10 equiv. of F^-, Cl^-, Br^-, ClO_4^-, HSO_4^-, I^- and NO_3^- anions.

Once the selectivity of this family of receptors was determined, the limits of detection (LOD) were estimated. In all cases LOD values of *ca*. 10 μM were determined for fluoride and cyanide anions.

Moreover, the interaction of **3a–f** and **4** with basic anions in water and acetonitrile–water mixtures (1:1, 5:1 and 10:1 v/v) was also tested. Unfortunately, in all cases changes neither in colour nor in fluorescence were observed. This was most likely due to the reduced basicity of the anions in aqueous environments due to solvation and the poor acidity of the receptors when compared with other reported ligands (*vide infra*).

On the whole, the changes observed in acetonitrile are in agreement with the expectation that the interaction between an electron-rich anion and a donor group in a push–pull system will induce a bathochromic shift. In fact, similar shifts in the presence of fluoride have also been reported to occur using other amide-, urea-, thiourea-, or pyrrole-containing hosts.[16] This interaction is attributed to the formation of strong hydrogen bonding complexes between these groups and to the highly basic F^- anion that is eventually able to originate the deprotonation of the binding site.[17] In fact, we believe that this dual complex +

deprotonation process is active in all of our receptors in the presence of fluoride: a first step consisting in the formation of a hydrogen- bonding complex and a second step in which the receptor is deprotonated by the anion. Usually the formation of hydrogen- bonding complexes, via receptor-interactions, is reflected in relatively minor variations in the absorption band of the receptor, whereas the deprotonation processes are revealed with the clear appearance of a new absorption band at longer wavelengths.[18] From a more physical viewpoint, the negative charge generated upon deprotonation induces an increase in the intensity of the electrical dipole that results in a substantial red shift of the absorption band. In most cases, the observation of complexation or/and deprotonation depends on a delicate balance between the acidity of the N–H protons of the receptor and the basicity of the anion. In our case, a close look at the results indicated that the final response of receptors **3a–f** and **4** to the tested basic anions strongly depends on the chemical nature of the functional groups attached to the thiosemicarbazone framework, which modulated the acidity of the N–H protons; i.e. for a certain anion (fluoride) at a given concentration, the development of the band due to deprotonation grew more or less in intensity depending on the receptors used.

When comparing the behaviour of similar compounds **3a–f**, it was apparent that the presence of electron-withdrawing moieties, such as a nitro group in **3b** and **3f**, induced an increase in the acidity of the N–H protons of the thiosemicarbazone, thus favouring the interaction with the fluoride and cyanide anions and deprotonation, whereas the presence of electron-donor groups, such as bromo (**3a**) and ethoxy (**3d**), respectively induced a certain decrease in acidity and the red-shifted band due to deprotonation developed to a lesser extent.

Stability constants

As stated above in the interaction of basic anions with semithio- carbazone-containing receptors **3a–f** and **4**, two different behaviours could be expected; *i.e.*, (i) hydrogen bonding interactions and (ii) deprotonation (see eqn (1) and (2)).

$$\mathrm{LH} + \mathrm{A}^- \rightleftarrows \mathrm{LH}\cdots\mathrm{A}^- \qquad (1)$$

$$\mathrm{LH}\cdots\mathrm{A}^- + \mathrm{A}^- \rightleftarrows \mathrm{L}^- + \mathrm{A_2H}^- \qquad (2)$$

In order to complete the characterization of the interaction of receptors **3a–f** and **4** with anions, the strength of both processes (coordination and deprotonation) was studied via the evaluation of the corresponding stability constants, which were determined by the UV-Vis spectroscopic titrations between receptors **3a–f** and **4** and fluoride and acetate anions using the HypSpec software V1.1.18. The data set was adjusted to the two consecutive equilibriums in eqn (1) and (2); the results are shown in Table 2.

Table 2. Logarithms of the stability constants measured for the interaction of receptors 3**a-f** with fluoride and acetate

	F^-		AcO^-	
	$LH + A^- \leftrightarrows LH\cdots A^-$	$LH\cdots A^- + A^- \leftrightarrows L^- + A_2H^-$	$LH + A^- \leftrightarrows LH\cdots A^-$	$LH\cdots A^- + A^- \leftrightarrows L^- + A_2H^-$
3a	3.46(6)	2.48(7)	3.40(6)	0.31(8)
3b	4.56(2)	4.24(4)	3.91(1)	1.53(4)
3c	4.20(5)	3.51(8)	3.60(1)	0.13(4)
3d	4.23(4)	3.81(8)	- [a]	- [a]
3e	4.37(1)	3.57(7)	3.56(8)	0.31(2)
3f	4.47(7)	4.47(1)	4.56(8)	1.64(1)

[a] No reliable results were obtained.

In all cases, the formation of anion–ligand 2:1 complexes shown in eqn (2) was confirmed for the method of continuous variation (Job's plots). As an example, Figure 5 shows the studies for the interaction of **3b** with fluoride. It is noticeable that despite the presence of two potential binding sites in **4**, this receptor showed

the same response as **3a–f**, namely the formation of 2:1 anion–ligand stoichiometry complexes.

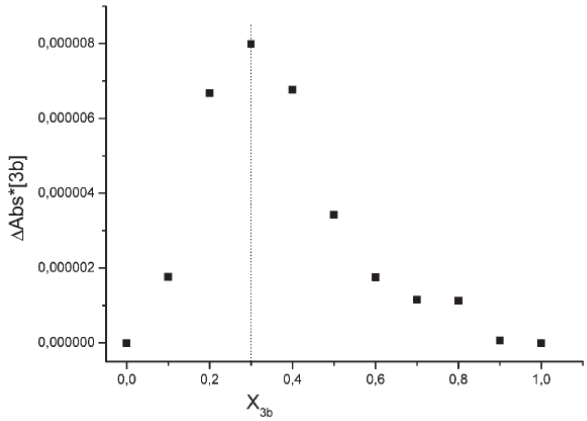

Figure 5. Job's plot for complexation of **3b** with the fluoride anion determined by UV-Vis spectrophotometry in acetonitrile at 540 nm and [**3b**] + [F^-] = 1.2 × 10^{-4} mol dm^{-3}.

Table 2 shows that, as a general trend, the logarithms of the stability constants measured for both equilibriums with fluoride were higher than those obtained for acetate. This is in agreement with the more basic character of fluoride in acetonitrile when compared with acetate. The logarithms of the stability constants for the formation of the Y-shaped hydrogen-bonding complexes were about one order of magnitude larger than the logarithms of the stability constants for the deprotonation for fluoride, and about three orders of magnitude larger for acetate. It is also apparent in Table 2 that the deprotonation logarithms of constants for all the receptors were more important for fluoride than for acetate.

The stability constants for the formation of the corresponding hydrogen-bonding complexes remained approximately the same for both anions. It is noteworthy that the logarithms of stability constants determined in this study for thiosemicarbazones were generally lower than those reported for the other urea/thiourea receptors functionalized with benzene rings containing electron withdrawing moieties. This is a clear consequence of the reduced acidity of the

receptors studied herein when compared with other reported ligands. For instance, compound 1,3-bis-(4-nitrophenyl)urea has also been reported to display the two-step process (coordination + deprotonation) upon addition of fluoride with logarithms of the stability constants for the formation of the complex and for the deprotonation of 7.38 and 6.37 respectively.[19] Another urea-based receptor (1-nitrobenzo[1,2,5]oxadia-zol-4-yl)-3-(4-nitrophenyl)urea showed logarithm values higher than 6 for the formation of the hydrogen-bonding complexes and 4.2 for the deprotonation step.[20] Finally, the thiourea receptor 1-(2-methyl-1,3-dioxo-2,3-dihydro-1*H*-isoindol-5-yl)-3-phenyl-thiourea also underwent a first coordination step and a second proton transfer process with the basic anions, with a logarithm of stability constants 5.7 and 5.5 for fluoride, and 6.02 and 3.23 for acetate.[21]

Fluorogenic studies involving anions

It is widely known that fluorescence, despite being a less extended technique in some cases, is much more sensitive to intermolecular interactions than colour changes. Therefore, fluorescence studies in acetonitrile solutions of the receptors upon addition of increasing amounts of the corresponding anion were carried out. Receptors were excited in the pseudo-isosbestic points observed in the course of UV-Vis titrations. In all cases, the emission consisted in a broad, unstructured band. Quantum yields in acetonitrile (see Table 1) ranged from quite low (receptor **3a**, Φ = 0.0016) to medium (compound **3d**, Φ = 0.0644). For all the receptors tested (i.e., **3a–f** and **4**), addition of the anions chloride, bromide, iodide, hydrogen sulphate and nitrate induced negligible changes in the emission intensity profiles. In contrast, the fluorescence emission in the presence of fluoride, cyanide, acetate and dihydrogen phosphate changed significantly.

A different general behaviour was found depending on the anion and the receptor used in the studies. As a general trend, and in the presence of fluoride, all the receptors **3a–f** and **4** showed enhanced fluorescence intensity upon the

addition of moderate amounts of fluoride followed by a quenching of the emission band at higher anion concentrations and the growth of a new band at longer wavelengths (λ_{em} in the 421–586 nm range, see Table 1).

In order to interpret this behaviour, we made a comparison between the changes observed in the emission and absorption spectra. A typical example is that shown in Figure 6, namely the behaviour found for ligand **3e** in the presence of fluoride. As seen, for small quantities of the fluoride anion, while the intensity of the absorption band at 364 nm remains unaltered, the fluorescence intensity at 429 nm progressively increased until 10 equiv. of fluoride had been added. Moreover, upon addition of larger amounts of fluoride, the intensity of the emission band at 429 nm diminished, suggesting the formation of a new compound that emits at longer wavelengths (λ_{em} = 476 nm). Thus, fluorescence measurements suggest that the interaction of the receptors with fluoride took place in two steps, as found in the UV-Vis studies. In the first step, the anion coordinates with the acidic NH protons of the thiourea moiety through hydrogen bonding interactions and led to an increase in the donor capacity of the binding site. Upon addition of more equivalents of the anion, deprotonation of the receptor occurred. This deprotonation process induced the appearance of the red-shifted visible and emission bands.

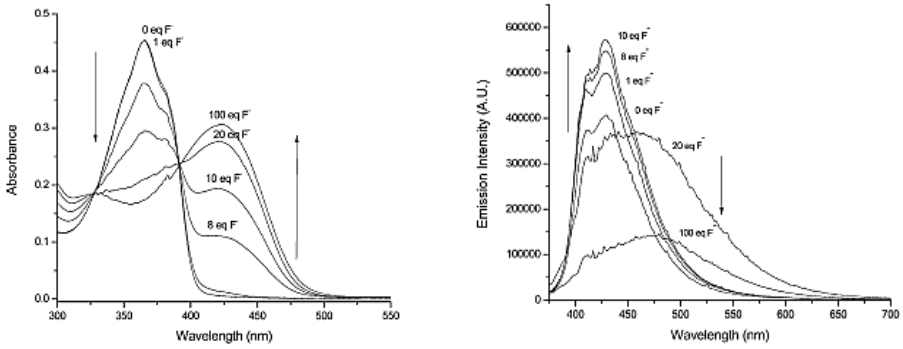

Figure 6. Interaction of receptor **3e** (1.2×10^{-5} mol dm^{-3}) with F^- anion (left): absorption spectra and (right): emission spectra of receptor in the presence of 0, 1, 8, 10, 20 and 100 equiv. of F^- anion.

The overall shape and intensity of the emission band for a certain receptor–anion pair depends on the LH/LH···A^-/L^- ratios. For instance, a closer look at the titration experiments with fluoride indicated that in order to induce the appearance of the red-shifted emission band, larger amounts of fluoride are required for receptor **3e** (functionalized with bromophenylfuryl) than for receptor **3f** (functionalized with nitrophenylfuryl), which is in agreement with the larger acidity of **3f** *versus* **3e**.

Figure 7 shows the emission and absorption spectra for receptor **3e** in the presence of acetate. The emission intensity was enhanced upon the addition of increasing quantities of the acetate anion. This enhancement in the emission intensity was assigned to the formation of the Y-shaped hydrogen-bonding complex between the NH thiourea protons of the receptor and the acetate anion. However, in this case, no significant deprotonation occurred and no red-shifted absorptions or emission bands were observed.

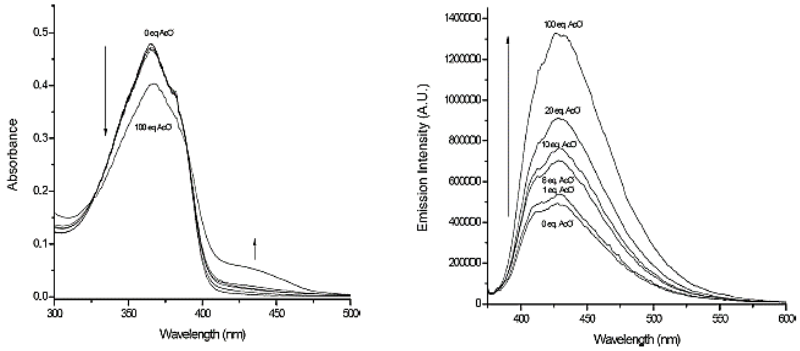

Figure 7. Interaction of receptor **3e** (1.2×10^{-5} mol dm^{-3}) with AcO^- anion (top): absorption spectra and (bottom): emission spectra of the receptor in the presence of 0, 1, 8, 10, 20 and 100 equiv. of AcO^- anion.

^{1}H-NMR spectroscopic studies in the presence of anions

As seen previously, the UV-Vis and fluorescence data of thiosemicarbazone receptors **3a–f** and **4** in the presence of anions displayed a varied response related

with the presence of hydrogen bonding interactions and the deprotonation of the receptors. In particular, the colorimetric behaviour observed for these receptors depends on the deprotonation tendencies of the thiosemicarbazone units in receptors **3a–f** and **4** and on the proton affinities of the anions.

In order to study the coordination/deprotonation processes in these systems in more detail, the interaction of receptor **3b** with the fluoride anion was investigated by means of ^{1}H NMR titration experiments in DMSO-d_6. Deuterated DMSO was selected as the solvent due to the poor solubility of **3b** in deuterated acetonitrile.

The ^{1}H NMR spectrum of **3b** showed the expected signals in the aromatic zone due to the presence of one benzene ring and one furan heterocycle. The monosubstituted benzene ring showed resonances at 7.21–7.26 (1H, multiplet, H_p), 7.39 (2H, broad triplet, H_m), 7.52–7.56 (2H, multiplet, H_o) ppm, whereas the protons of the 2,5-disubstituted furan ring (H_d and H_c) appeared as a broad doublet at 7.50 (H_d) and at 7.83 (H_c) ppm. Finally, the imine proton (–*CH*=N) was a broad singlet at 8.08 (H_e) ppm, and the N–*H* protons of the thiosemicarbazone group were also broad singlets at 10.18 (H_g) and 12.23 (H_f) ppm (Scheme 2).

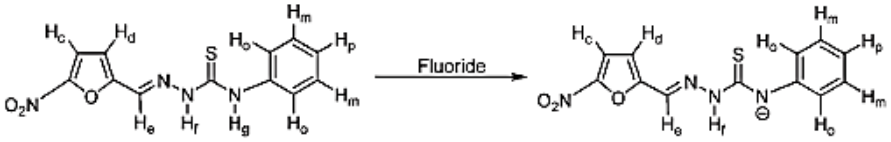

Scheme 2 Proposed mode for fluoride-induced deprotonation of receptor **3b.**

In a first step, we studied the shifts of the protons of receptor **3b** upon addition of increasing quantities of the fluoride anion. The most important fact was the disappearance of the H_f and H_g protons upon addition of 1 equiv. of fluoride. Additionally, the variation in the chemical shifts Δδ (ppm) for other protons in **3b**, during the titration with fluoride is shown in Figure 8.

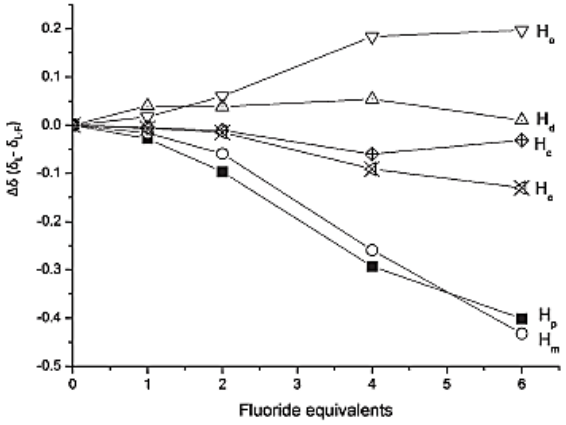

Figure 8. ^{1}H NMR shifts for the protons of receptor **3b** in the presence of increasing quantities of F^- anion (DMSO-d_6).

As seen, protons H_c, H_d and H_e showed negligible changes in their position in the NMR spectrum. In contrast, remarkable shifts were noted for H_o, H_m and H_p, suggesting that deprotonation took place in the N–H group closer to the phenyl group. It has been reported that upon the deprotonation of the N–H group, two effects might become active: (i) an increase in the electron density in the phenyl ring according to a π-mechanism, which should induce a shielding effect (an upfield shift of the C–H signals is expected), and (ii) a polarization of the C–H bonds induced by a through-space electrostatic mechanism, which is expected to cause a deshielding effect. Figure 8 shows how the H_o protons underwent important downfield shifts, indicating strong electrostatic effects due to the proximity of a negatively charged thiourea nitrogen atom. Protons H_m and H_p underwent upfield shifts as a result of the through-bond effect which, in this case, dominated (through-space effects vanished with distance). Fabbrizzi *et al*. and ourselves have observed a similar behaviour in closely related thioureas; *i.e.*, deprotonation apparently occurred in the protons of the nitrogen attached to the phenyl ring.[22]

Quantum mechanical studies

One way of describing the hydrogen bond-donating or -accepting ability of a molecule in a particular group can be accessed by gas-phase deprotonation energy studies determined by quantum chemical calculations by subtracting the energy of the receptor alone from that of the deprotonated form. For these studies, receptors **3a–f** containing furyl heterocycles were selected in order to obtain data that would be comparable. Calculations were carried out using a PM3 semi-empirical model. These thiosemicarbazone receptors contained two N–H groups and the deprotonation studies were performed by assuming that both protons could be eliminated. The data in Table 3 strongly suggest that the most acidic one was that attached to the imine carbon directly bonded to the furyl heterocycle (the more negative the value of the difference, the stronger the hydrogen-bond donor character). However, these results obtained from theoretical calculations contrast with the apparent conclusion of the ^{1}H NMR titrations, which suggested that deprotonation occurred at the H_g proton. The literature describes similar contradictory results obtained from the theoretical and experimental NMR data.[14]

Table 3. Stabilization energy of the deprotonation for receptors

	$E_{(L)} - E_{(LH)}$ (kcal mol^{-1})	
Receptor	R = N-NH-C(S)-N-Ph[a]	R = N-N-C(S)-NH-Ph[b]
3a	−5.87	−13.66
3b	−5.18	−14.56
3c	−6.16	−14.93
3d	−6.35	−14.33
3e	−6.84	−14.67
3f	−10.20	−18.86

[a] Deprotonation at the Hg proton (see Scheme 2). [b]Deprotonation at the Hf proton (see Scheme 2).

Despite this apparent contradiction, the theoretical calculations roughly agree with the chromogenic behaviour observed for the receptors. Among the compounds studied using a PM3 semi-empirical model, we can observe that the presence of an extra phenyl ring next to the furyl moiety (compounds **3c–3f**) made the receptors more acidic when compared with derivative **3a**. Moreover, the quantum mechanical studies indicate that derivative **3f** was the most acidic one. In fact, the acidity of the studied receptors followed this order **3f > 3c ~ 3e ~ 3b ~3d > 3a** (see Table 3). Basically, these data are in agreement with the chromo-fluorogenic behaviour of the receptors and with the expected basicity of anions in acetonitrile (*i.e.*, $F^- > CN^- > AcO^- > H_2PO_4^-$, Cl^-, HSO_4^-, SCN^-, NO_3^-, Br^-, I^-). Thus, the most basic anions fluoride and cyanide induced substantial spectroscopic changes for all the receptors, whereas acetate generally showed more minor changes in the optical properties of the receptors.

Electrochemical studies in the presence of fluoride

The electrochemical behaviour of receptor **3b** was studied alone (5×10^{-4} mol dm^{-3}) and in the presence of fluoride anion in acetonitrile using platinum as the working electrode and $[Bu_4N]$-$[ClO_4]$ as the supporting electrolyte (see Figure 9). Receptor **3b** showed a poorly defined irreversible oxidation band sweeping to anodic potentials at 0.7 V. Addition of 1 equiv. of fluoride induced an intensity increase, a small shift of the original oxidation band (band 1) and the appearance of a new oxidation band (band 2) at 0.2 V. Addition of 10 equiv. of fluoride enhanced the intensity of both bands. The fact that band 1 did not completely disappear with excess fluoride suggests the presence of a complex electrochemical mechanism involving both electrochemical and chemical reactions.

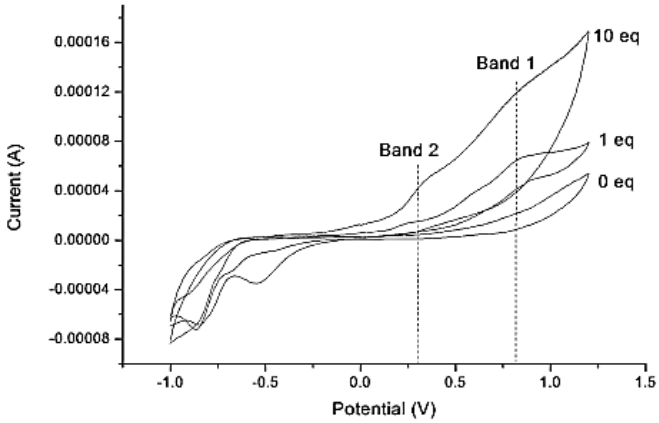

Figure 9. Cyclic voltammogram of receptor **3b** (5×10^{-4} mol dm^{-3}) in a solution of 1×10^{-2} mol dm^{-3} $[Bu_4N][ClO_4]$/acetonitrile alone (left) with 1 (centre) and 10 (right) equiv. of F^- anion at the scan rate of 20 mV s^{-1}.

Moreover, Figure 10 shows the plot showing the current of band 1 versus the equivalents of the fluoride added in the **3b** receptor. As observed, an almost linear increase took place up to 2 equiv. This behaviour is in agreement with fluoride reaction with **3b**, inducing deprotonation and the formation of the F_2H^- species.

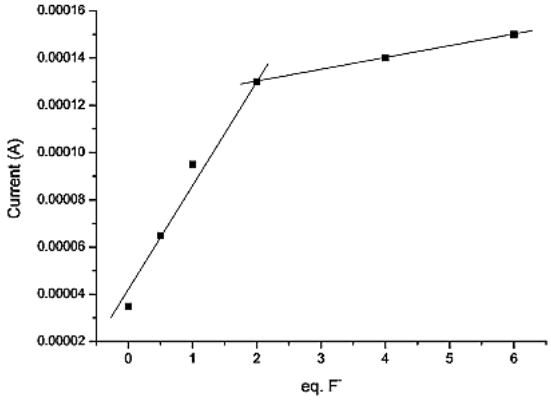

Figure 10. Current (*A*) of oxidation band 1 of **3b** *versus* the equivalents of F^- added.

3.4.3.4. Conclusions

A family of novel heterocyclic thiosemicarbazones containing furyl moieties (derivatives **3a–f** and **4**) has been prepared and characterized, and their interactions with anions have been studied *via* UV-Vis and fluorescence titrations, quantum chemical calculations and electrochemical techniques. The thiosemicarbazone dyes show a modulation of their donor hydrogen bonding abilities as a function of the electronic nature of the attached chemical groups. Two distinctive chromo-fluorogenic behaviours in the presence of anions in acetonitrile solutions are observed. The more basic anions fluoride and cyanide are capable of inducing dual coordination–deprotonation for all the receptors studied, whereas acetate and dihydrogen phosphate display poorer coordination ability and deprotonation is observed only upon the addition of large amounts of anion. Coordinative hydrogen-bonding interactions result in a slight bathochromic shift, while deprotonation is indicated by the appearance of a new band at *ca.* 400–450 nm. The fluorescence studies evidence that hydrogen-bonding interactions become visible through the enhancement of the emission band, whereas deprotonation induces the appearance of a new red-shifted emission. The PM3 studies are in agreement with the experimental behaviour. The electrochemical studies carried out with receptor **3b** show an irreversible oxidation process at 0.7 V, whereas the addition of fluoride also induces the growth of a new oxidation band at 0.2 V. The observed response toward basic anions of the receptors described in this paper clearly resembles that obtained with other derivatives containing hydrogen bonding binding sites (ureas, thioureas and amides). The selectivity trend is the same and only basic anions were able to induce a chromo-fluorogenic response. Despite the lack of response of these receptors in aqueous environments, the ease of synthesis of thiosemicarbazones opens the possibility to design more complex and pre-organized neutral receptors for anions with enhanced selectivity and applicability in aqueous environments.

3.4.3.5. Experimental section

Materials and methods

Thin-layer chromatography was carried out on 0.25 mm thick precoated silica plates (Merck Fertigplatten Kieselgel $60F_{254}$). All the melting points were measured on a Gallenkamp melting point apparatus. NMR spectra were obtained on a Varian Unity Plus Spectrometer at an operating frequency of 300 MHz for ^{1}H and 75.4 MHz for ^{13}C or with a Bruker Avance III 400 at an operating frequency of 400 MHz for ^{1}H and 100.6 MHz for ^{13}C, using the solvent peak as an internal reference. Solvents are indicated in parentheses before the chemical shift values (δ relative to TMS and given in ppm). The IR spectra were run on a FTIR Perkin-Elmer 1600 spectrophotometer in Nujol. The elemental analyses were carried out on a Leco CHNS 932 instrument. Mass spectrometry analyses were performed at the C.A.C.T.I.–Unidad de Espectrometria de Masas of the University of Vigo, Spain, in a Hewlett Packard 5989 A spectrometer for low resolution spectra and in a VG Autospec M spectrometer for high resolution mass spectra. All the solvents were of spectro-photometrical grade. Air-/water-sensitive reactions were per- formed in flame-dried glassware under argon. Aldehydes **1a–c**, **1e–f** and 4-phenyl-3-thiosemicarbazide **2** were purchased from Sigma-Aldrich and were used without further purification.

General procedure for the synthesis of formyl-furans 1d and 1g through Suzuki cross-coupling

5-Bromofuran-2-carbaldehyde (1.2 mmol) was coupled with 4-ethoxyphenylboronic acid or with 4-formylphenylboronic acid (1.6 mmol), in a mixture of DME (15 mL) and aqueous 2 mol dm^{-3} Na_2CO_3 (1 mL) and $Pd(PPh_3)_4$ (6 mol%) at 80 °C in an argon atmosphere for 5–12 h. After cooling, the mixture was filtered. Ethyl acetate and a saturated solution of NaCl were added and the phases were separated. The organic phase was washed with water (3 × 50 mL) and with an aqueous solution of NaOH (10%). The organic phase obtained was dried

($MgSO_4$), filtered and solvent removal gave a crude mixture which was submitted to column chromatography on silica with increasing amounts of diethyl ether in light petroleum as an eluent, thus affording the coupled products.

5-(4′-Ethoxyphenyl)furan-2-carbaldehyde (1d).[15] Yellow solid (75%). Mp: 120.1–122.3 °C. IR (Nujol) ν 1670 (C=O), 1608, 1291, 1254, 1119, 1041, 1029, 959, 919, 838, 797, 772 cm^{-1}. ^{1}H NMR (CDCl3) δ 1.39 (t, 3H, J = 7.2 Hz, C*H*$_3$), 4.02 (q, 2H, J = 7.2 Hz, CH2), 6.66 (d, 1H, 3H, *J* = 3.6 Hz, 4-H), 6.89 (dd, 2H, *J* = 6.4 and 2.0 Hz, H3′ and H5′), 7.25 (d, 1H, *J* = 3.6 Hz, H3), 7.69 (dd, 2H, *J* = 6.4 and 2.0 Hz, H2′ and H6′), 9.54 (s, 1H, C*H*O). ^{13}C NMR ($CDCl_3$) δ 14.54 (*C*H_3), 63.46 (CH2), 106.10 (C4), 114.17 (C3′ and C5′), 121.38 (C5), 124.32 (C3), 126.78 (C2′ and C6′), 151.37 (C2), 159.72 (C1′), 160.12 (C4′), 176.60 (CHO). MS (EI) *m/z* (%): 216 (M+, 100), 188 (93), 187 (35), 160 (33), 131 (43), 77 (17). HRMS: (EI) m/z (%) for C13H12O3; calcd 216.079; found 216.078.

5-(4′-Formylphenyl)furan-2-carbaldehyde (1g). Orange solid (91%). Mp: 124.6–126.0 °C. IR (Nujol) ν 1659 (C=O), 1602, 1309, 1157, 1117, 1093, 1020, 966, 946, 810, 722 cm^{-1}. ^{1}H NMR ($CDCl_3$) δ 7.01 (d, 1H, J = 3.6 Hz, H4), 7.36 (d, 1H, J = 3.6 Hz, H3), 7.98 (m, 4H, H2′, H6′, H3′ and H5′), 9.72 (s, 1H, CHO), 10.05 (s, 1H, CHO). ^{13}C NMR ($CDCl_3$) δ 110.0 (C4), 123.0 (C3), 125.6 (C2′ and C6′), 130.3 (C3′ and C5′), 134.1 (C1′), 136.5 (C4′), 152.7 (C2), 157.4 (C5), 177.5 (CHO), 191.3 (C*H*O). MS (EI) m/z (%): 200 (M^+, 100), 199 (84), 171 (18), 143 (23), 115 (56). HRMS: (EI) *m/z* (%) for $C_{12}H_8O_3$; calcd 200.047; found 200.048.

General procedure for the synthesis of heterocyclic phenylthiosemicarbazones 3-4

Equal amounts (0.4 mmol) of the appropriate aldehyde and thiosemicarbazide were dissolved in MeOH (30 mL) at room temperature. A solution was obtained, which was stirred overnight. Compounds were precipitated as microcrystalline solids, and were collected by suction filtration, washed with cold

MeOH and diethyl ether, then dried by vacuum. Further recrystallizations using $CHCl_3$–petroleum ether mixtures were performed when was necessary.

1-((5-Bromofuran-2-yl)methylene)-4-phenylthiosemicarbazone. 3a was obtained as a yellow solid (76%). Mp: 149.5–150.8 °C. ^{1}H NMR (DMSO-d_6): δ = 6.76 (d, *J* = 3.9 Hz, 1H, H3′), 7.10 (d, *J* = 3.9 Hz, 1H, H4′), 7.15–7.21 (m, 1H, H4), 7.34 (br t, *J* = 7.2 Hz, 2H, H3 and H5), 7.55 (br d, *J* = 7.2 Hz, 2H, H2 and H6), 7.99 (s, 1H, –C*H*=N), 9.88 (s, 1H, S=C–N*H*), 11.85 (s, 1H, C=N–N*H*) ppm. ^{13}C NMR (DMSO-d_6): δ = 114.5 (C3′), 115.6 (C4′), 124.3 (C5′), 125.3 (C4), 125.5 (C2 and C6), 128.1 (C3 and C5), 131.67 (–CH=N), 138.9 (C1), 151.4 (C2′), 175.8 (C=S) ppm. IR (Nujol) *v* 3332, 3132, 1593, 1558, 1538, 1515, 1448, 1274, 1266, 1205, 1125, 1016, 920, 781, 739, 689 cm^{-1}. $C_{12}H_{10}BrN_3OS$ (322.97): calcd C 44.46, H 3.11, N 12.96, S 9.89; found C 44.33, H 3.12, N 12.93, S 9.81.

1-((5-Nitrofuran-2-yl)methylene)-4-phenylthiosemicarbazone. 3b was obtained as a yellow solid (81%). Mp: 188.0–188.7 °C. ^{1}H NMR (DMSO-d_6): δ = 7.20–7.25 (m, 1H, H4), 7.38 (br t, *J* =7.8 Hz, 2H, H3 and H5), 7.49–7.55 (m, 3H, H3′, H2 and H6), 7.82 (d, *J* = 3.9 Hz, 1H, H4′), 8.07 (s, 1H, –C*H*=N), 10.18 (s, 1H, S=C–N*H*), 12.23 (s, 1H, C=N–N*H*) ppm. ^{13}C NMR (DMSO-d_6): δ = 113.5 (C3′), 115.2 (C4′), 125.7 (C4), 125.9 (C2 and C6), 128.2 (C3 and C5), 130.2 (–CHvN), 138.7 (C1), 151.6 (C5′), 152.6 (C2′), 176.3 (C=S) ppm. IR (Nujol) ν 3313, 3135, 1554, 1529, 1514, 1344, 1251, 1188, 1098, 1015, 964, 810, 760, 741, 693 cm^{-1}. $C_{12}H_{10}N_4O_3S$ (290.05): calcd C 49.65, H 3.47, N 19.30, S 11.05; found C 49.24, H 3.53, N 19.18, S 11.11.

4-Phenyl-1-((5-phenylfuran-2-yl)methylene)thiosemicarbazone. 3c was obtained as a yellow solid (76%). Mp: 176.0–176.8 °C. ^{1}H NMR (DMSO-d_6): δ = 7.14 (d, *J* = 3.3 Hz, 1H, H3′), 7.18–7.23 (m, 2H, H4 and H4′), 7.32–7.47 (m, 5H, H3′′, H4′′, H5′′, H3 and H5), 7.58 (br d, *J* = 7.5 Hz, 2H, H2 and H6), 7.83 (br d, *J* = 6.9 Hz, 2H, H2′′ and H6′′), 8.09 (s, 1H, –C*H*=N), 9.93 (s, 1H, SvC–NH), 11.89 (s, 1H, C=N–N*H*) ppm. ^{13}C NMR (DMSO-d_6): δ = 108.5 (C3′), 115.8 (C4′), 124.0 (C2′′ and

C6''), 125.3 (C4), 125.7 (C2 and C6), 128.1 (C3 and C5), 128.3 (C4''), 129.0 (C3'' and C5''), 129.5 (C1''), 132.4 (–*C*H=N), 139.0 (C1), 148.9 (C5'), 154.8 (C2'), 175.6 (*C*=*S*) ppm. IR (Nujol) ν 3270, 3147, 1622, 1595, 1553, 1530, 1491, 1259, 1188, 1092, 1026, 980, 922, 908, 754, 685 cm^{-1}. $C_{18}H_{15}N_3O_5S$ (321.09): calcd C 67.27, H 4.70, N 13.07, S 9.98; found C 67.19, H 4.76, N 12.91, S 9.65.

1-((5-(4-Ethoxyphenyl)furan-2-yl)methylene)-4-phenylthio-semicarbazone. **3d** was obtained as a yellow solid (78%). Mp: 178.8–179.9 °C. ^{1}H NMR (DMSO-d_6): δ = 1.32 (t, *J* = 7.2 Hz, 3H, OCH_2CH_3), 4.05 (q, *J* = 7.2 Hz, 2H, OCH_2CH_3), 6.96–7.01 (m, 3H, H3', H3'' and H5''), 7.13 (d, J = 3.6 Hz, 1H, H4'), 7.17–7.23 (m, 1H, H4), 7.37 (br t, *J* = 7.2 Hz, 2H, H3 and H5), 7.58 (br d, *J* = 7.2 Hz, 2H, H2 and H6), 7.76 (dd, *J* = 6.9 and 2.1 Hz, 2H, H2'' and H6''), 8.01 (s, 1H, –CHvN), 9.89 (s, 1H, S=C–N*H*), 11.84 (s, 1H, C=N–N*H*) ppm. ^{13}C NMR (DMSO-d_6): δ = 14.6 (OCH_2CH_3), 63.2 (OCH_2CH_3), 106.7 (C3'), 114.8 (C3'' and C5''), 116.2 (C4'), 122.2 (C1''), 125.3 (C4), 125.6 (C2 and C6), 125.7 (C2'' and C6''), 128.1 (C3 and C5), 132.5 (–*C*H=N), 139.0 (C1), 148.1 (C5'), 155.2 (C2'), 158.7 (C4''), 175.5 (*C*=S) ppm. IR (Nujol) ν 3339, 3133, 1621, 1606, 1548, 1505, 1269, 1251, 1219, 1176, 1116, 1037, 975, 919, 833, 786, 740 cm^{-1}. $C_{20}H_{19}N_3O_2S$ (365.12): calcd C 65.73, H 5.24, N 11.50, S 8.77; found C 65.23, H 5.21, N 11.49, S 8.69.

1-((5-(4-Bromophenyl)furan-2-yl)methylene)-4-phenylthio-semicarbazone. **3e** was obtained as a yellow solid (87%). Mp: 197.3–198.7 °C. ^{1}H NMR (DMSO-d_6): δ = 7.18–7.23 (m, 3H, H3', H4' and H4), 7.37 (br t, *J* = 8.0 Hz, 2H, H3 and H5), 7.58 (br d, 1H, *J* = 8.0 Hz, 2H, H2 and H6), 7.63 (dd, *J* = 6.4 and 2.0 Hz, 2H, H2'' and H6''), 7.78 (dd, *J* = 6.4 and 2.0 Hz, 2H, H3'' and H5''), 8.08 (s, 1H, –C*H*=N), 9.92 (s, 1H, S=C–N*H*), 11.89 (s, 1H, C=N–N*H*) ppm. ^{13}C NMR (DMSO-d_6): δ = 109.2 (C3'), 115.8 (C4'), 121.2 (C4''), 125.3 (C4), 125.7 (C2 and C6), 125.9 (C3'' and C5''), 128.1 (C3 and C5), 128.6 (C1''), 131.9 (C2'' and C6''), 132.2 (–CHvN), 139.0 (C1), 149.3 (C5'), 153.6 (C2'), 175.7 (*C*=S) ppm. IR (Nujol) *v* 3287, 3143, 1683, 1667, 1594, 1552, 1504, 1445, 1265, 1197, 1974, 1021, 1008, 926, 822, 785, 766, 735 cm^{-1}. MS (ESI): *m/z* (%) = 402 (M + H + ^{81}Br, 100), 400 (M + H + ^{79}Br, 100), 399 (M+,

82), 370 (41), 368 (41). HRMS (ESI): calcd for $C_{18}H_{15}{}^{81}BrN_3OS$ 402.00929, found 402.00905; calcd for $C_{18}H_{15}{}^{79}BrN_3OS$ 400.0114, found 400.0111.

1-((5-(4-Nitrophenyl)furan-2-yl)methylene)-4-phenylthiosemi-carbazone. 3f was obtained as a yellow solid (96%). Mp: 205.4–206.8 °C. ^{1}H NMR (DMSO-d_6): δ = 7.19–7.25 (m, 1H, H4), 7.28 (d, *J* = 3.9 Hz, 1H, H3′), 7.38 (br t, *J* = 7.8 Hz, 2H, H3 and H5), 7.48 (d, *J* = 3.9 Hz, 1H, H4′), 7.57 (br d, *J* = 7.8 Hz, 2H, H2 and H6), 8.05–8.11 (m, 3H, H2′′, H6′′ and –*C*H=N), 8.28 (dd, *J* = 7.2 and 2.1 Hz, 2H, H3′′ and H5′′), 9.99 (s, 1H, S=C–NH), 12.00 (s, 1H, C=N–NH) ppm. ^{13}C NMR (DMSO-d_6): δ = 112.6 (C3′), 115.7 (C4′), 124.4 (C3′′ and C5′′), 124.6 (C2′′ and C6′′), 125.5 (C4), 125.8 (C2 and C6), 128.2 (C3 and C5), 131.8 (–*C*H=N), 135.2 (C1′′), 138.9 (C1), 146.3 (C4′′), 151.0 (C5′), 152.4 (C2′), 175.8 (*C*=S) ppm. IR (Nujol) ν 3316, 3135, 1600, 1592, 1552, 1510, 1341, 1265, 1212, 1201, 1114, 1084, 1029, 809, 849, 798, 711, 693, 637 cm^{-1}. $C_{18}H_{14}N_4O_3S$ (366.08): calcd C 59.01, H 3.85, N 15.29, S 8.75; found C 58.39, H 3.92, N 15.25, S 8.77.

1,1-((5-Phenylfuran-2-yl)methylene)-bis-4-phenylthiosemicarbazone. 4 was obtained as a yellow solid (90%). Mp: 203.9–204.8 °C. ^{1}H NMR (DMSO-d_6): δ = 7.18–7.23 (m, 3H, 2 × (H4 and H4′)), 7.27 (d, *J* = 3.6 Hz, 1H, H3′), 7.37 (br t, *J* = 7.9 Hz, 4H, 2 × (H3 and H5)), 7.55–7.62 (m, 4H, 2 × (H2 and H6)), 7.88 (d, *J* = 8.4 Hz, 2H, H2′′ and H6′′), 7.97 (d, *J* = 8.4 Hz, 2H, H3′′ and H5′′), 8.10 (s, 1H, –C*H*=N), 8.16 (s, 1H, –C*H*=N), 9.96 (s, 1H, S=C–N*H*), 10.15 (s, 1H, S=C–N*H*), 11.86 (s, 1H, C=N–N*H*), 11.91 (s, 1H, C=N–N*H*) ppm. ^{13}C NMR (DMSO-d_6): δ = 109.7 (C3′), 115.9 (C4′), 124.1 (C2′′ and C6′′), 125.3 (C4), 125.4 (C4), 125.5 (C2 and C6), 126.0 (C2 and C6), 128.0 (C3 and C5), 128.1 (C3 and C5), 128.2 (C3′′ and C5′′), 130.5 (C1′′), 132.2 (–*C*H=N), 133.7 (C4′′), 138.9 (C1), 139.0 (C1), 142.2 (–*C*H=N), 149.4 (C2′), 154.3 (C5′), 175.6 (CvS), 176.0 (*C*=S) ppm. IR (Nujol) ν 3322, 3300, 3158, 1598, 1559, 1524, 1449, 1329, 1261, 1195, 1096, 1024, 943, 919, 747, 693 cm^{-1}. MS (ESI): *m/z* (%) = 499 (M + H+, 100), 467 (24), 437 (14), 415 (25), 350 (16), 298 (9). HRMS (ESI): calcd for $C_{26}H_{22}N_6OS_2$ 499.1369, found 499.1364.

Spectroscopic studies

Stock solutions of the anions (F^-, Cl^-, Br^-, I^-, NO_3^-, $H_2PO_4^-$, HSO_4^-, AcO^-, BzO^-, CN^- as tetrabutylammonium salts) were prepared at 10^{-2} and 10^{-3} mol dm^{-3} in acetonitrile. The concentrations of ligands used in these measurements were *ca.* 1.2×10^{-4} and 1.2×10^{-5} mol dm^{-3}. We took care that the maximum addition of anion solutions did not exceed 5% of the volume of the receptor to avoid significant changes in the solution concentration. In the experiments that required the addition of excess of anion (50 equiv.), corrections of the volume and concentration were made. The UV-Vis titrations were carried out at room temperature (~25 °C).

In fluorimetric titrations, all receptors were excited at wavelengths of the pseudo-isosbestic points observed in the course of UV-Vis titrations with fluoride anion. The electronic absorption spectra were obtained on a Perkin Elmer Instruments Lambda 35 UV/visible spectrometer and fluorescence spectra were recorded on a Quanta Master 40 steady state fluorescence spectrofluorometer from Photon Technology Internation (PTI) all in quartz cuvettes (1 cm). ^{1}H NMR titration spectra were acquired with a Varian 300 spectrometer.

Electrochemical studies were carried out in a GPES V 4.9 Autolab 30 system using platinum as the working and reference electrodes, a $[Bu_4N][ClO_4]$ solution (1.0×10^{-2} mol dm^{-3}) as the supporting electrolyte and a scan rate of 20 mV s^{-1} in a thermostated cell at 25 °C.

Theoretical studies

Quantum chemical calculations at the semi-empirical level (PM3, within restricted Hartree–Fock level) were carried out in vacuum with the aid of Hyperchem V6.03. The Polar–Ribiere algorithm was used for optimization. The convergence limit and the RMS gradient were set to 0.01 kcal mol^{-1}. Stability

constants were estimated with the HypSpec Software V1.1.18 using the data of the titration of receptors with selected anions.

3.4.3.6. Acknowledgements

We thank the Spanish Government (project MAT2009-14564- C04-01) and the Generalitat Valenciana (project PROMETEO/ 2009/016) for support. We are also grateful to the Fundação para a Ciência e Tecnologia (Portugal) and FEDER-COMPETE for financial support through the Centro de Química – Universidade do Minho, Project PEst-C/QUI/UI0686/2011 (F-COMP-01- 0124-FEDER-022716) and a Post-doctoral grant to R.M.F. Batista (SFRH/BPD/79333/2011). The NMR spectrometer Bruker Avance III 400 is part of the National NMR Network and was purchased within the framework of the National Program for Scientific Re-equipment, with funds from FCT. The authors are also indebted to the programme "Acções Integradas Luso-Espanholas/CRUP", for bilateral agreement number E-144/10. Thanks also go to the Fundación Carolina and UPNFM-Honduras for a doctoral grant to L.E. Santos-Figueroa and the Spanish Ministry of Science and Innovation for an FPU grant to M.E. Moragues.

3.4.3.7. References and Notes

1 (a) L. Basabe-Desmonts, D. N. Reinhoudt and M. Crego-Calama, Chem. Soc. Rev., 2007, **36**, 993–1017; (b) J. H. R. Tucker, Supramolecular Chemistry: From Molecules to Nanomaterials, ed. P. A. Gale and J. W. Steed, 2012, vol. 5, pp. 2523–2537; (c) R. Martínez-Máñez, F. Sancenón, M. Hecht, M. Biyikal and K. Rurack, Anal. Bioanal. Chem., 2011, **399**, 55–74; (d) S. Karuppannan and J.-C. Chambron, Chem.– Asian J., 2011, 6, 964–984.

2 (a) V. Amendola, M. Bonizzoni, D. Estebán-Gómez, L. Fabbrizzi, M. Licchelli, F. Sancenón and A. Taglietti, Coord. Chem. Rev., 2006, **250**, 1451–1470; (b) C. Suksai and T. Tuntulani, Chem. Soc. Rev., 2003, **32**, 192–202.

3 (a) E. M. Nolan and S. J. Lippard, Chem. Rev., 2008, **108**, 3443–3480; (b) M. Formica, V. Fusi, L. Giorgi and M. Micheloni, Coord. Chem. Rev., 2012, **256**, 170–192; (c) P. Pallavicini, Y. A. Diaz-Fernandez and L. Pasotti, Coord. Chem. Rev., 2009, **253**, 2226–2240.

4 (a) R. Martínez-Máñez and F. Sancenón, Chem. Rev., 2003, **103**, 4419–4476; (b) M. E. Moragues, R. Martínez-Máñez and F. Sancenón, Chem. Soc. Rev., 2011, **40**, 2593–2643; (c) R. Martínez-

Máñez, F. Sancenón, M. Biyikal, M. Hecht and K. Rurack, J. Mater. Chem., 2011, **21**, 12588–12604.

5 (a) R. Martínez-Mañéz and F. Sancenón, Coord. Chem. Rev., 2006, **250**, 3081–3093; (b) A. P. Davis, Coord. Chem. Rev., 2006, **250**, 2939–2951; (c) E. García-España, P. Díaz, J. M. Llinares and A. Bianchi, Coord. Chem. Rev., 2006, **250**, 2952–2986; (d) E. A. Katayev, Y. A. Ustynyuk and J. L. Sessler, Coord. Chem. Rev., 2006, **250**, 3004–3037; (e) J. M. Lloris, R. Martínez-Máñez, M. E. Padilla-Tosta, T. Pardo, J. Soto, P. D. Beer and J. Cadman, J. Chem. Soc., Dalton Trans., 1999, 2359–2369; (f) B. García-Acosta, R. Martínez-Máñez, F. Sancenón, J. Soto, K. Rurack, M. Spieles, E. García-Breijo and L. Gil, Inorg. Chem., 2007, **46**, 3123–3135.

6 (a) P. A. Gale, Acc. Chem. Res., 2006, 39, 465–475; (b) J. Yoon, S. K. Kim, N. J. Singh and K. S. Kim, Chem. Soc. Rev., 2006, **35**, 355– 360; (c) P. Blondeau, M. Segura, R. Pérez-Fernández and J. de Mendoza, Chem. Soc. Rev., 2007, **36**, 198–210.

7 (a) F. Li, S. Carvalho, R. Delgado, M. G. B. Drew and V. Félix, Dalton Trans., 2010, **39**, 9579–9587; (b) Y.-S. Lin, G.-M. Tu, C.-Y. Lin, Y.-T. Chang and Y.-P. Yen, New J. Chem., 2009, **33**, 860–867.

8 For recent papers of thiourea-based anion receptors see: (a) D. Makuc, J. R. Hiscock, M. E. Light, P. A. Gale and J. Plavec, J. Org. Chem., 2011, 7, 1205–1214; (b) Y.-S. Lin, J.-X. Zheng, Y.-K. Tsui and Y.-P. Yien, Spectrochim. Acta, Part A, 2011, **79**, 1552–1558; (c) M. O. Odago, D. M. Colabello and A. J. Lees, Tetrahedron, 2010, **66**, 7465–7471; (d) P. A. Gale, S. E. García-Garrido and J. Garric, Chem. Soc. Rev., 2008, **37**, 151–190; (e) S. Devaraj, D. Saravanakumar and M. Kandaswamy, Sens. Actuators, B Chem., 2009, **136**, 13–19; (f) Z. Li, F.-Y. Wu, L. Guo, A.-F. Li and Y. B. Jiang, J. Phys. Chem. B, 2008, **112**, 7071–7079; (g) J. V. Ros-Lis, R. Martínez-Máñez, F. Sancenón, J. Soto, K. Rurack and H. Weißhoff, Eur. J. Org. Chem., 2007, **17**, 2449–2458.

9 For recent examples see: (a) J. Krishnamurthi, T. Ono, S. Amemori, H. Komatsu, S. Shinkai and K. Sada, Chem. Commun., 2011, **47**, 1571– 1573; (b) P. Piątek, Chem. Commun., 2011, **47**, 4745–4747; (c) X. He, F. Herranz, E. C.-C. Cheng, R. Vilar and V. W.-W. Yam, Chem.–Eur. J., 2010, **16**, 9123–9131.

10 (a) D. Esteban-Gómez, L. Fabbrizzi and M. Licchelli, J. Org. Chem., 2005, 70, 5717–5720; (b) L. S. Evans, P. A. Gale, M. E. Light and R. Quesada, New J. Chem., 2006, **30**, 1019–1025; (c) L. S. Evans, P. A. Gale, M. E. Light and R. Quesada, Chem. Commun., 2006, 965–967; (d) G. Jakab, C. Tancon, Z. Zhang, K. M. Lippert and P. R. Schreiner, Org. Lett., 2012, **14**, 1724–1727.

11 (a) S. P. G. Costa, R. M. F. Batista, P. Cardoso, M. Belsley and M. M. M. Raposo, Eur. J. Org. Chem., 2006, 17, 3938–3946; (b) M. M. M. Raposo, M. C. R. Castro, P. Schellenberg, A. M. C. Fonseca and M. Belsley, Tetrahedron, 2011, 67, 5189– 5198.

12 (a) J. Withnall, J. Howard, P. Ponka and D. R. Richardson, Proc. Natl. Acad. Sci. U. S. A., 2006, **103**, 14901–14906; (b) H.-J. Zhang, X. Qin, K. Liu, D.-D. Zhu, X.-M. Wang and H. L. Zhu, Bioorg. Med. Chem., 2011, **19**, 5708–5715.

13 (a) Y.-P. Tian, C.-Y. Duan, C.-Y. Zhao and X.-Z. You, Inorg. Chem., 1997, **36**, 1247–1252; (b) R. Ramachandran, M. Rani and S. Kabilan, Bioorg. Med. Chem., 2009, **19**, 2819–2823.

14 (a) M. M. M. Raposo, B. García-Acosta, T. Ábalos, P. Calero, R. Martínez-Máñez, J. V. Ros-Lis and J. Soto, J. Org. Chem., 2010, **75**, 2922–2933; (b) V. Amendola, M. Boiocchi, L. Fabbrizzi and L. Mosca, Chem.–Eur. J., 2008, 14, 9683–9696; (c) L. E. Santos-Figueroa, M. E. Moragues, M. M. M. Raposo, R. M. F. Batista, R. C. M. Ferreira, S. P. G. Costa, F. Sancenón, R. Martínez-Máñez, J. Soto and J. V. Ros- Lis, Tetrahedron, **68**, 7179–7186.

15 A. Mitsch, P. Wissner, K. Silber, P. Haebel, I. Sattler, G. Klebe and M. Schlitzer, Bioorg. Med. Chem., 2004, 12, 4585–4600.

16 For recent examples see: (a) A. Aldrey, C. Núñez, V. García, R. Bastida, C. Lodeiro and A. Macías, Tetrahedron, 2010, **66**, 9223–9230; (b) A. K. Atta, I.-H. Ahn, A.-Y. Hong, J. Heo, C. K. Kim and D.-G. Cho, Tetrahedron Lett. 2012, **53**, 575–578; (c) V. Amendola, L. Fabbrizzi, L. Mosca and F.-P. Schmidtchen, Chem.–Eur. J., 2011, **17**, 5972–5981; (d) V. Amendola, G. Bergamaschi, M. Boiocchi, L. Fabbrizzi and M. Milani, Chem.–Eur. J., 2010, **16**, 4368–4380.

17 For recent examples see: (a) T. H. Kim, M. S. Choi, B.-H. Sohn, S.-Y. Park, W. S. Lyoo and T. S. Lee, Chem. Commun., 2008, 2364–2366; (b) V. Amendola and L. Fabbrizzi, Chem. Commun., 2009, 513–531; (c) C. Caltagirone, A. Mulas, F. Isaia, V. Lippolis, P. A. Gale and M. A. Light, Chem. Commun., 2009, 6279–6281; (d) C. Pérez-Casas and A. K. Yatsimirsky, J. Org. Chem., 2008, **73**, 2275–2284; (e) C. M. G. dos Santos, T. McCabe, G. W. Watson, P. E. Kruger and T. Gunnlaugsson, J. Org. Chem., 2008, **73**, 9235–9244; (f) P. Dydio, T. Zielinski and J. Jurczak, J. Org. Chem., 2009, **74**, 1525–1530; (g) Z. Xu, S. K. Kim, S. J. Han, C. Lee, G. Kociok-Kohn, T. D. James and J. Yoon, Eur. J. Org. Chem., 2009, 3058–3065.

18 V. Amendola, D. Esteban-Gómez, L. Fabbrizzi and M. Licchelli, Acc. Chem. Res., 2006, **39**, 343–353.

19 M. Boiocchi, L. Del Boca, D. Estebán-Gómez, L. Fabbrizzi, M. Licchelli and E. Monzani, J. Am. Chem. Soc., 2004, **126**, 16507–16514.

20 M. Boiocchi, L. Del Boca, D. Estebán-Gómez, L. Fabbrizzi, M. Licchelli and E. Monzani, Chem. – Eur. J., 2005, **11**, 3097–3104.

21 D. Esteban-Gómez, L. Fabbrizzi, M. Licchelli and E. Monzani, Org. Biomol. Chem., 2005, **3**, 1495–1500.

22 M. Bonizzoni, L. Fabbrizzi, A. Taglietti and F. Tiengo, Eur. J. Org. Chem., 2006, 3567–3574.

3.4.3.8. Supporting information

Synthesis and Evaluation of Thiosemicarbazones Functionalized with Furyl Moieties as New Chemosensors for Anion Recognition.

Luis E. Santos-Figueroa, María E. Moragues, M. Manuela M. Raposo, Rosa M. F. Batista, Susana P. G. Costa, R. Cristina M. Ferreira, Félix Sancenón, Ramón Martínez-Máñez, José Vicente Ros-Lis and Juan Soto.

I. Characterization data of receptors 3a-f and 4 by ^{1}HNMR and IR

Table 1. Yields, ^{1}H NMR and IR data of furyl-thiosemicarbazone receptors **3a-f** and **4**.

Formyl precursor	Receptor	Yield (%)	δH (ppm)[a]			IRb ν (cm-1)	
			(C*H*=N)	(C=N-N*H*)	(S=C-N*H*)	(CH=N)	(NH)
1a	**3a**	76	7.99	11.85	9.88	3132	3332
1b	**3b**	81	8.07	12.23	10.18	3135	3313
1c	**3c**	76	8.09	11.89	9.93	3147	3270
1d	**3d**	78	8.01	11.84	9.89	3133	3339
1e	**3e**	87	8.08	11.89	9.92	3143	3287
1f	**3f**	96	8.11	12.00	9.99	3135	3316
1g	**4**	90	8.10	11.86	10.15	3158	3322

[a] For the NH proton of the furyl-thiosemicarbazone receptors **3a-f** and **4** (300 or 400 MHz, DMSO-*d6*). b IR recorded in Nujol.

II. UV–Vis titration of receptors 3a-f and 4 (1.2×10^{-5} mol dm^{-3}) with fluoride (left) and acetate (rigth) anions (0 - 10 equiv.) in acetonitrile.

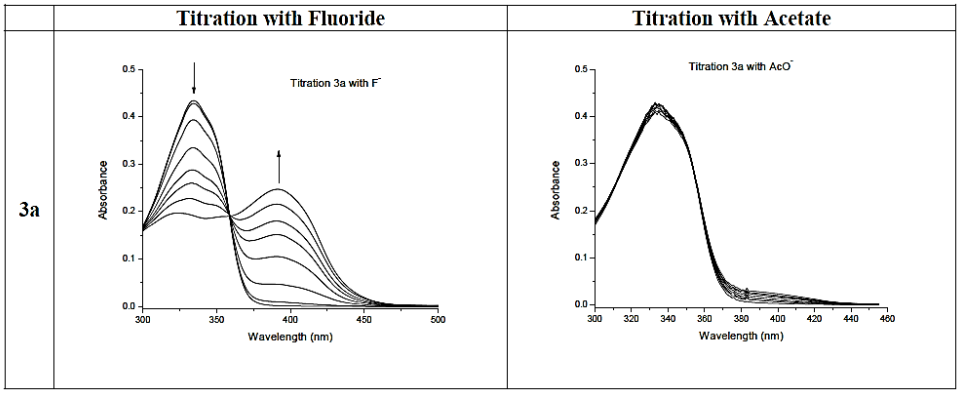

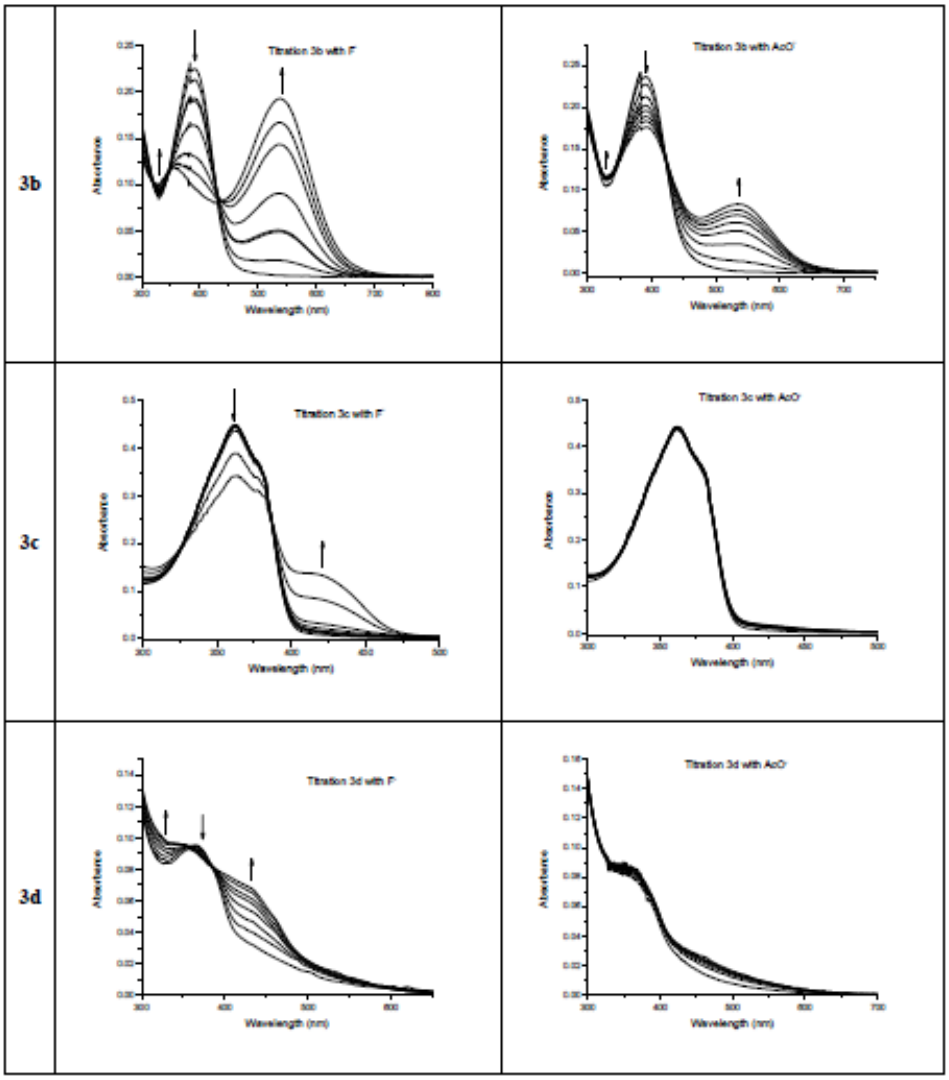
3b
Titration 3b with F
Absorbance
Wavelength (nm)
Titration 3b with AcO
Absorbance
Wavelength (nm)
3c
Titration 3c with F
Absorbance
Wavelength (nm)
Titration 3c with AcO
Absorbance
Wavelength (nm)
3d
Titration 3d with F
Absorbance
Wavelength (nm)
Titration 3d with AcO
Absorbance
Wavelength (nm)

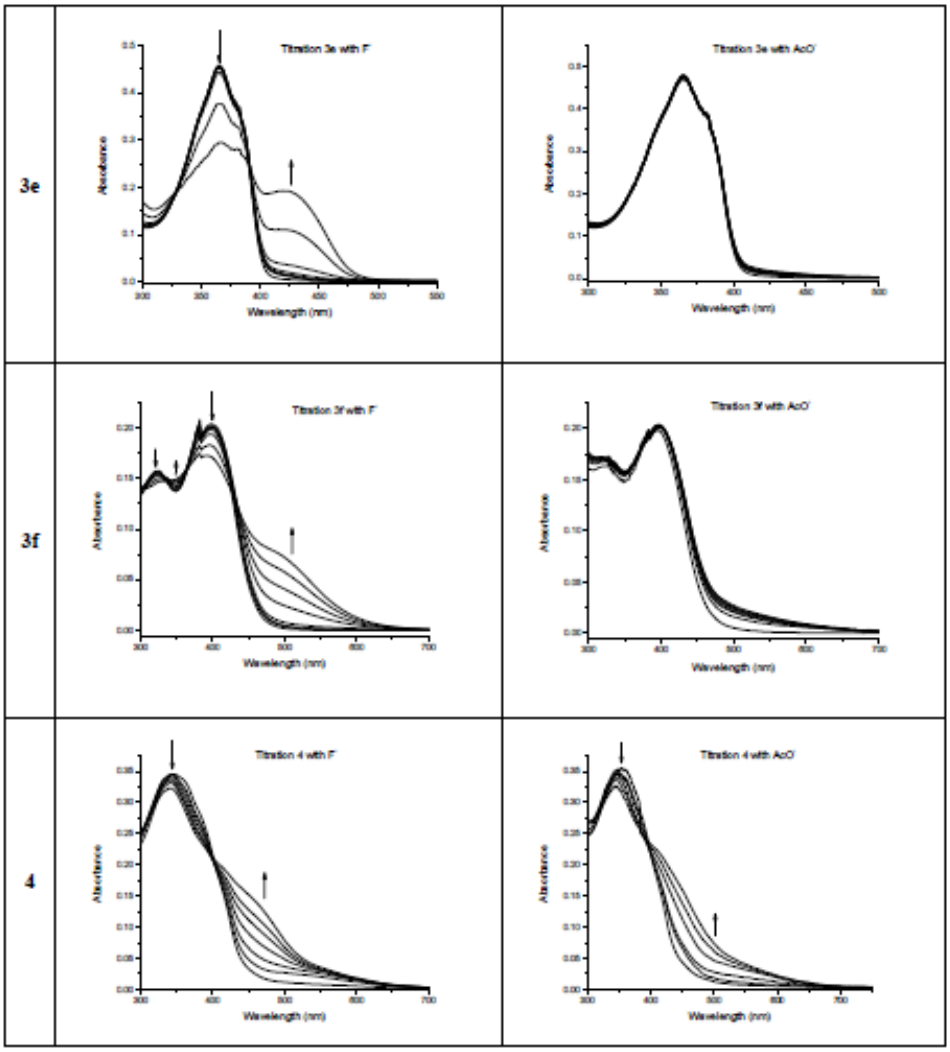
3e
Titration 3e with F⁻
Titration 3e with AcO⁻
3f
Titration 3f with F⁻
Titration 3f with AcO⁻
4
Titration 4 with F⁻
Titration 4 with AcO⁻
Absorbance
Wavelength (nm)

III. Study of selectivity of 3b (1 x 10^{-5} mol dm^{-3}) for F^- (10 equiv.) in presence of 10 equiv. of other anions (Br^-, Cl^-, ClO_4^-, HSO_4^-, I^- and NO_3^-) evaluated.

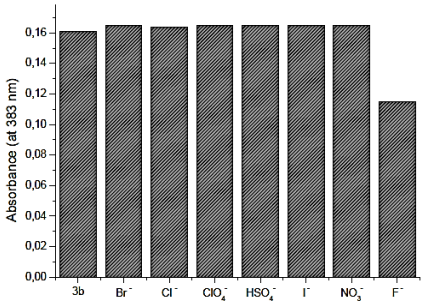

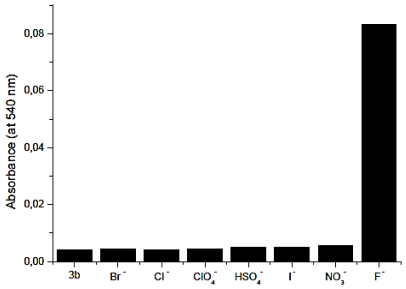

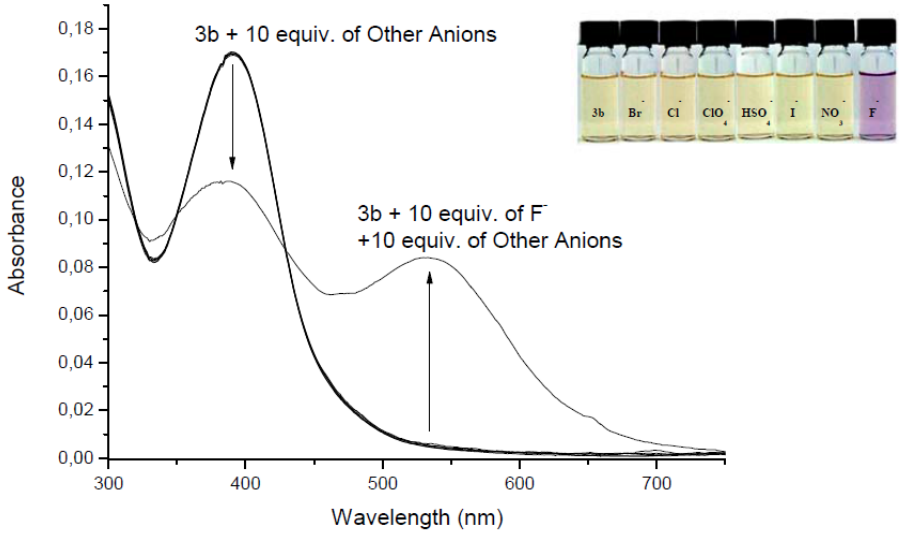

IV. Schematic representation of the dual coordination/deprotonation process for the interaction of thiosemicarbazone receptors with basic anions.

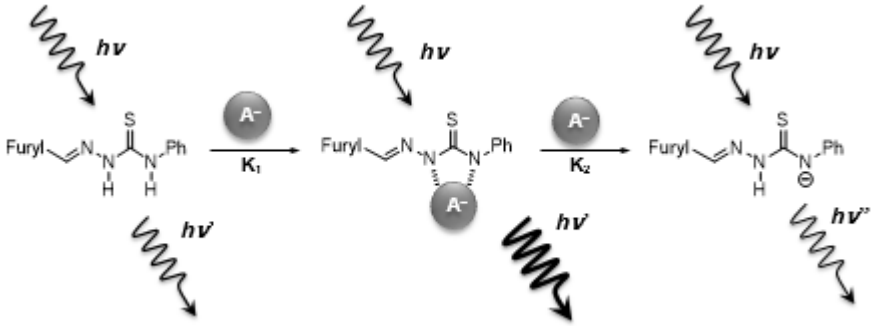

V. UV-Vis kinetic study of 3b (wavelength at 390 nm) with 10 equiv. of fluoride anion in acetonitrile, from 0 to 10 min of interaction.

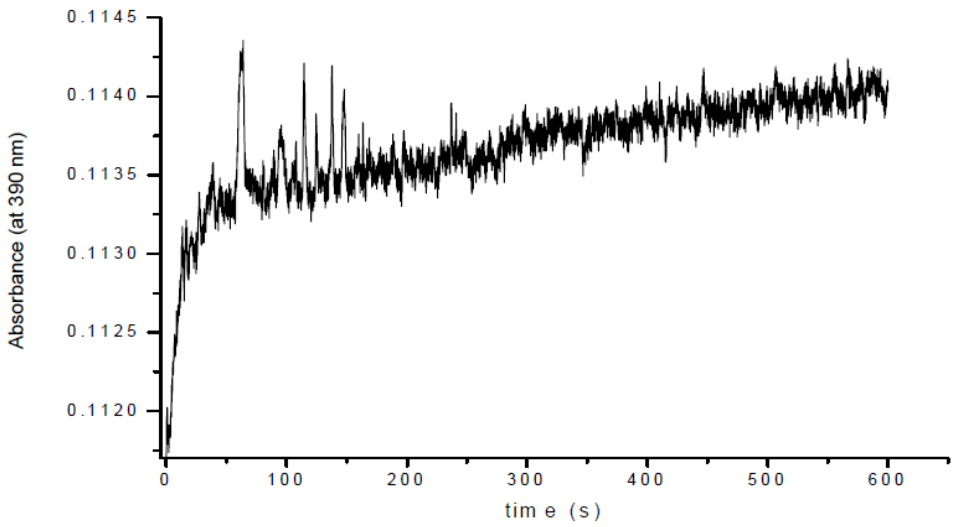

3.4.4. Synthesis and evaluation of fluorimetric and colorimetric chemosensors for anions based on (oligo)thienyl-thiosemicarbazones

Following with the study of thiosemicarbazone-based chemosensors, the results of synthesis and evaluation of a second family of thiosemicarbazone-based probes functionalized with thienyl moieties for chromo-fluorogenic sensing of anions is presented (Figure 33).

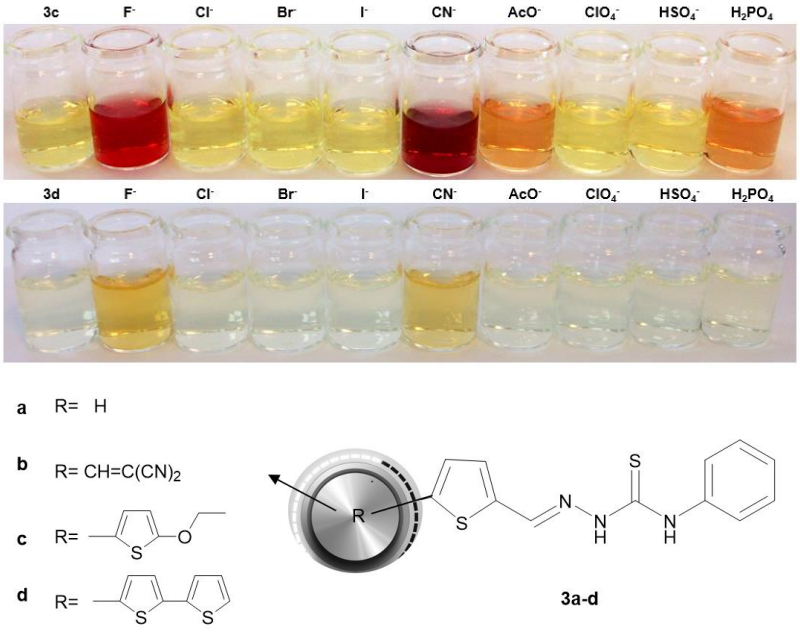

Figure 33. Schematic representation of (oligo)thienyl-thiosemicarbazones family for anions sensing.

Synthesis and evaluation of fluorimetric and colorimetric chemosensors for anions based on (oligo)thienyl-thiosemicarbazones

Luis E. Santos-Figueroa, [a, b, c] María E. Moragues, [a, b, c] M. Manuela M. Raposo, [d]* Rosa M. F. Batista, [d] R. Cristina M. Ferreira, [d] Susana P. G. Costa, [d] Félix Sancenón, Ramón Martínez-Máñez, [a, b, c]* Juan Soto [a, b] and José Vicente Ros-Lis [a, b, c]

[a] Instituto de Reconocimiento Molecular y Desarrollo Tecnológico (IDM), Centro Mixto Universidad Politécnica de Valencia-Universidad de Valencia (Spain)

[b] Departamento de Química, Universidad Politécnica de Valencia, Camino de Vera s/n, 46022 Valencia (Spain)

[c] CIBER de Bioingeniería, Biomateriales y Nanomedicina (CIBER- BBN)

[d] Centro de Química, Universidade do Minho, Campus de Gualtar, 4710-057 Braga, Portugal.

Received: March 29, 2012

Published online: June 15, 2012

Tetrahedron, **2012**, 68, 7179–7186

(Reproduced with permission of Elsevier Ltd.)

3.4.4.1. Abstract

A family of heterocyclic thiosemicarbazone dyes (**3a-d**) containing thienyl groups has been synthesized, characterized, and their chromo-fluorogenic response in acetonitrile in the presence of selected anions was studied. Acetonitrile solutions of **3a-d** show absorption bands in the 338-425 nm range, which are modulated by the groups attached to the thiosemicarbazone moiety. The fluoride, chloride, bromide, iodide, dihydrogen phosphate, hydrogen sulfate, nitrate, acetate, and cyanide anions were used in the recognition studies. Only sensing features were observed for fluoride, cyanide, acetate, and dihydrogen phosphate anions. Two different chromogenic responses were found, (i) a small shift of the absorption band due to coordination of the anions with the thiourea protons and (ii) the appearance of a new red-shifted band due to deprotonation of the receptor. For the latter process changes in the color solutions from pale-yellow to orange-red were observed. Fluorescence studies showed a different emission behavior according to the number of thienyl rings in the π-conjugated bridges. Stability constants for the two processes (complex formation+deprotonation) for receptors **3a-d** in the presence of fluoride and acetate anions were determined from spectrophotometric titrations using the HypSpec program. The interaction of **3d** with fluoride was studied through ^{1}H NMR titrations. Semiempirical calculations to evaluate the hydrogen-donating ability of the receptors were also performed.

3.4.4.2. Introduction

The development of new molecular-based receptors able to detect anions, cations, or neutral molecules has recently gained significance due to the importance of detecting some target species in biological and environmental samples. In these systems the receptors are able to transform host-guest interactions into a measurable signal, which allows analyte sensing via electrochemical or optical modulations.[1] In this field, apart from the interest in

developing fluorescent probes, chromogenic sensing has gained attention due to the possible semi-quantitative detection to the 'naked-eye' or using very simple instrumentation.[2] Optical chemosensors for metal cations have been developed for more than two decades,[3] whereas in contrast anionic chromogenic probes have only recently been investigated.[4,5] In particular, the supramolecular chemistry of anions has advanced a great deal in the last years and today a number of receptors for anion binding have been described.

In most cases they are based on hydrogen bonding, electrostatic interactions or coordination with suitable metal complexes.[6] In this area hydrogen bonding ligands are attractive because show the advantage of being directional allowing discrimination between anions of different hydrogen-bonding requirements or geometries.[7] Among neutral anion binding groups thioureas and thiourea-containing fragments have been widely used for the formation of complexes with anions.[8] In particular thiourea derivatives have been intensively studied as anion receptors and a number of ligands containing different number of thiourea moieties and thioureido NH protons with different acidities have been described.[9] A means of tuning the acidity of thioureido NH protons is to introduce electron-donating or electron-withdrawing substituents.[10]

On the other hand, among molecules containing thiourea fragments the use of thiosemicarbazones has gained interest recently as potential receptors. For instance Schiff-base compounds containing thiosemicarbazone groups have also grown in the areas of biology and chemistry due to their fungicidal, bactericidal, antiviral,[11] and antitumor properties.[12] Recently, we have demonstrated that (oligo)thiophenes, electronically connected to recognition sites, are efficient π-conjugated bridges for the fluorimetric and/or colorimetric sensing of certain anions (e.g., F^-, CN^-) and cations (H^+,Na^+,Pd^{2+},Cu^{2+},Zn^{2+},Hg^+,Ni^{2+}).[13] Moreover recently thiosemicarbazones have also gained attention as anion receptors. In fact we and others have recently demonstrated that π-conjugated heterocyclic

derivatives, containing thiosemicarbazone moieties are suitable systems for the colorimetric and fluorimetric sensing of anions.[14]

Taking into account our interest in the development of probes for anions and inspired in this previous work on the use of thiosemicarbazones as binding sites we report herein the synthesis and characterization of new (oligo)thienyl-thiosemicarbazones. These derivatives contain heteroaromatic π-conjugated systems (instead of the more commonly used aryl groups) and have been tested as anion chemosensors.

3.4.4.3. Results and discussion

Synthesis and characterization

The new compounds **3a–d** with thiophene, bithiophene, and terthiophene π-conjugated bridges were synthesized in moderate to good yields (41-77%) through Schiff-base condensation of heterocyclic aldehydes **1a–d** with 4-phenyl-3-thiosemicarbazide **2** in methanol at room temperature (see Scheme 1).

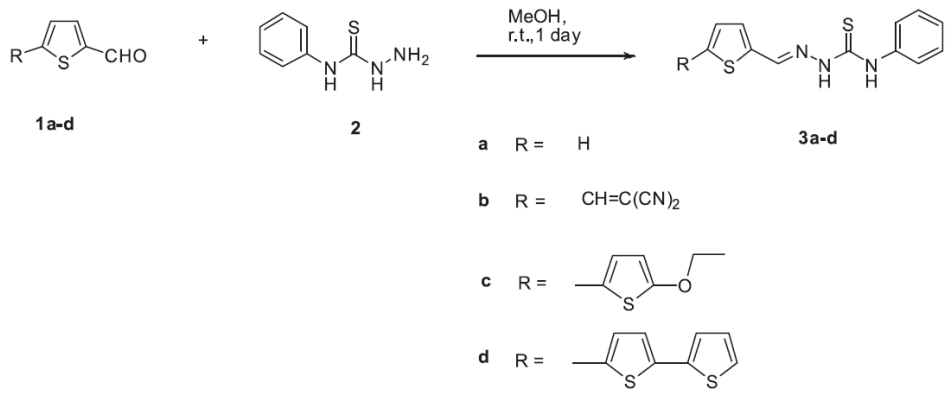

Scheme 1. Synthesis of the thienyl-thiosemicarbazone receptors **3a-d**.

Aldehyde **1a** was commercially available whereas aldehydes **1c** and **1d** were synthesized as reported elsewhere.[15] The 2-((5-formylthien-2-yl)methylene)malononitrile **1b** was synthesized through reaction of thiophene-2,5-dicarbaldehyde with malononitrile in dry DMF with a catalytic amount of piperidine. Purification of the crude product by column chromatography on silica with increasing amounts of diethyl ether in light petroleum as eluent, gave the pure compound in 22% yield. All the compounds were completely characterized by ^{1}H and ^{13}C NMR, IR, MS, EA or HRMS and the data obtained were in full agreement with the proposed formulation (see Table 1).

Table 1. Yields, ^{1}H NMR, and IR data of the oligothienyl-thiosemicarbazone receptors **3a-d**

Formyl thiophene	Product	Yield (%)	δ_H (ppm)[a]			IR[b] ν(cm^{-1})	
			(CH=N)	(C=N–NH)	(S=C–NH)	(=C–H)	(NH)
1a	**3a**	66	8.14	10.29	9.11	3141	3297
1b	**3b**	77	8.02	9.60	9.07	3122	3341
1c	**3c**	50	8.07	10.49	9.09	3127	3329
1d	**3d**	41	7.97	9.35	9.09	—	3310

[a] For the NH proton of the (oligo)thienyl-thiosemicarbazone receptors **3a–d** (300 MHz, $CDCl_3$).

[b] IR was recorded in Nujol.

The most characteristic signals in the ^{1}H NMR spectrum of this family of thiosemicarbazones were those corresponding to N–H and CH=N protons. ^{1}H NMR studies in deuterated chloroform showed CH=N protons in the 7.97-8.14 ppm range whereas thiourea-N–H protons were found in the 9.07–9.11 and 9.35–10.49 ppm interval for N–H adjacent to the phenyl ring and for the N–H adjacent to the CH=N moiety, respectively. When four compounds are considered the highest variation in δ were found for the N–H protons located in the vicinity of the CH=N moiety adjacent to thiophene (Δδ=0.94 ppm). Moreover, the N – H protons adjacent to the phenyl ring were the less affected (Δδ=0.04 ppm).

Spectroscopic behaviour of 3a–d

Acetonitrile solutions (C=1.2x10^{-5} mol dm^{-3} at 25 ^{o}C) of the thiosemicarbazone-functionalized receptors **3a–d** showed an intense absorption band (log ε ≈ 4.4) in the 338–425 nm region (see Table 2). Compound **3a** containing thiosemicarbazone moiety surrounded by a phenyl and a thienyl ring, showed an absorption band at 338 nm. The change of a hydrogen at the thienyl ring by a better electron acceptor moiety, such as a dicyanovinyl group (receptor **3b**) induced a red shift from 338 to 425 nm. The presence of one more thienyl group and an electron donor, such as an ethoxy group (receptor **3c**) induced a small red shift when compared with **3a** from 338 to 381 nm. Moreover the presence of two additional thienyl rings on the framework of **3a** (receptor **3d**) induced a bathochromic shift of the band (from 338 to 396 nm), which is most likely a consequence of the extension of the conjugation.

Table 2. Spectroscopic data for compounds **3a-d.**

Receptor	λ_{ab} LH (nm)	λ_{ab} L$^-$ (nm) [a]	Log ε (LH)	λ_{em} LH (nm)	$\Delta\lambda_{em}$ L$^-$ (nm) [a]	Φ	$\Delta\lambda_{ab-em}$ LH (nm)	$\Delta\nu_{ab-em}$ LH (cm^{-1})
3a	338	397	4.25	439	447	0.0064	101	6806
3b	425	626	4.35	560	539	0.0019	135	5672
3c	381	515	4.51	483	482	0.065	102	5542
3d	396	503	4.39	489	517	0.088	93	4802

[a] Measured upon addition of 100 equiv of fluoride anion.

UV-Vis studies involving anions

The UV−vis behavior of receptors **3a–d** in acetonitrile solutions (C=1.2x10^{-5} mol dm^{-3}) was studied at 25 ^{o}C in the presence of the fluoride, chloride, bromide, iodide, cyanide, nitrate, acetate, perchlorate, hydrogen sulfate, and dihydrogen phosphate anions. For all the receptors the presence (up to 100 equiv) of chloride, bromide, iodide, hydrogen sulfate, and nitrate induced insignificant changes in the UV–vis spectra strongly suggesting that no coordination takes place. This behavior

contrasts with that observed in the presence of basic anions, such as fluoride, cyanide, acetate, and dihydrogen phosphate (see Fig. 1).

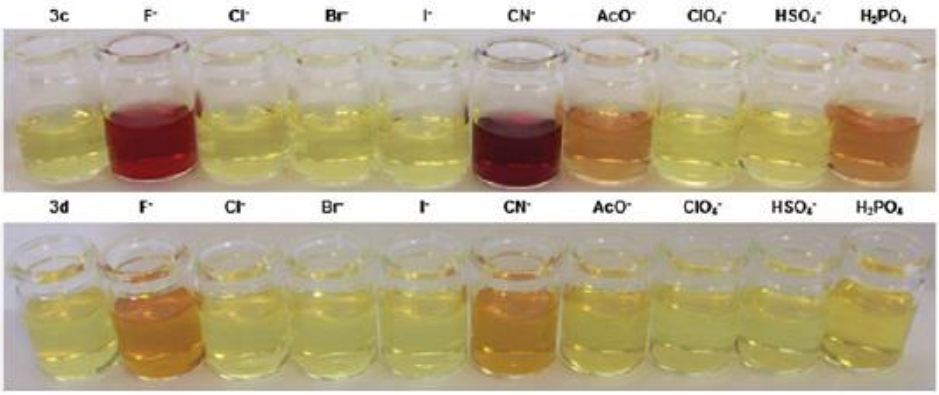

Figure 1. Color changes of **3c** (top) and **3d** (bottom) solution ($5x10^{-4}$ mol dm^{-3}) seen in the presence of 10 equiv of F^-, Cl^-, Br^-, I^-, CN^-, AcO^-, ClO_4^-, HSO_4^- and $H_2PO_4^-$.

For instance UV – vis titrations of receptors **3a-d** with fluoride showed an intensity decrease and a small bathochromic shift of the absorption band together with a simultaneous growth of a new red-shifted band. Moreover both the position of the new band and the relative intensity of the absorption band of the receptor with respect to the band upon addition of fluoride were dependent on the receptor used. For instance, the behavior observed in the presence of F^- for receptors **3c** and **3d** is shown in Figures 2 and 3.

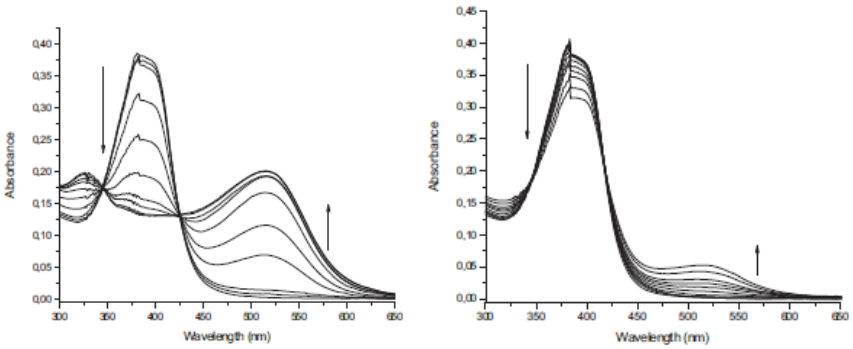

Figure 2. UV-vis titration of receptors **3c** ($1.2x10^{-5}$ mol dm^{-3}) with fluoride (left) and acetate (right) anions (0-30 equiv) in acetonitrile.

Receptor **3c** in acetonitrile was yellow due to the band at 381 nm. Upon addition of increasing quantities of fluoride this band progressively decreased while a new absorption at 515 nm (Δλ=134 nm) increased in intensity (see left of Figure 2). This induced a color modulation from pale-yellow to orange. This was in agreement with the expectation that the coordination of an anion in a donor group in a push-pull system will induce a bathochromic shift. Receptor **3d** showed a similar behavior with fluoride; i.e., the band at 396 nm suffered a small hypochromic effect and a new absorption band at 503 nm (Δλ=107 nm) grew in intensity (see left of Figure 3). As can be seen, it is apparent from the figure that the ratio between both bands was different for receptors **3c** and **3d**. Also it was clear that for a certain receptor the change observed depends on the anion used in the titration experiments. It was observed that fluoride and cyanide anions induced UV – vis changes for all the receptors whereas acetate and hydrogen phosphate displayed a poorer response and only gave noticeable changes with **3b** and **3c** (see for instance the right of Figures 2 and 3). When receptors **3a** and **3d** were compared it was found that **3a** was able to induce some changes with acetate, although to a much lesser extent than **3b** and **3c**.

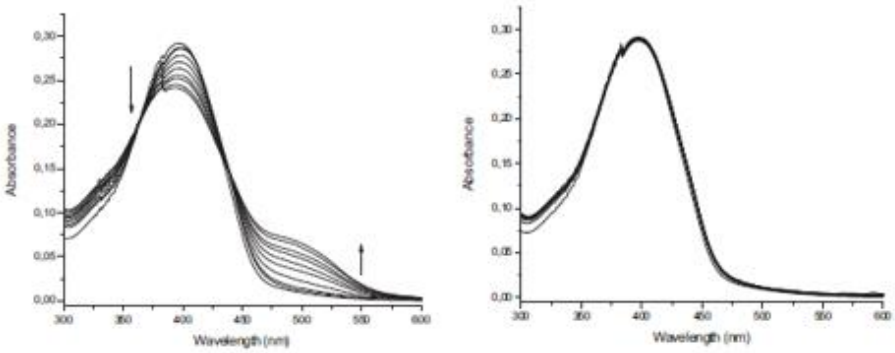

Fig. 3. UV-vis titration of receptors **3d** (1.2×10^{-5} mol dm^{-3}) with fluoride (left) and acetate (right) anions (0-30 equiv) in acetonitrile.

The changes observed in the UV–vis spectrum upon fluoride addition were attributed to the formation of hydrogen-bonding complexes with the thiosemicarbazone groups that eventually resulted in a deprotonation.[16,17] The formation of hydrogen-bonding complexes was reflected in relatively small variations in the absorption band of the receptor whereas deprotonation processes was related with the appearance of a new absorption band at longer wavelengths.[18]

Moreover a close view of the results indicated that the final response of the receptors **3a-d** towards the tested anions is dependent on the functional groups attached to the thiosemicarbazone group that modulated the acidity of the N–H protons. In our case the UV-vis studies suggested that the acidity of the receptors follows the order **3b>3c>3a>3d**. In fact, whereas **3b** and **3c** were able to display color changes (deprotonation) with fluoride, cyanide, acetate and dihydrogen phosphate, receptors **3a** and **3d** only showed significant color modulations in the presence of fluoride and cyanide.

Stability constants

As stated above, in the interaction of basic anions with the semithiocarbazone-containing receptors **3a-d** two different behaviors were observed: (i) hydrogen bonding interactions and (ii) deprotonation (see Eqs. 1 and 2). In order to complete the characterization of **3a-d** coordination and deprotonation processes were studied via the evaluation of the corresponding stability constants that were determined by UV – vis spectroscopic titrations between receptors **3a-d** and the fluoride and acetate anions, using the software HypSpec V1.1.18. The obtained data were adjusted to two consecutive equilibriums corresponding to coordination and deprotonation (see Eqs. 1 and 2) and the results are shown in Table 3.

$$\mathrm{LH} + \mathrm{A}^- \rightleftarrows \mathrm{LH}\cdots\mathrm{A}^- \qquad (1)$$

$$\mathrm{LH}\cdots\mathrm{A}^- + \mathrm{A}^- \rightleftarrows \mathrm{L}^- + \mathrm{A_2H}^- \qquad (2)$$

Table 3. Logarithms of the stability constants measured for the interaction of receptors 3a-d with fluoride and acetate

	F^-		AcO^-	
	$LH+A^- \leftrightarrows LH\cdots A^-$	$LH\cdots A^-+A^- \leftrightarrows L^-+A_2H^-$	$LH+A^- \leftrightarrows LH\cdots A^-$	$LH\cdots A^-+A^- \leftrightarrows L^-+A_2H^-$
3a	3.46(4)	2.75(3)	1.29(3)	[a]
3b	5.39(8)	4.19(4)	3.46(2)	1.52(7)
3c	3.62(6)	2.06(8)	2.36(5)	0.48(2)
3d	3.55(6)	1.06(6)	[a]	[a]

[a]No reliable results were obtained.

From Table 3 it can be observed that, as a general trend, the logarithms of the stability constants measured for both equilibriums with fluoride were higher than those obtained for acetate when using receptors **3a**, **3b** and **3c**. This was in agreement with the results detailed above and with the more basic character of fluoride in acetonitrile when compared with acetate. It can be observed in Table 3 that the stability constants for the formation of the corresponding hydrogen-bonding complexes were, for fluoride, at least one order of magnitude larger than the stability constants for the deprotonation and about two orders of magnitude for acetate. Table 3 also shows that deprotonation constants were more important for fluoride than for acetate. The stability constants determined in this study are similar than those reported for other thiosemicarbazones receptors but lower than those found for other urea/thiourea receptors functionalized with benzene.[19-21]

Fluorogenic studies involving anions

Fluorescence studies in acetonitrile solutions of the receptors upon addition of increasing amounts of the corresponding anion were also carried out. Receptors were excited in the pseudo-isosbestic points observed in the course of UV–vis titrations. All receptors displayed a broad and unstructured emission band. Quantum yields in acetonitrile (see Table 2) ranged from quite low (receptor **3a**, ϕ=0.0064) to medium (compound **3d**, ϕ=0.088). The addition of chloride, bromide, iodide, hydrogen sulfate, and nitrate anions to receptors **3a–d** resulted

in negligible changes in the emission intensity profiles. In contrast, the fluorescence emission in presence of fluoride, cyanide, acetate, and dihydrogen phosphate changed significantly.

A different general behavior was found depending on the anion and the receptor used in the studies. Figures 4 shows the changes observed in the emission of **3a** in the presence of increasing amounts of fluoride or acetate. In presence of fluoride, an enhancement of the fluorescence intensity upon the addition of moderate amounts of fluoride followed by a quenching of the emission band at higher anion concentrations and the shift of the final band at longer wavelengths were observed. This behavior is in agreement with the changes observed in the absorption titrations and the coordination plus deprotonation equilibriums. Thus enhancement of the fluorescence emission is attributed to the formation of the corresponding hydrogen-bonding complex (Eq. 1), whereas further quenching and shift of the band is related with the formation of the deprotonated species.

Figure 4 (rigth) also shows the emission behavior found for **3a** in the presence of acetate. In this case only an enhancement of the fluorescence was found in agreement with the formation of hydrogen-bonding complex (note that no clear deprotonation was found for **3a** with acetate). A similar emission behavior in the presence of fluoride and acetate was found when using receptor **3b**.

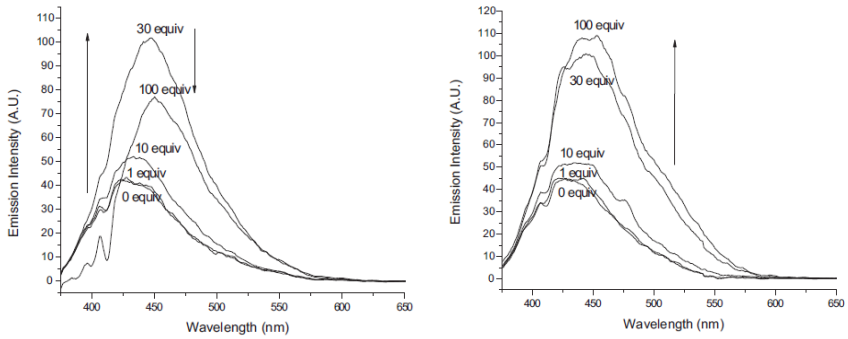

Fig. 4. Emission changes in **3a** (1.2×10^{-5} mol dm^{-3}) in the presence of fluoride (left) and acetate (right) anions. Emission spectra of the receptor in the presence of 0, 1, 10, 30 and 100 equiv of the corresponding anion.

This behavior observed for **3a** and **3b** contrasts with the emission behavior found for **3c** and **3d**. For these latter receptors, a quenching of the fluorescence was observed in the presence of increasing amounts of both fluoride and acetate. Taking into account that all four receptors showed a similar UV–vis behavior with anions the strong difference in emission properties should most likely be attributed to the presence of two and three thienyl groups in **3c** and **3d** that would favor deactivations paths that were not active in compounds **3a** and **3b**, which contain only one thio-phene moiety.

^{1}H-NMR spectroscopic studies in the presence of anions

UV –vis and fluorescence studies of thiosemicarbazone receptors **3a-d** displayed a varied response in the presence of anions related with hydrogen bonding interactions and deprotonation of the receptors. In order to study in more detail this dual coordination/deprotonation process the interaction of receptor **3d** with fluoride anion was investigated by means of ^{1}H NMR titration experiments in DMSO-d_6.

^{1}H NMR spectrum of **3d** showed resonances for the benzene ring at 7.20 (1H, broad triplet, H_p), 7.39–7.36 (2H, broad multiplet, H_m), 7.58 (2H, broad doublet, H_o) ppm, whereas protons of the two 2,5-disubstituted thiophene rings (H_d,H_e and H_f,H_g) appeared as doublets at 7.31(H_f) and at 7.49 (H_g) ppm for the first ring and as a broad multiplet in the 7.39-7.36 ppm range (H_d and H_e) for the second. Protons of the third 2-monosubstituted thienyl ring appeared as a double doublet at 7.11 (H_b), a doublet at 7.54 (H_c), which overlapped with a doublet at 7.35(H_a). Finally, the imine proton (–*C*H=N) appeared as a broad singlet at 8.30 (H_j) ppm and the N–*H* protons of the thiosemicarbazone group also were broad singlets at 11.88 (H_k) and 9.84 (H_l) ppm (Scheme 2).

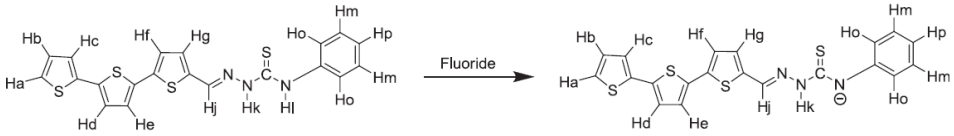

Scheme 2. Proposed mode for the fluoride-induced deprotonation of receptor **3d**.

In the presence of fluoride (5 equiv) the most remarkable observation was the disappearance of the H_k and H_l signals. Moreover the observed variation in the chemical shifts Δδ (ppm) over the course of the titration with fluoride for other protons in **3d** is shown in Figure 5.

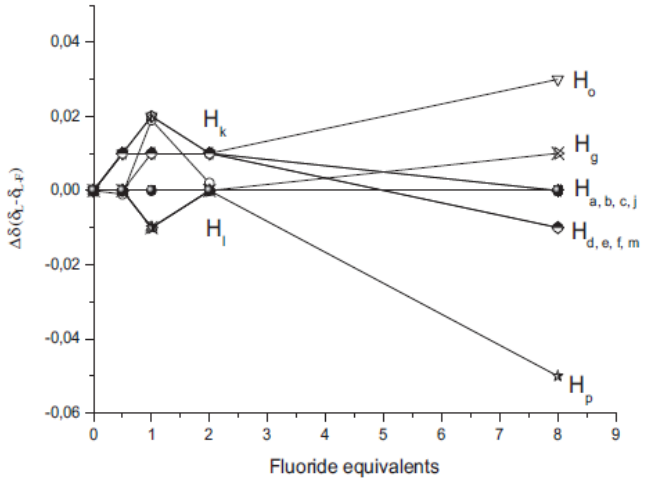

Figure 5. ^{1}H NMR shifts for the protons of receptor **3d** in the presence of increasing quantities of fluoride anion (DMSO-d_6).

As could be seen, H_a–H_g protons showed minor changes, whereas, in contrast, remarkable shifts were observed for H_o and H_p suggesting that deprotonation occurs in the N–H group closer to the phenyl group. Fabbrizzi et al. and ourselves have observed in closely related thioureas a similar behavior; i.e., the deprotonation apparently occurs in the protons of the nitrogen attached to the phenyl ring from NMR studies.[22]

Quantum mechanical studies

The hydrogen bond donating or accepting ability of a molecule at a particular site can be known by studying the deprotonation energy in gas-phase using quantum chemical calculations via the subtraction of the energy of the receptor alone from that of the deprotonated form. Following this concept, calculations were carried out using a PM3 semiempirical model that was applied to all the receptors **3a–d**. As these thiosemicarbazone receptors contain two N–H groups, the deprotonation studies were performed assuming that both protons could be eliminated. The results of this study are shown in Table 4. Data strongly suggests that the most acidic proton is H_k (see Scheme 2). As it can be observed there is not an agreement between the data obtained from the theoretical calculations and ^{1}H NMR titrations that suggested that deprotonation occurs at the H_l proton.

Table 4. Stabilization energies calculated for the deprotonation of the receptors **3a-d**

Receptors	$E_{(L)}$–$E_{(LH)}$ (Kcal/mol)	
	R=N–NH–C(S)–*N*–Ph[a]	R=N–N–C(S)–NH–Ph[b]
3a	−4.81	−12.3
3b	−10.54	−19.85
3c	−6.39	−14.19
3d	−0.57	−3.46

[a]Deprotonation at the H_l proton (see Scheme 2).

[b]Deprotonation at the H_k proton (see Scheme 2).

Despite this contradiction, theoretical calculations agree with the chromogenic behavior observed for the receptors. Quantum mechanical studies indicated that the dicyanovinyl derivative **3b** is the most acidic followed by the receptor **3c**. In fact the theoretical studies indicated that the acidity of the receptors follow the order **3b>3c>3a>3d** (see Table 4). This is in agreement with the chromo-fluorogenic behavior of the receptors (vide ante) and with the expected basicity of anions in (i.e., F^- > CN^-> AcO^-> $H_2PO_4^-$, Cl^-, HSO_4^-, SCN^-, NO_3^-, Br^-, I^-); i.e., the most acidic receptors **3b** and **3c** showed color changes in the

presence of fluoride, cyanide, acetate, and dihydrogen phosphate, whereas the less acidic **3a** and **3d** ligands were only able to show a remarkable color modulation in the presence of the most basic anions fluoride and cyanide anions.

3.4.4.4. Conclusions

A family of novel heterocyclic thiosemicarbazones containing thienyl groups, derivatives **3a-b**, has been prepared, characterized and their interactions with anions were studied through UV-vis, fluorescence, ^{1}H NMR and quantum chemical calculations. Two different chromo-fluorogenic behaviors in the presence of anions in acetonitrile were observed. The more basic anions fluoride and cyanide were able to induce dual coordination-deprotonation for all **3a-d** receptors studied, whereas acetate and dihydrogen phosphate showed poorer coordination ability and deprotonation was only observed on the more acidic receptors **3b** and **3c**. Hydrogen bonding interactions resulted in a small bathochromic shift, whereas deprotonation was indicated by the appearance of a new band at longer wavelengths. Color changes from pale-yellow to yellow-red were observed. In fluorescence studies it was apparent that hydrogen bonding interactions were visible through the enhancement or the decay of the emission band according to the number of thienyl rings at the π-conjugated bridges. Quantum mechanical studies suggested that the acidity of the receptors follows the order **3b > 3c > 3a > 3d**, which was in agreement with the experimentally observed behavior.

3.4.4.5. Experimental section

Materials and methods

Thin layer chromatography was carried out on 0.25 mm thick precoated silica plates (Merck Fertigplatten Kieselgel 60F_{254}). All melting points were measured on a Gallenkamp melting point apparatus and are uncorrected. NMR spectra were obtained on a Varian Unity Plus Spectrometer at an operating frequency of 300 MHz for ^{1}H and 75.4 MHz for ^{13}C or a Bruker Avance III 400 at an operating frequency of 400 MHz for ^{1}H and 100.6 MHz for ^{13}C, using the solvent peak as

internal reference. The solvents are indicated in parenthesis before the chemical shift values (δ relative to TMS and given in parts per million). IR spectra were run on a FTIR PerkineElmer 1600 spectrophotometer. Elemental analyses were carried out on a Leco CHNS 932 instrument. Mass spectrometry analyses were performed at the C.A.C.T.I. e Unidad de Espectrometria de Masas of the University of Vigo, Spain, on a Hewlett Packard 5989 A spectrometer for low resolution spectra and a VG Autospec M spectrometer for high resolution mass spectra. All the solvents were of spectrophotometrical grade. The aldehyde **1a** and 4-phenyl-3-thiosemicarbazide **2** were purchased from Sigma-Aldrich reagents and used without further purification. The synthesis of the aldehydes **1c** and **1d** was reported elsewhere.[15]

Synthesis of 2-((5-formylthiophen-2-yl)methylene) malononitrile 1b

To a solution of malononitrile (0.094 g, 1.4 mmol) and thiophene-2,5-dicarbaldehyde (0.2 g, 1.4 mmol) in dry DMF (15 mL), was added piperidine (1 drop). The solution was heated at 120 ^{o}C during 2 h. After cooling the mixture the solvent was removed under reduced pressure to give 2-((5-formylthiophen-2-yl)methy-lene)malononitrile **1b**, which was purified by column chromatography on silica with increasing amounts of diethyl ether in light petroleum as eluent.

2-((5-Formylthiophen-2-yl)methylene)malononitrile ***1b****. Orange solid (22%). Mp 161.1-165.3* ^{o}*C. IR (*$CHCl_3$*) v 2221 (CN), 1663 (C=O), 1571, 1432, 1215, 1069, 795 cm*$^{-1}$*.* ^{1}*H NMR (*$CDCl_3$*) δ 7.83 (br d, 1H, J=3.9 Hz, 4-H), 7.80-7.90 (m, 2H, 3-H and=CH), 10.03 (s, 1H, CHO). MS (EI) m/z (%): 188 (*M^+*, 60), 187 (100), 159 (11), 115 (9). HRMS: (EI) m/z (%) for* $C_9H_4N_2OS$*; calcd 188.0044; found 188.0049.*

General procedure for the synthesis of heterocyclic phenylthiosemicarbazones 3a-d

Equal amounts (0.4 mmol) of the appropriate aldehyde and thiosemicarbazide were dissolved in MeOH (30 mL) at room temperature. A solution was obtained, which was stirred overnight. Compounds precipitated as microcrystalline solids, which were collected by suction filtration, washed with cold MeOH and diethyl ether and dried in vacuum. Further recrystallization steps using $CHCl_3$/petroleum ether mixtures were performed if necessary.

4-Phenyl-1-((thiophen-2-yl)methylene)thiosemicarbazone **3a**[23] was obtained as a yellow solid (66%). Mp 185.6-186.9 °C. ^{1}H NMR ($CDCl_3$): δ=7.07-7.10 (m, 1H, 4´-H), 7.25-7.29 (m, 1H, 4-H), 7.32 (dd, *J*=3.9 and 0.9 Hz, 1H, 3´-H), 7.39-7.48 (m, 3H, 3- and 5- and 5´-H), 7.66 (br d, *J*=9.0 Hz, 2H, 2- and 6-H), 8.11 (s, 1H, -CH=N), 9.11 (s, 1H, S=C-N*H*), 10.29 (s, 1H, C=N-N*H*) ppm. IR (Nujol) *v* 3297(NH), 3141(=C-H), 1588, 1547, 1521, 1505, 1445, 1386, 1311, 1268, 1220, 1204, 1068, 1041, 922, 855, 817, 784, 763, 742, 726, 712, 701, 687, 622, 541 cm^{-1}. MS (FAB): *m/z* (%)=262 ($[M+H]^+$, 100), 228 (3), 168 (17). FAB-HRMS: calcd for $C_{12}H_{11}N_3S_2$ 262.0475; found 262.0467.

1-((5-(2,2-Dicyanovinyl)thiophen-2-yl)methylene)-4-phenyl-thiosemicarbazone **3b** was obtained as a red solid (77%). Mp 185.0-186.0 °C. ^{1}H NMR ($CDCl_3$): δ=7.22-7.28 (br t, *J*=7.2 Hz, 1H, 4-H), 7.37 (br d, *J*=7.8 Hz, 2H, 3- and 5-H), 7.52 (br d, *J*=7.2 Hz, 2H, 2-and 6-H), 7.82 (br s, 1H, 4´-H), 7.87 (br s, 1H, 3´-H), 7.96 (s, 1H, -CH=N), 8.02 (s, 1H, -C*H*=C$(CN)_2$), 9.08 (s, 1H, S=C-N*H*), 9.60 (s, 1H, C=N-N*H*) ppm. IR (Nujol) *v* 3341 (NH), 3122 (=C-H), 2223 (CN), 1596, 1579, 1568, 1540, 1517, 1498, 1261, 1198, 1097, 1061, 915, 811, 748, 705, 690, 610 cm^{-1}. MS (FAB): *m/z* (%)=338 ($[M+H]^+$, 100), 306 (9). FAB-HRMS: calcd for $C_{16}H_{11}N_5S_2$ 338.0529; found 338.0526.

*1-((5-(5-Ethoxythiophen-2-yl)thiophen-2-yl)methylene)-4-phenylthiosemicarbazone **3c** was obtained as a brown solid* (50%). Mp 171.3-171.6 °C.

^{1}H NMR ($CDCl_3$): δ=1.44 (t, *J*=7.2 Hz, 3H, OCH_2CH_3), 4.14 (q, *J*=7.2 Hz, 2H, OCH_2CH_3), 6.15 (d, *J*=3.9 Hz, 1H, 4´´-H), 6.91 (d, *J*=3.9 Hz, 1H, 3´´-H), 6.93 (d, *J*=3.9 Hz, 1H, 3´-H), 7.15 (d, *J*=3.9 Hz, 1H, 4´´-H), 7.25-7.32 (m, 1H, 4-H), 7.43 (br t, *J*=7.5 Hz, 2H, 3- and 5-H), 7.67 (br d, J=7.5 Hz, 2H, 2- and 6-H), 8.07 (s, 1H, -C*H*=N), 9.09 (s, 1H, S=C-NH), 10.50 (s, 1H, C=N-N*H*) ppm. ^{13}C NMR ($CDCl_3$): δ=14.6 (OCH_2CH_3), 69.6 (OCH_2CH_3), 105.7 (C4´´), 122.2 (C3´´), 122.9 (C3´), 123.0 (C2´), 124.7 (C2 and C6), 126.3 (C4), 128.8 (C3 and C5), 132.4 (C4´), 134.8 (C5´), 137.6 (CH=N), 137.8 (C1), 141.7 (C2´´), 165.7 (C5´´), 175.0 (C=S) ppm. IR (Nujol) *v* 3329 (NH), 3127 (=C-H), 1588, 1550, 1509, 1483, 1465, 1384, 1322, 1274, 1245, 1206, 1079, 1039, 912, 873, 779, 764, 743, 729, 703, 692, 614 cm^{-1}.$C_{18}H_{17}N_3OS_3$ (387.54): calcd. C 55.79, H 4.42, N 10.84, S 24.82; found C 56.21, H 4.51, N 10.51, S 25.09.

4-Phenyl-1-((5-(5-(thiophen-2-yl)thiophen-2-yl)thiophen-2-yl) methylene)thiosemicarbazone ***3d*** *was obtained as an orange solid (41%).* Mp >216 ^{o}C. ^{1}H NMR ($CDCl_3$): δ=7.05-7.18 (m, 8H, 4-H and thienyl-H), 7.21 (t, 2H, 3- and 5-H), 7.70 (d, 2H, 2- and 6-H), 7.97 (s, 1H, -C*H*=N), 9.09 (s, 1H, S=C-N*H*), 9.35 (s, 1H, C=N-N*H*) ppm. ^{13}C NMR (DMSO-d_6): δ=124.6, 124.7, 125.2, 125.3, 125.6, 125.9, 126.1, 128.1, 128.6, 132.3, 134.8, 135.8, 136.3, 137.4, 137.6, 138.3, 139.0, 175.5 (C=S) ppm. IR (Nujol) *v* 3310 (NH), 1742, 1586, 1546, 1463, 1456, 1377, 1307, 1270, 1202, 1169, 1156, 1076, 1059, 967, 922, 892, 783, 722, 703, 514 cm^{-1}. MS (FAB): *m/z* (%)=426 ([M+H]$^+$, 100), 424 (98), 394 (47), 338 (47), 288 (11). FAB-HRMS: calcd for $C_{20}H_{15}N_3S_4$ 426.0221; found 426.0218.

Physical measurements

Stock solutions of the anions (F^-, Cl^-, Br^-, I^-, NO_3^-, $H2PO_4^-$, HSO_4^-, AcO^-, BzO^-, CN^- as tetrabutylammonium salts) were prepared at 10^{-2} and 10^{-3} mol dm^{-3} in acetonitrile. The concentrations of ligands used in these measurements were ca. 1.2x10^{-4} and 1.2x10^{-5} mol dm^{-3}. ^{1}H NMR experiments were carried out in DMSO-d_6. At high concentrations the receptors showed low solubility in acetonitrile.

In fluorimetric titrations, all receptors were excited in wavelength of the pseudo-isosbestic points observed in the course of UV-vis titrations with fluoride anion. The electronic absorption spectra were obtained on a Perkin Elmer Instruments Lambda 35 UV/visible spectrometer and fluorescence spectra were recorded on a Quanta Master 40 steady state fluorescence spectrofluorometer from Photon Technology Internation (PTI); all in quartz cuvettes (1 cm). ^{1}H NMR titrations spectra were acquired with Varian 300 spectrometer.

Theoretical studies

Quantum chemical calculations at semiempirical level (PM3, within restricted Hartree-Fock level) were carried out in vacuum with the aid of Hyperchem V6.03. The Polar-Ribiere algorithm was used for the optimization. The convergence limit and the rms gradient were set to 0.01 kcal mol^{-1}. The stability constants were estimated with the HypSpec Software V1.1.18 with data of titration of receptors with selected anions.

3.4.4.6. Acknowledgements

We thank the Spanish Government (project MAT2009-14564-C04-01) and the Generalitat Valencia (project PROMETEO/2009/ 016) for support. Thanks are due to the Fundaçao para a Ciencia e Tecnologia (Portugal) and FEDER-COMPETE for financial support through the Centro de Química - Universidade do Minho, Project PEst-C/QUI/UI0686/2011 (F-COMP-01-0124-FEDER-022716) and a Post-doctoral grant to R.M.F.B. (SFRH/BPD/79333/2011). The NMR spectrometer Bruker Avance III 400 is part of the National NMR Network and was purchased within the framework of the National Program for Scientific Re-equipment, with funds from FCT. The authors are also indebted to program 'Acçoes Integradas Luso-Espanholas/CRUP', for the bilateral agreement number E-144/10. Thanks also to Fundación Carolina and UPNFM-Honduras for a doctoral grant to L.E.S.-F. and the Spanish Ministerio de Ciencia e Innovación for an FPU grant to M.E.M.

3.4.4.7. References and notes

1. (a) Fabrizzi, L.; Poggi, A. *Chem. Soc. Rev*. **1995**, 197-202; (b) De Silva, A. P.; Fox, D. B.; Huxley, A. J. M.; Moody, T. S. *Coord. Chem. Rev*. **2000**, 205, 41-57; (c) Beer, P. D. *Chem. Commun*. **1996**, 689-696; (d) Martínez-Máñez, R.; Soto, J; Lloris, J. M.; Pardo, T. *Trends Inorg. Chem*. **1998**, 5, 183-203; (e) P. D. Beer, *Chem. Soc. Rev*. **1989**, 18, 409-450.
2. (a) Löhr, H. G.; Vögtle, F. *Acc. Chem. Res*. **1985**, 18, 65-72; (b) Inouye, M. *Color. Non-Text. Appl*. **2000**, 238-274; (c) Amendola, V.; Bonizzoni, M.; Estebán-Gómez, D.; Fabbrizzi, L.; Licchelli, M.; Sancenón, F.; Taglietti, A. *Coord. Chem. Rev*. **2006**, 250, 1451-1470.
3. (a) De Silva, A. P.; Gunaratne, H. Q. N.; Gunnlaugsson, T.; Huxley, A. J. M.; McCoy, C. P.; Rademacher, J. T.; Rice, T. E. *Chem. Rev*. **1997**, 97, 1515-1566; (b) Prodi, L.; Bolletta, F.; Montalti, M.; Zaccheroni, N. *Coord. Chem. Rev*. **2000**, 205, 59-83; (c) Valeur, B.; Leray, I. *Coord. Chem. Rev*. **2000**, 205, 3-40; (d) Rurack, K. Spectrochim. *Acta, Part A* **2001**, 57, 2161-2195; (e) De Silva, A. P.; McCaughan, B.; McKinney, B. O. F.; Querol, M. *Dalton Trans.* **2003**, 1902-1913; (f) Callan, J. F.; De Silva, A. P.; Magri, D. C. *Tetrahedron* **2005**, 61, 8551-8588; (g) Formica, M.; Fusi, V.; Giorgi, L.; Micheloni, M. *Coord. Chem. Rev*. **2012**, 256, 170-192.
4. (a) Martínez-Máñez, R.; Sancenón, F. *Chem. Rev*. **2003**, 103, 4419-4476; (b) Moragues, M. E.; Martínez-Máñez, R.; Sancenón, F. *Chem. Soc. Rev*. **2011**, 40, 2593-2643; (c) Martínez-Máñez, R.; Sancenón, F. *J. Fluoresc*. **2005**, 15, 267-285; (d) Beer, P. D.; Gale, P. A. Angew. *Chem. Int. Ed*. **2001**, 40, 486-516; (e) Suksai, C.; Tuntulani, T. *Chem. Soc. Rev*. **2003**, 32, 192-202; (f) Xu, Z.; Chen, X.; Kim, H. N.; Yoon, J. *Chem. Soc. Rev*. **2010**, 39, 127-137.
5. (a) Schmidtchen, F. P.; Berger, M. *Chem. Rev*. **1997**, 97, 1609-1646; (b) Gale, P. A. *Coord. Chem. Rev*., Ed. Special issue: 35 years of Synthetic Anion Receptor Chemistry **2003**, 240, 1-2; (c) Bondy, C. R.; Loeb, S. J. *Coord. Chem. Rev*. **2003**, 240, 77-99; (d) Martínez-Mañéz, R.; Sancenón, F. *Coord. Chem. Rev*. **2006**, 250, 3081-3093.
6. (a) Gale, P. A. *Acc. Chem. Res*. **2006**, 39, 465-475; (b) Yoon, J.; Kim, S. K.; Singh, N. J.; Kim, K. S. *Chem. Soc. Rev*. **2006**, 35, 355-360; (c) Blondeau, P.; Segura, M.; Pérez-Fernández, R.; De Mendoza, J. *Chem. Soc. Rev*. **2007**, 36, 198-210; (d) Fitzmaurice, F. J.; Kyne, G. M.; Douheret, D.; Kilburn, J. D. *J. Chem. Soc., Perkin Trans. 1* **2001**, 841-864.
7. (a) Li, F.; Carvalho, S.; Delgado, R.; Drew, M. G. B.; Félix, V. *Dalton Trans.* **2010**, 39, 9579-9587; (b) Lin, Y. –S.; Tu, G. –M.; Lin, C. –Y.; Chang, Y. –T.; Yen, Y. –P. *New J. Chem.* **2009**, 33, 860-867.
8. For recent papers of thiourea-based anion receptors see: (a) Makuc, D.; Hiscock, J. R.; Light, M. E.; Gale, P. A.; Plavec, J.; Beils. *J. Org. Chem.* **2011**, 7, 1205-1214; (b) Lin, Y. –S.; Zheng, J. –X.; Tsui, Y. –K.; Yien, Y. –P.; *Spectrochim. Acta, Part A* **2011**, 79, 1552-1558; (c) Odago, M. O.; Colabello, D. M.; Lees, A. J. *Tetrahedron* **2010**, 66, 7465-7471; (d) Gale, P. A.; García-Garrido, S. E.; Garric, J. *Chem. Soc. Rev*. **2008**, 37, 151-190; (e) Devaraj, S.; Saravanakumar, D.; Kandaswamy, M. *Sensors Act. B Chem*. **2009**, 136, 13-19; (f) Li, Z.; Wu, F. –Y.; Guo, L.; Li, A. –F.; Jiang, Y. B. *J. Phys. Chem. B.* **2008**, 112, 7071-7079; (g) Ros-Lis, J. V.; Martínez-Máñez, R.; Sancenón, F.; Soto, J.; Rurack, K.; Weißhoff, H. Eur. *J. Org. Chem.* **2007**, 17, 2449-2458; (h) Nie, L.; Li, Z.; Han, J.; Zhang, X.; Yang, R.; Liu, W. –X.; Wu, F. –Y.; Xie, J. –W.; Zhao, Y. –F.; Jiang, Y. –B. *J. Org. Chem.* **2004**, 69, 6449-6454; (i) Jose, D. A.; Kumar, D. K.; Ganguly, B.; Das, A. *Org. Lett.* **2004**, 6, 3445-3448; (j) Jiménez, D.; Martínez-Máñez, R.; Sancenón, F.; Soto, J. *Tetrahedron Lett*. **2002**, 43, 2823-2825
9. For recent examples see: (a) Krishnamurthi, J.; Ono, T.; Amemori, S.; Komatsu, H.; Shinkai, S.; Sada, K. *Chem. Commun*. **2011**, 47, 1571-1573; (b) Piątek, P. *Chem. Commun*. **2011**, 47, 4745-4747; (c) He, X.; Herranz, F.; Cheng, E. C. –C.; Vilar, R.; Yam, V. W. –W. *Chem. Eur. J*. **2010**, 16, 9123-9131; (d) Jun E. J.; Swamy, K. M. K.; Bang, H.; Kim, S-J; Yoon, J. *Tetrahedron Lett.* **2006**, 47,3103-3106

10. (a) Camiolo, S.; Gale, P. A.; Hursthouse, M. B.; Light, M. E. *Org. Biomol. Chem.* **2003**, 1, 741-744; (b) Gunnlaugsson, T.; Kruger, P. E.; Jensen, P.; Pfeffer, F. M.; Hussey, G. M. *Tetrahedron Lett*. **2003**, 44, 8909-8913; (c) Esteban-Gómez, D.; Fabbrizzi, L.; Licchelli, M. *J. Org. Chem.* **2005**, 70, 5717-5720; (d) Evans, L. S.; Gale, P. A.; Light, M. E.; Quesada, R. *New J. Chem.* **2006**, 30, 1019-1025.
11. (a) Withnall, J.; Howard, J.; Ponka, P.; Richardson, D. R. *Proc. Natl. Acad. Sci. USA* **2006**, 103, 14901-14906; (b) Zhang, H. –J.; Qin, X.; Liu, K.; Zhu, D. –D.; Wang, X. –M.; Zhu, H. L. *Bioorg. Med. Chem.* **2011**, 19, 5708-5715.
12. See for example: Tian, Y. –P.; Duan, C. –Y.; Zhao, C. –Y.; You, X. –Z. *Inorg. Chem*. **1997**, 36, 1247-1252.
13. (a) Batista, R. M. F.; Oliveira, E.; Costa, S. P. G.; Lodeiro, C.; Raposo, M. M. M. *Org. Lett.* **2007**, *9*, 3201-3204. (b) Costa, S. P. G.; Oliveira, E.; Lodeiro, C.; Raposo, M. M. M. *Tetrahedron Lett.* **2008**, *49*, 5258-5261. (c) Batista, R. M. F.; Oliveira, E.; Costa, S. P. G.; Lodeiro, C.; Raposo, M. M. M. *Tetrahedron Lett*. **2008**, *49*, 6575-6578. (d) Batista, R. M. F.; Oliveira, E.; Nuñez, C.; Costa, S. P. G.; Lodeiro, C.; Raposo, M. M. M. *J. Phys. Org. Chem.* **2009**, *22*, 362-366. (e) Batista, R. M. F.; Oliveira, E.; Costa, S. P. G.; Lodeiro, C.; Raposo, M. M. M. *Tetrahedron* **2011**, *67*, 7106-7113. (f) Batista, R. M. F.; Oliveira, E.; Costa, S. P. G.; Lodeiro, C.; Raposo, M. M. M. *Talanta* **2011**, *85*, 2470-2478.
14. (a) Raposo, M. M. M.; García-Acosta, B.; Ábalos, T.; Calero, P.; Martínez-Máñez, R.; Ros-Lis, J. V.; Soto, J. *J. Org. Chem.* **2010**, 75, 2922-2933; (b) Amendola, V.; Boiocchi, M.; Fabbrizzi, L.; Mosca, L. *Chem. Eur. J*. **2008**, 14, 9683-9696.
15. (a) Raposo, M. M. M.; Kirsch, G. *Tetrahedron* **2003**, 59, 4891-4899. (b) Batista, R. M. F.; Costa, S. P. G.; Belsley, M.; Lodeiro, C.; Raposo, M. M. M. *Tetrahedron* **2008**, 64, 9230-9238
16. For recent examples see: (a) Aldrey, A.; Núñez, C.; García, V.; Bastida, R.; Lodeiro, C.; Macías, A. *Tetrahedron* **2010**, 66, 9223-9230; (b) Atta, A. K.; Ahn, I. –H.; Hong, A. –Y.; Heo, J.; Kim, C. K.; Cho, D. –G. *Tetrahedron Lett*. **2012**, 53, 575-578; (c) Amendola, V.; Fabbrizzi, L.; Mosca, L.; Schmidtchen, F. –P. *Chem. Eur. J*. **2011**, 17, 5972-5981; (d) Amendola, V.; Bergamaschi, G.; Boiocchi, M.; Fabbrizzi, L.; Milani, M. *Chem. Eur. J*. **2010**, 16, 4368-4380.
17. For recent examples see: (a) Kim, T. H.; Choi, M. S.; Sohn, B. –H.; Park, S. –Y.; Lyoo, W. S.; Lee, T. S. *Chem. Commun*. **2008**, 2364-2366; (b) Amendola, V.; Fabbrizzi, L. *Chem. Commun*. **2009**, 513-531; (c) Caltagirone, C.; Mulas, A.; Isaia, F.; Lippolis, V.; Gale, P. A.; Light, M. A. *Chem. Commun*. **2009**, 6279-6281; (d) Pérez-Casas, C.; Yatsimirsky, A. K. *J. Org. Chem.* **2008**, 73, 2275-2284; (e) Dos Santos, C. M. G.; McCabe, T.; Watson, G. W.; Kruger, P. E.; Gunnlaugsson, T. *J. Org. Chem.* **2008**, 73, 9235-9244; (f) Dydio, P.; Zielinski, T.; Jurczak, J. *J. Org. Chem.* **2009**, 74, 1525-1530; (g) Xu, Z.; Kim, S. K.; Han, S. J.; Lee, C.; Kociok-Kohn, G.; James, T. D.; Yoon, J. *Eur. J. Org. Chem.* **2009**, 3058-3065.
18. Amendola, V.; Esteban-Gómez, D.; Fabbrizzi, L.; Licchelli, M. *Acc. Chem. Res*. **2006**, 39, 343-353.
19. Boiocchi, M.; Del Boca, L.; Estebán-Gómez, D.; Fabbrizzi, L.; Licchelli, M.; Monzani, E. *J. Am. Chem. Soc.* **2004**, 126, 16507-16514.
20. Boiocchi, M.; Del Boca, L.; Estebán-Gómez, D.; Fabbrizzi, L.; Licchelli, M.; Monzani, E. *Chem. Eur. J*. **2005**, 11, 3097-3104.
21. Esteban-Gómez, D.; Fabbrizzi, L.; Licchelli, M.; Monzani, E. *Org. Biomol. Chem.* **2005**, 3, 1495-1500.
22. Bonizzoni, M.; Fabbrizzi, L.; Taglietti, A.; Tiengo, F. *Eur. J. Org. Chem.* **2006**, 3567-3574.
23. Mapathy, P.; Budhkar, A.P.; Dorai, C.S. *Ind. J. Chem*. **1986**, 63, 714-721.

3.5. Anion chemosensor by displacement assay approach

3.5.1. Experimental objectives

Taking into account the particular importance of hydrogen sulfide monitoring as industrial pollutant, the recently discovery of relevance of hydrogen sulfide anions in several biological proces and the growing attention in the development of new optical chemosensors for the detection of chemical species with biological and environmental interest; we decided to design a new system for the detection of hydrogen sulfide in aqueous media.

Consequently our main aims in this project were:

- Design and synthesize a new very selective fluorescent chemosensor for fast detection of hydrogen sulfide in aqueous environments.

- Characterize the new probe by standard methods (NMR, HRMS, IR, UV/Vis and emission spectroscopy).

- Evaluate the real potential of use of new probe to detect and monitor abnormal levels of hydrogen sulfide in living cells.

3.5.2. Chemosensor design

The main consideration into chemosensor design was the preparation of an eficient fluorescent probe able of hydrogen sulfide recognition in aqueous media. Thus, a "displacement assay" approach was selected for the chemosensors design in order to obtain the remarkable fluorescente changes in aqueous solution and avoid the solvatation interference, which is very relevant in other approaches.

The cyclam group was selected as binding site by their reported ability to coordinate with transition metals and their known cell viability. Especially, Cu(II)-cyclam complex was chose after of several preliminar test with other metal-complex of nickel and iron.

In addition, anthracene moiety was selected as fluorophore due to their known photophysical properties, their pH stability and for showing an emission easily to measure by simple fluorescence microscopy thechnique.

3.5.3. Highly selective fluorescence detection of hydrogen sulfide by using an anthracene-functionalized cyclam–Cu(II) complex

In the following section, we reported the synthesis, characterization and sensing properties of a new anthracene-functionalised cyclam–copper (II) complex which acts as a turn-on fluorogenic probe for HS^- anion in water and in living cells (Figure 34).

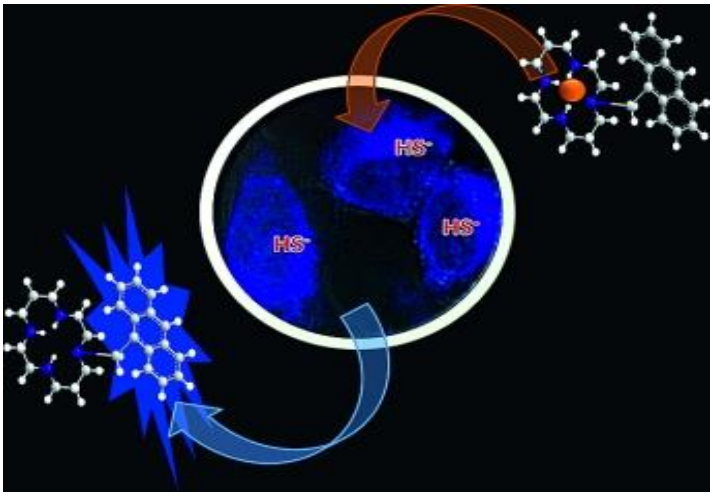

Figure 34. Schematic representation of a new chemosensor for HS^- sensing in aqueous media and living cells (front cover of published communication)

Highly Selective Fluorescence Detection of Hydrogen Sulfide by Using an Anthracene-Functionalized Cyclam–Cu^{II} Complex

Luis E. Santos-Figueroa, [a, b, c] Cristina de la Torre, [a, b, c] Sameh El Sayed, [a, b, c] Félix Sancenón, [a, b, c] Ramón Martínez-Máñez, [a, b, c]* Ana M. Costero, [a, d] * Salvador Gil [a, d] and Margarita Parra [a, d]

[a] Instituto de Reconocimiento Molecular y Desarrollo Tecnológico (IDM), Centro Mixto Universidad Politécnica de Valencia-Universidad de Valencia (Spain)

[b] Departamento de Química, Universidad Politécnica de Valencia, Camino de Vera s/n, 46022 Valencia (Spain)

[c] CIBER de Bioingeniería, Biomateriales y Nanomedicina (CIBER- BBN)

[d] Departamento de Química, Universitat de València, Dr. Moliner 50, 46100, Burjassot, Valencia, Spain

Received: October 5, 2013
Published online: November 19, 2013

European Journal of Inorganic Chemistry, **2014**, 41-45.

3.5.3.1. Abstract

An anthracene-functionalised cyclam–copper(II) complex for the detection of HS^- in aqueous environments has been prepared. This probe displays poor fluorescence but can selectively and sensitively detect HS^- anions in water over other anions, biothiols and common oxidants such as H_2O_2 through remarkably enhanced emission. This turn-on response in the presence of the HS^- anion is ascribed to a demetallation reaction that inhibits emission quenching observed in the initial complex as a result of the presence of the paramagnetic Cu^{2+} centre. Moreover, real-time fluorescence imaging measurements confirm that probe $[Cu(\mathbf{1})]^{2+}$ can be easily used to detect intracellular HS^- at micromolar concentrations with a remarkable enhancement in the FI/FI_0 ratio.

3.5.3.2. Introduction

Hydrogen sulfide (H_2S), a colourless, flammable gas with high solubility in water and organic solvents, is well known for its disagreeable “rotten eggs” smell. Hydrogen sulfide has been traditionally studied for its known toxicity[1] and for its presence in several industrial[2] and environmental processes.[3] Very recently, hydrogen sulfide was also discov-ered to play a role as an endogenous gasotransmitter[4] and to be of relevance in a number of biological processes, in-cluding neurotransmission,[5] vasorelaxation,[4b,6] cardio-protection[7] and anti-inflammation.[8]

Moreover, abnormal hydrogen sulfide production has been associated with diseases such as chronic kidney disease, liver cirrhosis,[9] Alzheimer’s disease[10] and Down’s syndrome.[11] As a result, and given the important roles that hydrogen sulfide plays in environmental, industrial and biological processes, the development of quick, selective and sensitive detection systems for this chemical has recently become an important focal point.[12]

In the last few years, some probes for the detection of hydrogen sulfide have been described. In particular, the re-duction of azide,[13] hydroxylamine[14] and nitro[15] moieties to the amine group has been used as a key reaction in the design of hydrogen sulfide selective fluorescent probes. Moreover, HS^--induced hydrolysis reactions of disulfide bonds,[16] dinitrophenyl ethers[17] and several nucleophilic additions,[18] linked with selected fluorophores, have also been used for the fluorescent recognition of this anion. Furthermore, some of us have reported colorimetric sulfide sensing on the basis of the sulfide-induced transformation of a pyrylium heterocycle into the corresponding thiopyrylium derivative.[19]

Despite these advances, some shortcomings of these probes typically involve slow response and poor selectivity, as in other cases in which thiol-containing biomolecules (e.g., Cys, Hcy and GSH) and anions (e.g., SO_3^{2-} and $S_2O_3^{2-}$) also induce a chromo-fluorogenic response.[20] An interesting alternative approach that has recently been used for the detection of this anion is based on hydrogen sulfide induced demetallation reactions of nonfluorescent complexes.[21] In particular, the research groups of Nagano[21a] and Yu[21b] have very recently reported the use of cyclen–Cu^{II} complexes conjugated with common fluorophores as selective probes for HS^- in pure water.

This interesting approach is highly modular, as it allows the design of different probes through the selection of certain complexes and fluorophores. However, regardless of the huge potential of this paradigm, the use of hydrogen sulfide induced demetallation reactions to design probes for HS^- is still a barely explored field. Also, the potential application of these chromo-fluorogenic probes for monitoring natural endogenous hydrogen sulfide production in living cells has been recently demonstrated.[22]

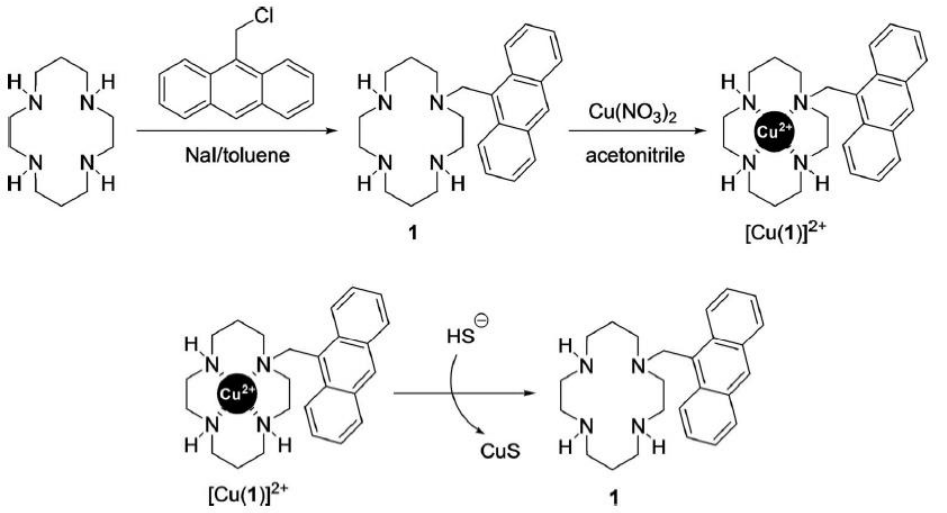

Scheme 1. Synthesis of probe $[Cu(\mathbf{1})]^{2+}$ and its reaction with HS^- in pure water.

On the basis of these concepts, we paid attention to designing a simple probe for hydrogen sulfide that can be easily applied to the detection of this anion in pure water and living cells. The probe was designed on the basis of two well-known systems: a cyclam azamacrocycle (cyclam = 1,4,8,11-tetraazacyclotetradecane) as a ligand for Cu^{2+} and anthracene as a fluorophore (Scheme 1). Ligand **1** was prepared according to literature procedures, which involved a nucleophilic substitution reaction between cyclam and 9-(chloromethyl)anthracene in the presence of sodium iodide.[23] Moreover, the reaction of **1** with $Cu(NO_3)_2$ in re-fluxing acetonitrile yielded final complex $[Cu(\mathbf{1})]^{2+}$ (see the Supporting Information for details).

3.5.3.3. Results and discussion

Aqueous solutions [4-(2-hydroxyethyl)-1-piperazineethanesulfonic acid (HEPES) 30 mm, pH 7.5] of $[Cu(\mathbf{1})]^{2+}$ show a very weak structured fluorescence band in the 350–475 nm interval (λ_{ex} = 256 nm), typical of the anthracene fluorophore.[24] The weak emission of the complex was ascribed to quenching resulting from the coordination of **1** with the paramagnetic Cu^{2+} centre.

Moreover, the emission behaviour of the $[Cu(\mathbf{1})]^{2+}$ probe in the presence of several anions (HS^-,Cl^-,Br^-,I^-,F^-,OH^-, AcO^-,CN^-,N_3^-,NO_3^-, HCO_3^-,SO_4^{2-},$S_2O_3^{2-}$,SO_3^{2-}, HPO_4^{2-} and citrate), bio-thiols (Cys, Hcy and GSH) and a common oxidant (H_2O_2) was studied. The results obtained are shown in Figure 1.

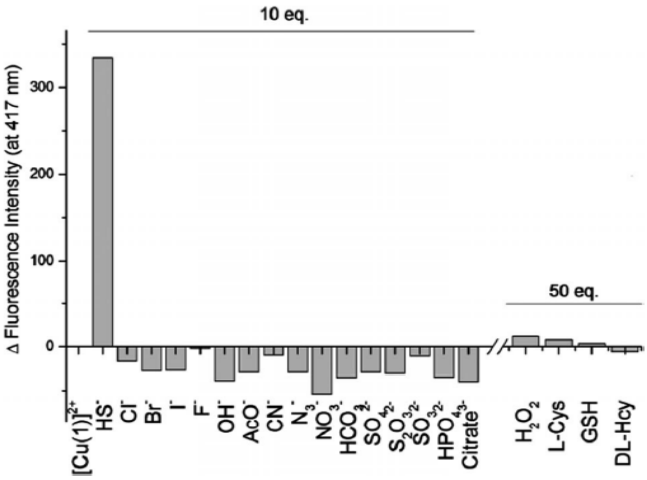

Figure 1. Fluorescence intensity at 417 nm (λ_{ex} = 256 nm) of $[Cu(\mathbf{1})]^{2+}$ ($2.0X10^{-5}$ m) in HEPES (30 mm at pH 7.5) in the presence of selected anions (10 equiv.), biothiols (50 equiv.) and oxidants (50 equiv.).

As the figure shows, of all the anions tested, only $HS^-$was able to induce a remarkable enhancement in the emission. In contrast, other tested anions induced a slight quenching of the emission band. Moreover, the addition of up to 50 equiv. of certain biothiols and H_2O_2 resulted in negligible changes in the emission profile of $[Cu(\mathbf{1})]^{2+}$. The selective fluorescence enhancement in the presence of HS^- is ascribed to a demetallation reaction of the $[Cu(\mathbf{1})]^{2+}$ complex that renders emissive ligand **1** free. In fact, the emission spectrum obtained upon demetallation of $[Cu(\mathbf{1})]^{2+}$ with HS^- is very similar to that of free receptor **1**, and this confirms the proposed mechanism.

Having assessed the highly selective response of $[Cu(\mathbf{1})]^{2+}$ to the HS^- anion, the sensitivity of the probe was studied by monitoring the emission change of $[Cu(\mathbf{1})]^{2+}$ (2.0 X 10^{-5} m) in HEPES (30 mM, pH 7.5) upon the addition of the HS^- anion. Increasing the concentration of HS^- (up to 100 equiv.) resulted in a progressive and immediate growth in fluorescence intensity (Figure 2). This figure also shows the colour change observed for the probe in the absence and presence of HS^- under UV irradiation. A clear-to-the-naked-eye colour modulation in water was also observed. From these studies, a remarkable limit of detection (LOD) of 3.9 μm was calculated. Moreover, $[Cu(\mathbf{1})]^{2+}$ presented accurate sensitivity, which was below the concentration of H_2S required to elicit physiological responses (10–1000 μm).[25]

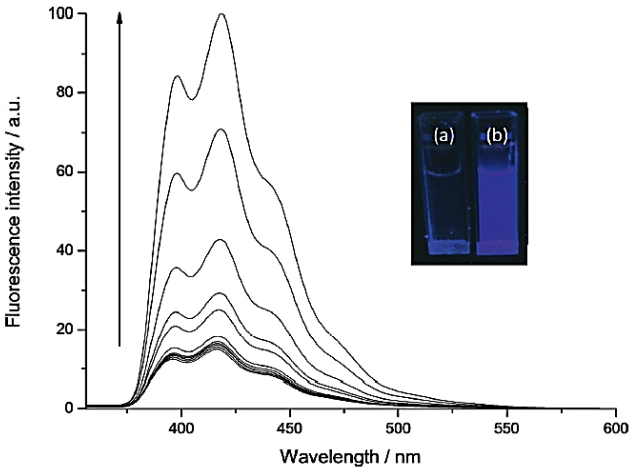

Figure 2. Emission spectra of $[Cu(\mathbf{1})]^{2+}$ (2.0X10^{-5} m) in HEPES (30 mm, pH 7.5) with the addition of increasing quantities (0–100 equiv.) of HS^-. Inset: photograph under UV radiation of (a) $[Cu(\mathbf{1})]^{2+}$ probe alone and (b) $[Cu(\mathbf{1})]^{2+}$ upon the addition of an excess amount of HS^-.

The sensing features of the $[Cu(\mathbf{1})]^{2+}$ probe are quite similar to those reported for analogous Cu^{II} complexes with an instantaneous response upon the addition of hydrogen sulfide and limits of detection in the 1–10 μm range. Other chemodosimeters based on addition, hydrolysis and reduction reactions present higher reaction times (in the 1–100 min interval) than those based on

demetallation processes, yet they show similar limits of detection (see the Supporting Information for a comparative table).

In a second step, and to verify the feasibility of the developed probe to detect HS^- in complex environments, we prospectively used complex $[Cu(\mathbf{1})]^{2+}$ for the fluorescence imaging of HS^- in living cells. The control experiment (HeLa cells with no probe) displayed no fluorescence, whereas the HeLa cells incubated with $[Cu(\mathbf{1})]^{2+}$ showed minor emission, which is tentatively ascribed to the basal fluorescence of the probe. In contrast, a large enhancement in intracellular emission was observed in the HS^--treated cells (Figure 3).

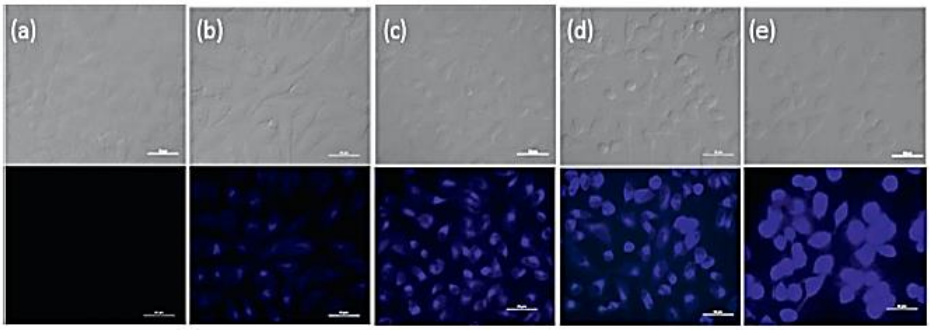

Figure 3. Detection of HS^- levels in living cells by using $[Cu(\mathbf{1})]^{2+}$. HeLa cells were incubated with $[Cu(\mathbf{1})]^{2+}$ (30 μm) for 30 min at 37 °C in DMEM. Transmitted light and fluorescence images were captured for (a) HeLa cells, (b) HeLa cells incubated with $[Cu(\mathbf{1})]^{2+}$ and (c) HeLa cells incubated with $[Cu(\mathbf{1})]^{2+}$ in the presence of HS^- at concentrations of 100 μm, (d) 200 μm and (e) 500 μm. The range of excitation was 330–380 nm and emission was monitored for wavelengths exceeding 420 nm.

Moreover, Figure 4 shows the ratio of average fluorescence after 10 min as compared to that found in the absence of the probe (FI/FI_0) for the fluorescence images of cells after the addition of 0, 100, 200 and 500 μm NaHS. A very clearly enhanced fluorescence ratio is observed, which related well with the increment in HS^- concentration. For instance, the FI/FI_0 ratio was found to be remarkably ca. 9 times higher for the cells incubated with 500 μm. Moreover, to complete our study, the WST-1 cell viability assays show that $[Cu(\mathbf{1})]^{2+}$ exhibited no toxicity at concentrations up to 100 μm (see the Supporting Information).

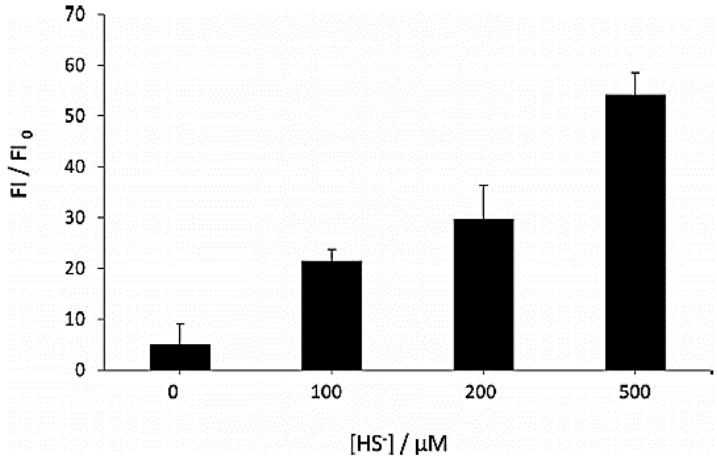

Figure 4. Average FI/FI_0 ratios from the fluorescence images of HeLa cells incubated with $[Cu(\mathbf{1})]^{2+}$ after the addition of 0, 100, 200 and 500 μm NaHS. Error bars are ± (standard deviation) from replicate experiments (*n* = 3).

3.5.3.4. Conclusions

We have prepared a sensitive and highly selective fluorescence probe for the detection of HS^- in aqueous environments. This probe consists of a Cu^{II} complex of an anthracene-functionalised cyclam ligand, which displays poor fluorescence. The probe can selectively and sensitively detect HS^- anions in water over other anions, biothiols and common oxidants such as H_2O_2 through remarkably enhanced emission. This turn-on response in the presence of the HS^- anion is ascribed to a demetallation reaction that inhibits the emission quenching observed in the initial complex as a result of the presence of the paramagnetic Cu^{2+} centre. Moreover, real-time fluorescence imaging measurements confirmed that probe $[Cu(\mathbf{1})]^{2+}$ can be easily used to detect intracellular HS^- at micromolar concentrations with a remarkable enhancement in the FI/FI_0 ratio. Chemosensor $[Cu(\mathbf{1})]^{2+}$ is one of the very few probes that exhibits a turn-on response for HS^- detection on the basis of the use of simple demetallation reactions. Similar

designs with the use of other available dyes for the straightforward signalling of HS^- are currently being investigated in our laboratory.

Supporting Information (see footnote on the first page of this article): General techniques, synthesis and characterisation of **1** and $[Cu(\mathbf{1})]^{2+}$; sensing features of $[Cu(\mathbf{1})]^{2+}$; cell viability assay of $[Cu(\mathbf{1})]^{2+}$ and fluorescence microscopy studies.

3.5.3.5. Acknowledgements

The authors thank the Spanish Government (Project MAT2012-38429-C04-01), the Generalitat Valenciana (Project PROMETEO/2009/016) and the Centro de Investigación Biomédica en Red en Bioingeniería, Biomateriales y Nanomedicina (CIBER-BBN) for their support. We are also grateful to the Carolina Foundation and the Universidad Pedagógica Nacional Francisco Morazán (UPNFM) Honduras for a doctoral grant to L. E S.-F.

3.5.3.6. References and notes

[1] T. L. Guidotti, *Int. J. Toxicol.* **2010**, *29*, 569–581.
[2] H. Ma, X. Cheng, G. Li, S. Chen, Z. Quan, S. Zhao, L. Niu,*Corros. Sci.* **2000**, *42*, 1669–1683.
[3] M. N. Bates, N. Garrett, P. Shoemack, *Arch. Environ. Health* **2002**, *57*, 405–411.
[4] A) L. Li, P. Rose, P. K. Moore, *Annu. Rev. Pharmacol. Toxicol.***2011**, *51*, 169–187; b) C. Szabo, *Nat. Rev. Drug Discovery* **2007**, *6*, 917–935.
[5] K. Abe, H. Kimura, *J. Neurosci.* **1996**, *16*, 1066–1071.
[6] G. Yang, L. Wu, B. Jiang, W. Yang, J. Qi, K. Cao, Q. Meng, K. Mustafa, W. Mu, S. Zhang, S. H. Snyder, R. Wang, *Sci- ence* **2008**, *322*, 587–590.
[7] D. J. Lefer, *Proc. Natl. Acad. Sci. USA* **2007**, *104*, 17907–17908.
[8] C. Szabo, *Critical Care* **2009**, *13*, P365.
[9] S. Fiorucci, E. Antonelli, A. Mencarelli, S. Orlandi, B. Renga, G. Rizzo, E. Distrutti, V. Shah, A. Morelli, *Hepatology* **2005**, *42*, 539–548.
[10] K. Eto, T. Asada, K. Arima, T. Makifuchi, H. Kimura, *Bio- chem. Biophys. Res. Commun.* **2002**, *293*, 1485–1488.
[11] P. Kamoun, M.-C. Belardinelli, A. Chabli, K. Lallouchi, B. Chadefaux-Vekemans, *Am. J. Med. Genet. A* **2003**, *116A*, 310– 311.
[12] a) J. Chen, S. C. Dodani, C. J. Chang, *Nature Chem.* **2012**, *4*, 973–984; b) Y. Yang, Q. Zhao, W. Feng, F. Li, *Chem. Rev.* **2013**, *113*, 192–270.
[13] a) A. R. Lippert, E. J. New, C. J. Chang, *J. Am. Chem. Soc.* **2011**, *133*, 10078–10080; b) S. Chen, Z.-J. Chen, W. Ren, H. W. Ai, *J. Am. Chem. Soc.* **2012**, *134*, 9589–9592; c) S. K. Das, C. S. Lim, S. Y. Yang, J. H. Han, B. R. Cho, *Chem. Commun.* **2012**, *48*, 8395–8397; d) H. Peng, Y. Cheng, C. Dai, A. L. King, B. L. Predmore, D. J. Lefer, B. Wang, *Angew. Chem.* **2011**, *123*, 9846– 9849; *Angew. Chem. Int. Ed.* **2011**, *50*, 9672–9675; e) Z. Wu, Z. Li, L. Yang, J. Han, S. Han, *Chem. Commun.* **2012**, *48*, 10120– 10122.

[14] W. Xuan, R. Pan, Y. Cao, K. Liu, W. Wang, *Chem. Commun.* **2012**, *48*, 10669–10671.
[15] L. A. Montoya, M. D. Pluth, *Chem. Commun.* **2012**, *48*, 4767–4769.
[16] a) C. Liu, J. Pan, S. Li, Y. Zhao, L. Y. Wu, C. E. Berkman, A. R. Whorton, M. Xian, Angew. *Chem.* **2011**, 123, 10511– 10513; *Angew. Chem. Int. Ed.* **2011**, *50*, 10327–10329; b) Z. Xu, L. Xu, J. Zhou, Y. Xu, W. Zhu, X. Qian, *Chem. Commun.* **2012**, *48*, 10871–10873.
[17] a) X. Cao, W. Lin, K. Zheng, L. He, *Chem. Commun.* **2012**, *48*, 10529–10531; b) X.-F. Yang, L. Wang, H. Xu, M. Zhao, *Anal. Chim. Acta* **2009**, *631*, 91–91.
[18] C. Liu, B. Peng, S. Li, C.-M. Park, A. R. Whorton, M. Xian, *Org. Lett.* **2012**, *14*, 2184–2187.
[19] D. Jiménez, R. Martínez-Máñez, F. Sancenón, J. V. Ros-Lis, A. Benito, J. Soto, *J. Am. Chem. Soc.* **2003**, *125*, 9000–9001.
[20] L. E. Santos-Figueroa, M. E. Moragues, E. Climent, A. Agos- tini, R. Martinez-Manez, F. Sancenon, *Chem. Soc. Rev.* **2013**, *42*, 3489–3613.
[21] a) K. Sasakura, K. Hanaoka, N. Shibuya, Y. Mikami, Y. Ki- mura, T. Komatsu, T. Ueno, T. Terai, H. Kimura, T. Nagano, *J. Am. Chem. Soc.* **2011**, *133*, 18003–18005; b) M.-Q. Wang, K. Li, J.-T. Hou, M.-Y. Wu, Z. Huang, X.-Q. Yu, *J. Org. Chem.* **2012**, *77*, 8350–8354; c) C. Gao, X. Liu, X. Jin, J. Wu, Y. Xie, W. Liu, X. Yao, Y. Tang, *Sensors Acta B: Chem.* **2013**, *185*, 125–131; d) X. Hou, F. Zeng, F. Du, S. Wu, *Nanotechnology* **2013**, *24*, 335502; e) J. Wang, L. Long, D. Xie, Y. Zhan, *J. Lumin.* **2013**, *139*, 40–46.
[22] V. S. Lin, A. R. Lippert, C. J. Chang, *Proc. Natl. Acad. Sci. USA* **2013**, *110*, 7131–7135.
[23] G. De Santis, L. Fabbrizzi, M. Licchelli, C. Mangano, D. Sac- chi, *Inorg. Chem.* **1995**, *34*, 3581–3582.
[24] L. Fabbrizzi, A. Poggi, *Chem. Soc. Rev.* **1995**, *24*, 197–202. [25] M. Hoffman, A. Rajapakse, X. Shen, K. S. Gates, *Chem. Res. Toxicol.* **2012**, *25*, 1609–1615.

3.5.3.7. Supporting information

Highly Selective Fluorescence Detection of Hydrogen Sulfide by Using an Anthracene-Functionalized Cyclam–Cu^{II} Complex

Luis E. Santos-Figueroa, Cristina de la Torre, Sameh El Sayed, Félix Sancenón, Ramón Martínez-Máñez, Ana M. Costero, Salvador Gil and Margarita Parra.

Chemicals

The chemicals 9-(chloromethyl)anthracene, sodium iodide, 1,4,8,11-tetraazacyclotetradecane (cyclam), sodium hydroxide, copper(II) nitrate, hydrochloric acid and paraformaldehyde were provided by Sigma-Aldrich. Analytical-grade solvents and anhydrous magnesium sulfate were purchased from Scharlau (Barcelona, Spain). Cell proliferation Reagent WST-1 was obtained from Roche Applied Science. DMEM with L-glutamine, piruvate and Fetal Bovine Serum (FBS), trypan blue solution (0.4%) cell culture grade and trypsin were provided by Gibco-Invitrogen. For the spectroscopy studies L-cysteine (Cys), DL-homocysteine (Hcy), glutathione (GSH), hydrogen peroxide and tetrabutylammonium or sodium salts of hydrogen sulfide, fluoride, chloride, bromide, iodide, hydroxide, acetate, cyanide, azide, nitrate, hydrogen carbonate, sulfate, thiosulfate, hydrogen phosphate and citrate were used. Sodium hydrogen sulfide solutions in HEPES (30 mM, pH 7.5) were freshly prepared each time before use.

General Techniques

UV-visible spectra were recorded with a JASCO V-650 Spectrophotometer. Fluorescence measurements were carried out in a Jasco FP-8500 Spectrophotometer. 1H and 13C-NMR spectra were acquired in a Bruker Advance III (400 MHZ). Mass spectra were carried out in a Triple TOF T5600 (ABSciex, USA) spectrometer. Fluorescence images were captured using an epifluorescence microscopy Eclipse E600 with a Nikon DS-Ri digital cooler CCD camera using a UV-2A (Ex 330-380 nm, DM 400, BA 420) filter cube. Cell viability measurements were carried out with a Wallac 1420 workstation.

Synthesis of 1

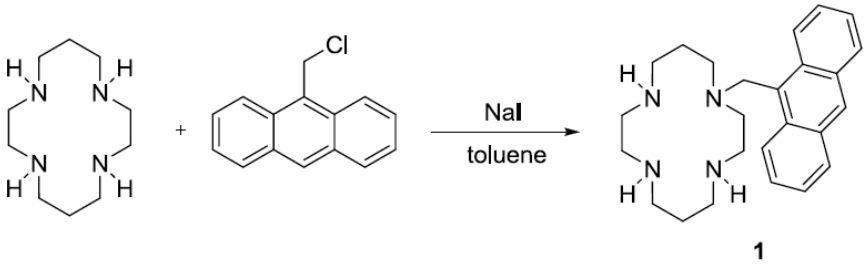

1

Scheme S1. Synthesis of **1**.

9-(chloromethyl)anthracene (560 mg, 2.5 mmol) was dissolved in toluene (10 mL) and then sodium iodide (370 mg, 2.5 mmol) was added under constant stirring. Then, 1,4,8,11-tetraazacyclotetradecane (520 mg, 2.6 mmol) was added and the resulting solution was heated under reflux for 8 h. After this time, the precipitated salts were removed by filtration and the solution was washed with 5% aqueous sodium hydroxide solution (2 x 10 mL) and water (3 x 10 mL). The organic phase was separated, dried with anhydrous magnesium sulfate, filtered, and concentrated to dryness. The resulting product was dissolved in ethanol (10 mL) and concentrated hydrochloric acid (1.5 mL) was added. The hydrochloride salt was precipitated on cooling and collected by filtration. Then, the

hydrochloride was dissolved in basic water and then extracted with diethyl ether in order to obtain the free base. The ether layer was then dried (Na_2SO_4), filtered and the solvent removed by rotary evaporation. Finally, the product (**1**) was purified by chromatography on silica using ethyl acetate/hexane (3:1 v/v) as eluent to afford pure **1** (296 mg, 0.75 mmol, 53% yield) as a yellow solid. The ^{1}H and ^{13}C data of **1** are in full agreement with those published in the literature.[1] HRMS-EI m/z: calcd for $C_{25}H_{35}N_4$ 391.2856; found 392.2848 ($M+H^+$). ^{1}H NMR (400 MHz, CDCl3) δ 8.51 (d, J = 9.0 Hz, 2H, 2xCH), 8.41 (s, 1H, CH), 7.99 (d, J = 7.8 Hz, 2H, 2xCH), 7.56 – 7.39 (m, 4H, 4xCH), 4.51 (s, 2H, CH_2), 3.36 (s, 1H, NH), 2.76 – 2.65 (m, 6H, 3xCH_2), 2.64 – 2.54 (m, 6H, 3xCH_2), 2.48 – 2.41 (m, 4H, 2xCH_2), 1.88 – 178 (m, 2H, CH_2), 1.57 – 1.49 (m, 2H, CH_2), 1.25 (s, 2H, 2NH) ppm.

Synthesis of [Cu(1)]$^{2+}$complex

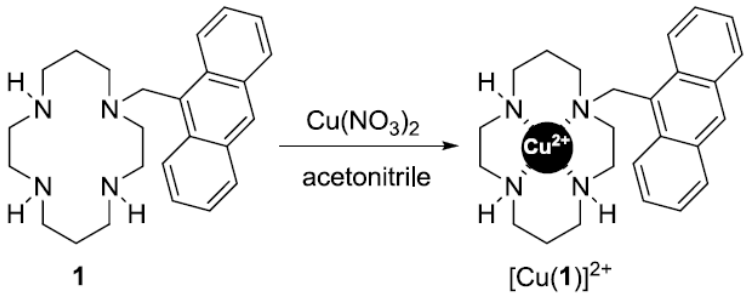

Scheme S2. Synthesis of [Cu(**1**)]$^{2+}$ complex.

The [Cu(**1**)]$^{2+}$ complex was prepared by the addition of an equimolar amount of copper(II) nitrate (13.5 mg, 0.072 mmol) to **1** (28.1 mg, 0.072 mmol) in hot acetonitrile (10 mL). The solution was stirred at reflux, under argon for 14 h.

[1] a) G. De Santis, L. Fabbrizzi, M. Licchelli, C. Mangano, and D. Sacchi, *Inor. Chem.* **1995**, 34, 3581; b) L. Fabbrizzi, M. Licchelli, P. Pallavicini, A. Perotti, A. Taglietti and D. Sacchi, *Chem. Eur. J*. **1996**, 2, 75.

Finally, $[Cu(\mathbf{1})]^{2+}$ was precipitated on cooling as a purple solid (32.74 mg, 0.072 mmol). HRMS-EI *m/z*: calcd for $C_{25}H_{32}N_4Cu^{2+}$ 452.1996; found 452.2011.

UV-visible behavior of $[Cu(1)]^{2+}$

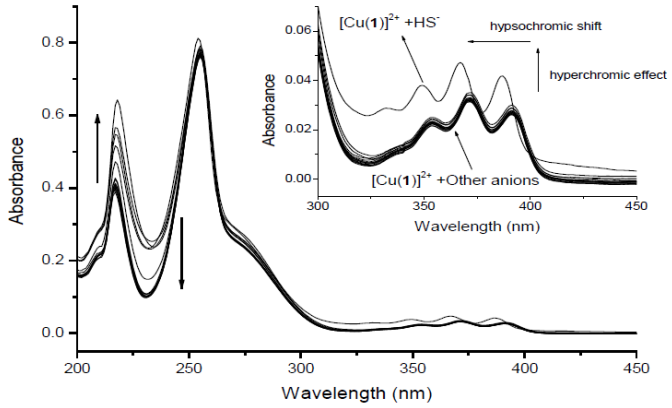

Figure S1. UV-visible spectra of $[Cu(\mathbf{1})]^{2+}$ (2.0×10^{-5} M) in HEPES (30 mM, pH 7.5 at 25 °C) alone and in the presence of 10 eq. of selected anions (HS^-, Cl^-, Br^-, F^-, OH^-, AcO^-, CN^-, N_3^-, HCO_3^-, SO_4^{2-}, $S_2O_3^{2-}$, SO_3^{2-}, HPO_4^{2-} and citrate). Inset: absorption spectra in the 300-450 nm range.

Emission behavior of $[Cu(1)]^{2+}$

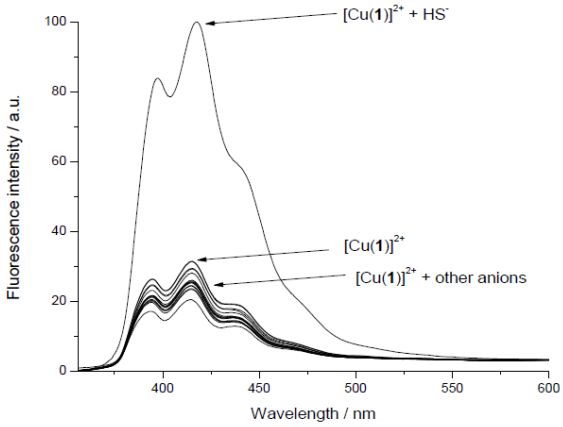

Figure S2. Emission spectra of $[Cu(\mathbf{1})]^{2+}$ solution (2.0×10^{-5} M) in HEPES (30 mM, pH 7.5 at 25 °C) alone and in the presence of 10 eq. of selected anions (HS^-, Cl^-, Br^-, I^-, F^-, OH^-, AcO^-, CN^-, SCN^-, N_3^-, NO_3^-, HCO_3^-, SO_4^{2-}, $S_2O_3^{2-}$, SO_3^{2-}, HPO_4^{2-} and citrate) upon excitation at 256 nm.

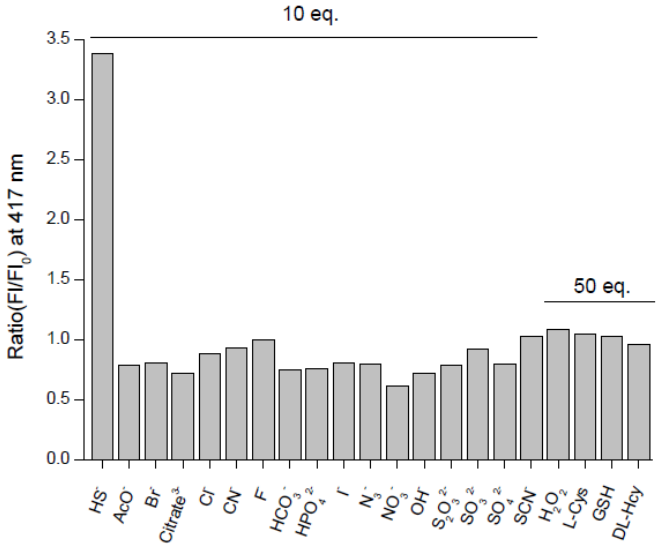

Figure S3. Emission intensity at 417 nm (F/F_0), upon excitation at 256 nm, of $[Cu(\mathbf{1})]^{2+}$ solution (2.0×10^{-5} M) in HEPES (30 mM, pH 7.5 at 25 °C) alone and in the presence of 10 eq. of selected anions and 50 eq. of H_2O_2 and thiol-containing derivatives.

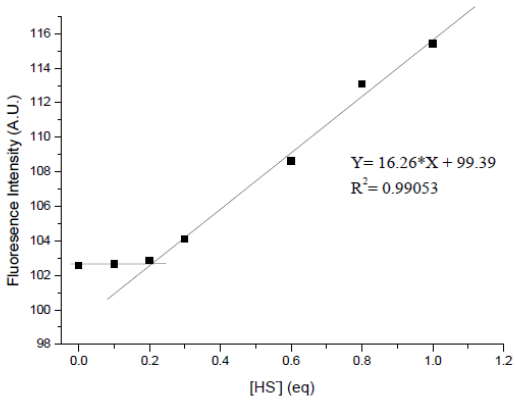

Figure S4. Fluorescence calibration curve for HS^- anion using $[Cu(\mathbf{1})]^{2+}$ (2.0×10^{-5} M) in HEPES (30 mM, pH 7.5 at 25 °C) at 417 nm, upon excitation at 256 nm.

WST-1 Cell viability assay and fluorescence imaging

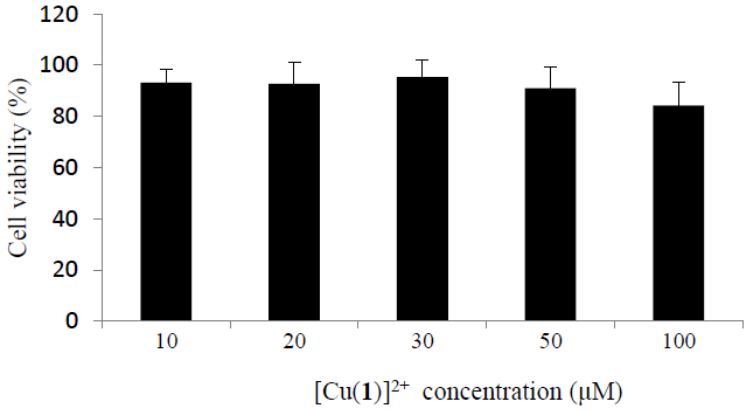

Figure S5. Evaluation of cell viability of $[Cu(\mathbf{1})]_{2+}$ in HeLa cells.

The HeLa cervix adenocarcinoma cells were purchased from the German Resource Centre for Biological Materials (DSMZ) and were grown in Dulbecco's modified Eagle's medium (DMEM) supplemented with 10% fetal bovine serum. Cells were maintained in a humidified atmosphere (5% carbon dioxide and 95 % air at 37 ^{o}C) and underwent passage twice a week.

To develop the cell viability assays HeLa cells were cultured in sterile 96-well plate at a seeding density of 2.5 x 10^3 cells/well and they were allowed to settle for 24h. Then, the medium was replaced and $[Cu(\mathbf{1})]^{2+}$ in DMSO was added to cells at final concentrations of 5, 10, 30, 50 and 100 μM. Incubation was continued for 30 min, then the medium was removed, replaced and 10 μL/well of a NaHS solution in PBS was added (final concentration of 500 μM) and the cells were further incubated for 30 min. The medium was replaced and WST-1 (10 μL of a 5 mg/ml solution) was added to each well, and cells were further incubated for 1 h. Then shaked thoroughly for 1 minute on a shaker and the absorbance was measured at 450 nm against a background control as blank using an ELISA microplate reader. The reference wavelength was 690 nm. The results of the WST-

1 cell viability assay are shown in Figure S5. As it can be seen $[Cu(\mathbf{1})]^{2+}$ is non-toxic for HeLa cells at the tested concentrations.

To develop the fluorescence microscopy studies, HeLa cells were seeded in 24 mm glass coverslips in six-well plates at a seeding density of 1.5 x 10^5 cells/well, and they were allowed to settle for 24 h. Cells were treated with $[Cu(\mathbf{1})]^{2+}$in DMSO (1%) at a final concentration of 30 μM. After 20 minutes, the medium was removed to eliminate compounds. Then solution of NaHS in PBS was added to the culture at a final concentration of 0, 100, 200 and 500 μM and the cells were incubated for another 10 min. All the fluorescence imaging was carried out after washing the cells with PBS buffer three times and then fixed with paraformaldehyde using an epifluorescence microscopy ECLIPSE E600.

Selected fluorogenic probes for detection of hydrogen sulfide

Mechanism	Solvent	Time	LOD	Reference
Demetallation of a Cu(II)-cyclam complex	HEPES pH 7.5	instantaneous	3.9 μM	this paper
demetallation of a Cu(II)-cyclen complex	HEPES pH 7.4	instantaneous	not reported	*J. Am. Chem. Soc.* **2011**, *133*, 18003
demetallation of a Cu(II)-cyclen complex	HEPES pH 7.4	instantaneous	16 μM	*J. Org. Chem.* **2012**, *77*, 8350
demetallation of a Cu(II)-quinoline complex	HEPES (pH 7.2)-DMSO 1:9 v/v	not reported	1 μM	*Sensors Act. B: Chem.* **2013**, *185*, 125-131
demetallation of a Cu(II) complex	HEPES pH 7.0	10 seconds	0.78 μM	*Nanotechnology* **2013**, *24*, 335502
demetallation of a Cu(II) complex	TRIS-DMF 6:4 v/v	1 minute	0.18 μM	*J. Lumin.* **2013**, *139*, 40
Pyrylium to thiopyrylium transformation	water-ACN 1:1 v/v	2 minutes	not reported	*J. Am. Chem. Soc.* **2003**, *125*, 9000
Michael addition-cyclization	phosphate buffer pH 7.4	30 minutes	1 μM	*Org. Lett.* **2012**, *14*, 2184
Michael addition-cyclization	PBS (pH 7.4)-ACN 9:1 v/v	60 minutes	1 μM	*Angew. Chem. Int. Ed.* **2011**, *50*, 10327
Michael addition-cyclization	TRIS (pH 7.4)-ethanol 6:4 v/v	2 minutes	0.12 μM	*Chem. Commun.* **2012**, *48*, 10871
hydrolysis of 2,4-dinitrophenylether	PBS (pH 7.0 with CTAB)-	5 minutes	0.05 μM	*Chem. Commun.* **2012**, *48*, 10529

	ethanol 9:1 v/v			
hydrolysis of 2,4-dinitrobenzenesylfonyl	water (pH 7.4)-acetone 75-25 v/v	30 minutes	0.05 μM	*Anal. Chim. Acta* **2009**, *631*, 91
hydroxylamine-amine reduction	phosphate buffer pH 7.4	120 minutes	0.5 μM	*Chem. Commun.* **2012**, *48*, 10669
azide-amine reduction	PIPES pH 7.4	45 minutes	1 μM	*Chem. Commun.* **2012**, *48*, 4767
azide-amine reduction	HEPES pH 7.4	60 minutes	5 μM	*J. Am. Chem. Soc.* **2011**, *133*, 10078
azide-amine reduction	HEPES pH 7.2	120 minutes	5 μM	*Chem. Commun.* **2012**, *48*, 8395
sulfonylazide-sulfonylamine reduction	phosphate buffer pH 7.5	10 minutes	1 μM	*Angew. Chem. Int. Ed.* **2011**, *50*, 9672
azide-amine reduction and cyclization	phosphate buffer (pH 7.4)-ACN 8:2 v/v	60 minutes	100 μM	*Chem. Commun.* **2012**, *48*, 10120

3.6. Anion chemosensor by chemodosimeter paradigm approach

3.6.1. Experimental objectives

Following our interest in the preparation of efficient chemosensor for enviromental and biorelevant hydrogen sulfide anion sensing and focusing in the search of a chromo-fluorogenic probe; we decided to design a new chemosensor for the detection of HS^- anion by using the chemodosimeter paradigm.

Taking into account the above mentioned facts, our main aims in this project were:

- Design and synthesize a new sensitive and selective chromo-fluorogenic chemosensor for HS^- recognition.

- Characterize the new probe by standard methods (NMR, HRMS, IR, UV/Vis and emission spectroscopy).

- Evaluate the real potential of use of new probe to detect HS^- by color change to the naked eye and by intracelular fluorescence images.

3.6.2. Chemosensor design

In the same line of the previously reported projet (section 3.5.3), the new chemosensor design was also centred into preparation of a probe able of immediate hydrogen sulfide detection in aqueous medium. In particular, this project seach the preparation of a new chromo-fluorogenic chemosensor with an easily noticeable optical output.

Chemodosimeter paradigm was prefered as design approach, due their specificity and versatility especially to chromogenic recognition in aqueous media. In this case, the chemical reduction of an azide to an amine was selected as mechanism for the chromo-fluorogenic response.

We chose sulfonyl azide dyes in the preparation of chemodosimeter, due to their straightforward synthesis and their well-known spectroscopic properties. Besides, azo dyes are widely used in organic products and cellular studies by its low toxicity, which was suitable for the development of chemosensors for hydrogen sulfide in cellular medium. Other families of dyes, such as bodipy and nitro dyes were also considering on the design steps and were discarded later because showed poor chromo-fluorogenic changes.

3.6.3. A chemosensor bearing sulfonyl azide moieties for selective chromo-fluorogenic hydrogen sulfide recognition in aqueous media and in living cells

In this section a sensitive and selective chromogenic and fluorogenic detection of hydrogen sulfide in aqueous environments and intracellular by a simple sulfonyl azide derivative is reported (**Figure 35**).

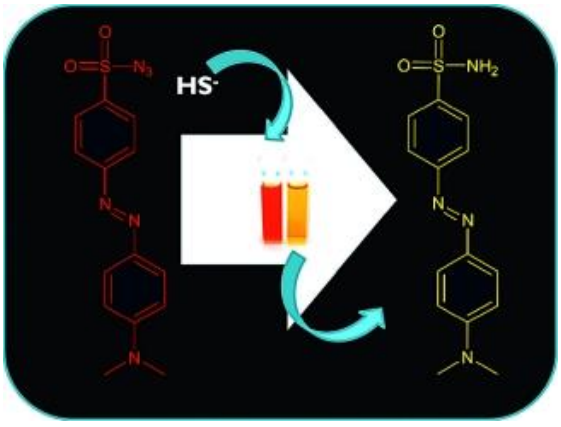

Figure 35. Schematic representation of a new chemodosimeter for HS^- recognition in aqueous media and living cells (front cover of publised communication)

A Chemosensor Bearing Sulfonyl Azide Moieties for Selective Chromo-Fluorogenic Hydrogen Sulfide Recognition in Aqueous Media and in Living Cells

Luis E. Santos-Figueroa,[a,b,c] Cristina de laTorre,[a,b,c] Sameh El Sayed,[a,b,c] Félix Sancenón,[a,b,c] Ramón Martínez-Máñez,*[a,b,c] Ana M. Costero,*[a,d] Salvador Gil,[a,d] and Margarita Parra[a,d]

[a] Instituto de Reconocimiento Molecular y Desarrollo Tecnológico (IDM), Centro Mixto Universidad Politécnica de Valencia-Universidad de Valencia (Spain)

[b] Departamento de Química, Universidad Politécnica de Valencia, Camino de Vera s/n, 46022 Valencia (Spain)

[c] CIBER de Bioingeniería, Biomateriales y Nanomedicina (CIBER- BBN)

[d] Departamento de Química, Universitat de València, Dr. Moliner 50, 46100, Burjassot, Valencia, Spain

Received: October 5, 2013

Published online: January 28, 2014

European Journal of Organic Chemistry, **2014**, 1848-1854.

3.6.3.1. Abstract

A simple chemodosimeter based on a sulfonyl azide dye (**1-**Az), which displayed a highly selective response toward hydrogen sulfide anion in mixed aqueous media, was synthesised and characterised. Addition of hydrogen sulfide to acetonitrile/HEPES 1:1 solutions of **1-**Az induced a clear colour change from red-orange to yellow, which was easily detected by the naked eye, and by an enhancement in the emission intensity. Other common anions, thiol-containing biomolecules and oxidants did not induce any noticeable colour or fluorescence modulation in the probe. The chemodosimeter also showed a good sensitivity, with limits of detection of 11.91 and 0.63 μM by using UV/Vis or fluorescence measurements, respectively. Moreover, **1-**Az could be used for real-time fluorescence imaging of intracellular HS^- at micro- molar concentrations.

3.6.3.2. Introduction

Hydrogen sulfide (H_2S), a colourless and flammable gas with high solubility in water and in organic solvents, is well-known for its disagreeable "rotten eggs" smell. Hydrogen sulfide has been traditionally studied for its known toxicity[1] its presence as a corrosive industrial waste product,[2] and emission in the energy industry,[3] as a parameter for geological activity,[4] as quality control of foods with high protein content,[5] and as an important compound related to microbial activity in anaerobic processes. Moreover, recently, hydrogen sulfide has been discovered to have a role as a gasotransmitter[6] and has relevance in a number of biological processes, such as neurotransmission,[7] vasorel- axation,[8] cardioprotection,[9] and anti-inflammation.[10] In fact, some H_2S-releasing drugs are currently being used to treat these pathologies. Furthermore, the abnormal production of H_2S has been associated with diseases such as chronic kidney disease, liver cirrhosis,[11] Alzheimer[12] and Down's syndrome.[13] Due to the important roles that hydrogen sulfide plays in environmental and in biological processes, the development of selective detection systems for this compound has recently become a focus of significance.

In the last years, several probes for the fluorogenic detection of hydrogen sulfide in water or in mixed organic-aqueous environments have been described.[14] In most cases, the probes follow a chemodosimeter approach in which an irreversible chemical reaction induced by hydrogen sulfide is coupled with effective fluorescence modulations. In particular, the reduction of azide,[15] hydroxylamine[16] and nitro[17] moieties to amine have been used as key reactions in the development of hydrogen sulfide-selective fluorescent probes. Moreover, the hydrogen sulfide-induced hydrolysis of disulfide bonds,[18] dinitrophenyl ethers,[19] and cyano-vinyl moieties,[20] linked with fluorophores have also been used for the fluorescent recognition of this anion. Another interesting approach is the use of demetallation reactions of nonfluorescent Cu^{II} complexes induced by hydrogen sulfide that resulted in a turn-on of the emission.[21] Recently, Han and co-workers prepared several fluorescent BODIPY dyes that were functionalised with selenoxide moieties for the detection of hydrogen sulfide through HS^--promoted reduction of the selenoxide group to selenide, which resulted in quenching of the initial emission.[22]

In addition to fluorescence changes, three of the examples mentioned above also show colour modulations in the presence of hydrogen sulfide. For instance, Han and co-workers prepared a cyanine derivative functionalised with an azide moiety that showed an absorption band at 610 nm (blue) in water at pH 7.4 that was shifted to 660 nm in the presence of hydrogen sulfide.[15b] Some other examples involve reduction of the nitro moiety to amino in dimethyl sulfoxide (DMSO) in certain coumarin derivatives,[17b] the demetallation reaction in a Cu^{II} complex,[21c] nucleophilic addition to tricyanovinyl dyes,[22a] and nucleophilic aromatic substitution reactions.[23] Furthermore, some of us have reported colorimetric sulfide-sensing based on sulfide-induced transformation of a pyrylium group into the corresponding thiopyrylium derivative.[24]

In particular, we believe that the design of chromogenic chemodosimeters for hydrogen sulfide has a special interest, because they offer the possibility of straightforward use of widely available instrumentation and simple semi-quantitative detection of this toxic anion with the naked eye. Such simple systems may be used to control H_2S concentrations in target industrial processes or for environmental and geological monitoring in situ. Nevertheless, in spite of these possible applications, relatively few examples of selective and sensitive chromogenic probes for the detection of hydrogen sulfide have been reported (see above).

Bearing in mind the concepts mentioned above and following our interest in the development of new approaches for optical sensing,[25] we attempted to develop a simple probe for the detection of sulfide in mixed aqueous media. In the design of the probe, among the possible signaling subunits, we chose azo dyes, which have been widely used due to their straightforward synthesis and their well-known spectroscopic properties. In fact the simple reaction between *N,N*-disubstituted anilines and diazonium salts of a great variety of aniline derivatives results in the preparation of azo dyes with characteristic charge-transfer absorption bands in the 400–500 nm interval and compounds that range from pale-yellow to red-orange. Moreover, as a signalling reporter we took advantage of the strategy recently reported by Wang and co-workers that used the accelerated reduction of azide groups directly attached to sulfonyl moieties to amine in the presence of hydrogen sulfide.[15] By following this approach we report herein the development of **1-**Az (see Scheme 1) as a new probe for the selective colorimetric detection of hydrogen sulfide. The probe contains a sulfonyl azide signalling moiety attached to an azo dye framework.

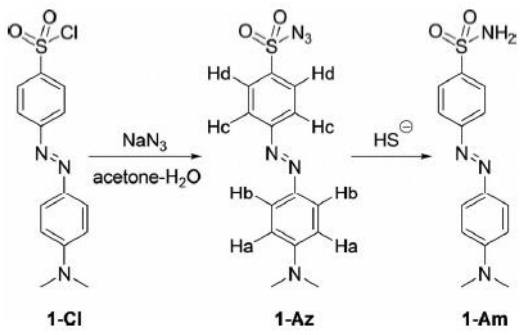

Scheme 1. Synthesis of chemodosimenter **1**-Az and its reaction with hydrogen sulfide to yield **1**-Am.

3.6.3.3. Results and Discussion

Probe **1**-Az was prepared by following a slight modification of previously reported procedures.[26] In particular, commercially available dabsyl chloride (**1**-Cl) was dissolved in acetone and then an aqueous concentrated solution of sodium azide was carefully added with constant stirring at 0 °C (see Scheme 1). The structure of the **1**-Az probe was fully confirmed by ^{1}H and ^{13}C NMR, IR and HRMS analyses (see the Supporting Information for full details). ^{1}H NMR spectra of **1-**Az showed the typical doublets centred at δ = 6.88 and 7.87 ppm ascribed to the 1,4 disubstituted benzene ring bearing the *N,N*-dimethylamine moiety and other AB system with signals centred at δ = 8.01 and 8.15 ppm, ascribed to the 1,4-disubstituted benzene ring bearing the sulfonyl azide group. Moreover, the protons of the *N,N*-dimethylamine moiety appeared as a singlet centred at δ = 3.12 ppm. HRMS-EI measurements confirmed the structure of the final product (*m/z* calcd. for $C_{14}H_{15}N_6O_2S^+$: 331.0972; found: 331.0969).

MeCN/HEPES (30 mM, pH 7.5; 1:1 v/v) solutions of **1**-Az (1.0 X 10^{-5} M) presented an intense CT absorption band (centred at 478 nm) due to the presence of a *N,N*-dimethylamino donor moiety and an electron-acceptor sulfonyl azide group (see Figure 1). The UV/Vis behaviour of **1**-Az was tested in the presence of 10 equiv. of selected anions (i.e., HS^-, Cl^-, Br^-, I^-, F^-, OH^-, AcO^-, CN^-, N_3^-, NO_3^-,

HCO_3^-, SO_4^{2-}, $S_2O_3^{2-}$, HPO_4^{2-} and citrate), other thiol-containing derivatives [i.e., L-cysteine (L-Cys), DL-homocysteine (DL-Hcy), and glutathione (GSH)] and certain oxidants (i.e., H_2O_2). As can be seen in Figure 1, only hydrogen sulfide induced a hypsochromic shift of 28 nm (from 478 to 450 nm) of the visible band of **1**-Az together with a moderate hypochromic effect that was reflected in a colour modulation from orange-red to yellow (see Figure 2). This observed change in colour (that was practically instantaneous) was ascribed to hydrogen sulfide-induced reduction of the sulfonyl azide moiety in **1**-Az to a sulfonamide (see structure **1**-Am in Scheme 1). The reduced electron-acceptor character of the sulfonamide moiety, when compared with the initial sulfonyl azide, accounts for the observed hypsochromic shift.

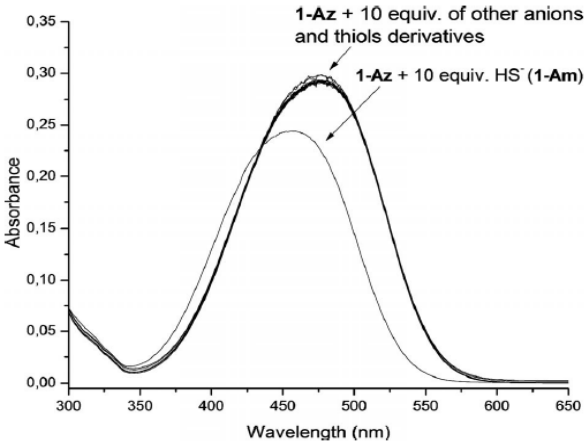

Figure 1. UV/Vis spectra of **1**-Az (1.0 X 10^{-5} M) in MeCN/HEPES (30 mM, pH 7.5; 1:1 v/v) upon addition of 10 equiv. of HS^-, Cl^-, Br^-, I^-, F^-, OH^-, AcO^-, CN^-, N_3^-, NO_3^-, HCO_3^-, SO_4^{2-}, $S_2O_3^{2-}$, HPO_4^{2-}, citrate, L-Cys, DL-Hcy, GSH or H_2O_2.

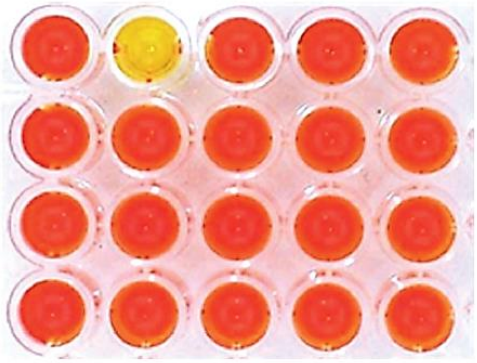

Figure 2. Photograph of MeCN/HEPES (30 mM, pH 7.5; 1:1 v/v) solutions of **1**-Az upon addition of 10 equiv. of target chemicals. From left to right and top to bottom: blank, HS^-, Cl^-, Br^-, I^-, F^-, OH^-, AcO^-, CN^-, N_3^-, NO_3^-, HCO_3^-, SO_4^{2-}, $S_2O_3^{2-}$, HPO_4^{2-}, citrate, L-Cys, DL-Hcy, GSH and H_2O_2.

The mechanism of the chromogenic response was fully corroborated by the synthesis and isolation of compound **1**-Am upon reaction of **1**-Az with sodium sulfide in acetonitrile (see the Supporting Information for full synthetic details). Figure 3 shows the ^{1}H NMR spectra of the aromatic part of chemodosimeter **1**-Az compared to that of sulfonamide 1-Am obtained upon reaction of **1**-Az with HS^-. Reduction of the sulfonyl azide moiety in **1**-Az induced upfield shifts of the signals centred at 8.01 (Hc) and 8.15 (Hd) ppm to 7.90 and 7.96 ppm, respectively, which is indicative of the formation of sulfonamide moieties (see Scheme 1 for proton assignation). Furthermore, the protons of the sulfonamide group appeared as a broad singlet centred at δ = 7.42 ppm. HRMS (EI) measurements confirmed the formation of **1**- Am (*m/z* calcd. for $C_{14}H_{17}N_4O_2S^+$ 305.1072; found: 305.1068).

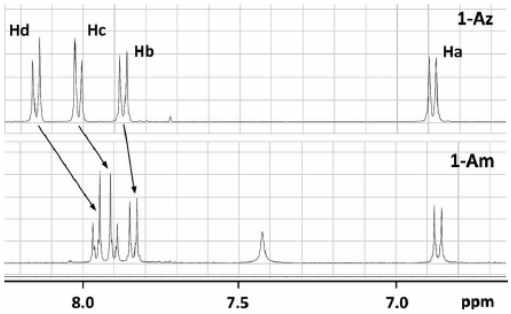

Figure 3. ^{1}H NMR spectra of the aromatic protons of chemodosi- meter **1**-Az and of **1**-Am (both at 1.0 X 10^{-3} M) in CD_3CN.

The response observed was highly selective and, from all the species tested (see above), only HS^- induced shifts of the visible band. Moreover, in competitive experiments it was found that the same chromogenic response of **1**-Az took place upon addition of HS^- alone or HS^- in the presence of 10 equiv. of the above studied species (see Figure 4).

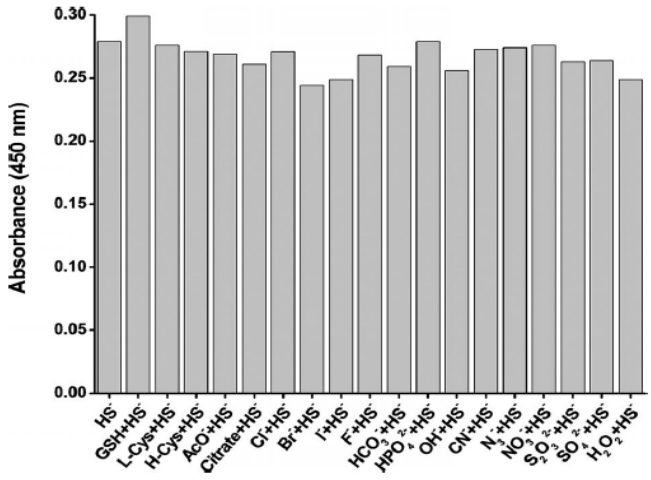

Figure 4. Absorbance at 450 nm of **1**-Az (1.0 X 10^{-5} M) in MeCN/ HEPES (30 mM, pH 7.5; 1:1 v/v) upon addition of 10 equiv. of HS^- alone and in the presence of 10 equiv. of HS^- and 10 equiv. of selected anions, oxidants and biological thiols.

Having assessed the selective chromogenic response of **1**-Az toward HS^- anions, the sensitivity of the probe was studied. In particular, the changes in the visible band centred at 478 nm, of MeCN/HEPES (30 mM, pH 7.5; 1:1 v/v) solutions of **1**-Az (1.0 X 10^{-5} M) was monitored upon addition of HS^- anions. The addition of increasing quantities of HS^- anions induced a progressive hypsochromic shift of the visible band in **1**-Az (see the Supporting Information). From typical calibration curves, a remarkable detection limit of 11.91 ± 0.09 μM (δ = 0.4 ppm) was calculated by using a simple conventional UV/Vis spectrophotometer. Furthermore, the highly selective response of **1**-Az to HS^- anions was also studied by monitoring the emission change. Thus, **1**-Az

(MeCN/HEPES, 1:1 v/v solutions) was weakly emissive (quantum yield of 0.036), showing a broad emission band centred at 557 nm with a shoulder at ca. 520 nm (upon excitation at 478 nm). Solutions of **1**-Az were tested in the presence of several anions (i.e., HS^-, Cl^-, Br^-, I^-, F^-, OH^-, AcO^-, CN^-, N_3^-, NO_3^-, HCO_3^-, SO_4^{2-}, $S_2O_3^{2-}$, $HPO4^{2-}$ and citrate), thiol-containing derivatives (i.e., L-Cys, DL-Hcy and GSH) and H_2O_2. Only HS^- induced a moderate emission enhancement at 557 nm (quantum yield of 0.048). From the corresponding calibration curves a remarkable detection limit for sulfide of 0.63 ± 0.05 μM (δ = 0.02 ppm) was determined (see the Supporting Information). The sensitivity of the system was sufficient to determine levels of **1**-Az below the concentration of H_2S required to elicit physiological responses (10– 1000 μM).[27]

Further experiments were carried out in the presence of higher concentrations of L-Cys, DL-Hcy and GSH. In particular, it is known that common physiological concentrations of biothiols are in the range of 1–20 mM for GSH, 0.14–0.37 mM for Cys, and 0.004–0.018 mM for Hcy. Taking into account these data, the chromo-fluorogenic response of **1**-Az (1.0×10^{-5} M) in MeCN/HEPES (30 mm, pH 7.5; 1:1 v/v) solutions in the presence of 0.2, 0.3 and 0.4 mM of DL-Cys, 0.5, 1, 5, 10 and 20 mM of GSH, and 0.2 mM of DL-Hcy was studied. Neither L-Cys, GSH or DL-Hcy (in the range of concentrations tested) induced changes in either the absorption or the emission bands of **1**-Az.

Finally, the stability of probe **1**-Az in the presence of water-containing mixtures and air was studied. It was found that the intensity of the absorption and emission bands at 480 and 557 nm, respectively, of MeCN/HEPES solutions (1:1, v/v) of the probe (measured in open cuvettes to evaluate possible degradation by air) remained unchanged for at least 12 h.

The selective emission enhancement of **1**-Az in the presence of HS^- and the negligible response observed upon the addition of biothiols (GSH, L-Cys and DL-Hcy) at physiological concentrations strongly suggest that the probe can be used

for HS^- imaging in living cells. Based on these observations, the cytotoxicity of **1**-Az was first evaluated. In this respect, HeLa cells were treated with **1**-Az at different concentrations over a 24-hour period and cell viability was determined by a WST-1 assay. The obtained results are shown in Figure 5. As seen, probe **1**-Az is essentially nontoxic in the range of concentrations tested (10–100 μM).

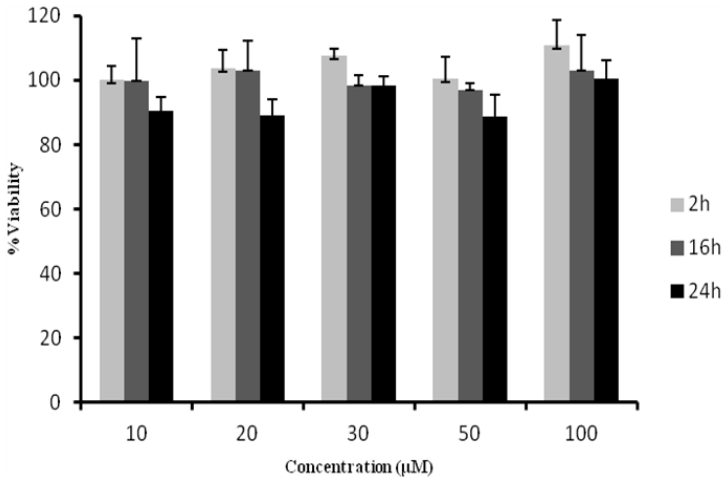

Figure 5. Cell viability test of different concentrations of **1**-Az at 24 h in HeLa cells using WST-1 assay.

In a second step, to verify the feasibility of the developed probe to detect HS^- in highly competitive environments, we used **1**-Az for the fluorescence imaging of sulfide in living cells. HeLa cells were incubated in DMEM supplemented with 10 % fetal bovine serum. To conduct fluorescence microscopy studies, HeLa cells were seeded in 24 mm glass coverslips in 6-well plates and were allowed to settle for 24 h. Cells were treated with **1**-Az in DMSO at a final concentration of 30 μM. After 20 min at 37 °C, the medium was removed and the cells were washed with PBS. Solutions of different concentrations of NaHS (0, 60, 80, 200 and 500 μM) in PBS were added and the cells were incubated for a further 30 min period. The results are shown in Figure 6. The control experiment (HeLa cells without probe **1**-Az) showed no fluorescence, whereas cells incubated with **1**-Az showed a very weak fluorescence (ascribed to the endogenous HS^-). In contrast, a marked

enhancement in intracellular emission was observed in the HS^--treated cells, clearly indicating the possible use of **1**-Az to detect hydrogen sulfide in complex media. However, HeLa cells treated with 10 and 40 μM of HS^- showed no emission enhancement.

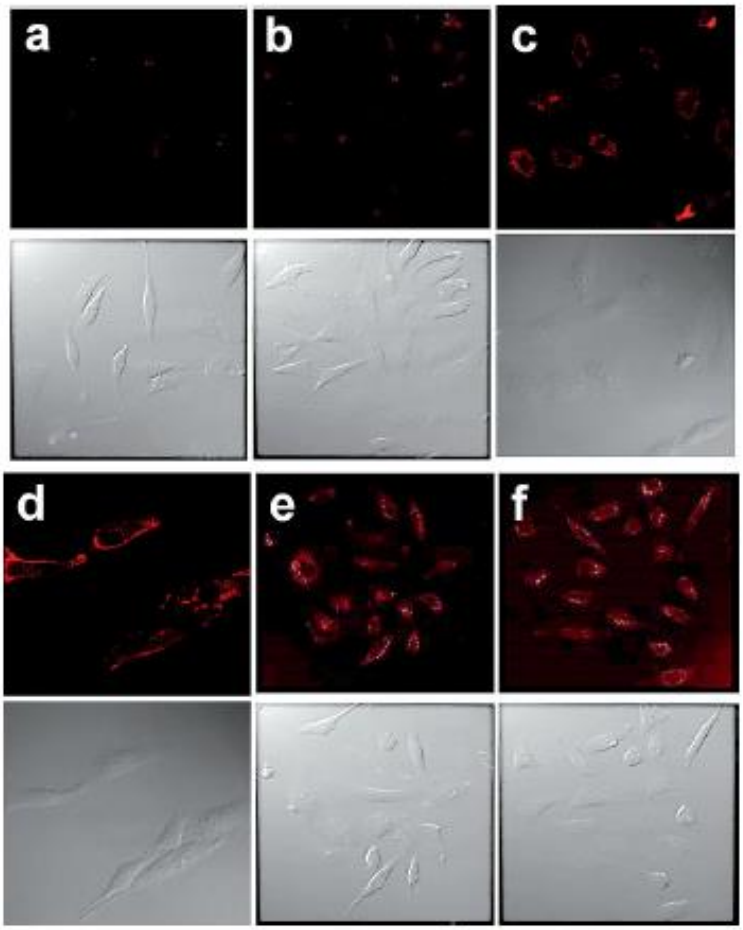

Figure 6. Confocal fluorescence images of HeLa cells: (a) cells untreated; (b) cells incubated with **1**-Az (30 μM); (c), (d), (e) and (f) cells incubated with **1**-Az (30 μM) in the presence of HS^- (60, 80, 200 and 500 μm for c, d, e and f respectively).

Moreover, Figure 7 shows the ratio of average fluorescence after 10 min as compared to that found in the absence of the probe (FI/FI_0) for the fluorescence

images of cells after the addition of 0, 200 and 500 μM NaHS. A clearly enhanced fluorescence ratio is observed, which related well with the increment in HS^- concentration.

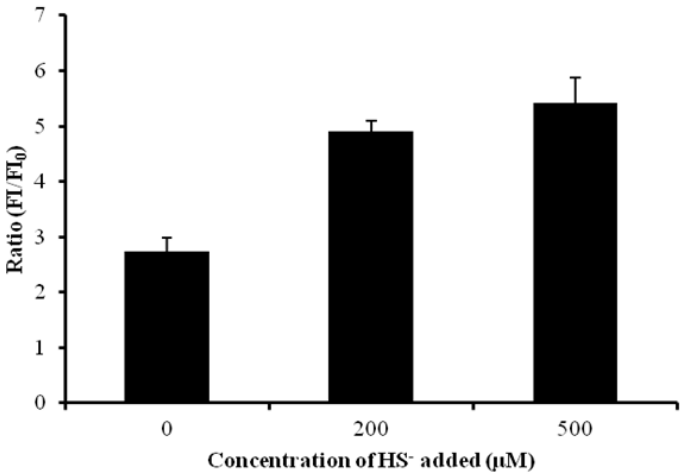

Figure 7. Average FI/FI_0 ratios from the fluorescence images of HeLa cells incubated with **1**-Az after the addition of 0, 200 and 500 μM of NaHS. Error bars are ±SD from replicate experiments (*n* = 3).

3.6.3.4. Conclusions

We have prepared a simple chemodosimeter based on a sulfonyl azide dye (**1**-Az) that displayed a highly selective response toward hydrogen sulfide anions in mixed aqueous media. In the presence of this anion a clear colour change from red-orange to yellow, which was easily detected by the naked eye, and an enhancement of emission intensity were observed. Other common anions, thiol-containing biomolecules, and oxidants did not induce any noticeable colour or fluorescence modulation in the probe. The chemodosimeter also showed a good sensitivity, with limits of detection of 11.91 and of 0.63 μM by using UV/Vis or fluorescence measurements, respectively. The prepared probe is easy to synthesise and allows an efficient, fast and low-cost detection of hydrogen sulfide anions in mixed aqueous solutions. Moreover, real-time fluorescence imaging measurements confirm that probe **1**-Az can be used to detect intracellular HS^- at

micromolar concentrations. Similar designs using other available dyes for the straightforward signalling of HS^- are being investigated in our laboratory.

3.6.3.5. Experimental Section

Chemicals: Sodium azide, dabsyl chloride (**1**-Cl), L-cysteine (Cys), DL-homocysteine (Hcy), glutathione (GSH), and hydrogen peroxide were purchased from Sigma–Aldrich. Analytical-grade solvents, sodium hydrogen carbonate, and anhydrous magnesium sulfate were purchased from Scharlau (Barcelona, Spain). For the chromo-fluorogenic studies, tetrabutylammonium or sodium salts of hydrogen sulfide, fluoride, chloride, bromide, iodide, hydroxide, acetate, cyanide, azide, nitrate, hydrogen carbonate, sulfate, thiosulfate, hydrogen phosphate and citrate were used. For cell culture experiments, cell proliferation Reagent WST-1 was obtained from Roche Applied Science. DMEM with L-glutamine, piruvate and Fetal Bo- vine Serum (FBS), trypan blue solution (0.4 %) cell culture grade and trypsin were purchased from Gibco-Invitrogen.

All studies with **1**-Az and hydrogen sulfide were performed by using freshly prepared MeCN/HEPES (30 mM, pH 7.5; 1:1 v/v) sodium hydrogen sulfide solutions.

General Techniques: UV/Vis spectra were recorded with a JASCO V-650 Spectrophotometer. Fluorescence measurements were carried out with a JASCO FP-8500 spectrophotometer. ^{1}H and ^{13}C NMR spectra were acquired with a BRUKER AVANCE III (400 MHz) instrument, and mass spectra were recorded with a TRIPLETOF T5600 (ABSciex, USA) spectrometer. Cell viability measurements were carried out with a Wallac 1420 Workstation.

Synthesis of 1-Az: Dabsyl chloride (**1**-Cl; 710 mg, 2.19 mmol) was dissolved in acetone (10 mL) and cooled to 0 °C with an ice bath. A solution of sodium azide (142 mg, 2.19 mmol) in water (2 mL) was then slowly added dropwise under vigorous stirring. The crude mixture was stirred for 2 h at 0 °C and then for 4 h at

room temperature. Finally, to achieve complete transformation of the sulfonyl chloride into sulfonyl azide, sodium azide (32 mg, 0.1 mmol) dissolved in water (500 µL) was added dropwise at room temperature and the reaction was stirred for 3 h. Dichloromethane (200 mL) was added and the organic phase was washed with water (2 X 100 mL), sodium hydrogen carbonate 5 % solution (100 mL), and again with water (2 X 100 mL). The organic phase was then dried with anhydrous magnesium sulfate, filtered, and concentrated in a rotary evaporator. The solid residue was suspended in acetonitrile (2 mL) and filtered. The final product **1**-Az (280 mg, 0.85 mmol, 39 %) was isolated as an orange-red solid. ^{1}H NMR (400 MHz, [D_6]DMSO): δ = 3.12 (s, 6 H), 6.88 (d, J = 6.5 Hz, 2H), 7.87 (d, J = 6.5 Hz, 2 H), 8.01 (d, J = 6.0 Hz, 2 H), 8.15 (d, J= 6.0 Hz, 2 H) ppm. ^{13}C NMR (100 MHz, [D_6]DMSO): δ = 40.2, 111.7, 122.9, 125.9, 128.9, 136.5, 142.7, 153.5, 156.2 ppm. HRMS(EI): *m/z* calcd. for C14H15N6O2S+ 331.0972; found 331.0969.

Synthesis of 1-Am: Sodium sulfide (45 mg, 0.58 mmol) dissolved in water (450 µL) was added into a solution of **1**-Az (40.7 mg, 0.12 mmol) in acetonitrile (15 mL). The reaction was stirred for 6 h at room temperature, then the solvents were evaporated under reduced pressure to give **1**-Am (29.3 mg, 0.096 mmol, 78 %) as an orange-yellow solid. ^{1}H NMR (400 MHz, [D_6]DMSO): δ = 3.10 (s, 6 H), 6.87 (d, *J* = 7.0 Hz, 2 H), 7.42 (br. s, 2 H), 7.84 (d, *J* = 7.0 Hz, 2 H), 7.90 (d, *J* = 6.0 Hz, 2 H), 7.96 (d, *J* = 6.0 Hz, 2 H) ppm. ^{13}C NMR (100 MHz, [D_6]DMSO): δ = 40.1, 112.1, 122.5, 125.8, 127.4, 143.0, 144.5, 153.5, 154.6 ppm. HRMS (EI): *m/z* calcd. For $C_{14}H_{17}N_4O_2S^+$ 306.1072; found 306.1068.

Quantum Yield Measurements: The quantum yield of **1**-Az (f = 0.036) and **1**-Am (f = 0.048) were calculated by using an acid solution of quinine sulfate (0.5 N in H_2SO_4) as reference and by the known comparative method following equation:

$$\phi = \phi_R \times \frac{I}{I_R} \times \frac{A_R}{A} \times \frac{n^2}{n_R^2}$$

where ϕ is the quantum yield, I is the integrated of fluorescent intensity, *n* is the refractive index, and *A* is the absorbance intensity. The subscript *R* refers to the reference fluorophore (quinine sulfate).

Limit of Detection by UV/Vis Spectroscopy: Changes in the visible band centred at 478 nm, of MeCN-HEPES (30 mm, pH 7.5; 1:1 v/v) solutions of **1**-Az (1.0 X 10^{-5} m), were monitored upon addition of increasing amounts of HS^- anions. Addition of increasing quantities of HS^- anions induced a progressive hypsochromic shift of the visible band. From the typical titration profile (representation of absorbance at 478 nm vs. log [HS^-]), a detection limit of 1.2 X 10^{-5} m (δ = 0.4 ppm) was calculated by using a conventional UV/Vis spectrophotometer. The experiments were carried out three times to calculate the standard deviation.

Limit of Detection by Fluorescence: Changes in the emission band centred at 557 nm (upon excitation at 478 nm) of MeCN-HEPES (30 mM, pH 7.5; 1:1 v/v) solutions of **1**-Az (1.0 X 10^{-5} m) were monitored upon addition of increasing amounts of HS^- anions. This addition induced a progressive enhancement of the emission band at 478 nm. From the calibration curve (representation of the emission intensity at 557 nm vs. log [HS^-]), a detection limit for HS^- of 6.0 X 10^{-7} M (δ = 0.02 ppm) was calculated. The experiments were carried out three times to calculate the standard deviation.

Cell Culture Conditions: HeLa human cervix adenocarcinoma cells were purchased from the German Resource Centre for Biological Materials (DSMZ) and were grown in DMEM supplemented with 10 % FBS. Cells were maintained at 37 °C in an atmosphere of 5 % carbon dioxide and 95 % air and underwent passage twice a week

WST-1 Cell Viability Assay: HeLa cells were seeded in a 96-well plate at a density of 2.5 X 10^3 cells/well in 100 µL DMEM and were incubated 24 h in a CO_2 incubator at 37 °C. Then, **1**-Az in DMSO was added to cells in sextuplicate at final

concentrations of 10, 20, 30, 50 and 100 μM and 1, 15 and 23 h later, 7 μL of WST-1 was added to each well and the plate was incubated for 1 h. Thus, a total of 24 h of incubation was studied. Before reading the plate, it was shaken for 1 min to ensure homogeneous distribution of colour; the absorbance was measured at a wavelength of 450 nm.

Live Confocal Microscopy Studies: HeLa cells were seeded on 24 mm Ø glass coverslips in six-well plates at a seeding density of 1 X 10^5 cells/well. After 24 h, cells were treated with **1**-Az for 20 min at a final concentration of 30 μM. The medium was changed and the well was washed with PBS. A solution of Na_2S in PBS was then added at a final concentration of 0, 10, 40, 60, 80, 200 and 500 μM for 30 min. Then the coverslips were washed twice to eliminate compounds and were visualized under a confocal microscope employing Leica TCS SP2 AOBS (Leica Microsystems Heidelberg GmbH, Mannheim, Germany) inverted laser scanning confocal microscope using oil objectives: 63X Plan-Apochromat-Lambda Blue 1.4 N.A. Confocal microscopy studies were performed by Confocal Microscopy Service (CIPF). The images were acquired with an excitation wavelength of 474 nm (argon laser) and an emission wavelength of 470–570 nm. Two-dimensional pseudo colour images (255 colour levels) were gathered with a size of 1024 X 1024 pixels and Airy 1 pinhole diameter. All confocal images were acquired by using the same settings and the distribution of fluorescence was analyzed by using the Image J Software. Three independent experiments were performed, giving similar results.

Supporting Information (see footnote on the first page of this article): ^1H NMR, ^{13}C NMR and IR spectra of **1**-Az and **1**-Am, UV/ Vis changes of **1**-Az in the presence of selected anions, UV/Vis changes of **1**-Az upon addition of increasing quantities of HS^- and fluorescence titration of **1**-Az with HS^-.

3.6.3.6. Acknowledgments

The authors thank the Spanish Government (project MAT2012- 38429-C04-01), the Generalitat Valenciana (project PROMETEO/ 2009/016) and CIBER de

Bioingeniería, Biomateriales y Nanomedicina (CIBER-BBN) for their support. The authors are also grateful to Fundación Carolina and UPNFM Honduras (doctoral grant to L. E. S.-F.) and the Generalitat Valenciana for Santiago Grisolia (fellowship to S. E. S.).

3.6.3.7. References and Notes

Keywords: Analytical methods / Sensors / Hydrogen sulfide / Sulfur / Azides

1 a) Hydrogen Sulfide, Geneva, World Health Organization, **1981** (Environmental Health Criteria, No. 19); b) R. E. Gosselin, R. P. Smith, H. C. Hodge, Hydrogen Sulfide, in: Clinical Toxicology of Commercial Products, 5th ed.; c) S. A. Pat- wardhan, S. M. Abhyankar, Colourage **1988**, 35, 15.

2 H. Ma, X. Cheng, G. Li, S. Chen, Z. Quan, S. Zhao, L. Niu, Corros. Sci. **2000**, 42, 1669.

3 Official Journal of the European Union (June 29, **1999**), L 163/ 41, Council Directive 1999/30/EC.

4 a) M. L. Carapezza, B. Badalamenti, L. Cavarra, A. Scalzo, J. Volcanol. Geotherm. Res. **2003**, 123, 81; b) A. J. Sutton, T. Elias, R. Navarrete, U. S. Geological Survey Open-File **1994**, Report 94–569, 34; c) M. N. Bates, N. Garrett, P. Shoemack, Arch. Environ. Health **2002**, 57, 405.

5 a) D. S. Mottram, Food Chem. **1998,** 62, 415; b) P. M. Schweizer-Berberich, S. Vaihinger, W. Göpel, Sens. Actuators, B **1994**, 18, 282; c) P. J. A. Vos, R. S. Gray, Am. J. Enol. Viti. **1979**, 3, 187.

6 a) C. Szabo, Nat. Rev. Drug Discovery **2007**, 6, 917; b) L. Li, P. Rose, P. K. Moore, Annu. Rev. Pharmacol. Toxicol. **2011**, 51, 169; c) R. d'Emmanuele di Villa Bianca, R. Sorrentino, V. Mi- rone, G. Cirino, Nat. Clin. Pract. Oncol. **2011**, 8, 286.

7 K. Abe, H. Kimura, J. Neurosci. **1996**, 16, 1066.

8 G. Yang, L. Wu, B. Jiang, B. Yang, J. Qi, K. Cao, Q. Meng, A. K. Mustafa, W. Mu, S. Zhang, S. H. Snyder, R. Wang, Sci- ence **2008**, 322, 587.

9 a) D. J. Lefer, Proc. Natl. Acad. Sci. USA **2007**, 104, 17907; b) G. Szabó, G. Veres, T. Radovits, D. Gero, K. Módis, C. Miesel- Gröschel, F. Horkay, M. Karck, C. Szabó, Nitric Oxide **2011**, 25, 201.

10 Y. J. Peng, J. Nanduri, G. Raghuraman, D. Souvannakitti, M. M. Gadalla, G. K. Kumar, S. H. Snyder, N. R. Prabhakar, Proc. Natl. Acad. Sci. USA **2010**, 107, 10719.

11 S. Fiorucci, E. Antonelli, A. Mencarelli, S. Orlandi, B. Renga, G. Rizzo, E. Distrutti, V. Shah, A. Morelli, Hepatology **2005,** 42, 539.

12 K. Eto, T. Asada, K. Arima, T. Makifuchi, H. Kimura, Bio- chem. Biophys. Res. Commun. **2002**, 293, 1485.

13 P. Kamoun, M.-C. Belardinelli, A. Chabli, K. Lallouchi, B. Chadefaux-Vekemans, Am. J. Med. Gen., Part A **2003**, 116, 310.

14 a) L. E. Santos-Figueroa, M. E. Moragues, E. Climent, A. Agostini, R. Martínez-Máñez, F. Sancenón, Chem. Soc. Rev. **2013**, 42, 3489; b) M. Moragyes, R. Martínez-Máñez, F. San- cenón, Chem. Soc. Rev. **2011**, 40, 2593; c) R. Martínez-Máñez, F. Sancenón, Chem. Rev. **2003**, 103, 4419.

15 a) A. R. Lippert, E. J. New, C. J. Chang, J. Am. Chem. Soc. **2011**, 133, 10078; b) B. Chen, C. Lv, X. Tang, Anal. Bioanal. Chem. **2012**, 404, 1919; c) S. Chen, Z.-J. Chen, W. Ren, H.-W. Ai, J. Am. Chem. Soc. **2012**, 134, 9589; d) T. Chen, Y. Zheng, Z. Xu, M. Zhao, Y. Xu, J. Cui, Tetrahedron Lett. **2013**, 54, 2980; e) S. K. Das, C. S. Lim, S. Y. Yang, J. H. Han, B. R. Cho, Chem. Commun. **2012**, 48, 8395; f) H. Peng, Y. Cheng, C. Dai, A. L. King, B. L. Predmore, D. J. Lefer, B. Wang, Angew. Chem. **2011**, 123, 9846; Angew. Chem. Int. Ed. **2011**, 50, 9672; g) Z. Wu, Z. Li, L. Yang, J. Han, S. Han, Chem. Commun. **2012**, 48, 10120; h) F. Yu, P. Li, P. Song, B. Wang, J. Zhao, K. Han, Chem. Commun. **2012**, 48, 2852; i) S. Singha, D. Kim, A. S. Rao, T. Wang, K. H. Kim, K.-H. Lee, K.-T. Kim, Ahn, Dyes Pigm. **2013**, 99, 308.

16 W. Xuan, R. Pan, Y. Cao, K. Liu, W. Wang, Chem. Commun. **2012**, 48, 10669.

17 a) L. A. Montoya, M. D. Pluth, Chem. Commun. **2012**, 48, 4767; b) M.-Y. Wu, K. Li, J.-T. Hou, Z. Huang, X.-Q. Yu, Org. Biomol. Chem. **2012**, 10, 8342.

18 a) C. Liu, J. Pan, S. Li, Y. Zhao, L. Y. Wu, C. E. Berkman, A. R. Whorton, M. Xian, Angew. Chem. **2011**, 123, 10511; Angew. Chem. Int. Ed. **2011**, 50, 10327; b) Z. Xu, L. Xu, J. Zhou, K. H. Y. Xu, W. Zhu, X. Quian, Chem. Commun. **2012**, 48, 10871.

19 X. Cao, W. Lin, K. Zheng, L. He, Chem. Commun. **2012**, 48, 10529.

20 C. Liu, B. Peng, S. Li, C.-M. Park, A. R. Whorton, M. Xiang, Org. Lett. **2012**, 14, 2184.

21 a) K. Sasakura, K. Hanaoka, N. Shibuya, Y. Mikami, Y. Ki- mura, T. Komatsu, T. Ueno, T. Terai, H. Kimura, T. Nagano, J. Am. Chem. Soc. **2011**, 133, 18003; b) F. Hou, J. Cheng, P. Xi, F. Chen, L. Huang, G. Xie, Y. Shi, H. Liu, D. Bai, Z. Zeng, Dalton Trans. **2012**, 41, 5799; c) F. Hou, L. Huang, P. Xi, J. Cheng, X. Zhao, G. Xie, Y. Shi, F. Cheng, X. Yao, D. Bai, Z. Zeng, Inorg. Chem. **2012**, 51, 2454; d) M.-Q. Wang, K. Li, J.-T. Hou, M.-Y. Wu, Z. Huang, X.-Q. Yu, J. Org. Chem. **2012**, 77, 8350.

22 a) B. Wang, P. Li, F. Yu, P. Song, X. Sun, S. Yang, Z. Lou, K. Han, Chem. Commun. **2013**, 49, 1014; b) B. Wang, P. Li, F. Yu, J. Chen, Z. Qu, K. Han, Chem. Commun. **2013**, 49, 5790.

23 a) Y. Zhao, X. Zhu, H. Kan, W. Wang, B. Zhu, B. Du, X. Zhang, Analyst **2012**, 137, 5576; b) L. A. Montoya, T. F. Pe- arce, R. J. Hansen, L. N. Zakharov, M. D. Pluth, J. Org. Chem. **2013**, 78, 6550.

24 D. Jimenez, R. Martínez-Máñez, F. Sancenón, J. V. Ros-Lis, A. Benito, J. Soto, J. Am. Chem. Soc**. 2003**, 125, 9000.

25 E. Climent, L. Mondragón, R. Martínez-Máñez, F. Sancenón, M. D. Marcos, J. R. Murgia, P. Amorós, K. Rurack, E. Pérez- Payá, Angew. Chem. Int. Ed. **2013**, 52, 8938; E. Aznar, R. Villa- longa, C. Giménez, F. Sancenón, M. D. Marcos, R. Martínez- Máñez, P. Diez, J. M. Pingarrón, P. Amorós, Chem. Commun. **2013**, 49, 6391; E. Climent, D. Gröninger, M. Hecht, M. A. Walter, R. Martínez-Máñez, M. Weller, F. Sancenón, P. Amorós, K. Rurack, Chem. Eur. J. **2013**, 19, 4117; Y. Salinas, R. Martínez-Máñez, J. O. Jeppesen, L. H. Petersen, F. San- cenón, M. D. Marcos, J. Soto, C. Guillem, P. Amorós, ACS Appl. Mater. Interfaces **2013**, 5, 1538; Y. Salinas, A. Agostini, E. Pérez-Esteve, R.

Martínez-Máñez, F. Sancenón, M. D. Mar- cos, J. Soto, A. Costero, S. Gil, M. Parra, P. Amorós, J. Mater. Chem. **2013**, 1, 3561; D. Jiménez, R. Martínez-Máñez, F. San- cenón, J. V. Ros-Lis, J. Soto, A. Benito, E. García-Breijo, Eur. J. Inorg. Chem. **2005**, 12, 2393; M. E. Padilla-Tosta, J. M. Lloris, R. Martínez-Máñez, A. Benito, J. Soto, T. Pardo, M. A. Miranda, M. D. Marcos, Eur. J. Inorg. Chem. **2000**, 741; C. Coll, R. Casasús, E. Aznar, M. D. Marcos, R. Martínez- Máñez, F. Sancenón, J. Soto, P. Amorós, Chem. Commun. **2007**, 1957; F. Sancenón, A. Benito, F. J. Fernandez, J. M. Lloris, R. Martínez-Máñez, T. Pardo, J. Soto, Eur. J. Inorg. Chem. **2002**, 866; J. V. Ros-Lis, R. Martínez-Máñez, F. San- cenón, J. Soto, K. Rurack, H. Weisshoff, Eur. J. Org. Chem. **2007**, 2449.

26 H. A. Dabbagh, A. Teimouri, A. N. Chermahini, Dyes Pigm. **2009**, 73, 239.

27 M. Hoffman, A. Rajapakse, X. Shen, K. S. Gates, Chem. Res. Toxicol. **2012**, 25, 1609–1615.

3.6.3.8. Supporting information

A Chemosensor Bearing Sulfonyl Azide Moieties for Selective Chromo-Fluorogenic Hydrogen Sulfide Recognition in Aqueous Media and in Living Cells

Luis E. Santos-Figueroa, Cristina de la Torre, Sameh El Sayed, Félix Sancenón, Ramón Martínez-Máñez, Ana M. Costero, Salvador Gil and Margarita Parra.

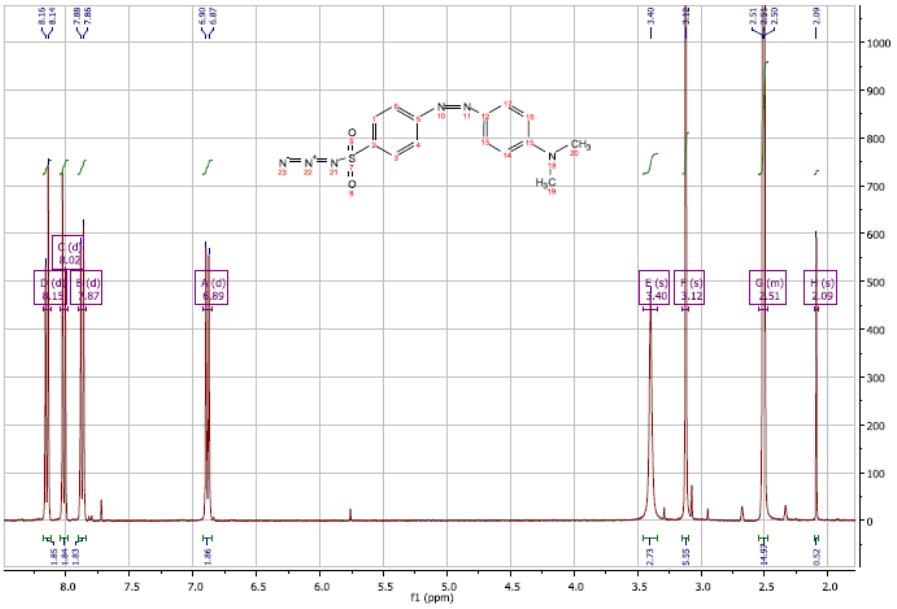

Figure S1. ^{1}H-NMR spectra of probe **1-Az** in DMSO-D$_6$.

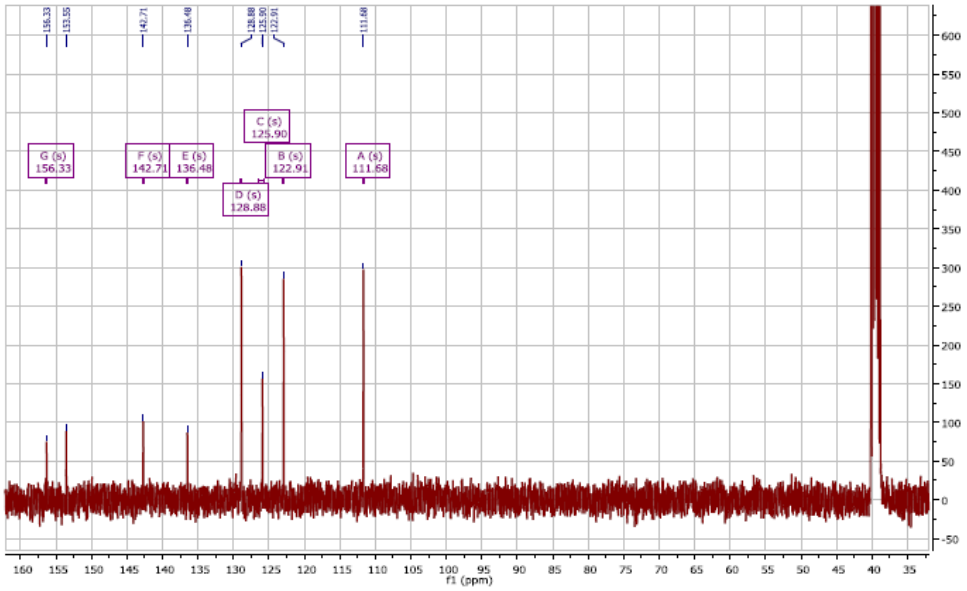

Figure S2. ^{13}C-NMR spectra of probe **1-Az** in DMSO-D$_6$.

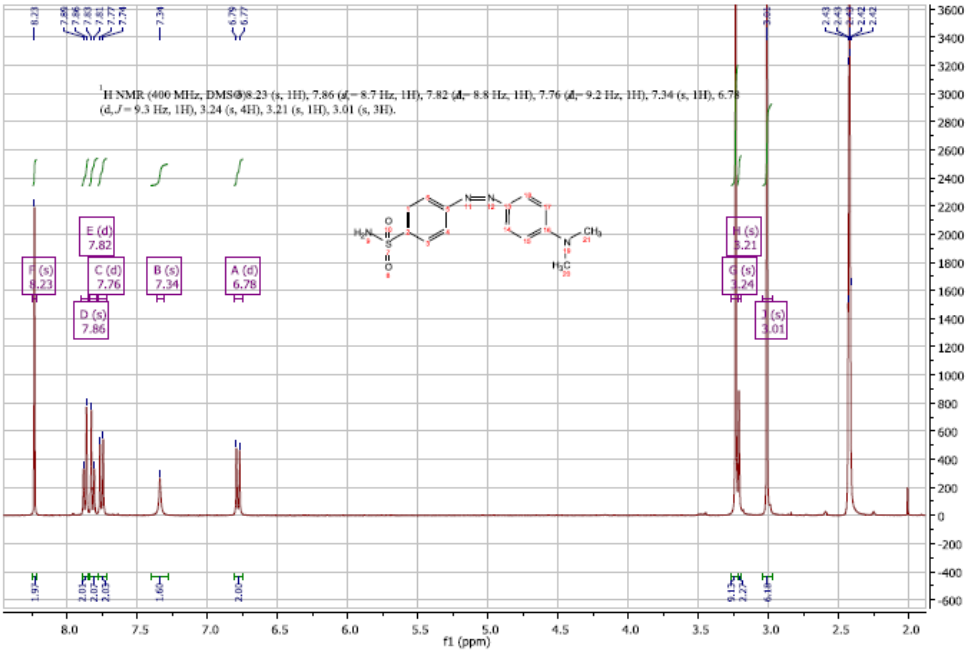

Figure S3. ^{1}H-NMR spectra of **1-Am** in DMSO-D$_6$.

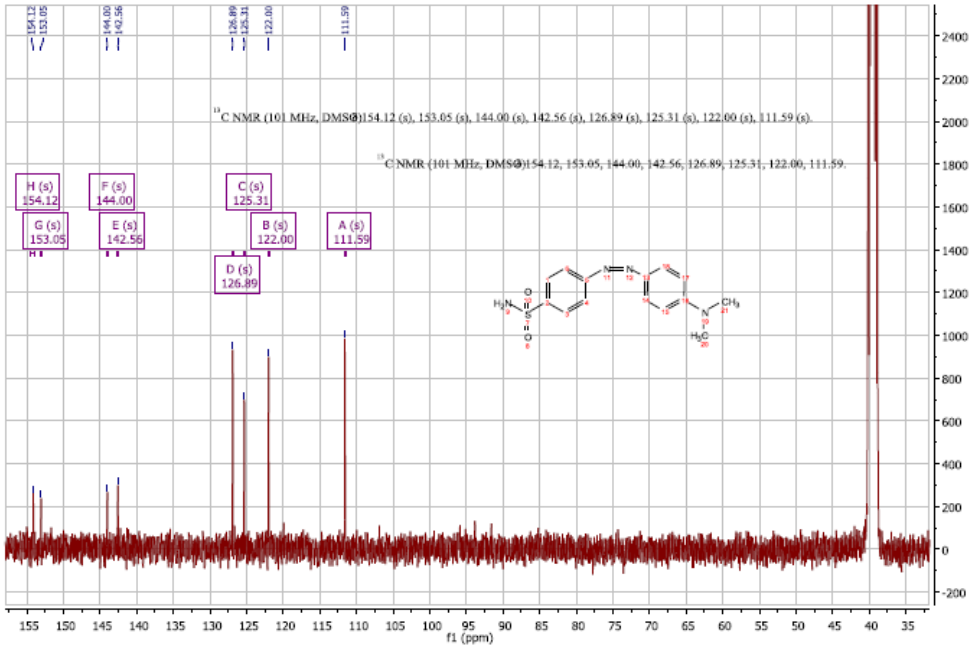

Figure S4. ^{13}C-NMR spectra of **1-Am** in DMSO-D6.

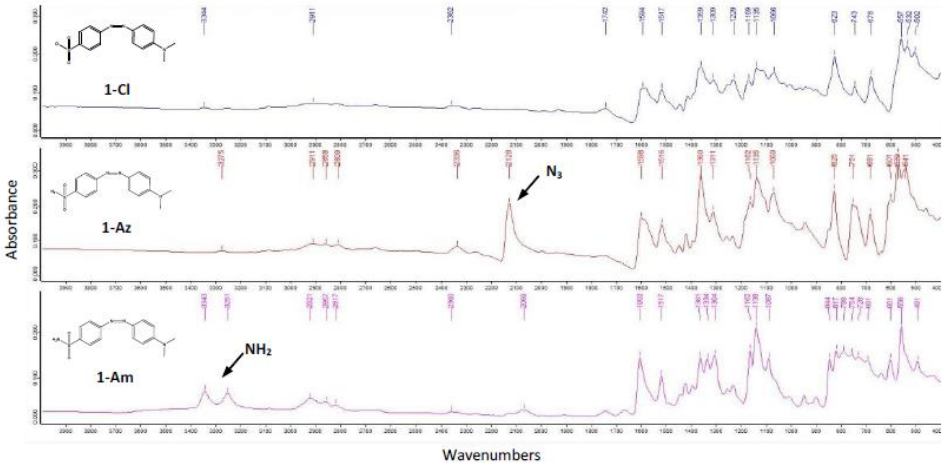

Figure S5. IR spectra of **1-Cl**, the chemodosimeter **1-Az** and the product **1-Am** isolated after the reaction with HS^- anion.

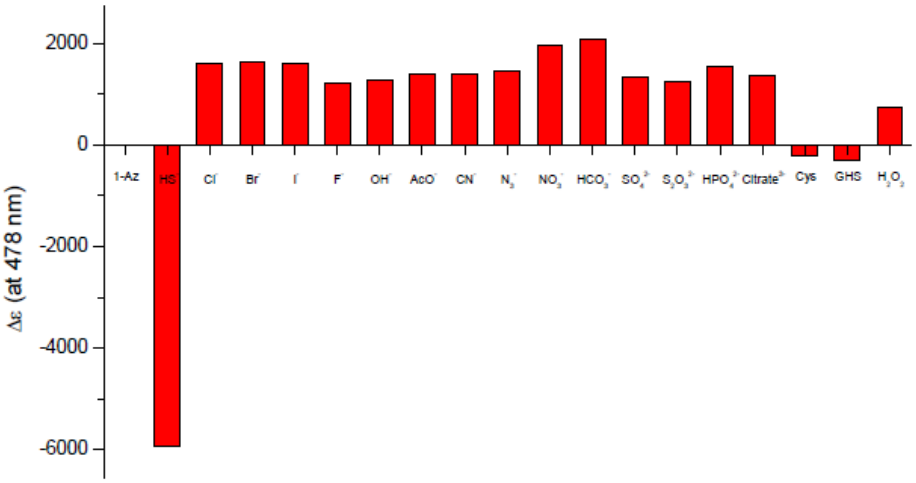

Figure S6. Δε at 478 nm of **1-Az** (1.0 x 10^{-5} M) in ACN-HEPES (30 mM, pH 7.5) 1:1 v/v in the presence of 10 eq. of selected anions, other thiol containing derivatives and oxidants.

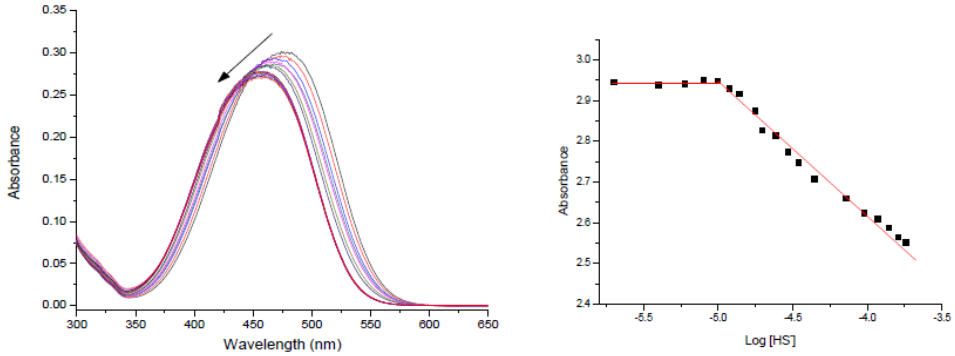

Figure S7. Left: visible spectra of **1-Az** (1.0 x 10^{-5} M) in ACN-HEPES (30 mM, pH 7.5) 1:1 v/v upon addition of increasing amounts of hydrogen sulfide (0-10 eq.). Right: Calibration curve for HS^- using chemodosimeter **1-Az** (1.0 x 10^{-5} M) in ACN-HEPES (30 mM, pH 7.5) 1:1 v/v.

Figure S8. Photograph showing ACN-HEPES (30 mM, pH 7.5) 1:1 v/v solutions of probe **1-Az** (1.0 x 10^{-3} M) in the presence of increasing quantities of HS^- anion. From left to right: no anion, 0.1, 0.5, 0.8, 1.5, 5 and 10 eq. of HS^-.

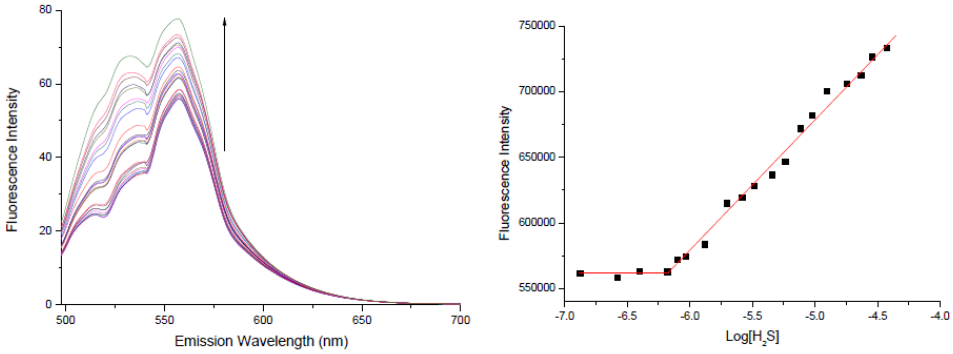

Figure S9. Left: fluorescence of **1-Az** (1.0 x 10^{-5} M) in ACN-HEPES (30 mM, pH 7.5) 1:1 v/v solution upon addition of increasing quantities of HS^- anion (excitation at 478 nm). Right: Calibration curve for HS^- using chemodosimeter **1-Az** (1.0 x 10^{-5} M) in ACN-HEPES (30 mM, pH 7.5) 1:1 v/v (λ_{ex} = 478 nm, λ_{em} = 557 nm).

Chapter 4: Supramolecular nanosystems as chemosensors

4. SUPRAMOLECULAR NANOSYSTEMS AS CHEMOSENSORS

4.1. About this chapter

The final chapter of this PhD thesis is centered on the development of one functional system for molecular recognition in complex samples. The new system is constituted by a selective probe for sulfite encapsulated inside of functionalized cavities of silica mesoporous nanoparticles.

In this case, the preliminary discussion and the theoretical considerations are focused in the presentation of the major features of the solid scaffolding used to develop the new sensing system.

Later, as in previous chapters, the main objetives and the major considerations into design are presented prior the published experimental results.

4.2. Preliminary discussion

The blending of material science and supramolecular chemistry has lead to the preparation of sophisticated hybrid materials with very interesting properties and with novel applications in several scientific and technological fields.

While the implementation of self-assembly for the preparation of new nanostructured materials has been a big step for materials science, the preparation and application of new functionalised pre-organised nanoscopic solid structures or polymers in sensing protocols has caused simultaneous evolution of supramolecular area.

As already mentioned above in chapter 1 (section 1.1.5), the combination of molecular recognition and self-assembly processes in interdisciplinar applications of supramolecular chemistry allow to prepare highly sophisticated functional systems which have results in new processes and applications.

4.3. Theoretical considerations

Molecular and supramolecular chemosensors are based on the simple interaction of target species with a binding site or reactive centre. Whereas, the use of combined molecular probe with functionalised pre-organised nanoscopic solid structures in sensing protocols may result in the development of novel sensing systems with new properties and new binding modes where the solid scaffolding itself could plays a role in sensing or signalling protocols.

Some examples of this new approach using as inorganic scaffoldings gold/silica nanoparticles and mesoporous supports have been reported as functional supramolecular systems.[1] In some of this cases, the use of solid scaffolding not only provides a support but also enhance the original sensing capabilities, specially on selectivity and solubility.

The new solids are hybrid materials with selective funtionalization. The hybrid materials are not simply physical mixtures of organic and inorganic moieties, but they are really nanocomposites with organic and inorganic components. The synergy among components gives them new properties different from those of its components separately and not only the sum of the individual contributions of both phases.[2]

[1] Descalzo, A. B.; Martínez-Máñez, R.; Sancenón, F.; Hoffmann, K.; Rurack, K., *Angew. Chem. Int. Ed*. **2006**, 45, 5924-5948.

[2] Sanchez, C.; Julian, B.; Belleville, P.; Popall, M., *J. Mat. Chem.* **2005,** *15*, 3559-3592.

In the nature, encapsulation of binding sites in simple pockets on a protein surface allows the selective interaction with small molecules, which are discriminated by steric hindrance, hydrophobicity or other additional features to the host-guest interactions promoted by the pocket properties.[3] Biomimetically, some hybrid materiales can be used to prepare a binding pocket-based chemosensor. In these materials a selective functionalization of cavities creates hydrophobic (or hydrophilic) binding pockets which are adequate in size and shape to the inclusion of a specific binding-signaling units. On similar form to nature, these materials shown an improved selectivity to some guest and new binding properties.

In general, the use of functionalised pre-organised nanoscopic solid structures or polymers in sensing protocols can improved the binding properties of several sensing systems and could yield materials with novel applications in industry, medicine and science.

4.4. Hybrid sensor material as a functional system

4.4.1. Experimental objectives

Taking into account the above mentioned facts and the importance of anions sensing in water and in real comercial samples for development of real applications; we decided to prepare a hybrid sensor material for sulfite detection in pure water.

With this purpose, we proposed the next main aims:

- Design and synthesize a selective chromo-fluorogenic probe for sulfite recognition.

[3] Glaser, F.; Morris, R. J.; Najmanovich, R. J.; Laskowski, R. A.; Thornton, J. M., *Proteins,* **2006,** *62*, 479-488.

- Prepare a functionalized hybrid material equipped with binding pockets to encapsulate the molecular probe.

- Prepare and evaluate a commercially viable format to use the new functional system for determine sulfite in real samples.

4.4.2. Chemosensor design

In this project, the design of new functional system was centred into two main focuses: (i) the synthesis of an efficient molecular probe for chromo-fluorogenic sulfite sensing and (ii) the preparation of a hybrid material composed by a mesoporous solid with the probe inside the porous network for application in real samples.

We chose to design a pyrylium-based probe by their properties as Michael acceptor, able to suffer nucleophilic attacks and by have a strong electronic conjugation with hight potential to displayed optical output.

MCM-41 mesoporous nanoparticles were selected as inorganic scaffolds because have desirable structural properties such an ordered mesoporous system, a high specific surface chemical inertness and well known functionalization procedures.

The specific use of a binding pocket system in this case was inspired by nature. As already mentioned above, the use of binding pocket in proteins enables selective molecular recognition of small molecules. Based on this, we modified the inner surface of the pores in MCM-41 in order to achive a corret encapsulation of the molecular probe.

Finally, a ceramic foam monolith was selected as final format because of its trimodal hierarchical pore system with a high external surface, good mechanical

properties, possibility to achieve a high degree of coverage with silica nanoparticles and easy synthesis by replication of a commercially available and inexpensive polyurethane foam with a ceramic slip.

4.4.3. Selective and Sensitive Chromofluorogenic Detection of the Sulfite Anion in Water Using Hydrophobic Hybrid Organic–Inorganic Silica Nanoparticles.

In the following section, we reported the synthesis, characterization and sensing properties of a new hybrid organic–inorganic material that contained a probe encapsulated in hydrophobic biomimetic cavities for chromo-fluorogenic detection of the sulfite anion in pure water and in red wine (Figure 36).

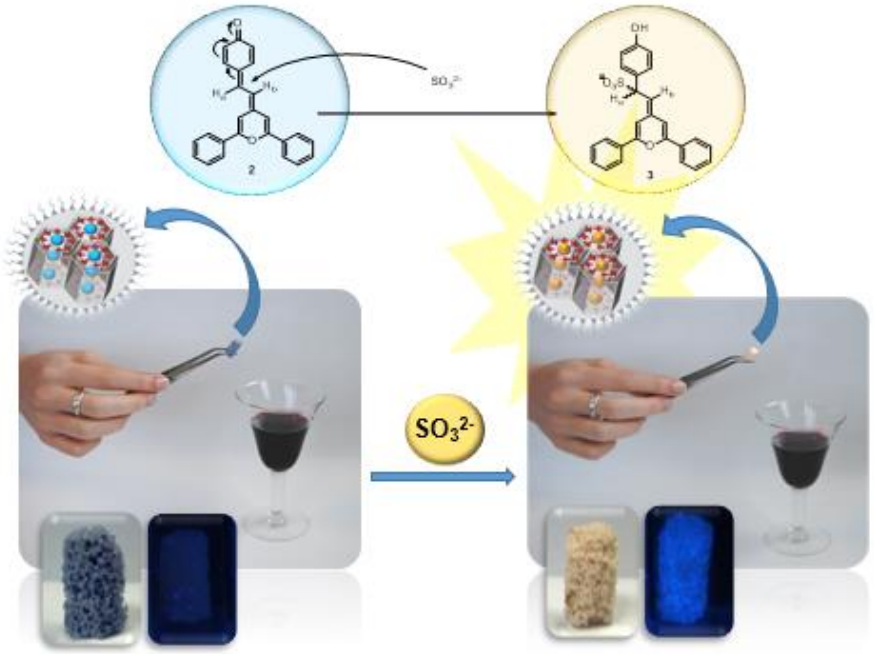

Figure 36. Schematic representation of a new hybrid sensor material for chromo-fluorogenic detection of the sulfite anion in pure water and in red wine

Selective and Sensitive Chromofluorogenic Detection of the Sulfite Anion in Water Using Hydrophobic Hybrid Organic–Inorganic Silica Nanoparticles

Luis Enrique Santos-Figueroa, [a, b, c] Cristina Giménez, [a, b, c] Alessandro Agostini, [a, b, c] Elena Aznar, [a, b, c] María D. Marcos, [a, b, c] Félix Sancenón, [a, b, c] Ramón Martínez-Máñez [a, b, c] and Pedro Amorós [d]

[a] Instituto de Reconocimiento Molecular y Desarrollo Tecnológico (IDM), Centro Mixto Universidad Politécnica de Valencia-Universidad de Valencia (Spain)

[b] Departamento de Química, Universidad Politécnica de Valencia, Camino de Vera s/n, 46022 Valencia (Spain)

[c] CIBER de Bioingeniería, Biomateriales y Nanomedicina (CIBER- BBN)

[d] Instituto de Ciencia de los Materiales (ICMUV), Universidad de Valencia (Spain)

Received: July 31, 2013
Published online: November 7, 2013

*Angewandte Chemie International Edition, **2013**, 52, 13712 –13716*
(Reproduced with permission of Wiley-VCH Verlag GmbH & Co. KGaA, Weinheim)

4.4.3.1. Introduction

Nowadays, sulfites or sulfiting agents such as sodium, calcium, and potassium sulfite (SO_3^{2-}); metabisulfite ($S_2O_5^{2-}$); and bisulfites (HSO_3^-) as well as sulfur dioxide (SO_2) are compounds widely used as preservative and antimicrobial agents to prevent browning of foods and beverages (E220–228 additives).[1] However, several studies had associated topical, oral, or parenteral exposure to high doses of sulfite with adverse reactions as dermatitis, urticaria, flushing, hypotension, abdominal pain, and diarrhoea.[2] In fact, several reports confirmed that some people can be extremely sensitive even to very low sulfite levels [3] and that bronchoconstriction can occur in many asthmatic patients[4] or in people exposed to high doses.[5] Exposure to high doses of sulfite can occur for consumption of food and drinks that contain this additive (as fruits, vegetables, salads, meat, gelatin, juices, vinegar, soft drinks, beer, wine, and others), through the use of several drugs (adrenaline, phenylephrine, corticosteroids, and local anesthetics), some cosmetics (hair colors and bleaches, creams, and perfumes) or in some occupational settings (leather, textile, mineral, pulp, rubber, agriculture, and chemical industries).[2a] The addition of low levels of sulfite (as low as 0.7 mg kg^{-1} of body weight dictated by FAO/WHO)[6] are permitted in beer, wine, and some food under rigorous control, but in many countries their addition, especially in fresh products as salads, fruit, mincemeat, or sausages, is prohibited.[1, 7]

Sulfur dioxide is an important and very common air pollutant. When SO_2 is dissolved in aqueous media, a pH-dependent equilibrium occurs and it favors the formation of sulfite and bisulfite at neutral pH value.[8] Many studies suggested that extended exposition to SO_2 and/or its derivatives could produce different toxicological effects such as cancer, cardiovascular diseases, neurological disorders, and the change of the characteristics of voltage-gated sodium and potassium channels.[9]

Taking into account the above mentioned facts, the interest in the development of fast and efficient methods for sulfite detection has increased in the last years. In particular, methods based on electrochemistry,[10] spectrophotometry,[11] chromatography,[12] capillary electrophoresis,[13] and titration[8b, 14] have been extensively used for the detection and quantification of sulfite. Recently, the development of chromo-fluorogenic sensors for anion detection has become a field of interest, since they usually offer several advantages in terms of sensitivity, selectivity, and simplicity of operation over classic, nonportable, and expensive instrumental analysis.[15] In spite of these advantages, few chemosensors for the chromo-fluorogenic detection of the sulfite anion have been described. In this field, specific reactions of sulfite with aldehydes,[16] levulinate esters,[17] Michael-type additions,[18] and coordinative interactions[19] have been recently used. However, some of those reported probes show certain drawbacks such as low sensitivities and selectivities, poor performance in pure water, the need for using acidic environment (pH < 5.5), or large response times. Moreover, very recently, some chemosensors for sulfite detection with good stability based on the use of carbon quantum dots,[20] gold nanoparticles,[21] and polymers[22] have been reported. In addition, some sulfite biosensors have been described based on the aerobic oxidation of sulfite by immobilized sulfite oxidase and its electrochemical breakdown under high voltage.[23] These biosensors are sensitive even in pure water; however, have generally low stability, significant metabolite interference, short life, and high cost.

We herein report the development of a simple material for the selective and sensitive chromo-fluorogenic recognition of sulfite in aqueous solution. We have used functionalized MCM-41 nanoparticles containing a suitable sulfite probe within highly hydrophobic mesopores. The structure of the used organic probe **2** and the synthetic procedure for the preparation of the hybrid sensing nanoparticles (**N1**) are shown in Scheme 1.

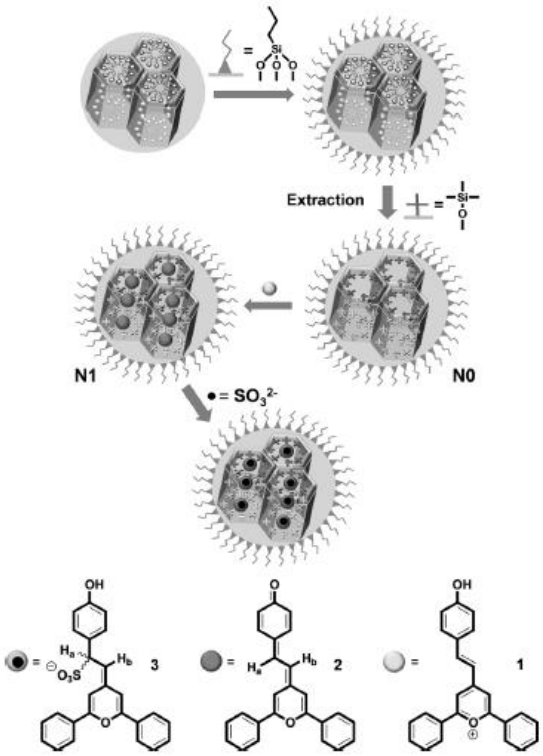

Scheme 1. Representation of the preparation of **N0** nanoparticles, the final sensing material **N1** (with probe **2** located inside the hydrophobic cavities), and proposed chromo-fluorogenic reaction with sulfite anion.

4.4.3.2. Results and Discussion

The design of the probe involves the preparation of a sensing material that should ideally be hydrophobic enough to maintain the probe in the nanopores but not too hydrophobic in order to obtain stable suspensions of the nanoparticles (note that highly hydrophobic nanoparticles tend to float in water, which inhibits fast reaction with the analyte). After several attempts, (see the Supporting Information for a detailed discussion) the following procedure was selected for the preparation of **N1**. MCM-41 mesoporous nanoparticles (diameter of ca. 100 nm) were selected as inorganic scaffolds.[24, 25] Before the extraction of the

cetyltrimethylammonium bromide (CTAB; used as structure-directing agent), the external surface of the silica nanoparticles was functionalized with propyltrimethoxysilane. Then the CTAB located inside the pores was extracted with hydrochloric acid. Finally, the inner sides of the pore walls were hydrophobized with hexamethyldisilazane (see the Supporting Information for details). These experimental procedures yield inorganic nanoparticles (**N0**) containing hydrophobic pockets. The organic content in **N0** was determined by thermogravimetric and elemental analysis and amounts to 0.22 mg of organic matter per mg SiO_2.

The final hybrid nanoparticles **N1** were prepared by suspending **N0** in an acetone solution of **1** (red) and allowing its diffusion into the hydrophobic cavities for 24 h. During the preparation of **N1**, the color of the solid changes from white to blue. This is a consequence of the inclusion of probe **1** into the hydrophobic cavities, through a simple adsorption process, which transformed the red pyrylium stilbene **1** into the blue quinone **2** (formed by the spontaneous deprotonation of probe 1). By thermogravimetric and elemental analysis, a content of 0.038 mmol of **2** per g SiO_2 in the final **N1** sensing material was determined.

To characterize this red-to-blue color change, a solution of probe **1** in acetonitrile was reacted with 1,8-diazabicyclo-[5.4.0]undec-7-ene (DBU, a non-nucleophilic base) to give an immediate color modulation from red to blue (attributed to **2**, see the Supporting Information). This final blue color was the same as that observed in the sensing **N1** nanoparticles. Moreover, this color transformation went along with changes in the ^{1}H-NMR spectrum: the signals of the double bond protons (H_a and H_b) of **1** showed significant upfield shifts with a reduction of the coupling constant (from 16 to 12 Hz) upon addition of DBU to give **2**. Moreover, the hydroxy proton signal of **1** centered at 10.8 ppm disappeared.

The nanoparticles **N0** and **N1** were characterized by standard procedures. Powder X-ray diffraction (PXRD) of as-synthesized siliceous MCM-41 (see the Supporting Information) shows four low-angle reflections typical of a hexagonal array that can be indexed as (100), (110), (200), and (210) Bragg peaks. The PXRD patterns of **N0** and **N1** (see also the Supporting Information) clearly preserve the reflections (100), (110), and (200), thereby evidencing that the surface functionalization and the further loading process with **1** did not damage the mesoporous scaffold. The presence of the mesoporous structure in the starting MCM-41 samples, hydrophobic nanoparticles **N0**, and final sensory material **N1** was also observed by using TEM analysis (see the Supporting Information).

To further explore different formats and to potentially enhance applicability of **N1**, the nanoparticles were included (as a coating) in a rigid monolith with the aim to design ready-and simple-to-use dipsticks for the rapid “in situ” chromo-fluorimetric screening of sulfite. In particular, a ceramic foam monolith was selected because of its trimodal hierarchical pore system with a high external surface, good mechanical properties, and the possibility to achieve a high degree of coverage with silica nanoparticles.[26]

The ceramic foam monolith was prepared through the replication of commercially available and inexpensive polyurethane foam with a ceramic slip. Then, the surface area of the ceramic foam was activated by using an alkaline-hydro-thermal treatment. After the activation process, the coating of the monolith with MCM-41 was carried out by successive impregnation cycles (4 times) in water suspensions of the nanoparticles followed by a soft thermal treatment. Then, the MCM-41-coated ceramic foam was hydrophobized, thereby yielding the monolith **M0**. Finally, their pores were loaded with derivative **1** resulting in the final blue ceramic foam sensing monolith **M1** (see Figure 1).

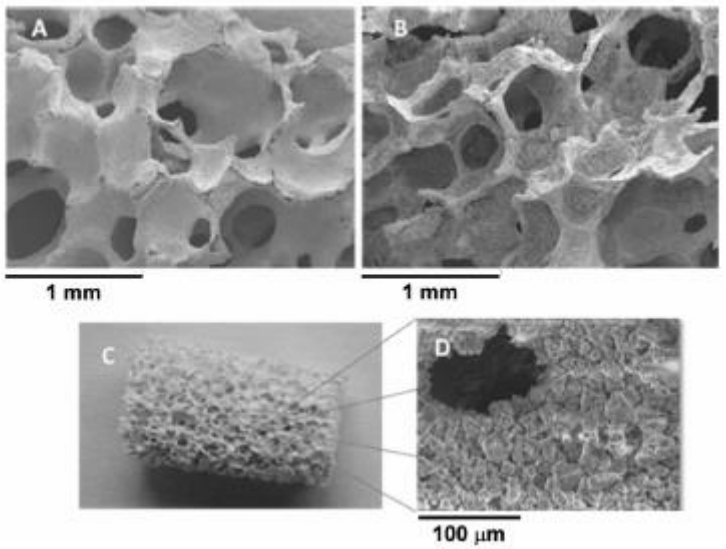

Figure 1. SEM images of A) the ceramic foam before coating and B) after four impregnation cycles with MCM-41 nanoparticles. C) Monolith **M1** and D) SEM image of **M1** macropores.

A preliminary study demonstrated that aqueous solutions of sulfite in the presence of **N1** or **M1** were able to change the color of the solids from blue to pale yellow and at the same time, the solids became fluorescent. The pH dependence of color stability of **N1** was also evaluated. **N1** nanoparticles were suspended in water at different pH values and the blue color remained in the 6–9 pH range, with an optimum blue color at pH 7.5 (see the Supporting Information for details).

Figure 2 shows the emission behavior of aqueous buffered (HEPES 30 mm, pH 7.5) suspensions of **N1** nanoparticles in the absence and in the presence of selected anions (HS^-, Cl^-, Br^-, I^-, F^-, AcO^-, N_3^-, NO_3^-, HCO_3^-, SO_4^{2-}, SO_3^{2-}, $S_2O_3^{2-}$, HPO_4^{2-}, and citrate), biological thiols (Cys, Hcy, and GSH) and oxidants (H_2O_2). In a typical experiment **N1** (5 mg) was suspended in buffered water (200 μL) containing the corresponding analyte. Then the solid was isolated by centrifugation and the fluorescence at 460 nm (λ_{ex} = 355 nm) was measured. The addition of sulfite anions induced a selective enhancement of the emission (Figure 2) with a

concomitant visible color change of the solid from blue to pale-yellow (see the Supporting Information). The HS^- anion also induced the appearance of the fluorescence band at 460 nm, but of less intensity. Remarkably, the addition of the other selected analytes induced negligible changes in the emission of **N1** nanoparticles. The same selective chromo-fluorogenic response was observed when using the blue ceramic foam monolith **M1** (data not shown).

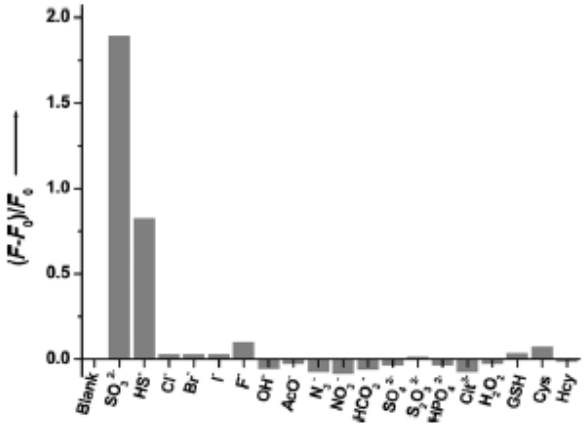

Figure 2. Fluorescence intensity at 460 nm (λ_{ex}=355 nm) of **N1** nanoparticles in HEPES buffer (30 mm at pH 7.5) in the presence of10 equivalents of selected anions, biological thiols, and oxidants. Hcy=homocysteine, GSH=glutathione, Cys=cysteine.

The change in color and in emission of **2** upon addition of sulfite anions is ascribed to a 1,6-conjugated addition reaction, which yielded the phenol **3** (Scheme 1). This addition was confirmed by NMR experiments (Figure 3) carried out with quinone **2** (obtained upon deprotonation of **1** with DBU). As shown in Figure 3, the most remarkable signals of quinone **2** are two doublets centered at 8.1 (proton H_b in Scheme 1) and at 6.7 ppm (proton H_a in Scheme 1). Addition of sulfite to **2** induced a marked upfield shift of both H_a and H_b protons to 5.45 (H_a) and 4.65 ppm (H_b) attributed to a loss of aromatic character upon reaction with sulfite anion. HSQC studies (see the Supporting Information) indicated the existence of a clear correlation between proton H_b and a benzylic carbon (at 63.4 ppm) and also between proton H_a and an olefinic carbon (at 116.8 ppm).

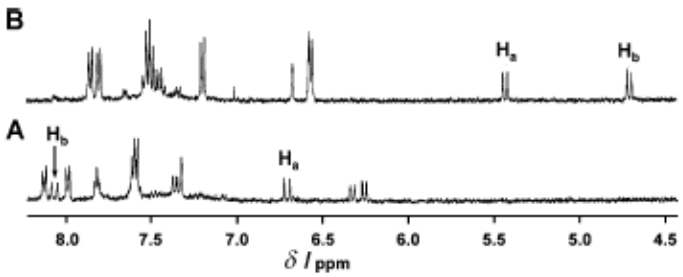

Figure 3. ^{1}H NMR spectra of **2** (A) and **3** (B, obtained upon addition of an excess of sulfite to probe **2**) in DMSO-d_6.

The selective response toward sulfite, shown by **2** when incorporated in **N1** nanoparticles, is ascribed to the preferential inclusion of sulfite into the highly hydrophobic pockets in **N1**, which favors the 1,6-conjugated addition reaction. The more hydrophilic HS^- anion was partially included in the hydrophobic cavities, whereas nucleophilic biological thiols (such as Cys, Hcy, and GSH) are too polar and too large to be internalized in the porous network of **N1** nanoparticles. In fact parallel assays carried out using DMSO solutions of **2** demonstrated that **2** is poorly selective and reacted similarly with different nucleophiles such as sulfite, sulfide, GSH, Cys, and Hcy.

Having assessed the selective response of **N1** nanoparticle suspensions to sulfite anions, the sensitivity of the probe was studied by monitoring the emission changes of aqueous buffered (HEPES 30 mM, pH 7.5) suspensions of **N1** nanoparticles upon addition of increasing quantities of sulfite. Increasing the concentration resulted in a progressive and immediate enhancement of fluorescence intensity at 460 nm (Figure 4). From these studies, a remarkable limit of detection (LOD) of 8 μm (0.32 ppm) was calculated. Besides, **N1** presents an accurate sensitivity for its potential application in food and in environmental analysis, based on both U.S.A.[6–7] and E.U.[1] standards.

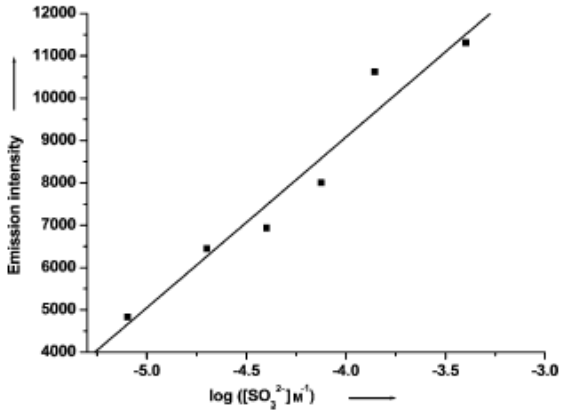

Figure 4. Emission intensity at 460 nm (λ_{ex}=355 nm) of buffered (HEPES 30 mm, pH 7.5) suspensions of **N1** nanoparticles upon addition of increasing quantities of sulfite.

Based on this promising proof-of-principle and taking into account the favorable spectroscopic response of **N1** and **M1**, we explored the possibility of using these materials for the detection of sulfite in complex real samples. In particular, we selected sulfite-free red wine that was bleached by simple addition of active carbon and spiked with 20 ppm of sulfite. Then, **M1** monolith was dipped in the doped wine samples and a remarkable and immediate color change from blue to pale yellow was observed (A in Figure 5), whereas when the same material was used in bleached sulfite-free red wine no color change was found. The chromogenic response (visible to the naked eye) was accompanied by a clear emission enhancement (under irradiation with 355 nm UV light) as it can be seen in Figure 5B.

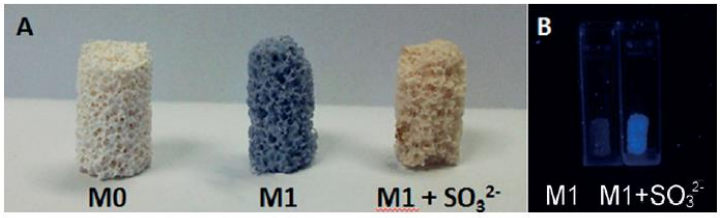

Figure 5. A) Photograph showing the **M0** and **M1** monoliths before (blue) and after (yellow) their reaction with bleached red wine containing 20 ppm of sulfite. B) Fluorescence response under UV irradiation (355 nm).

In an additional experiment, the same sulfite-free wine sample was spiked with a known amount of sulfite (6.0 ppm)[27] and the solid **N1** was used to determine sulfite concentration using the well-known standard addition method. In a typical experiment, **N1** nanoparticles (5 mg) were suspended in the bleached wine (200 μL); then increasing volumes of a standard sulfite solution were added and the emission intensity at 460 nm (λ_{ex} = 355 nm) of the samples was measured. By using this procedure, a concentration of 5.6 ppm of sulfite was determined (88 % of recovery).

4.4.3.3. Conclusions

In summary, we have reported here a sensing hybrid material (**N1**) for the simple chromo-fluorogenic detection of sulfite anions in pure water. The hybrid material was based in MCM-41 mesoporous nanoparticles with hydrophobic cavities able to encompass the chromo-fluorogenic probe **2**. Of all the anions tested, only sulfite was able to induce a remarkable color change (from blue to pale yellow) with a high emission enhancement. The sulfite detection was selective and sensitive with a limit of detection of 0.32 ppm. In addition, **N1** nanoparticles and **M1** monolith were used for sulfite detection in a complex matrix such as wine. Especially the use of systems such as **M1** opens the possibility of sensing sulfite with the naked eye by using a simple dipstick assay, which may find applications in food and environmental analysis. Moreover the study also demonstrated that the inclusion of chromo-fluorogenic probes into hydrophobic biomimetic cavities of mesoporous supports is a very simple and promising approach to design sensing materials for anions able to display sensing features in pure water.

4.4.3.4. References and Notes

Keywords: Sulfite sensing · Mesoporous nanoparticles · Silica monoliths · Food analysis·Hybrid materials

1 Council Directive 95/2/EC of the European Parliament and of the Council of 20 February 1995 on food additives other than colours and sweeteners, *Official Journal of the European Communities* L 61, 18.3.1995, pp.1-53

2 a) H. Vally, N. L. A. Misso, V. Madan, *Clin. Exp. Allergy* **2009**, *39*, 1643-1651; b) H. Niknahad, P. J. O'Brien, *Chem. Biol. Interact.* **2008**, *174*, 147-154.

3 a) T. Oliphant, A. Mitra, M. Wilkinson, *Contact Dermatitis* **2012**, *66*, 128-130; b) P. García-Ortega, E. Scorza, A. Teniente, *Clin. Exp. Allergy* **2010**, *40*, 688-690.

4 a) H. Vally, P. J. Thompson, N. L. A. Misso, *Clin. Exp. Allergy* **2007**, *37*, 1062-1066; b) R. K. Bush, S. L. Taylor, K. Holden, J. A. Nordlee, W. W. Busse, *Am. J. Med.* **1986**, *81*, 816-820; c) D. D. Stevenson, R. A. Simon, *J. Allergy Clin. Immunol.* **1981**, *68*, 26-32.

5 S. Iwasawa, Y. Kikuchi, Y. Nishiwaki, M. Nakano, T. Michikawa, T. Tsuboi, S. Tanaka, T. Uemura, A. Ishigami, H. Nakashima, T. Takebayashi, M. Adachi, A. Morikawa, K. Maruyama, S. Kudo, I. Uchiyama, K. Omae, *J. Occup. Health* **2009**, *51*, 38-47.

6 W. J. FAO, in *WHO food additives series, 60* (Ed.: World Health Organization), Geneva, **2009**.

7 USEPA, (Ed.: EPA), Virginia, USA, **2007**.

8 a) X. Shi, *J. Inorg. Biochem.* **1994**, *56*, 155-165; b) J. H. Karchmer, J. W. Dunahoe, *Anal. Chem.* **1948**, *20*, 915-919.

9 a) G. Li, N. Sang, *Ecotoxicol. Environ. Saf.* **2009**, *72*, 236-241; b) J. Li, R. Li, Z. Meng, *Eur. J. Pharmacol.* **2010**, *645*, 143-150; c) P. J. T. H. Vally, *Thorax* **2001**, *56*, 763-769; d) Y. Y. Nan Sang, Hongyan Li, Li Hou, Ming Han, and Guangke Li, *Toxicol. Sci.* **2010**, *114*, 226-236.

10 a) R. Keil, R. Hampp, H. Ziegler, *Anal. Chem.* **1989**, *61*, 1755-1758; b) D. Huang, B. Xu, J. Tang, J. Luo, L. Chen, L. Yang, Z. Yang, S. Bi, *Anal. Meth.* **2010**, *2*, 154-158.

11 a) M. S. Abdel-Latif, *Anal. Lett.* **1994**, *27*, 2601-2614; b) Y. Li, M. Zhao, *Food Control* **2006**, *17*, 975-980; c) J. E. Haskins, H. Kendall, R. B. Baird, *Water Res.* **1984**, *18*, 751-753.

12 a) K. Akasaka, H. Matsuda, H. Ohrui, H. Meguro, T. Suzuki, *Agric. Biol. Chem.* **1990**, *54*, 501-504; b) L. Pizzoferrato, G. Di Lullo, E. Quattrucci, *Food Chem.* **1998**, *63*, 275-279; c) R. F. McFeeters, A. O. Barish, *J. Agric. Food. Chem.* **2003**, *51*, 1513-1517; d) H. J. Kim, *Journal of the Association of Official Analytical Chemists* **1990**, *73*, 216-222.

13 a) Z. Daunoravicius, A. Padarauskas, *Electrophoresis* **2002**, *23*, 2439-2444; b) W. C. Fazio T, *Food Addit Contam.* **1990**, *7*, 433-454; c) G. Jankovskiene, Z. Daunoravicius, A. Padarauskas, *J. Chromatogr. A* **2001**, *934*, 67-73.

14 a) M. o. Health, *Analyst* **1927**, *52*, 343-344; b) N. T. K. Thanh, L. G. Decnop-Weever, W. T. Kok, *Fresenius J. Anal. Chem.* **1994**, *349*, 469-472; c) J. B. Thompson, E. Toy, *Industrial & Engineering Chemistry Analytical Edition* **1945**, *17*, 612-615.

15 L. E. Santos-Figueroa, M. E. Moragues, E. Climent, A. Agostini, R. Martinez-Manez, F. Sancenon, *Chem. Soc. Rev.* **2013**, *42*, 3489-3613.

16 a) G. J. Mohr, *Chem. Commun.* **2002**, *0*, 2646-2647; b) K. Chen, Y. Guo, Z. Lu, B. Yang, Z. Shi, *Chin. J. Chem* . **2010**, *28*, 55-60; c) X.-F. Yang, M. Zhao, G. Wang, *Sensors Actuators B: Chem.*

2011, *152*, 8-13; d) Y.-Q. Sun, P. Wang, J. Liu, J. Zhang, W. Guo, *Analyst* **2012**, *137*, 3430-3433; e) Y. Yang, F. Huo, J. Zhang, Z. Xie, J. Chao, C. Yin, H. Tong, D. Liu, S. Jin, F. Cheng, X. Yan, *Sensors Actuators B: Chem.* **2012**, *166–167*, 665-670; f) C. Yu, M. Luo, F. Zeng, S. Wu, *Anal. Meth.* **2012**, *4*, 2638-2640; g) X. Cheng, H. Jia, J. Feng, J. Qin, Z. Li, *Sensors Actuators B: Chem.* **2013**, *184*, 274-280; h) G. Wang, H. Qi, X.-F. Yang, *Luminescence* **2013**, *28*, 97-101.

17 a) X. Gu, C. Liu, Y.-C. Zhu, Y.-Z. Zhu, *J. Agric. Food. Chem.* **2011**, *59*, 11935-11939; b) M. G. Choi, J. Hwang, S. Eor, S.-K. Chang, *Org. Lett.* **2010**, *12*, 5624-5627; c) S. Chen, P. Hou, J. Wang, X. Song, *RSC Advances* **2012**, *2*, 10869-10873.

18 a) M.-Y. Wu, T. He, K. Li, M.-B. Wu, Z. Huang, X.-Q. Yu, *Analyst* **2013**, *138*, 3018-3025; b) Y.-Q. Sun, J. Liu, J. Zhang, T. Yang, W. Guo, *Chem. Commun.* **2013**, *49*, 2637-2639.

19 a) J. Xu, K. Liu, D. Di, S. Shao, Y. Guo, *Inorg. Chem. Commun.* **2007**, *10*, 681-684; b) R. C. Rodríguez-Díaz, M. P. Aguilar-Caballos, A. Gómez-Hens, *J. Agric. Food. Chem.* **2004**, *52*, 7777-7781; c) Y. Sun, C. Zhong, R. Gong, H. Mu, E. Fu, *The Journal of Organic Chemistry* **2009**, *74*, 7943-7946.

20 A. Zhu, Q. Qu, X. Shao, B. Kong, Y. Tian, *Angew. Chem. Int. Ed.* **2012**, *51*, 7185-7189.

21 a) J. Zhang, X. Xu, X. Yang, *Analyst* **2012**, *137*, 3437-3440; b) J. Zhang, Y. Yuan, X. Wang, X. Yang, *Anal. Meth.* **2012**, *4*, 1616-1618.

22 H. Xie, F. Zeng, C. Yu, S. Wu, *Polymer Chemistry* **2013**.

23 C. Pundir, R. Rawal, *Anal. Bioanal. Chem.* **2013**, *405*, 3049-3062.

24 a) E. Climent, R. Martínez-Máñez, F. Sancenón, M. D. Marcos, J. Soto, A. Maquieira, P. Amorós, *Angew. Chem. Int. Ed.* **2010**, *49*, 7281-7283; b) C. Coll, A. Bernardos, R. Martínez-Máñez, F. Sancenón, *Acc. Chem. Res.* **2012**, *46*, 339-349.

25 a) G. Kickelbick, *Angew. Chem. Int. Ed.* **2004**, *43*, 3102-3104; b) A. Stein, *Adv. Mater.* **2003**, *15*, 763-775; c) A. P. Wight, M. E. Davis, *Chem. Rev.* **2002**, *102*, 3589-3614; d) S.-H. Wu, C.-Y. Mou, H.-P. Lin, *Chem. Soc. Rev.* **2013**, *42*, 3862-3875.

26 a) J. El Haskouri, D. O. d. Zarate, C. Guillem, J. Latorre, M. Caldes, A. Beltran, D. Beltran, A. B. Descalzo, G. Rodriguez-Lopez, R. Martinez-Manez, M. D. Marcos, P. Amoros, *Chem. Commun.* **2002**, *0*, 330-331; b) L. Huerta, J. El Haskouri, D. Vie, M. Comes, J. Latorre, C. Guillem, M. D. Marcos, R. Martínez-Mañez, A. Beltrán, D. Beltrán, P. Amorós, *Chem. Mater.* **2007**, *19*, 1082-1088.

27 Concentrations of less that 10 ppm were selected because this is the macimum concentration limit allowed for sale red wine as SO32- free wine acordin to E.U. regulations.

4.4.3.5. Supporting information

Selective and Sensitive Chromofluorogenic Detection of the Sulfite Anion in Water Using Hydrophobic Hybrid Organic–Inorganic Silica Nanoparticles

Luis Enrique Santos-Figueroa, Cristina Giménez, Alessandro Agostini, Elena Aznar, María D. Marcos, Félix Sancenón, Ramón Martínez-Máñez and Pedro Amorós

Chemicals

The chemicals, sodium sulfite, acetophenone, triethylorthoformiate, magnesium, methyl iodide, perchloric acid, ammonium chloride, sodium sulfate, tetraphenylphosphonium tetrafluoroborate, 4-hydroxybenzaldehyde, 1,8-diazabicyclo[5.4.0]undec-7-ene (DBU), tetraethylorthosilicate (TEOS), *n*-cetyltrimethylammonium bromide (CTAB), sodium hydroxide, (propyl)trimethoxysilane (PTMS), hexamethyldisilazane (HMDS) and hydrochloric acid were provided by Sigma-Aldrich. Analytical-grade solvents (diethyl ether, acetonitrile, acetone, absolute ethanol and dimethyl sulfoxide) and anhydrous magnesium sulfate were purchased from Scharlau (Barcelona, Spain). For the

spectroscopy studies tetrabutylammonium or sodium salts of hydrogen sulfide, fluoride, chloride, bromide, iodide, hydroxide, acetate, cyanide, azide, nitrate, hydrogen carbonate, sulfate, thiosulfate, hydrogen phosphate and citrate were provided by Sigma-Aldrich. Also, L-cysteine (Cys), DL-homocysteine (Hcy), glutathione (GSH) and hydrogen peroxide were provided by Sigma-Aldrich.

General Techniques

UV-visible spectra were recorded with a JASCO V-650 Spectrophotometer. Fluorescence measurements were carried out in a JASCO FP-8500 Spectrophotometer. ^{1}H and ^{13}C-NMR spectra were acquired in a BRUKER ADVANCE III (400 MHZ). The NMR samples were dissolved in deuterated solvents purchased from Cambridge Isotope Labs or Sigma-Aldrich, and TMS or the residual solvent were used as internal standard. Electron impact ionization mass spectrometry (MS-EI) was performed on a Thermo Finnigan MAT SSQ710 single stage quadropole instrument and high resolution mass spectra (HRMS) were carried out in a TRIPLETOF T5600 (ABSciex, USA) spectrometer. Matrix-assisted laser-desorption/ionization mass spectrometry was performed on a Bruker Autoflex III Smartbeam mass spectrometer, utilizing a 2,5-dihydroxybenzoic acid (DHB) matrix. X-ray measurements were performed on a Seifert 3000TT diffractometer using Cu-K_{α} radiation. Thermo-gravimetric analysis were carried out on a TGA/SDTA 851e Mettler Toledo equipment, using an oxidant atmosphere (Air, 80 mL/min) with a heating program consisting on a heating ramp of 10 °C per minute from 393 K to 1273 K and an isothermal heating step at this temperature during 30 minutes. N2 adsorption-desorption isotherms were recorded on a Micromeritics ASAP2010 automated sorption analyser. The samples were degassed at 120 °C in vacuum overnight. The specific surfaces areas were calculated from the adsorption data in the low pressures range using the BET model. Pore size was determined following the BJH method. Scanning electron microscope (SEM) images were acquired in a JEOL JSM 6300 and transmission electron microscope (TEM) images were performed in a Philips CM-10.

Synthesis of 2,6-diphenylpyrylium perchlorate (b)

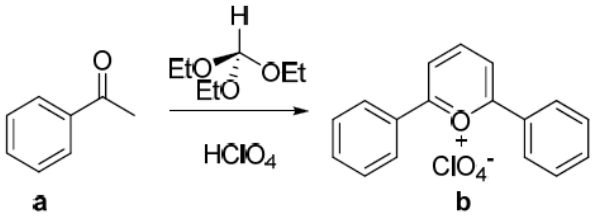

Acetophenone (**a**, 4 mL, 34.3 mmol) and triethylorthoformiate (10 mL) were placed in a round bottomed flask (250 mL) under Ar atmosphere and at 0 °C. After 15 minutes perchloric acid (7.4 mL, 86.5 mmol) was added dropwise during 30 minutes. Then, the crude reaction was allowed to react at room temperature for 60 minutes. The final 2,6-diphenylpyrylium perchlorate (**b**, 10.1 g, 30.4 mmol, 88.6% yield) was isolated as a yellow solid by addition of diethylether. ^{1}H- and ^{13}C-NMR data and mass spectra are coincident with the reported in the literature.[1]

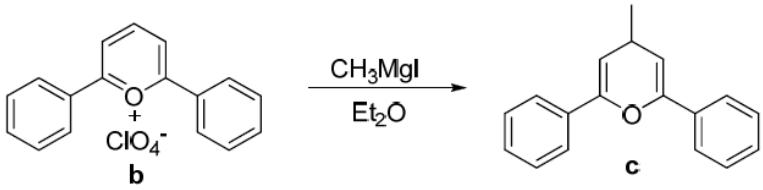

a) **Preparation of the Grignard reagent.** Magnesium (1 g, 0.042 mol) was placed in a round bottomed flask with refrigerant, septum and connected to a vacuum line. Firstly, the air was removed by vacuum and replaced by Argon. In a second step, a solution of methyl iodide (2.58 mL, 0.042 mol) in diethyl ether (30 mL) was added through the septum under inert Ar atmosphere to avoid the degradation of the just formed Grignard reagent. The mixture was stirred at room temperature for 1 hour.

[1] (a) R. Wizinger, P. Ulrich, Helv. *Chim. Acta* **1956**, 39, 207-216; (b) D. Markovitsi, C. Jallabert, H. Strzelecka, M. Veber, *J. Chem. Soc.,* Faraday Trans. **1990**, 86, 2819-2822.

b) **Nucleophilic addition of methylmagnesium iodide** to 2,6-diphenylpirilium perchlorate. The as-made Grignard reagent in diethyl ether was added, under inert Ar atmosphere, to a diethyl ether (10 mL) solution of 2,6-diphenylpyrylium perchlorate (**b**), 790 mg, 2.37 mmol). The reaction mixture was stirred at room temperature overnight. Subsequently the reaction mixture was washed twice with saturated aqueous NH_4Cl (2 x 30 mL), water (3 x 20 mL) and finally dried over sodium sulfate. The elimination of the diethyl ether gave the title product **c** (581 mg, 2.37 mmol) in nearly quantitative yield. ^{1}H-NMR ($CDCl_3$, 400 Mhz): δ: 1.43-1.51 (dd, 3H, J=3Hz, J=6Hz), 3.47 (m, 1H), 5.59-5.61 (dd, 2H, J=3Hz, J=6Hz), 7.61 (m,6H), 7.97 (m, 4H). ^{13}C-NMR ($CDCl_3$, 100 Mhz): δ: 21.1, 31.5, 107.3, 126.5, 128.3, 130.5, 133.5, 159.3. HRMS-EI *m/z*: calcd for $C_{18}H_{16}O$ 248.1201; found: 248.1205.

Synthesis of 4-methyl-2,6-diphenylpyrylium tetrafluoroborate (d)

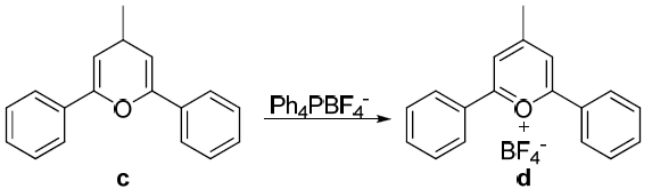

c **d**

A solution of **c** (520 mg, 2.1 mmol) in anhydrous CH_3CN (30 mL) was treate with tetraphenylphosphonium tetrafluoroborate (629 mg, 2.53 mmol) at room temperature overnight. Then, acetonitrile was eliminated by rotary evaporation and the dark-brown residue dissolved in the minimum amount of acetone (1 mL). Product **d** was isolated as a brown powder (580 mg, 1.7 mmol, 82% yield) through precipitation with diethyl ether.[2] ^{1}H-NMR ($CDCl_3$, 400 Mhz): δ: 2.84 (s, 3H), 7.82 (m, 6H), 8.42-8.45 (d, 4H, J=9Hz), 8.85 (s, 9H). ^{13}C-NMR ($CDCl_3$, 100 MHz): δ: 24.1,

[2] K. L. Hoffman, G. Maas, M. Regitz, *J. Org. Chem.* **1987**, 52, 3851-3857.

120.1, 127.8, 128.4, 130.7, 136.0, 170.9, 180.2. HRMS-EI *m/z*: calcd for $C_{18}H_{15}O^+$ 247.1123; found: 247.1121.

Synthesis of chemodosimeter (1)

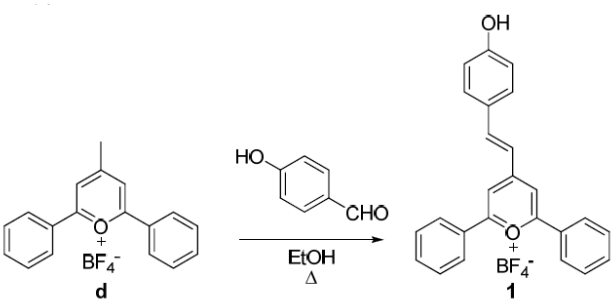

A solution of 4-methyl-2,6-diphenylpyrylium tetrafluoroborate (**d**, 3.03 g, 9.1 mmol) and 4-hydroxybenzaldehyde (1.11 g, 9.1 mmol) in absolute ethanol (150 mL) was refluxed overnight under argon atmosphere. Then, ethanol was removed by rotary evaporation and the dark-red residue taken up with the minimum amount of acetone. This solution was treated with diethyl ether (500 mL) to precipitate the final product **1** (3.59 g, 8.2 mmol, 89.8% yield) as a dark-red crystalline powder. ^{1}H-NMR ($CDCl_3$, 400 Mhz): δ: 7.00 (d, 2H, J = 6.5 Hz), 7.45 (d, 1H, J = 14 Hz), 7.76 (m, 6H), 7.83 (d, 2H, J = 6.5 Hz), 8.38 (d, 4H, J = 6.7 Hz), 8.67 (d, 1H, J = 14 Hz), 8.74 (s, 2H), 10.82 (s, 1H). ^{13}C-NMR ($CDCl_3$, 100 Mhz): δ:113.8, 117.2, 120.3, 125.5, 128.2, 129.5, 130.1, 133.0, 134.6, 150.8, 163.3, 167.6. HRMS-EI *m/z*: calcd for $C_{25}H_{19}O_2^+$ 351.1385; found: 351.1364.

Transformation of 1 to 2

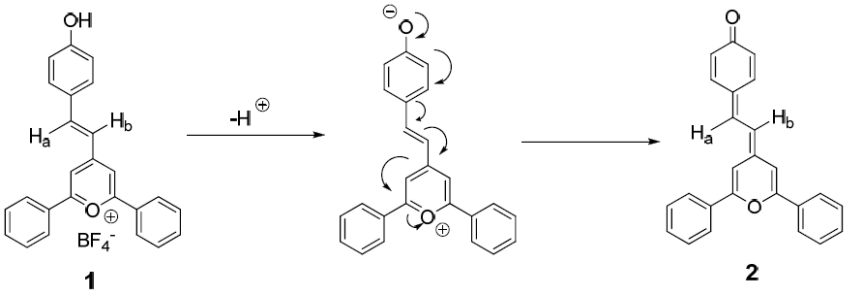

Figure SI-1. Transformation of **1** to **2**.

1 is transformed to **2** via a deprotonation of the acidic phenolic proton of **1** (pK_a = 7.10 in acetonitrile) favoured by the electronic conjugation with the electron withdrawing pyrylium ring. In order to confirm this deprotonation process, a solution of probe **1** (1.0 x 10^{-5} M) in acetonitrile was prepared and upon addition of 1,8-diazabicyclo[5.4.0]undec-7-ene (DBU, a non nucleophilic base) an immediate colour modulation from red-orange to blue with the appearance of intense absorptions in the 500-700 nm interval (peaks at 547, 583 and 640 nm) was observed (see Figure SI-2).

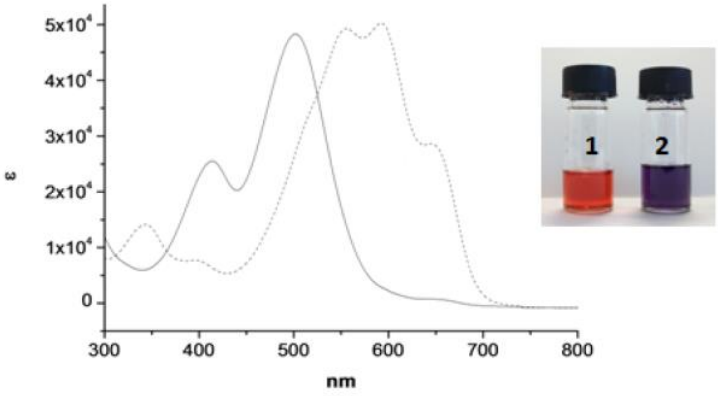

Figure SI-2. UV-visible spectra of chemodosimeter **1** (1.0 x 10^{-5} M) in acetonitrile (filled line) and probe **2** obtained upon DBU-induced deprotonation of chemodosimeter **1** (dashed line) Insert: colour of both **1** and **2** in acetonitrile solution.

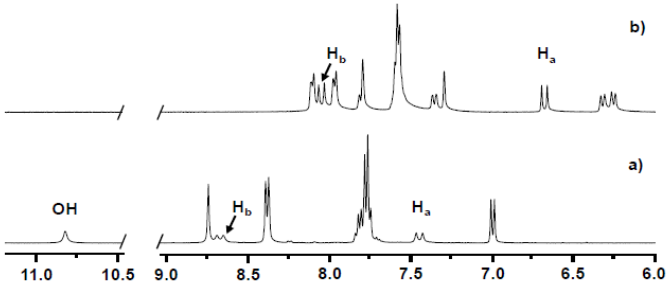

Figure SI-3. ^{1}H-NMR spectra of **1** (a) and **2**(b) obtained upon addition of DBU to probe **1** in DMSO-d_6.

The changes in absorbance spectrum went also along with a remarkable modulation in the ^{1}H-NMR spectrum. As could be seen in **Figure SI-3** the signals of the double bond protons (H_a and H_b) of **1** suffered a significant upfield shifts with a reduction of the coupling constant (from 16 to 12 Hz) upon addition of DBU. Also, the hydroxyl proton signal centred at 10.8 ppm disappeared upon addition of base.

Mechanism of the chromo-fluorogenic response of probe 2 in the presence of sulfite

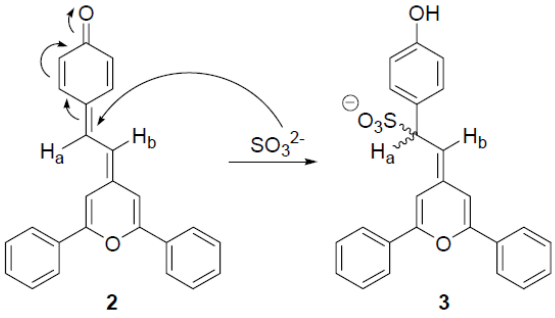

Figure SI-4. Mechanism of the 1,6-conjugated addition of sulfite to chemodosimeter **2.**

The mechanism of the chromo-fluorogenic response was studied by means of NMR measurements with quinone **2** (obtained upon addition of DBU to probe **1**) alone and with the addition of an excess of sulfite in DMSO-D6. At this respect, the most remarkable signals of quinone **2** are two doublets centred at 8.1 (proton H_b in Figure SI-4) and at 6.7 (proton H_a in Figure SI-4) ppm. Addition of sulfite to **2** induced a marked upfield shift of both H_a and H_b protons to 5.45 (H_a) and 4.65 (H_b) ppm (see Figure SI-5). These remarkable upfield shifts would be associated to a loss of aromatic character of chemodosieter **2** upon reaction with sulfite anion.

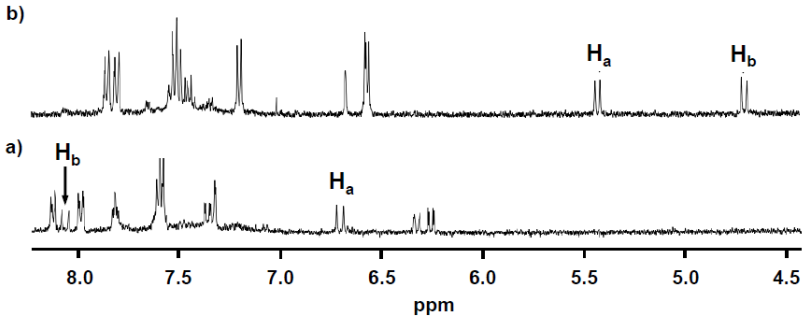

Figure SI-5. ^{1}H-NMR spectra of **2** (a) and **3** (b, obtained upon addition of an excess of sulfite to probe **2**) in DMSO-D6.

In order to further characterize the reaction of sulfite with probe **2**, two-dimensional NMR experiments were also carried out. Homonuclear correlation spectroscopy (COSY) sequence showed that H_a and H_b protons were coupled together (see Figure SI-6). Heteronuclear single quantum coherence (HSQC) spectra (see Figure SI-7) indicated the existence of a clearly correlation between H_b proton and a benzylic carbon (at 63.4 ppm) and also between H_a proton and an olefinic carbon (at 116.8 ppm). These correlations pointed to a sulfite 1,6-conjugated addition over probe **2** yielding **3** (see Figure SI-4).

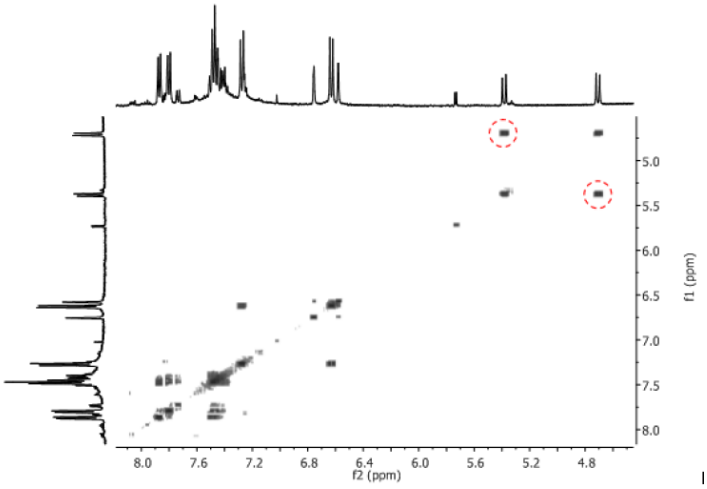

Figure SI-6. COSY spectra of **3** (obtained upon addition of sulfite to probe **2**) in DMSO-D6.

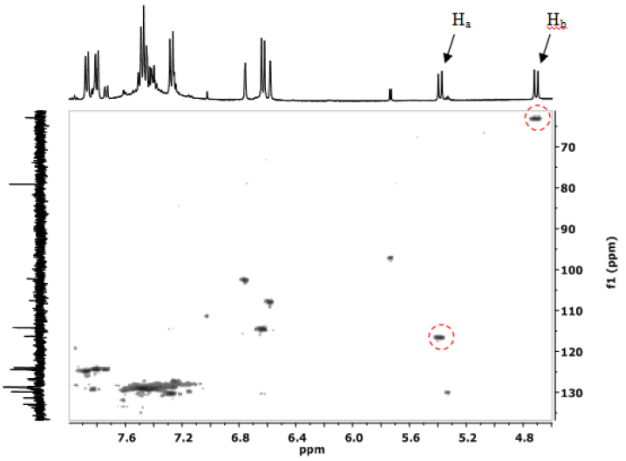

Figure SI-7. HSQC spectra of **3** (obtained upon addition of sulfite to probe **2**) in DMSO-D6.

Similar changes in colour and in emission of **2** (generated upon addition of DBU to chemodosimeter **1** in DMSO) were observed upon addition of several thiols (HS^-, Cys, Hcy and GSH) and ascribed to the same 1,6-conjugated addition reaction with the final formation of **3**.

Synthesis of the mesoporous silica nanoparticles support (MSN)

Mesoporous MCM-41 nanoparticles were synthesized by the following procedure: *n*-cetyltrimethylammonium bromide (CTAB, 1.00 g, 2.74 mmol) was first dissolved in deionized water (480 mL). Then, NaOH (3.5 mL, 2.00 M) in deionized water was added to the CTAB solution, followed by adjusting the temperature to 80 ^{o}C. TEOS (5.00 mL, 2.57 x 10^{-2} mol) was then added dropwise. The mixture was stirred for 2 h to give a white precipitate. Finally, the solid product was centrifuged, washed with deionized water and ethanol, and dried at 60 ^{o}C (MCM-41 as-synthesized).

A portion of the MCM-41 synthesized was reserved for use as support of **N0** and **N1** materials, while another portion was calcined at 550 ^{o}C using an oxidant atmosphere for 5 h in order to remove the template phase and be used in the preparation of the **M1** monolith.

Design of the probe

In a first approach calcined MCM-41 nanoparticles were fully hydrophobized using hexamethyldisilazane. Finally the probe **1** was adsorbed into the hydrophobic cavities of the support. This experimental procedure yielded a blue-colored (due to the formation of quinone **2** in the inner of the pores) hydrophobic material that was quite difficult to disperse in water (HEPES 30 mM, pH 7.5) due to the high hydrophobicity of the external surface of the nanoparticles. In fact the solid prepared in this way trend to float and did not react properly with sulfite contained in the solution. In order to enhance the water dispersion of the sensory nanoparticles we decided to functionalize the external surface of the inorganic scaffold with a linear alkylic chain bulky enough to allow a medium degree of functionalization but not too large to entail a high hydrophobic character. In particular we selected (propyl)trimethoxysilane (PTMS) as coating molecule. Taking these facts into account, the final solid was prepared via the functionalization of the external surface of the silica nanoparticles with (propyl)trimethoxysilane (several (propyl)trimethoxysilane/MCM-41 nanoparticles ratios were tested) followed by the extraction of the CTAB with hydrochloric acid located inside the pores. Finally, the inner of the pore walls were hydrophobized with hexamethyldisilazane. This experimental procedure yield inorganic nanoparticles (**N0**, see below) containing hydrophobic pockets. The presence of bulky propyl chains in the outer surface yielded hybrid nanoparticles with a medium hydrophobicity which are able to be dispersed properly in aqueous environments.

Synthesis of hydrophobic hybrid nanoparticles (N0)

The hydrophobic material was prepared as follows: 2.5 g of MCM-41 as-synthesized was suspended in acetonitrile (200 mL) and (propyl)trimethoxysilane (PTMS, 4.37 mL, 25 mmol) was added. The suspension was stirred for 5.5 h at room temperature with the aim of achieving the functionalization of the MCM-41 scaffolding. Then, the solid was isolated by centrifugation, washed with

acetonitrile and abundant water, and dried at 37 °C for 12 h. The template removal was carried out by acidic extraction. At this respect, 2 g of this solid was suspended in 200 mL of hydrochloride acid solution (1 M) and refluxed for 12 h. This procedure was repeated 3 times, washing the solid between each cycle. Finally, 2 g of the template-free solid was suspended in acetonitrile (160 mL) and hexamethyldisilazane (HMDS, 3.36 mL, 16.11 mmol) was added. The mixture was stirred 12 h at room temperature in order to achieve the maximum functionalization of the pores. Finally, the obtained solid (**N0**) was isolated by centrifugation, washed with abundant water and dried at 37 °C for 12 h.

Preparation of loaded sensing system (N1)

For the preparation of the sensing solid **N1** (containing the probe **2**), 2 g of solid **N0** were suspended in 4 mL of a red solution of probe **1** (8.0 mg, 0.023 mmol) in acetone. Then, the mixture was stirred for 12 hours at room temperature with the aim of achieving maximum loading of the pores of the MCM-41 scaffolding. Finally, the blue solid **N1** was isolated by centrifugation and dried under vacuum. Finally, excess of probe **1** was removed from the solid surface by washing with water and water- CTAB solutions. The final blue solid **N1** was dried in vacuum (see Figure SI-8).

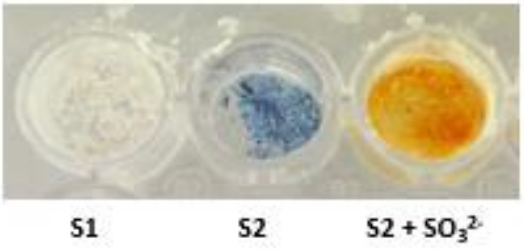

Figure SI-8. Colour of hydrophobic solid **N0**, solid **N1** and final solid **N1** upon reaction with sulfite.

Evaluation of pH stability of N1suspensions

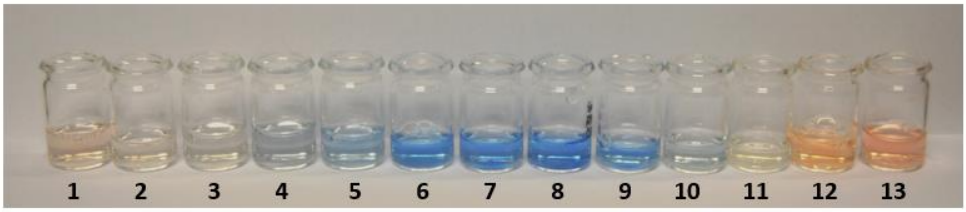

Figure SI-9. Suspensions of **N1** nanoparticles at different pH values.

Characterization of MCM-41 nanoparticles

The power X-ray diffraction (PXRD) of the as-synthesised siliceous nanoparticulated MCM-41 (see Figure SI-10, curve a) shows the typical low-angle reflections that index as (100), (110), (200) and (210) Bragg peaks. From the PXRD data of the as-synthesized MCM-41, a d100 spacing of 40.04 Å was calculated. A significant displacement of the peaks in the PXRD of the calcined MCM-41 was found corresponding to an approximate cell contraction of 3.28 Å (Figure SI-10, curve b). This displacement and broadening are related to further condensation of silanol groups during the calcination step.

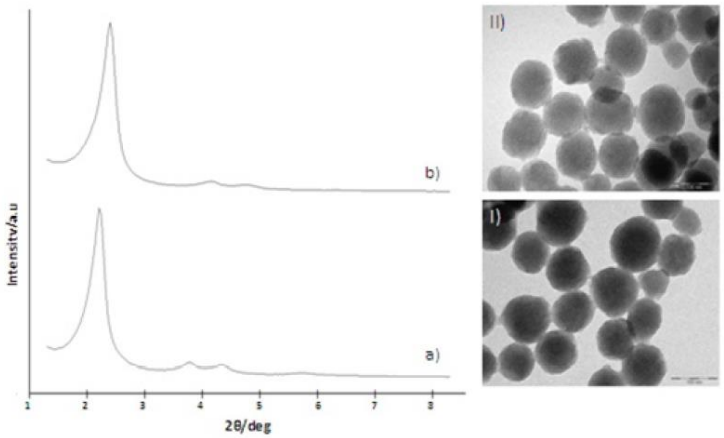

Figure SI-10. Left: Powder X-ray patterns of the solids (a) MCM-41 as synthesized (b) calcined MCM-41. Right: TEM images of (I) MCM-41 as synthesized (II) calcined MCM-41, showing the typical hexagonal porosity of the MCM-41 mesoporous matrix.

The N_2 adsorption-desorption isotherm of the MCM-41 calcined material shows a typical curve for this mesoporous solid (see Figure SI-11). The application of the BET model resulted in a value for the total specific surface of 1034.3 $m^2\ g^{-1}$. Pore size and volume were determined by using the BJH method with Halsey-Faas correction from the adsorption branch of the isotherm. From the PXRD, porosimetry and TEM studies, the pore volume (0.81 $cm^3\ g^{-1}$), the a_0 cell parameter (42.44 Å), the pore diameter (2.59 nm) and a value for the wall thickness of 1.65 nm can be calculated.

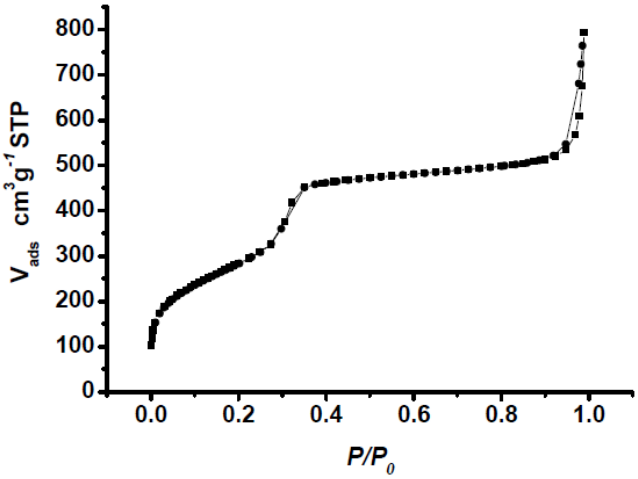

Figure SI-11. Nitrogen adsorption-desorption isotherms for the calcined MCM-41 material.

Characterization of N0 and N1

Figure SI-12 shows powder X-ray patterns of the **N0** functionalised material (curve a) and the final solid **N1** loaded with the probe **2** (curve b). PXRD of both **N0** and **N1**, display the (100), (110) and (200) reflections showing that the surface functionalization and the further loading process with the probe **2** have not damaged the mesoporous MCM-41 scaffolding. The presence of the mesoporous structure in functionalized solid **N0** and final loaded solid **N1** is also observed from the TEM analysis (see I and II respectively in Figure SI-12).

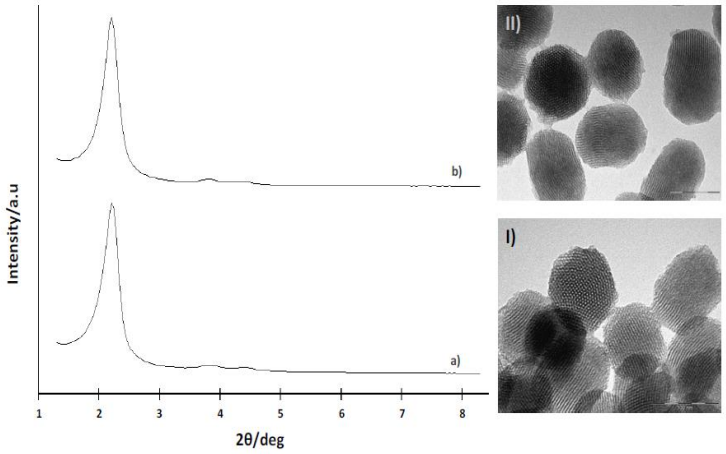

Figure SI-12. Left: Powder X-ray patterns of (a) functionalized solid **N0** and (b) final solid **N1**. Right: TEM images of (I) functionalized solid **N0** and (II) final solid **N1**, showing the typical hexagonal porosity of the MCM-41 mesoporous matrix.

N_2 adsorption-desorption studies of **N0** and **N1** nanoparticles were carried out. The **N0** material, functionalized with propyl and trimethyl silyl moieties, shows a typical curve for these mesoporous solids; i.e. an adsorption step at intermediate P/P_0 value 0.3 and an additional adsorption step at high P/P_0 values ascribed to surfactant-generated mesopores and large interparticle textural-type porosity, respectively (see Figure SI-13). The first adsorption step is typical of a type IV isotherm, and can be related to the nitrogen condensation inside the mesopores by capillarity. The absence of a hysteresis loop in this interval and the narrow pore distribution suggest the existence of uniform cylindrical mesopores (0.63 $cm^3\ g^{-1}$). The second adsorption step corresponds to the filling of the large pores among the primary MCM-41 functionalized particles and shows a characteristic H1 hysteresis loop and a wide pore size distribution with large pore size values falling in the border between meso and macropores. The application of the BET model resulted in a value for the total specific surface of 1012.4 $m^2\ g^{-1}$. From the XRD, porosimetry and TEM studies, the a_0 cell parameter (46.23 Å), the pore diameter (2.15 nm) and a value for the wall thickness of 24.73 Å can be calculated.

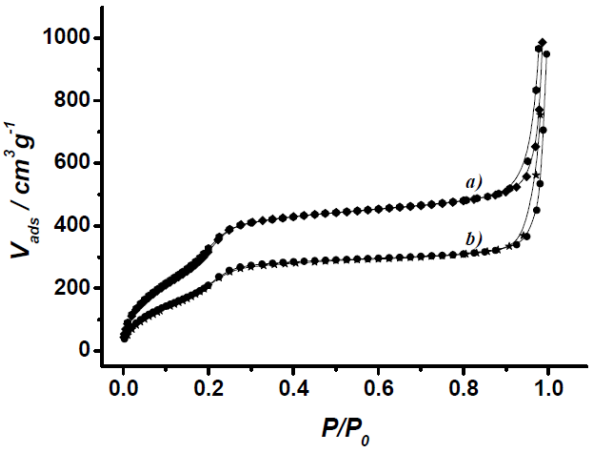

Figure SI-13. Nitrogen adsorption-desorption isotherms for (a) N0 nanoparticles and (b) the final **N1** material.

BET specific surface values, pore volumes, and pore sizes calculated from the N_2 adsorption-desorption isotherms for **N0** and **N1** are listed in Table 1. The BJH pore size and pore volume values in Table 1 correspond to the intraparticle mesopores (estimated from adsorption data at P/P_0 values < 0.8, and then excluding the large textural-type interparticle porosity).

Table 1. BET specific surface values, pore volumes and pore sizes calculated for **N0** and **N1** nanoparticles.

Solid	**S_{BET}** ($m^2 g^{-1}$)	**Pore Volume** ($cm^3 g^{-1}$)	**Pore Size** (nm)
N0	1012.4	0.63	2.15
N1	852.2	0.43	2.12

The thermal analysis of solids shows a typical behaviour of functionalized mesoporous materials, that is, an initial weight loss between 25 and 150 °C related to solvent evaporation, a second loss between 150 and 800 °C due to the combustion of organic material, and a final loss in the 800-1000 °C range related to the condensation of the silanol groups. The loading of the final solid **N1** was

determined by elemental analysis and thermogravimetric studies. A ratio of 0.038 mmol **2**/g SiO_2 was calculated.

Fluorescence calibration curve of N1 upon addition of sulfite

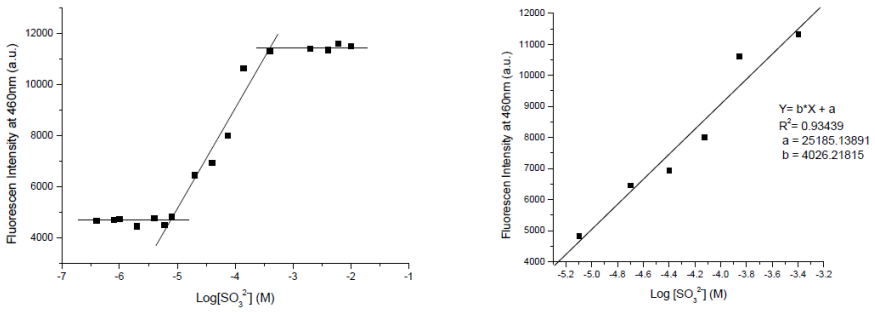

Figure SI-14. Right: Emission intensity at 460 nm (λ_{ex}=355 nm) of buffered (HEPES 30 mM, pH 7.5) suspensions of **N1** nanoparticles as a function of sulfite concentration. Left: Lineal range of the calibration curve and regression equation.

Preparation of M0 and M1 monoliths

A ceramic foam (CF) was prepared through of a typical replication process using commercially available and inexpensive polyurethane foams (PUF) and ceramic slip (barbotine). Then, the CF surface area was activated by inducing the formation of silanol groups using a strong alkaline-hydrothermal treatment (with heating at 110 °C in NaOH 1M solution for 2h). Next, a colloidal suspension in water of silica nanoparticles of MCM-41 (2% in weight) was prepared by means of ultrasound irradiation for 15 min at 350 W in water (using a high-power Branson 450 instrument). Then, the rigid hybrid monoliths **M0** were prepared by successive impregnation cycles (4 times) over the CF with the aqueous MCM-41 colloidal suspension followed by soft thermal treatment (120 °C for 2 h). Finally **M0** was reacted with hexamethyldisilazane (HMDS) and loaded with probe **2** in acetone to form the **M1** blue monolith (see Figures SI-15 and SI-16).

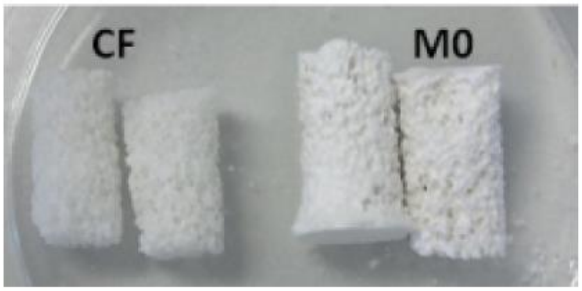

Figure SI-15. Photograph showing CF and **M0** monolith.

Figure SI-16. Photograph showing the **M0** and **M1** monoliths before (blue) and after (yellow-orange) their reaction with sulfite anion.

Chapter 5: Conclusions and Perspectives

5. CONCLUSIONS AND PERSPECTIVES

The preparation of optical chemosensors for chemical species of biological, industrial and environmental interest is one of the most promising sub-areas within the supramolecular chemistry field. In fact, progress on new approaches to make more effective and efficient chemosensors offer a new interdisciplinary area with wide horizons to the development of specific applications. This PhD thesis is an original scientific contribution to the evolution of this dynamic field.

We attempted to apply organic, analytical and inorganic chemistry in creative way and combined with the material science on the creation of new chromo-fluorogenic chemosensors systems for real problems.

The fundaments of supramolecular chemistry, especially about molecular recognition chemistry and self-assembly, are addressed in the general introduction presented in chapter one. Besides, more of 130 examples of new chemosensor for anion recognition are reported in an additional comprehensive review published during the first stage of development of this PhD thesis.

In the second chapter, the experimental results obtained with the development of a new chromo-fluorogenic chemosensor for selective detection of trivalent cations are reported. The design, synthesis and characterization of the recognition system have been described. A detailed study of the optical response of the new probe in presence of target guest and several common interferents was carried out. Finally, a new chalcone-based chemosensor able to selectively detect Al^{3+}, Fe^{3+} and Cr^{3+} with remarkables low limits of detection in nM concentration range and with a simple to detect to-naked-eye chromo-fluorogenic response are presented.

The chapter three of this PhD thesis is devoted to the study of optical chemosensors for anions recognition. The synthesis and evaluation of sensing behaviour of 13 new cromofluorogenic chemosensor are shown along this chapter.

In particular, a contribution to the study for understanding the behavior of the molecular recognition of basic anions using push-pull systems is presented at the beginning of chapter three. In this respect, two families of novel heterocyclic thiosemicarbazones containing furyl or thienyl moieties were prepared and characterized. Their interactions with anions have been thoroughly studied via UV-Vis, fluorescence and NMR spectroscopy, quantum chemical calculations and electrochemical techniques. The thiosemicarbazone dyes show a modulation of their donor hydrogen bonding abilities and optical output responses as a function of the electronic nature of the attached chemical groups. A delicate balance between the acidity of the N-H protons of the receptor and the basicity of the anion modulates a dual coordination–deprotonation process has been found. At the same time, the influenced of the incorporation into the probe of an aceptor or a donor moiety on the final acidity of N-H group was clearly observed.

Always in the third chapter, the design, synthesis, characterization and application of two new molecular probes for the detection of hydrogen sulfide in aqueous media and living cells are presented.

The first of these probes was design by "displacement assay" approach. In this case a new anthracene-functionalised cyclam–copper(II) complex weakly emissive was prepared as a fluorescent chemosensor. In presence of hydrogen sulfide anion, a selective turn-on response has been displayed due a demetallation reaction that inhibits the emission quenching observed in the initial complex because of the presence of the paramagnetic Cu^{2+} center. Moreover, real-time fluorescence imaging measurements confirm that the new probe can be easily

used to detect intracellular hydrogen sulfide at μM concentrations with a remarkable enhancement in the FI/FI_0 ratio.

On the other hand and in the same chapter, a sulfonyl azide-based chemodosimeter for chromogenic and fluorogenic detection of hydrogen sulfide in aqueous environments and intracellular is also exposed. The addition of hydrogen sulfide induce a clear colour change, easily detected by the naked eye, and an enhancement in the emission intensity. The selective and sensitive response is due to reduction of sulfonyl azide to sulfonyl amide group. The potential ability of this probe to sensing intracellular hydrogen sulfide at μM concentrations is also reported.

Finally, throughout the fourth chapter, the design, synthesis, characterization and application of a nanoscopic mesoporous silica based hybrid functional system able to selectively detect sulfite in pure water is reported. Evaluation of sensing abilities of the functional system for sulfite recognition was carried out. In presence of sulfite, a significant increase in fluorescence due to the reaction between the anion and the dosimeter within the cavities of the hybrid support has been showed. Additionally, the evaluation of functional system with the use of the prepared hybrid material and a polymeric monolith support confirms the potential use of the new system for detection of sulfite in real samples such as commercial wine.

In summary with this PhD thesis we explored several approach for the preparation of chromo-fluorogenic chemosensors for several chemical species of biological, industrial and environmental interest.

With the design and evaluation of the molecular probes prepared, the published of our scientific results of research done in the framework of this PhD thesis and the comprehensive review of other recently publications dealing with anion chemosensor, we provided the scientific community several contribution to

the theoretical and the pure science research. Besides, our successful results in sensing of specific targets in several aqueous and organic media, living cells and real samples also provide several potencial applications that address some real problems.

In addition, possible future development of new chemosensor are raised throughout all studies. In fact, some new systems inspired in this work have been designed and are currently being evaluated.

In this particular, further studies on the influence of organic changes in the recognition abilities of some quinoline derivatives and anthraquinones is being carried out. The preparation of novel functional binding pocket systems in order to enhance the sensing features of some chromo-fluorogenic probes, similar to the presented in this PhD thesis are also being evaluated by our research group and others. Besides, some of the chemical sensors reported here are being used as the basis for the preparation of molecular gates and as inspiration for the design of new molecular probes.

We also believe that with the experience gained during the development of this work and considering other systems that are not included in this thesis but were tested preliminarily in conjunction with the results reported here, we have opened new ways to continue with the design of even more sensitive and selective systems and of novel commercially viable applications.

Gracias a la Fundación Carolina, la OAI-UPV y a la UPNFM por la beca de formación doctoral que ha financiado el desarrollo de esta tesis.